U.S. Geological Survey
Open File Report # 94-637
October 15, 1994

Geophysical Database of the East Coast of the United States Northern Atlantic Margin: Cross Sections and Gridded Database

(Georges Bank Basin, Long Island Platform, and Baltimore Canyon Trough)

K.D. Klitgord, C.W. Poag, C.M. Schneider, and L. North
U.S. Geological Survey
Woods Hole MA 02543

This report is preliminary and has not been reviewed for conformity with U.S. Geological Survey editorial standards and nomenclature. Use of trade names is for the purposes of identification only and does not constitute endorsement by the U.S. Geological Survey.

Table of Contents

Introduction 3
The U.S. Atlantic Margin - General Geologic Framework 4
The Geoacoustic Database 5
Table 1: Geoacoustic parameters and formulas used to calculate them 7
Geoacoustic Parameters 8
Table 2: Example of profile geoacoustic database 8
Table 3: Example of gridded geoacoustic database 9
Seismotratigraphy 10
Table 4: U.S. Atlantic margin seismostratigraphy 10
Sediment types and lithologies 11
Table 5: General lithologic types identified on the U.S. Atlantic margin 11
Table 6: Seruficial sediment types and surface attenuation 11
Seismic velocities 12
Data gridding and contouring 12
Data Masks 12
Geological influences on geoacoustic parameters 13
Geoacoustic Database Displays 13
Multichannel seismic-reflection profiles (Appendix 3) 14
Depth to reflectors in time (Appendix 4) and distance (Appendix 5) 15
Thickness Isopachs for acoustic units (Appendix 6) 15
Interval velocities (Appendix 7) 16
Sediment types (Appendix 8) 16
Summary 16
Acknowledgements 17
References 17
Figure Captions 21
Figures 23
Appendix 1: U.S. Geological Survey CDP Seismic Lines 35
Line crossing and well crossing shot point numbers 36
Appendix 2: U.S. Atlantic margin wells used to calibrate database 39
Appendix 3: Stratigraphic time sections and layer interval velocity sections 40
Appendix 4: Time depth contour maps for base of acoustic units in digital database 88
Appendix 5: Depth (in meters) contour maps for the base of acoustic units in digital database 109
Appendix 6: Thickness Isopach maps for acoustic units in digital database 130
Appendix 7: Interval velocity contour maps for acoustic units in digital database 151
Appendix 8: Sediment-type distribution within acoustic units in digital database 169

Geophysical Database of the East Coast of the United States Northern Atlantic Margin: Cross Sections and Gridded Database (Georges Bank Basin, Long Island Platform, and Baltimore Canyon Trough)

K.D. Klitgord, C.W. Poag, C.M. Schneider, and L. North
U.S. Geological Survey, Woods Hole MA 02543

Introduction

Acoustic transmission characteristics in the submarine environment are influenced by the sound propagation properties of the rock units beneath the sea floor. Geoacoustic models of these rock units are "basic to underwater acoustics and to marine geological and geophysical studies of the earth's crust, including stratigraphy, sedimentology, geomorphology, structural and gravity studies, geologic history, etc." (Hamilton, 1980). Numerous geoacoustic models (e.g., Hamilton, 1980; Stoll, 1980; Hamilton and Bachman, 1982) have been developed from small, local data sets in acoustic transmission studies, but their general utility has been limited by the lack of regional geoacoustic data sets for model parameter determinations. A regional geoacoustic database on the northern U.S. Atlantic margin has been developed for the U.S. Naval Oceanographic Office by the U.S. Geological Survey as an initial step to meet this need. Multichannel seismic-reflection data are the primary sources of acoustic information used in this construction. It is recognized that these data have limited resolution in the upper 500 m of the sedimentary column, critical for transmission studies, but this database can be used in existing geoacoustic models to define the nature and extent of more detailed high-resolution acoustic studies of the upper sedimentary column.

This geoacoustic study of the northern U.S. Atlantic margin (Cape Hatteras to the Canadian boundary) is centered around two major sedimentary basins (Baltimore Canyon Trough and Georges Bank Basin) and the intervening crustal platform (Long Island Platform) (Figures 1, 2 and 3). The geoacoustic parameters in this database (Table 1) are derived from a combination of a seismostratigraphy developed from a grid of multichannel seismic-reflection profiles (Figure 3; Appendices 1 and 3) and acoustic velocity vs depth functions based on normal moveout velocity analyses on multichannel seismic-reflection profiles, velocity sonic logs and checkshot studies at selected industry drillholes (Appendix 2), and wide-angle seismic data from 2-ship seismic experiments. Construction and calibration of the velocity data component of this geoacoustic database is described by Klitgord and Schneider (1994). A digital database of these geoacoustic parameters (e.g., Tables 2 and 3) has been constructed from data along each seismic line and at a 5 minute grid spacing over the area of investigation. Graphical representations of this digital database are in the form of stratigraphic time sections and interval-velocity profiles for the seismic-reflection profiles (Appendix 3), travel-time (seconds) surface contour maps for the base of each stratigraphic unit (Appendix 4), depth (meters) surface contour maps for the base of each stratigraphic unit (Appendix 5), isopach maps of each stratigraphic unit (Appendix 6), interval-velocity contour maps for each stratigraphic unit (Appendix 7), and distribution of gross lithologies within these stratigraphic units (Appendix 8).

The U.S. Atlantic Margin - General Geologic Framework

The U.S. Atlantic continental margin incorporates the coastal plain and continental shelf, slope and rise of the U.S. East Coast. It is bordered on the west by the Appalachian Mountains and on the east by the deep sea of the Atlantic Ocean (Figures 1 and 2). The upper surface of the margin decreases slowly in elevation to seaward across the coastal plain and then is nearly flat across the continental shelf (~0.1° slope). Near the 200-m water-depth isobath, the gradient of the seafloor increases markedly (>2°) in the narrow zone called the continental slope. The sea-floor gradient decreases again (~0.5°) at about the 3000-m water-depth isobath, where it is now called the continental rise. The continental rise grades into the nearly flat deep sea floor with water depths >4500 m. The present continental slope is dissected by numerous submarine canyons where sedimentary material is transported from the shelf to the rise. For this study, we are focusing on the acoustic properties of rocks beneath the continental shelf, slope, and rise.

The geologic framework of the U.S. Atlantic continental margin is the product of a regional tectonic environment that evolved from continental rifting to sea-floor spreading and finally to that of a passive continental margin. Initially, an extensional tectonic regime caused continental rifting (similar to the present-day East African Rift) as the Pangea supercontinent (North American, South American, and African continents) rifted apart in the early Mesozoic (~230-187 m.a.; rift phase). The pre-existing continental crust was fragmented and intruded by new igneous material (rift-stage crust). The Atlantic Ocean formed as the continents moved apart and new igneous material (oceanic crust) was emplaced at the Mid-Atlantic Ridge (sea-floor spreading). As the Mid-Atlantic Ridge migrated eastward relative to the North American margin (remaining near the center of the expanding Atlantic Ocean Basin), the heat influx associated with this magmatic activity also moved away and the crust at the edge of the margin began to cool. Thermal contraction of the crust at the margin caused rapid sea-floor subsidence and enabled a thick pile of sediments from the eroding Appalachian Mountains to accumulate along the margin (e.g., Klitgord and others, 1988; Poag and Sevon, 1989). This later period (~187 m.a. to Present; postrift phase) is referred to as the passive margin phase of margin development; it is a time when thermal subsidence, sediment loading, and fluctuations in climate and oceanographic environments control the accumulation of sedimentary rock along and across the margin.

The continental margin is a wedge of sedimentary rock overlying basement rocks of igneous or metamorphic origin (Figure 3). This sedimentary wedge thickens in the seaward direction from zero at the Fall Line (the western edge of the coastal plain) to over 15 km beneath the outer continental shelf. A carbonate-bank, shelf-edge platform developed near the boundary between rift-stage and oceanic crust, trapped significant amounts of sedimentary material on the shelf, and formed a steep continental slope. The wedge thins to the east beneath the continental rise (6-10 km) and deep sea (< 6 km), and approaches zero thickness at the crest of the Mid Atlantic Ridge. A rapid thickening of this wedge from 4 km to 8+km occurs at a basement hinge zone beneath the inner continental shelf. Sedimentary rocks in this wedge range in age from Late Triassic (230 m.a.) to Present (Tucholke and Mountain, 1979; Klitgord and Grow, 1981; Poag, 1982, 1985b, 1991, 1992; Olsson and others, 1988; Manspeizer and others, 1989; Poag and Ward, 1993). The base of this sedimentary wedge is constructed of igneous, metavolcanic, and metasedimentary rocks of pre-Mesozoic age (>245 m.a.) west of the basement hinge zone (Manspeizer and others, 1989; Sheridan and others, 1991), Late Triassic and younger (<230 m.a.) beneath the continental shelf and slope (Klitgord and others, 1988;

Poag and Ward, 1993), and Middle Jurassic and younger (<187m.a.) beneath the continental rise (Tucholke and Mountain, 1979; Klitgord and Grow, 1980; Poag, 1992).

Between the sea floor and basement, numerous erosional and depositional unconformities (associated with sea-level fluctuations and combinations of oceanographic and tectonic processes) divide the sediment pile into subparallel, near-horizontal layers (Figure 4) (Poag and Schlee, 1984). The deepest of these unconformities, the postrift or breakup unconformity, separates synrift sedimentary rock deposited in a rift environment with extensive faulting and igneous activity, from postrift sediments that accumulated in a broadly subsiding basin. This latter basin of postrift sedimentary fill is usually divided into two basins; one beneath the continental shelf and one beneath the slope, rise and deep sea. The boundary between these two basins is a Jurassic shelf-edge carbonate platform (Poag, 1991) that is poorly imaged on seismic-reflection data (Figure 5) and represents a significant change in depositional environment. Relatively stratified units formed at the seaward base of the platform during the Jurassic and Early Cretaceous, but the development of extensive, overlapping fans during the Late Cretaceous and Tertiary has left a more chaotic stratigraphic record in the upper section (e.g., Figure 6). The ages of these unconformity-bounded units have been determined from biostratigraphic studies of drill hole material (e.g., Figure 4) and occasional bottom sampling where erosion on the continental slope has exposed deeper stratigraphic units (Poag, 1985b, 1991, 1992; Poag and Valentine, 1988).

Sedimentary rock types vary across the margin and were significantly different during various periods of the margin's construction. The synrift sediments included significant amounts of salt and anhydrite mixed with varying amounts of terrigenous clastic and volcaniclastic material. There also may be significant amounts of igneous rock in the synrift section. The primary postrift sediment source is terrigenous clastic material (sandstone and clay mixtures) flooding from onshore mixed with carbonate-rich material deposited near the shelf edge during the first 60 m.y. of the shelf development (Poag, 1991). This later material (limestone and dolomite) formed a carbonate shelf edge during the Jurassic and Early Cretaceous (187 to 130 m.a.) that trapped clastic material behind it and created a steep scarp at the shelf edge (e.g., Figure 5). The continental slope and rise were constructed from the clastic debris which swept over the shelf edge as debris flows and turbidites and mixed with calcareous and silicic pelagic material. Variations in the supply of shelf-derived material and fluctuations in the calcite compensation depth (CCD) are reflected in pelagic-dominated layers (carbonate-rich or shales) and turbidite-dominated layers of clastic material. Fluctuating sea level created an environment in which fan deposition shifted between the shelf and rise. During low stands of sea level, numerous canyons were incised into the shelf slope forming the conduits for sediment transport onto the continental rise. Extensive descriptions and summaries of the geology of the U.S. Atlantic margin have been published in Poag (1982, 1985a,b, 1987, 1991, 1992), Poag and Sevon (1989), Poag and Ward (1993), and in the Geological Society of America centennial series (Sheridan and Grow, 1988).

The Geoacoustic Database

The basic database is a suite of geoacoustic parameters (Tables 1, 2 and 3) for a layered set of acoustic stratigraphic units on the continental shelf and adjacent slope and rise of the Atlantic continental margin of the United States (Poag, 1985b, 1991, 1992; Schlee, 1984; Klitgord and

others, 1988; Sheridan and Grow, 1988; Grow and others, 1988). Each of these units is comprised of rocks with lithologies that can vary across and along the margin. All of the rock units in this data base are sedimentary; we have minimal velocity information from the underlying igneous and metamorphic rocks. Primary input data for the database are 1.) seismostratigraphic horizons (Table 4) from seismic-reflection profiles (Figure 2 and Appendix 3), 2.) bio- and litho-stratigraphic information from a sparse set of industry and stratigraphic test wells (e.g., Amato and Bebout, 1980; Amato and Simonis, 1980) (Appendix 2) and surficial sea-floor sampling sites, and 3.) seismic-velocity information from normal-moveout analyses of multichannel seismic- reflection data, sonic logs and checkshot velocity studies at industry and stratigraphic test drill wells (Appendix 2) and seismic-refraction studies (Sheridan and others 1988; Klitgord and Schneider, 1994). These data are used to determine the three-dimensional (horizontal and vertical) geometries of stratigraphic units for the database, lithologies and ages of these units, and RMS sound transmission velocities to the surfaces that bound these units. This set of observations is then expanded to include geologic and acoustic parameters that are derived from this initial set of parameters: density (ρ), compressional-wave (p-wave) velocity, shear-wave (s-wave) velocity, p-wave attenuation (k_p), and s-wave attenuation (k_s). These parameters have been determined at a 5 shot-point spacing along each seismic line (250 m or 500 m; see Appendix 3 for shot point spacings) for stratigraphic information, an ~30 or 60 shot point spacing (~ 3000 m) for velocity information (Figure 7), and at a 5-minute grid spacing (9250 m x 7100 m) over the area of investigation (Figure 8). Thus the database is actually two data sets: one confined to points along individual seismic lines and the second interpolated onto a regional grid.

A basic premise in this study is that the geoacoustic parameters of a given unit or reflector are influenced only by the material above it and the unit just below it. The acoustic units are defined by acoustic reflectors that bound them on top and bottom. Nomenclature has been developed for these units such that parameters are related to the surface (reflector) that defines the base of each unit. Two-way travel times (in seconds; sea surface to reflector to sea surface), depth below sea surface (in meters) and RMS velocities, properties related to the entire overlying crustal column, are given with respect to a particular reflector (Figure 9). Densities, thicknesses, p-wave velocities, s-wave velocities and attenuation properties pertaining to a given unit are related to the unit directly above a given reflector. Each reflector has been numbered (see Table 4) to facilitate digitizing and identification in the digital arrays. These numbers monotonically increase with depth (and age) but they have no meaning in a geologic sense. Most of these surfaces are erosional unconformities, some of which have eroded deeply enough into the sedimentary wedge to completely remove one or more underlying units on parts of the margin. In such cases, two or more reflectors merge and there could be ambiguity in identifying the age of the boundary between two units. In the situation shown in Figure 10, reflector 60 is the top of Eocene-Paleocene sediments in some places and the top of Cretaceous sediments in others. The mid-Oligocene unconformity (base of Upper Oligocene; reflector 60) has eroded down to the top of the Cretaceous (base of Paleocene-Eocene; reflector 70) and we have referred to that surface as reflector 60 (base of Upper Oligocene). To avoid ambiguity, we always refer to a reflector as the surface that defines the base of the overlying unit rather than as the top of the underlying unit. In this way, when we discuss the properties in the database, we can refer to material that *exists* above a reflector, since it is often possible that the original material below a reflector (in the case of reflector 60 it is Eocene-Paleocene material) is now missing. In this convention, prominent geologic boundaries, such as the surface forming the top

Table 1: Geoacoustic Parameters and Formulas used to calculate them.

For each horizon n (n=1,N) or each layer n bounded by horizons n-1 and n:

$T(n)$ = two-way travel time depth below sea level of reflector n (in seconds);
$T(0)$ = 0.0 = sea surface observed on seismic-reflection records.
$V_{rms}(n)$ = RMS velocity of all units above reflector n (in m/sec) calculated from NMO analysis of multichannel seismic data.
$A(n)$ = age of unit above reflector n based on correlation of acoustic units to biostratigraphic information at drill sites or dredge sites.
$ST(n)$ = sediment type within unit above reflector n based on correlation of acoustic units to lithostratigraphic information at drill or dredge sites (see symbol codes in Table 4).
$V_i(n)$ = interval velocity of unit above reflector n in m/sec
= $(V_{rms}(n)-V_{rms}(n-1))/(T(n)-T(n-1))$
$V_p(n)$ = compressional-wave velocity for unit above reflector n in m/sec
= $V_i(n)$
$V_p(water)$ = 1500 m/sec on all of profiles.
$DZ(n)$ = thickness of layer n in meters
= $(T(n)-T(n-1))\cdot V_i(n)$
$D(n)$ = depth of reflector n in meters
= $\Sigma(T(j)-T(j-1))\cdot V_i(j)$ for j=1,n
$Z(n)$ = depth to midpoint of unit above reflector n in meters
= $D(n) - DZ(n)/2$
$\rho(n)$ = density of rock within unit n in gm/cc calculated from V_p using the following formulae for terrigenous marine sediments (Hamilton, 1978, p. 368)
= $14.80\ V_p - 21.014$ gm/cc at V_p (seafloor)
= $1.135\ V_p - 0.190$ gm/cc 1.5 km/s $< V_p < 2.0$ km/s
= $-0.08\ V_p \cdot V_p + 0.744\ V_p + 0.917$ gm/cc 2.0 km/s $< V_p < 4.5$ km/s
$V_s(n)$ = shear-wave velocity in unit n calculated from V_p using the following formulae for terrigenous marine sediments (Hamilton, 1979, p. 1095):
= $3.884\ V_p(n) - 5.757$ km/s 1.512 km/s $< V_p < 1.555$ km/s
= $1.137\ V_p(n) - 1.485$ km/s 1.555 km/s $< V_p < 1.650$ km/s
= $+0.47\ V_p(n)\cdot V_p(n) - 1.136\ V_p(n) + 0.991$ km/s 1.650 km/s $< V_p < 2.150$ km/s
= $0.780\ V_p(n) - 0.962$ km/s 2.150 km/s $< V_p$
for mud stone (Castagna and others, 1985):
= $0.862\ V_p(n) - 1.172$ km/s
$\alpha_p(n)$ = compressional-wave attenuation in dB/m
= $F(k_0, V_p(n), D(n-1), D(n), f)$
where k_0 is a constant dependent on surface rock type, f is the frequency in kHz (Mitchell and Focke ,1980; Stoll, 1985).
$\alpha_s(n)$ = shear-wave attenuation in dB/m
= $k_s \cdot f$ where k_s is a constant in dB/m-kHz , f is frequency in kHz (Hamilton, 1976a,b; Castagna and others, 1985)

of the Cretaceous, will be represented by portions of several reflectors (e.g., reflector 70, then reflector 60 and finally reflector 70 again in Figure 10). This nomenclature (referencing the bottom of units) is different from the standard reference to the top of units, but it eliminates ambiguity in the layer reference frame and simplifies the bookkeeping.

Geoacoustic Parameters

The digital database contains the following information at a 3000-m spacing along each seismic-reflection line and at each of the 5-minute grid points in the study area where adequate data are available: labelling by line number, shot point, latitude-longitude pairs and an array of geoacoustic parameters at each of these points. This parameter array includes information determined from seismic or sample data: reflector number, two-way travel time (T) of each reflector, RMS velocity (V_{rms}) between sea surface and this reflector, layer age (A) and sediment type (ST). From these data we have calculated at each location: depth (D) in meters to the reflector and thickness (DZ), density (ρ), p-wave velocity (V_p), s-wave velocity (V_s), p-wave attenuation (k_p), and s-wave attenuation (k_s) for each layer (Tables 1, 2 and 3).

Table 2: Example of Profile Geoacoustic Database

Line No.	Shot Point No.	Latitude (deg.)	Longitude (deg.)	Layer No.	Sed. Type	Travel Time (sec.)	Depth (m)	Thick-ness (m)	Density (gm/cc)	RMS Vel. (m/s)	P-Wave Vel. (m/s)	S-Wave Vel. (m/s)	Surface Atten.	P-Wave Atten. (dB/m-kHz)	S -Wave Atten.
22	915	-71.0864	41.1034	001	02	0.070	052	052	1.000	1500	1500	-	0.01138	-	-
22	915	-71.0864	41.1034	020	02	0.210	169	117	1.715	1620	1678	408	-	0.01302	0.18339
22	915	-71.0864	41.1034	070	04	0.240	196	026	1.830	1641	1780	458	-	0.01672	0.12278
22	915	-71.0864	41.1034	080	04	0.400	350	153	1.989	1758	1920	542	-	0.04559	0.17813
22	915	-71.0864	41.1034	090	04	0.470	423	073	2.123	1811	2090	669	-	0.06491	0.14818
22	1002	-71.0644	41.0658	001	02	0.070	052	052	1.000	1500	1500	-	0.01150	-	-
22	1002	-71.0644	41.0658	020	02	0.211	171	118	1.727	1628	1689	413	-	0.01305	0.16945
22	1002	-71.0644	41.0658	070	04	0.250	206	035	1.859	1657	1805	471	-	0.01527	0.09843
22	1002	-71.0644	41.0658	080	04	0.420	372	166	2.028	1783	1954	565	-	0.03864	0.13345
22	1002	-71.0644	41.0658	090	04	0.510	468	095	2.138	1848	2127	701	-	0.05020	0.10421
22	1062	-71.0486	41.0406	001	02	0.070	052	052	1.000	1500	1500	-	0.01193	-	-
22	1062	-71.0486	41.0406	020	02	0.237	194	141	1.741	1643	1701	418	-	0.01364	0.16263
22	1062	-71.0486	41.0406	070	04	0.274	229	034	1.909	1673	1849	497	-	0.03769	0.19713
22	1062	-71.0486	41.0406	080	04	0.442	396	167	2.080	1804	2000	599	-	0.03401	0.10081
22	1062	-71.0486	41.0406	090	04	0.550	514	117	2.158	1883	2177	736	-	0.06548	0.12066
22	1122	-71.0339	41.0148	001	02	0.070	052	052	1.000	1500	1500	-	0.01279	-	-
22	1122	-71.0339	41.0148	020	02	0.260	214	162	1.750	1655	1709	422	-	0.01906	0.21511
22	1122	-71.0339	41.0148	070	04	0.300	252	037	1.939	1686	1876	513	-	0.07267	0.33819
22	1122	-71.0339	41.0148	080	04	0.460	415	163	2.101	1816	2039	628	-	0.05726	0.15071
22	1122	-71.0339	41.0148	090	04	0.572	540	124	2.178	1904	2228	775	-	0.11813	0.19468
22	1182	-71.0194	40.9890	001	02	0.070	052	052	1.000	1500	1500	-	0.01422	-	-
22	1182	-71.0194	40.9890	020	02	0.270	224	171	1.759	1663	1717	426	-	0.01929	0.20641
22	1182	-71.0194	40.9890	070	04	0.320	271	047	1.957	1701	1892	524	-	0.09098	0.39647
22	1182	-71.0194	40.9890	080	04	0.470	426	154	2.112	1825	2065	649	-	0.06493	0.15867
22	1182	-71.0194	40.9890	090	04	0.580	551	125	2.196	1918	2275	812	-	0.12349	0.18506
22	1242	-71.0040	40.9639	001	02	0.071	053	053	1.000	1500	1500	-	0.01642	-	-
22	1242	-71.0040	40.9639	020	02	0.260	215	161	1.753	1656	1712	423	-	0.01905	0.21069
22	1242	-71.0040	40.9639	070	04	0.312	264	049	1.964	1699	1898	528	-	0.07685	0.32696
22	1242	-71.0040	40.9639	080	04	0.470	428	164	2.116	1833	2074	656	-	0.06336	0.15102
22	1242	-71.0040	40.9639	090	04	0.600	577	148	2.202	1942	2292	825	-	0.11758	0.17052
22	1302	-70.9893	40.9386	001	02	0.072	053	053	1.000	1500	1500	-	0.02031	-	-
22	1302	-70.9893	40.9386	020	02	0.267	220	166	1.749	1654	1708	421	-	0.04753	0.54013
22	1302	-70.9893	40.9386	070	04	0.310	261	040	1.962	1689	1896	526	-	0.09897	0.42444
22	1302	-70.9893	40.9386	080	04	0.480	436	175	2.113	1831	2066	650	-	0.07543	0.18382
22	1302	-70.9893	40.9386	090	04	0.610	586	149	2.203	1940	2296	828	-	0.02376	0.03420
22	1302	-70.9893	40.9386	105	04	0.618	595	009	2.250	1947	2424	928	-	0.01955	0.02256
22	1362	-70.9747	40.9128	001	02	0.073	054	054	1.000	1500	1500	-	0.02491	-	-

Table 3: Example of Gridded Geoacoustic Database

Latitude (degrees): 40.500000
Longitude (degrees): -71.000000

Layer No.	Surface (Age)	Sed. Type	Travel Time (sec)	Depth (m)	Thick-ness (m)	Density (gm/cc)	Velocity RMS (m/s)	Velocity P-Wave (m/s)	Velocity S-Wave (m/s)	Atten. Surface	Atten. P-Wave (db/m-kHz)	Atten S-Wave
001	Seafloor	02	0.106	79	79	1.000	1500	1500	-	0.021	-	-
020	Base Quaternary	02	0.240	189	110	1.676	1581	1644	384	-	0.036	0.665
045	Base Mid Miocene	02	0.342	280	91	1.840	1646	1788	462	-	0.078	0.545
070	Base Tertiary	02	0.420	354	73	1.945	1692	1881	517	-	0.176	0.802
080	Base Campanian	02	0.671	619	264	2.133	1861	2115	691	-	0.167	0.358
090	Base Coniacian	02	0.982	1000	381	2.259	2065	2447	947	-	0.013	0.015
105	Base Aptian	02	1.126	1202	201	2.378	2175	2815	1234	-	0.010	0.007
140	Base Kimmeridgian	02	1.159	1252	49	2.431	2203	3007	1383	-	0.010	0.006
190	Base Aalenian	02	2.977	5238	3984	2.641	3690	4382	2456	-	0.010	0.003

Latitude (degrees): 40.583333
Longitude (degrees): -71.000000

Layer No.	Surface (Age)	Sed. type	Travel Time (sec)	Depth (m)	Thick-ness (m)	Density (gm/cc)	Velocity RMS (m/s)	Velocity P-Wave (m/s)	Velocity S-Wave (m/s)	Atten. Surface	Atten. P-Wave (db/m-kHz)	Atten. S-Wave
001	Seafloor	02	0.094	70	70	1.000	1500	1500	-	0.022	-	-
020	Base Quaternary	02	0.240	192	121	1.698	1601	1663	401	-	0.078	1.235
045	Base mid Miocene	02	0.316	260	67	1.838	1647	1786	461	-	0.036	0.259
070	Base Tertiary	02	0.377	317	56	1.940	1686	1876	514	-	0.161	0.746
080	Base Campanian	02	0.610	562	245	2.131	1860	2111	687	-	0.158	0.341
090	Base Coniacian	02	0.886	898	336	2.253	2055	2430	933	-	0.015	0.017
105	Base Aptian	02	1.022	1085	186	2.358	2160	2749	1182	-	0.010	0.008
190	Base Aalenian	02	2.621	4462	3376	2.632	3563	4223	2331	-	0.010	0.003

Latitude (degrees): 40.666667
Longitude (degrees): -71.000000

Layer No.	Surface (Age)	Sed. Type	Travel Time (sec)	Depth (m)	Thick-ness (m)	Density (gm/cc)	Velocity RMS (m/s)	Velocity P-Wave (m/s)	Velocity S-Wave (m/s)	Atten. Surface	Atten. P-Wave (db/m-kHz)	Atten. S-Wave
001	Seafloor	02	0.084	63	63	1.000	1500	1500	-	0.020	-	-
020	Base Quaternary	02	0.242	195	132	1.717	1619	1680	409		0.052	0.727
045	Base mid Miocene	02	0.300	247	51	1.834	1652	1783	459	-	0.110	0.797
070	Base Tertiary	02	0.343	287	40	1.926	1680	1864	506	-	0.029	0.144
080	Base Campanian	02	0.559	514	226	2.127	1854	2100	678	-	0.082	0.182
090	Base Coniacian	02	0.796	798	284	2.239	2030	2393	904	-	0.087	0.105
105	Base Aptian	02	0.916	957	159	2.330	2122	2659	1112	-	0.010	0.008
190	Base Aalenian	02	2.274	3710	2753	2.618	3410	4053	2199	-	0.010	0.003

Latitude (degrees): 40.750000
Longitude (degrees): -71.000000

Layer No.	Surface (Age)	Sed. Type	Travel Time (sec)	Depth (m)	Thick-ness (m)	Density (gm/cc)	Velocity RMS (m/s)	Velocity P-Wave (m/s)	Velocity S-Wave (m/s)	Atten. Surface	Atten. P-Wave (db/m-kHz)	Atten. S-Wave
001	Seafloor	02	0.075	56	56	1.000	1500	1500	-	0.021	-	-
020	Base Quaternary	02	0.234	190	134	1.724	1628	1686	411	-	0.053	0.706
070	Base Tertiary	02	0.318	267	77	1.896	1686	1838	490	-	0.070	0.386
080	Base Campanian	02	0.513	469	201	2.116	1843	2075	657	-	0.068	0.163
090	Base Coniacian	02	0.719	710	241	2.218	1997	2335	860	-	0.092	0.123
105	Base Aptian	02	0.808	823	113	2.295	2065	2553	1030	-	0.012	0.011
190	Base Aalenian	02	1.936	3009	2186	2.599	3246	3876	2061	-	0.010	0.004

Seismiostratigraphy

The acoustic units incorporated into the geoacoustic database are seismostratigraphic units defined by Poag (1982, 1985a,b, 1987, 1991, 1992; Schlee and others, 1985; Poag and Valentine, 1988; Poag and Ward, 1993) for the U.S. Atlantic margin. This comprehensive division of stratigraphic units has been developed from a seismostratigraphic analysis of seismic profiles on our multichannel seismic grid (Figure 2). This seismostratigraphy has been calibrated with biostratigraphic data from the suite of industry drill wells onshore and offshore (Poag, 1982, 1985b, 1987, 1991, 1992; Poag and Ward, 1993) plus dredge sample data from canyons that dissect the continental slope (Valentine, 1981) and the Blake Escarpment (Dillon and Popenoe, 1988). The two-way travel times to each reflector (sea surface to reflector to sea surface) were digitized along the length of each seismic-reflection profile, creating a seismostratigraphic cross section of time depth vs distance. As mentioned above, these reflectors represent the base of geologic units. Where reflectors intersect, only the youngest reflector is entered into the database. The reflector numbers used in the database are purely arbitrary and are given here to facilitate labelling of computer plots of seismostratigraphic cross sections. Ages assigned to the geologic units are based on the DNAG geologic timescale of Palmer (1983).

Table 4: U.S. Atlantic Margin Seismostratigraphy

Refl.No.*	Geologic Surface	Reflector Name**
1	Base of water column - seafloor	seafloor
20	Base Quaternary	
30	Base Pliocene	
40	Base Upper Miocene	
45	Base Middle Miocene	Mid-Miocene Unconformity
50	Base Lower Miocene	
60	Base Upper Oligocene	Mid-Oligocene Unconformity
70	Base Tertiary	Top Cretaceous
80	Base Campanian/Maastrichtian	Horizon A* in Deep Sea
90	Base Coniacian/Santonian	Late Cenomanian Unconformity
100	Base Cenomanian/Turonian	Mid Cretaceous Unconformity
105	Base Aptian/Albian	
110	Base Barremian	Horizon ß in Deep Sea
120	Base Berriasian/Hauterivian	Top Jurassic
130	Base Tithonian	
140	Base Kimmeridgian	
150	Base Oxfordian	Top Middle Jurassic
170	Base Upper Bathonian/Callovian	
180	Base Bajocian/Lower Bathonian	
190	Base Aalenian	Postrift Unconformity
230	Base synrift sediments	Crystalline basement
300	Base of crust	Moho

* Numbers have no geologic significance and are used only as a tag in the digital database. They correspond to the same geologic horizons throughout the data set.

** Names more commonly used in literature than those in the geologic surface column.

Sediment Types and Lithologies

Lithologies vary within these units as indicated in the database. The gross lithologies of stratigraphic units have been determined from lithologic logs at drill holes and dredge samples from submarine canyons that cut deep into the continental slope integrated with the analysis of acoustic character on seismic profiles in our multichannel seismic grid (Poag, 1982, 1985b, 1987, 1991, 1992; Poag and Ward, 1993). This technique is based on the association of distinctive acoustic signatures with specific depositional environments and lithologies (Vail and others, 1977; Poag and Schlee, 1984; Van Wagoner and others, 1988). The resulting estimates of sediment types are very subjective, therefore, only a small set of lithologies has been incorporated into the database (Table 5). There are few surface samples in deep water seaward of the shelf edge and this region has been assigned a general type of clay ($k_0 = 0.045$).

Table 5: General Lithologic Types Identified on the U.S. Atlantic Margin

Rock Type	Numerical Code in Database
Silt/Sand	02
Clay/Shale	03/04
Chalk/Limestone	06/08
Dolomite	10
Halite + Anhydrite	12
Halite	14

* Rock types are in approximate increasing grain size or proximity to siliciclastic sediment sources

Surficial sediment types (Table 6, Figure 11) along individual seismic lines and on the database grid were extracted from a digital database of over 40 years of surficial sampling compiled by Hathaway and others (1994). This compilation is based on the original work of Hathaway (1971), Schlee (1973), Hathaway and others (1979) and an updated study by Poppe and others (1989) mapping surficial sediment types on the U.S. Atlantic continental margin. The database of surficial sediment types is based on grain size analyses which are used to define sediment types by standard definitions of grain size for specific sediment types. These grain sizes have been correlated with the near-surface attenuation of compressional waves (k_0).

Table 6: Surficial Sediment Types and Surface Attenuation

Sediment Type*	Phi Class	Grain Size (mm)	Surface Attenuation (k_0)**
Coarse Sand	<1	>0.5	0.005
Medium Sand	<2	0.25-0.5	0.010
Fine Sand	<3	0.125-0.25	0.015
Sandy Silt	<4	0.0625-0.125	0.020
Silty Sand	<5	0.0312-0.0625	0.025
Silt	<6	0.0156-0.0312	0.030
Silty Clay	<7	0.0078-0.0156	0.035
Clayey Silt	<8	0.0039-0.0078	0.040
Clay	<9	0.00195-0.0039	0.045

* Sediment types arranged by decreasing grain size

** k_0 values are compressional-wave surface attenuation in dB/m-kHz where $\alpha = k_0 f^m$ based on the Biot-Stoll model and applicable only below 1 kHz (Stoll,1985)

Seismic Velocities

Velocity data for the northern U.S. Atlantic margin (Baltimore Canyon Trough, Long Island Platform, and Georges Bank Basin regions) are derived from the stacking velocities determined for the multichannel seismic profiles as part of the standard industry processing of seismic-reflection data. The velocity data for our grid of seismic profiles were calibrated at a suite of drill sites in each area, along three standard dip-line transects and on a strike-line transect (Figure 2). Local velocity calibration studies were undertaken along composite seismic profiles connecting industry wells in Georges Bank Basin (Composite CDP Line G1-G2) and in the Baltimore Canyon Trough (USGS CDP lines 14 and 15). One transect crosses Georges Bank Basin (USGS CDP Line 19), one crosses the central Baltimore Canyon Trough (USGS CDP Line 25), and a third goes through a navy test area south of Long Island (USGS CDP Line 22). USGS CDP Line 12 has been used to construct a velocity-structure profile that links these velocity calibration sites with the rest of the seismic grid. Figure 12 is an example of the stratigraphic and interval-velocity data along a seismic line (Line G1-G2). A comprehensive discussion of the velocity data used in this database is given by Klitgord and Schneider (1994).

Data Gridding and Contouring

The areal digital database was created from gridded data based on the two-way travel time to individual reflectors, thickness of units in time, and interval velocities of these units. The skewed data spacing of dense data along widely-spaced seismic lines is not ideal for creating a gridded data set and unrealistic gridded and contoured data can easily result. The character of the resulting data is highly dependent upon the gridding technique used. In many cases, the results are not "right" or "wrong" but merely reflect the representation of the data given the assumptions built into the particular technique. The closely-spaced stratigraphic data were initially smoothed to the velocity data spacing shown in Figure 7 to reduce aliasing in the gridding stage. A minimum-curvature cubic-spline technique (Smith and Wessel, 1990) with a tension of zero was used on the data displayed in Appendix 3 to create a 5-minute grid of data. The resultant "scalloped" character of the contoured data displayed in Appendices 4 to 7 is an artifact of the minimum curvature assumption. No additional data constraints, based on assumed distributions of the data between seismic lines, have been added to the data. This would have "improved" the appearance of the contoured data, but it also would have given the false impression of better control than exists.

Data Masks

The information portrayed in Appendices 4 to 8 for the individual surfaces or units have regions where the data are missing or unknown. Regions of missing data are where erosion has removed the unit, or perhaps it was never deposited. The units have zero thickness in these regions, which are indicated by shaded regions without contours. If an erosional unconformity has cut deep enough to remove an underlying horizon in a given region, that surface contour map (Appendices 4 and 5) has a shaded zone with no contours where the horizon is missing. This masking is consistent with the database construction used here, where surfaces refer to the bottom of units that exist. We have not attempted to construct composite surfaces that go across the entire margin, although this can be done with the information available in the digital database. There also are narrow zones within and beneath the carbonate bank shelf edge platform where the geoacoustic information is unknown. These zones are indicated by the blank region on all of the maps for units and surfaces below horizon 120.

Geological Influences on Geoacoustic Parameters

Variations in geoacoustic properties on the margin are caused by a general increase in density that results from an increasing depth of burial, by changes in the lithologies within and between the stratigraphic units, and by surficial and buried structures. The subdivision of the sedimentary wedge into a series of acoustic units separated by horizons or unconformities enables us to incorporate most of these variations into the database. The influence of depth of burial on interval velocities can be readily seen on all of the profiles in Appendix 3. Both these cross sections (top profiles in Appendix 3) and the depth-to-surface maps (Appendices 4 and 5) show the gradual seaward deepening of stratigraphic units beneath the shelf. The gradual increase in interval velocity across the shelf (see lower profiles in Appendix 3 and interval-velocity contour maps in Appendix 7) are partially caused by the change in lithology from sandstone and shale to limestone and dolomite (lithologic maps in Appendix 8), but the primary cause is the increasing depth of burial.

Sedimentary structures, such as the carbonate shelf edge, prograding deltas, fans, salt diapirs, and rift basins, create a distinct velocity structure that may be faster or slower than adjacent sedimentary units and often more opaque to acoustic transmission. These features are incorporated into the database as general changes in lithologies (velocity), but they also could have significant influences on sound transmission because of their modes of construction. The chaotic character of the carbonate bank (Figure 5) creates an acoustic barrier that is difficult to penetrate with seismic techniques. As a result, the underlying units are usually masked on seismic-reflection data and we can say little about their acoustic properties. The blank areas near the shelf edge for units beneath the Upper Jurassic unit is caused by this acoustic masking. Attempts to see through this zone with larger offset receivers such as in the LASE experiment (Keen and others, 1986) have met with some success, but there is a significant loss in resolution and such experiments are very expensive. Prograding fans and deltas are particularly important geologic units in the Cretaceous and Tertiary sections of the margins (Figures 6 and 13)(Poag, 1992). On seismic lines (e.g., see the Tertiary section on Figure 6), the lobate shape of these fans and deltas creates a suite of undulating stratigraphic packets of coalescing sedimentary structures. Distinct lithologic variations associated with grain-size partitioning of sediment within a single delta or fan can create small, but distinctive velocity anomalies. The extensive fan/delta systems found in the upper 1 km of the sedimentary section on the northern U.S. shelf and rise make them some of the most important geologic features on the margin. Although these small variations can not be resolved in this data set, an understanding of the velocity structure of these systems represents an important objective of any high-resolution velocity study for acoustic transmission.

The modification of sedimentary units by erosion can significantly modify acoustic signatures. The erosion of the seaward edge of geologic units by fluctuations in sea level has created "holes" in the acoustic information for many of the Cretaceous and Tertiary units. On the shelf and rise, these erosional holes (indicated by masked regions on the maps in Appendices 4-8) are actually regions where significant lithologic discontinuities can exist. Causes of these discontinuities include the juxtaposition of younger, less lithified strata, over significantly older strata that was at one time buried to a greater depth. The unconformity can juxtapose units deposited in significantly different environments. Canyons cut into the continental slope create a chaotic pattern of steep-sided structures that can diffract substantial amounts of acoustic energy. This chaotic pattern results in a very low coherence in the RMS velocity analyses in this region and causes some of the scatter displayed on the contour maps. In general,

the continental slope (both past and present day) represents of zone of poorly defined acoustic character.

Faulting has deformed sedimentary units in two distinctive zones. The deep synrift sections are cut by numerous faults (Klitgord and others, 1988), but most of these sections are beneath the region of reliable velocity analyses for our data. In the shallower postrift sedimentary sections there are two sources of faulting. Failure under sediment loading has created a series of large faults near the shelf edge that parallel the margin (Figure 3). These faults are partially localized by load failure as the continental shelf edge prograded over the older continental slope. This set of faults has been called the Gemini Fault system by Poag (1985b, 1987; 1991). Faulting and uplift of sedimentary units are associated with the rise of salt diapirs and the intrusion of igneous bodies during the Mid-Cretaceous. The Schlee Dome in northern Baltimore Canyon Trough (Poag, 1987; Grow and others, 1988) is the largest of these intrusive features. There is extensive faulting along the southeastern edge of Georges Bank where the intrusive bodies did not rise as high into the sedimentary wedge, but the faulting around them does extend into the Upper Cretaceous section. This fracturing and subsequent crack-filling can significantly modify the local velocity structure. Such variations are below the resolution of this study, but shallow fault systems have the potential for distorting transmission paths.

Geoacoustic Database Displays

The digital geoacoustic database is portrayed in cross-section perspective on the seismic-reflection profiles in Appendix 3 and in map perspective in Appendices 4 to 8. The map perspectives are based on the information related to individual surfaces (horizons) or to the unit just above each surface (see Figures 9 and 10). Therefore, there is a separate map for each of the surfaces or units in the database (see Table 4) based on data from all of the seismic lines in Appendix 3.

Multichannel Seismic-Reflection Profiles (Appendix 3)

All of the seismic-reflection profiles used in this data set are included in Appendix 3. The locations of these lines are shown on Figures 3 and 7. Most of the profiles (lines 1-38, IPOD, and 77-1, 77-2) were acquired by commercial firms under contract to the U.S. Geological Survey (USGS) in the 1970's. Two lines (BGR-79-202 and 79-204) were acquired by the German Geological Survey as part of a cooperative with USGS. Detailed discussions of these seismic data and their stratigraphic analyses are given by Poag (1985b, 1987, 1991, 1992), Grow and others (1988), Sheridan and others (1988), and Schlee and Klitgord (1988). Line crossing and well-crossing locations are given in Appendix 1 and labelled across the top of each profile. The time section (two-way travel time vs shot point distance) and the interval velocities for each stratigraphic unit (vs shot point distance) on this time section are displayed for each of these lines. All dip sections are plotted from northwest to southeast. All strike sections are plotted from southwest to northeast. The corresponding reflector number for each horizon or unit (Table 4) is labelled at each end of the profiles and at appropriate locations along the profile. On each time section the upper-most reflector is the sea floor (reflector 1). The bottom-most labelled reflector varies across the margin, but on most profiles it is the postrift unconformity or oceanic basement. Stratigraphic units and structures beneath the postrift unconformity and faults are plotted, but not labelled on the profiles. There is no velocity information associated with these latter features, therefore, they have not been

incorporated into the digital database. The interval velocities have been smoothed, using a contouring technique described by Klitgord and Schneider (1994). The locations of original velocity information are indicated by the x's. The velocity profiles are plotted with increasing velocity values (in m/sec) going down. In this way, the relative positions of reflectors and the velocity curves associated with the unit above each reflector are the same; in general, the lowermost velocity curve (i.e., highest velocity) corresponds to the deepest numbered horizon in the time section.

Depth to Reflectors in Time (Appendix 4) and Distance (Appendix 5)

The contoured surface depths of individual reflectors (horizons), in seconds two-way travel time or in meters, portray the expected increasing depth to older reflectors at any given location. The areal variations in depth, however, are best seen on the depth in meters surfaces in Appendix 5. The distortion in two-way travel time surfaces (Appendix 4) caused by vertical variations in velocity creates a surface dominated by the shape of the sea floor. Two of the most distinctive characters of the surface contours in Appendix 5 are the shifts in the location (and vertical relief) of the continental slope and the more extensive erosion found in the Georges Bank and Long Island Platform regions relative to the Baltimore Canyon Trough. The shifts in the location of the shelf edge and changes in the depth of the continental rise relative to the shelf are a consequence of shifting sediment supply, sea-level variations and the effectiveness of the shelf-edge barrier trapping sediment on the shelf. The pattern of eroded units concentrated around Georges Bank is caused by: 1.) the basement hinge zone being farther offshore than in the region of the Baltimore Canyon Trough; 2.) the slower subsidence of the Georges Bank region relative to the Baltimore Canyon Trough; and 3.) a smaller terrigenous sediment supply to the Georges Bank region. Sediment distribution patterns onshore west of the Baltimore Canyon Trough (which is landward of the basement hinge zone) show thinning or absence of Jurassic units similar to that found on the Long Island Platform and along the northern edge of Georges Bank basin. The greater subsidence rate in the Baltimore Canyon Trough was probably caused by a combination of greater sediment influx (loading) (Poag, 1991) as well as a more extensive modification of the rift-stage crust (Klitgord and others, 1988). Because Georges Bank Basin had a slower subsidence rate than the Baltimore Canyon Trough (Sawyer and others, 1983), the sedimentary units on the shelf were thinner and more likely to be completely eroded by a drop in sea level. Several of the reflectors are found only in the centers of the two basins. This occurs because the depocenters also are the regions of greatest subsidence rate across the margin, and thus the most likely zone for preserving material during sea level falls.

Isopachs of Acoustic Units (Appendix 6)

Isopach maps of stratigraphic units in the database provide a much clearer image of the deposition and erosion patterns on the margin (Poag, 1991, 1992) than that provided by the depth maps (Appendices 4 and 5). These maps show that there is almost no Tertiary sediment on Georges Bank Basin, but extensive deposition on the adjacent continental rise; sediment was bypassing the bank. The Mid-Miocene was the only period of major Cenozoic sediment accumulation in the Baltimore Canyon Trough region. The Tertiary was, in general, a period of major sediment influx to the continental rise (Poag, 1992). In contrast, the Jurassic was a period of major accumulation on both the shelf and rise. The depocenters during the Cretaceous appear to have straddled the older continental slope, as extensive terrigenous material prograded over the older platform complex and filled the adjacent continental rise. The shelf-rise transition was more gradual at this time, with major deltas and fans covering the margin (e.g., Figure 12).

Interval Velocities (Appendix 7)

Interval velocity patterns are dominated by the depth of burial influence mentioned previously. There are general velocity increases across the margin as well as smaller wavelength changes along the margin. The latter features correspond to major fans or deltas. Of note are the similar velocities in both Georges Bank Basin and Baltimore Canyon Trough for the Middle Jurassic deposits, despite the considerably greater depth of the Baltimore Canyon Trough units. This similarity may be a result of the sediments reaching a limit to their density increase at low temperatures or may be caused by the higher dolomite and anhydrite content in the lower section of the Georges Bank Basin. These maps also reaffirm the observation that on Georges Bank there are higher velocity sedimentary units at shallow depth than to the south.

Sediment Types (Appendix 8)

The sediment types for the various units are estimates based on the limited distribution of subsurface samples and seismic character evaluations (Poag, 1982, 1985b, 1991, 1992). Terrigenous fluxes of sand (s), sand and silt (s/s) and clay (c) dominate the Tertiary, with a minor phase of carbonate (carb) along the outer shelf during the early Tertiary. A similar pattern dominates the Cretaceous, with more extensive deep sea shales (sh) forming during the mid-Cretaceous. The Jurassic shelf edge is dominated by limestone accumulation from active shelf-edge reefs. Sand and silt filled the shelf behind the reef while pelagic shale mixed with lobes of terrigenous sands formed the continental rise. Changes in the upland sources of sediment caused along-shelf variations in sediment type (from sand/silt to clay), as the locus of delta and fan formation shifted (Poag and Sevon, 1989).

Summary:

The geoacoustic database constructed from multichannel seismic-reflection profiles and well data on the northern U.S. Atlantic margin provides the ability to investigate the three-dimensional acoustic character of the continental margin and its variation since the Middle Jurassic (187 m.a.). Both the isopach and interval-velocity patterns for individual acoustic units incorporated into this database display variations reflecting the depositional and erosional history of the margin and the distribution of major sedimentary features such as deltas, fans, and a carbonate-bank, shelf-edge platform. Geoacoustic consequences of the stratigraphic and velocity patterns incorporated in the database include:

1.) A general monotonic increase in velocities with depth on all parts of the margin. The increase in depth to reflectors and increasing overburden of geologic units creates a general increase in V_{rms}, V_i, V_s, and ρ across the shelf to the continental slope. Velocity inversions are known to exist from well log data (Klitgord and Schneider, 1994), but they can not be resolved with the multichannel seismic data used in this study.

2.) The erosion of portions of geologic units can cause some abrupt changes in transmission properties, bringing lower-velocity units into direct contact with higher-velocity units. This phenomenon will influence the refracted seismic energy in terms of abrupt changes in distant arrival times and the reflected seismic signal in terms of abrupt increases in reflected energy amplitudes. The presence of relatively high-velocity material at a shallow depth (<500 m) just south of Long Island is a consequence of either erosion or nondeposition of Tertiary material in the Long Island Platform and Georges Bank regions.

3.) Prograding deltas, overlapping fans, and faulting associated with mega-slumping at the shelf edge represent a set of geologic features in the upper sedimentary wedge of the margin (<1000 m) that may have a significant influence on acoustic transmission patterns.

Acknowledgements

This project was supported by the U.S. Naval Oceanographic Office. We gratefully acknowledge discussions and collaboration with Dr. Rudi Markl, the Naval Oceanographic Office's project manager during most of this work and P. Schexnayder, program manager during the early stages of the project, and thank Dr. M. Head, R. Hecht, and G. Michel, all of the Naval Oceanographic Office, for their support and technical assistance. Numerous discussions and detailed reviews by R. Markl, D. Hutchinson, and P. Popenoe have led to significant improvements in this study. D. Hutchinson provided the shot-gather refraction data along seismic line 22. Technical support from L. Morse, J. Taylor, K. Delorey, D. Senske, S. Harrison and E. Wright, all of the U.S. Geological Survey, is gratefully acknowledged. The seismic data-analysis system developed by E.Wright and the GMT data management system developed by Wessel and Smith (1991) were used in this project to construct the digital database and graphic output.

REFERENCES

Amato, R.V., and Bebout, J.W., eds., 1980, Geologic and operational summary, COST No. G-1 well, Georges Bank area, North Atlantic OCS: U.S. Geological Survey Open File Report 80-268, 117p.

Amato, R.V., and Simonis, E.K., eds., 1980, Geologic and operational summary, COST No. G-2 well, Georges Bank area, North Atlantic OCS: U.S. Geological Survey Open File Report 80-269, 120p.

Castagna, J.P., Batzle, M.L., and Eastwood, R.L., 1985, Relationships between compressional-wave and shear-wave velocities in clastic silicate rocks: Geophysics, v.50, p. 571-581.

Dillon, W.P., and Popenoe, P., 1988, The Blake Plateau Basin and Carolina Trough, *in* Sheridan, R.S., and Grow, J.A., eds.: The Atlantic Continental Margin, U.S., The Geology of North America, v. I-2, Geological Society of America, p. 291-328.

Grow, J.A., Klitgord, K.D., and Schlee, J.S., 1988, Structural and evolution of the Baltimore Canyon Trough, *in* Sheridan, R.S. and Grow, J.A., eds., The Atlantic Continental Margin, U.S., The Geology of North America, v. I-2, Geological Society of America, p. 269-290.

Hamilton, E.L., 1976a, Sound attenuation as a function of depth in the sea floor: Journal of the Acoustical Society of America, v. 59, no. 3, p. 528-535.

Hamilton, E.L., 1976b, Attenuation of shear waves in marine sediments: Journal of the Acoustical Society of America, v. 60, no. 2, p. 334-338.

Hamilton, E.L., 1978, Sound velocity-density relations in sea-floor sediments and rocks: Journal of the Acoustical Society of America: v. 63, no. 2, p. 366-377.

Hamilton, E.L., 1979, V_p/V_s and Poisson's ratios in marine sediments and rocks: Journal of the Acoustical Society of America, v. 66, no. 4, p. 1093-1101.

Hamilton, E.L., 1980, Geoacoustic modeling of the sea floor: Journal of the Acoustical Society of America, v. 68, no. 5, p. 1313-1340.

Hamilton, E.L., and Bachman, R.T., 1982, Sound velocity and related properties of marine sediments: Journal of the Acoustical Society of America, v. 72, no. 6, p. 1891-1904.

Hathaway, J.C., 1971, Data file - continental margin program Atlantic coast of the United States Vol. 2 - Sample collection and analytical data: Woods Hole Oceanographic Institution Ref. No. 71-15, 496 p.

Hathaway, J.C., Poag, C.W., Valentine, P.C., Miller, R.E., Schultz, D.M., Manheim, F.T., Kohout, F.A., Bothner, M.H., and Sangrey, D.A., 1979, U.S. Geological Survey core drilling on the Atlantic shelf: Sciences, v. 206, p. 515-527.

Hathaway, J.C., and others, 1994, Digital data base of surficial sediments on U.S. Atlantic Margin, USGS Open File Report, in review.

Keen, C., and others, 1986, Deep structure of the US East Coast passive margin from large aperture seismic experiments (LASE): Marine and Petroleum Geology, v. 3, p. 234-242.

Klitgord, K.D., and Grow, J.A., 1980, Jurassic seismic stratigraphy and basement structure of western Atlantic magnetic quiet zone: American Association of Petroleum Geologists Bulletin, v. 64, p. 1658-1680.

Klitgord, K.D., and Schneider, C.M., 1994, Geophysical database of the East Coast of the United States: Northern Atlantic margin: Velocity Analyses: U.S. Geological Survey Open File Report OF94-192, 74 pp.

Klitgord, K.D., Hutchinson, D.R., and Schouten, H., 1988, U.S. Atlantic continental margin; Structural and tectonic framework, *in* Sheridan, R.S., and Grow, J.A., eds., The Atlantic Continental Margin, U.S., The Geology of North America, v. I-2, Geological Society of America, p. 19-55.

Manspeizer, W., DeBoer, J., Costain, J.K., Froelich, A.J., Coruh, C., Olsen, P.E., McHone, G., Puffer, J.H., and Prowell, D.C., 1989, Post-Paleozoic activity, *in* Hatcher, R.D., Jr., Thomas, W.A., and Viele, G.W., eds, The Appalachian-Oachita Orogen in the United States: Geological Society of America, The Gology of North America, v. F-2, p. 319-374.

Mitchell, S.K., and Focke, K.C., 1980, New measurements of compressional wave attenuation in deep ocean sediments, Journal of Acoustic Society of America, v. 67, no. 5, p. 1582-1589.

Olsson, R.K., Gibson, T.G., Hansen, H.J., and Owens, J.P., 1988, Geology of the northern Atlantic coastal plain: Long Island to Virginia, *in* Sheridan, R.S. and Grow, J.A., eds., The Atlantic Continental Margin, U.S., The Geology of North America, Vol. I-2, Geological Society of America, p. 87-105.

Palmer, A.W., 1983, The Decade of North American Geology 1983 geologic timescale: Geology, v. 11, p. 503-504.

Poag, C.W., 1982, Stratigraphic reference section for the Georges Bank Basin: depositional model for New England passive margin: American Association of Petroleum Geologists Bulletin, v. 66, p. 1021-1041.

Poag, C.W., ed., 1985a, Geologic Evolution of the United States Atlantic Margin: New York, Van Nostrand Reinhold Company, 385 p.

Poag, C.W., 1985b, Depositional history and stratigraphic reference section for central Baltimore Canyon Trough, in Poag, C.W.,ed., Geologic Evolution of the United States Atlantic Margin: p. 217-263.

Poag, C.W., 1987, The New Jersey Transect: Stratigraphic framework and depositional history of a sediment-rich passive margin, *in* Poag, C.W., Watts, A.B., and others, eds., Initial Reports of the Deep Sea Drilling Project, Volume 95: Washington, D.C., U.S. Government Printing Office, p. 763-817.

Poag, C.W., 1991, Rise and demise of the Bahama-Grand Banks gigaplatform, northern margin of the Jurassic proto-Atlantic seaway: Marine Geology, v. 102, p. 63-130.

Poag, C.W., 1992, U.S. middle Atlantic continental rise: provenance, dispersal and deposition of Jurassic to Quaternary sediments: *in* Poag, C.W., and de Graciansky, P.C., eds., Geological evolution of Atlantic continetal rises: New York, Van Nostrand Reinhold, p. 100-156.

Poag, C.W., and Schlee, J.S., 1984, Depositional sequences and stratigraphy gaps on submerged United States Atlantic margin, in Schlee, J.S., ed., Interregional Unconformities and Hydrocarbon Accumulation, The American Association of Petroleum Geologists Memoir 36, p. 165-182.

Poag, C.W., and Sevon, W.D., 1989, A record of Appalachian denudation in postrift Mesozoic and Cenozoic sedimentary deposits of the U.S. middle Atlantic continental margin: Geomorphology, v. 2, p. 119-157.

Poag, C.W., and Valentine, P., 1988, Mesozoic and Cenozoic stratigraphy of the United States Atlantic continental shelf and slope, *in* Sheridan, R.S. and Grow, J.A., eds., The Atlantic Continental Margin, U.S., The Geology of North America, Vol. I-2, Geological Society of America, p. 67-85.

Poag, C.W., and Ward, L.W., 1993, Allostratigraphy of the U.S. Middle Atlantic Continental Margin -- characteristics, distribution and depositional history of principal unconformity bounded Upper Cretaceous and Cenozoic sedimentary units: U.S. Geological Survey Professional Paper 1542, 81pp.

Poppe, L., Schlee, J.S., Butman, B., and Lane, C., 1989, Map showing distribution of surficial sediment, Gulf of Maine and Georges Bank: U.S. Geological Survey, MI Map I-1986-A.

Sawyer, D.S., Toksoz, M.N., Sclater, J.G., and Swift, B.A., 1983, Thermal evolution of the Baltimore Canyon Trough and Georges Bank Basin: American Association of Petroleum Geologists Memoir 34, p. 743-762.

Sheridan, R.A., Grow, J.A., Behrendt, J.C., and Bayer, K.C., 1979, Seismic refraction study of the continental edge off the eastern United States: Tectonophysics, v. 59, p. 1-26.

Sheridan, R.A., and Grow, J.A., 1988, The Atlantic Continental Margin, U.S.: The Geology of North America, Vol. I-2, Geological Society of America, 610p.

Sheridan, R.A., Grow, J.A., and Klitgord, K.D., 1988, Geophysical data, *in* Sheridan, R.S., and Grow, J.A., eds., The Atlantic Continental Margin, U.S., The Geology of North America, v. I-2, Geological Society of America, p. 177-196.

Sheridan, R.E., Olsson, R.K., and Miller, J.J., 1991, Seismic reflection and gravity study of proposed Taconic suture under the New Jersey Coastal Plain: Geological Society of America Bulletin, v. 103, p. 402-414.

Schlee, J., 1973, Atlantic Continental Shelf and Slope of the United States -- Sediment Texture of the Northeastern Part, USGS Professional Paper 529-L.

Schlee, J.S., and Klitgord, K.D., 1986, Structure of the North American Atlantic continental margin: Journal of Geological Education, v. 34, p. 72-89.

Schlee, J.S., and Klitgord, K.D., 1988, Georges Bank Basin - A regional synthesis, *in* Sheridan, R.S., and Grow, J.A., eds., The Atlantic Continental Margin, U.S., The Geology of North America, v. I-2, Geological Society of America, p. 243-268.

Schlee, J.S., ed., 1984, Interregional Unconformities and Hydrocarbon Accumulation, American Association of Petroleum Geologists Memoir 36.

Schlee, J., Poag, C.W., and Hinz, C., 1985, Seismic stratigraphy of the continental slope and rise seaward of Georges Bank, in Poag, C.W., ed., Geologic Evolution of the United States Atlantic Margin: New York, Van Nostrand Reinhold Company, p. 265-292.

Scholle, P.A., ed., 1977, Geological studies on the COST No. B-2 well, U.S. mid-Atlantic outer continental shelf area: U.S. Geological Survey Circular 750.

Scholle, P.A., and Wenkam, C.R., eds., 1982, Geological studies of the COST Nos. G-1 and G-2 wells, United States North Atlantic outer continental shelf: U.S. Geological Survey Circular 861, 193p.

Smith, W.H.F., and Wessel, P., 1990, Gridding with continuous curvature splines in tension: Geophysics, v. 55, p. 293-305.

Stoll, R.D., 1980, Theoretical aspects of sound transmission in sediments: Journal of Acoustic Society of America, v. 68, p. 1341-1350.

Stoll, R.D., 1985, Acoustic waves in ocean sediments: Geophysics, v. 42, p. 715-725.

Tucholke, B.E., and Mountain, G.M., 1979, Seismic stratigraphy, lithostratigraphy and paleosedimentation patterns in the North American Basin, *in* Talwani, M., Hay, W., and Ryan, W.B.F., eds., Deep drilling results in the Atlantic Ocean: continetal margins and paleoenvironment: Maurice Ewing Series 3, American Geophysical Union, p. 58-86.

Vail, P.R, Mitchum, R.M., Jr., Todd, R.G., Widmier, J.M., Thompson III, S., Sangree, J.B., Bubb, J. N., and Hatlelid, W.G., 1977. Seismic stratigraphy and global changes of sea level, *in* Payton, C.E., ed., Seismic stratigraphy; Applications to hydrocarbon exploration: American Association of Petroleum Geologists Memoir 26, p. 49-212.

Valentine, P.C., 1981, Continental margin stratigraphy along the U.S. Geological Survey Seismic line 5 -- Long Island Platform and western Georges Bank Basin: U.S. Geological Survey Miscellaneous Field Studies Map MF-857, 2 sheets.

Van Wagoner, J.C., Posamentier, H.W., Mitchum, R.M., Vail, P.R., Sarg, J.D., Loutit, T.S., and Hardenbol, J., 1988, An overview of the fundamentals of sequence stratigraphy and key definitions, *in* Wilgus, C.K., and others, eds., Sea-level changes: An integrated approach: Society of Economic Paleontologists and Mineralogists Special Publication 42, p. 39-45.

Wessel, P., and Smith, W.H.F., 1991, Free software helps map and display data: EOS, Transactions of the American Geophysical Union, v. 72, pp. 441, 445-446.

Figure Captions

Figure 1: General geologic features on the U.S. Atlantic continental margin. Major sedimentary basins and intervening basement platforms offshore are indicated. Grid of multichannel seismic-reflection profiles is shown.

Figure 2: Multichannel seismic-reflection profile grid used in the construction of this geoacoustic database superimposed on bathymetric contour map of the northern U.S. Atlantic Continental Margin. Heavier weight lines indicate seismic-reflection profiles used as primary stratigraphic and velocity calibration lines for this study (USGS CDP Lines 12, 14, 15, 19, 22, and 25). G-1 and G-2 refer to the ends of the composite seismic line connecting the COST G-1 and COST G-2 wells.

Figure 3: General geologic features across the U.S. Atlantic margin based on seismic-reflection profile USGS CDP Lines 19, 25, and 28 (from Klitgord et al., 1988, Fig. 4). Note the location of the basement hinge zone, the Jurassic carbonate-bank paleoshelf edge, and major faults within the Cretaceous and Jurassic sections in the vicinity of the paleoshelf edge. Shading has been used to distinguish the different age sedimentary units across the margin. T=Tertiary, UK=Upper Cretaceous; LK=Lower Cretaceous; UJ=Upper Jurassic; MJ=Middle Jurassic. Small dash pattern on landward side of profiles represents continental crust. Oceanic crust underlies the surface labelled oceanic basement. From Klitgord and others (1988, Fig. 3).

Figure 4: A segment of USGS seismic line 19 across Georges Bank. A.) A simplified lithologic log of the COST G-2 well to a depth of 6,667 m (21,873 ft) has been projected onto the line of section from 12 km to the southwest. The arrows outline horizons along which reflections are terminated by truncation, downlap, or onlap; wavy lines indicate unconformities in hole. Such features are used to identify depositional environment and the influence of fluctuating sea-level and sea-floor depth on margin construction. B.) Ages of seismostratigraphic units and their bounding unconformities (heavy lines) on the same line section. The ages of the gaps older than Late Cretaceous were inferred by matching the horizons along which reflections were terminated. From Poag and Schlee (1984, Figs. 6 and 7).

Figure 5: A segment of USGS seismic line 6 across the outer edge of the Baltimore Canyon Trough showing the carbonate shelf-edge platform. Projected locations of exploration wells by Shell Oil Co. that drilled into the carbonate complex are indicated. A, A^*, and β refer to Cretaceous unconformities. OLIGO = Oligocene, CENOM> = Cenomanian; APT = Aptian; UJ = Upper Jurassic. From Schlee and Klitgord (1986, Fig. 10).

Figure 6: A segment of USGS seismic line 18 across the continental rise east of Georges Bank. Stratigraphic units labelled as in Table 4. A^u = Oligocene unconformity; T/K = Tertiary-Cretaceous boundary; β = top of Neocomian limestone unit; J_1 = top of Jurassic; J_2 = top of Middle Jurassic. From Klitgord and others (1988, Fig. 9a).

Figure 7: Location of velocity data points along the grid of multichannel seismic-reflection profiles used in this database. Seismic line numbers are indicated and cross sections are included in Appendix 3.

Figure 8: Location of 5-minute grid points for digital database of acoustic parameters.

Figure 9: Diagrammatic representation of the geometry of geologic features in the geoacoustic database. Parameters *X(n)* in Table 1 refer to either properties of the unit directly above reflector n or properties of the entire section between the sea surface (z=0) and the reflector n. A.) Time section. B.) Depth section.

Figure 10: Diagram portraying the nomenclature for acoustic reflectors used in this geoacoustic database based on the tags using the base of units. Note for example that the top of the Maastrichtian unit is reflector 70, then reflector 60 and then again reflector 70 whereas reflector 60 is always the base of the Upper Oligocene.

Figure 11: Surface attenuation (k_0) based on surface sediment type (Table 6) derived from the digital database of Hathaway and others (1994). Contour interval is 0.005 units. Plus symbol indicates location of data samples. Region seaward of the shelf edge where there are few samples has been assigned a general value of 0.045 for clay.

Figure 12: Composite CDP seismic line G1-G2 in Georges Bank Basin used to calibrate seismic-reflection profiles with COST Wells G-1 and G-2. A.) Time depth of acoustic reflectors in digital database (in seconds two-way travel time) vs distance (shot points). B.) Interval velocities (m/s) of units just above acoustic reflectors in Figure 11A vs distance (shot points). Shot point spacing is 100m. See Figure 2 for location.

Figure 13: Example of depositional features within a stratigraphic unit in this database. The sediment isochron map (in sec) for the Aptian-Albian unit corresponds to the stratigraphic unit between reflectors 100 and 105 (Table 4). Solid arrows indicate inferred primary routes of sediment dispersal: dashed arrows indicate secondary routes. Diagonal hachures indicate unite absent or too thin to resolve on seismic profiles. The major deltas on the shelf and fans in the slope-rise region are indicated. Shaded contour interval (0.0-0.1 sec) indicates thinnest parts of unit. Heavy dotted line indicates possible axis of eroding bottom current. J = ancient James River; P = ancient Potomac River; S = ancient Susquehanna River; D = ancient Delaware River; H = ancient Hudson River; C = ancient Connecticut River; EM = ancient river(s) in eastern Massachusetts; CF = confluent fan. From Poag (1992; Fig. 6-19).

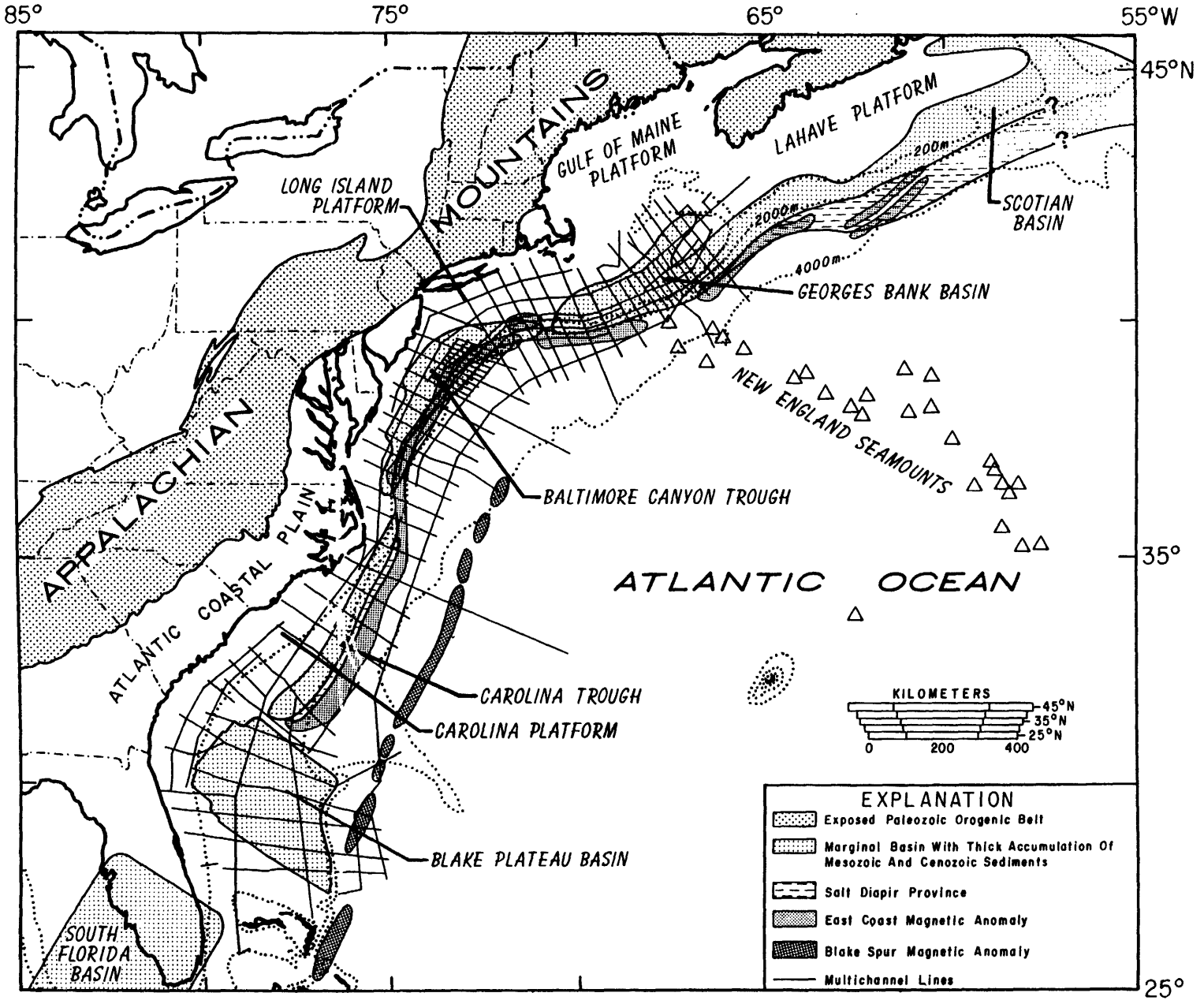
85°
75°
65°
55°W
45°N
35°
25°
APPALACHIAN MOUNTAINS
ATLANTIC COASTAL PLAIN
LONG ISLAND PLATFORM
GULF OF MAINE PLATFORM
LAHAVE PLATFORM
SCOTIAN BASIN
200m
2000m
4000m
GEORGES BANK BASIN
NEW ENGLAND SEAMOUNTS
BALTIMORE CANYON TROUGH
ATLANTIC OCEAN
CAROLINA TROUGH
CAROLINA PLATFORM
BLAKE PLATEAU BASIN
SOUTH FLORIDA BASIN
KILOMETERS
45°N
35°N
25°N
0
200
400
EXPLANATION
Exposed Paleozoic Orogenic Belt
Marginal Basin With Thick Accumulation Of Mesozoic And Cenozoic Sediments
Salt Diapir Province
East Coast Magnetic Anomaly
Blake Spur Magnetic Anomaly
Multichannel Lines

Figure 1

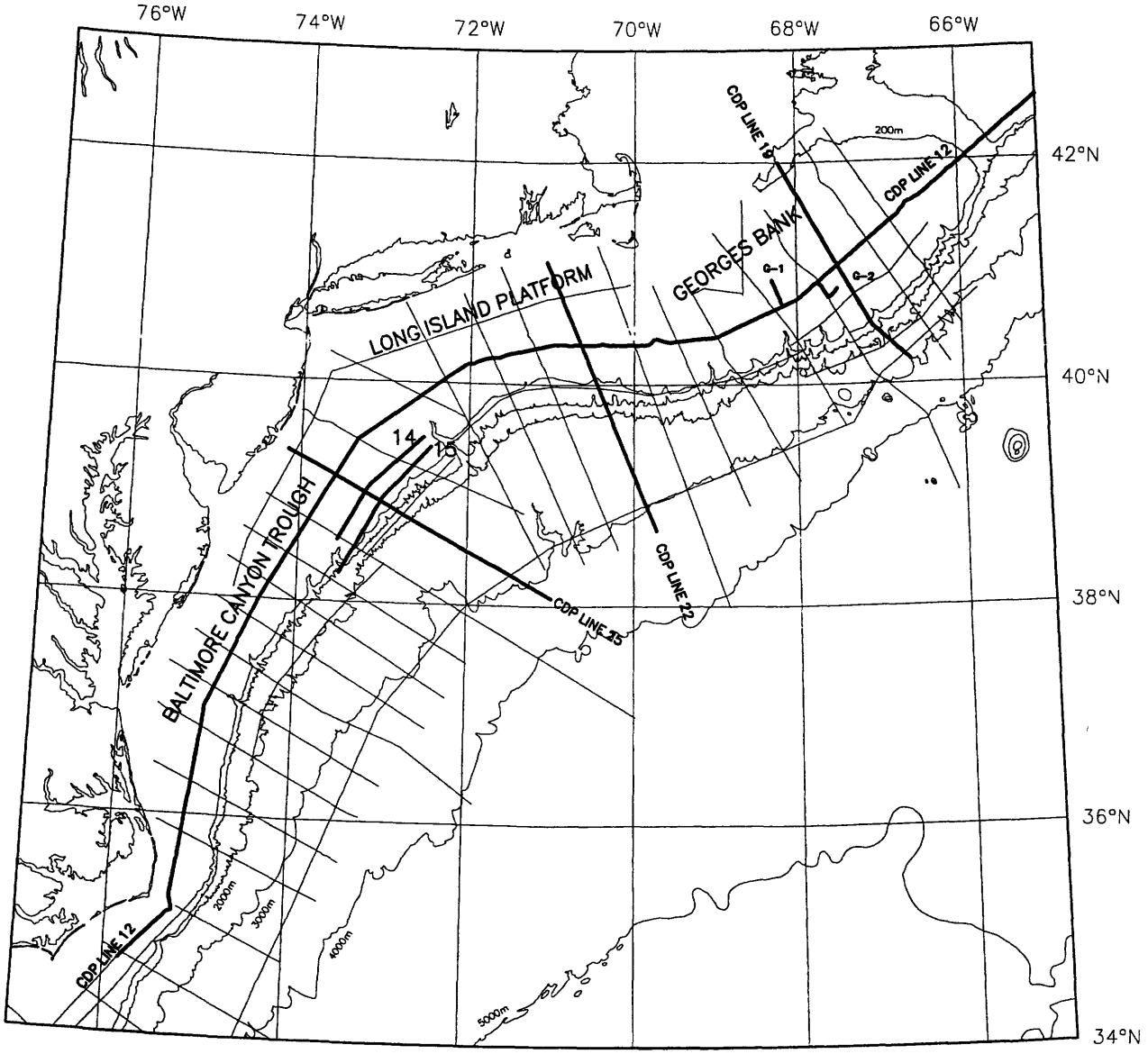
76°W
74°W
72°W
70°W
68°W
66°W
42°N
40°N
38°N
36°N
34°N
CDP LINE 19
CDP LINE 12
200m
GEORGES BANK
LONG ISLAND PLATFORM
14
15
BALTIMORE CANYON TROUGH
CDP LINE 22
CDP LINE 25
CDP LINE 12
2000m
3000m
4000m
5000m

Figure 2

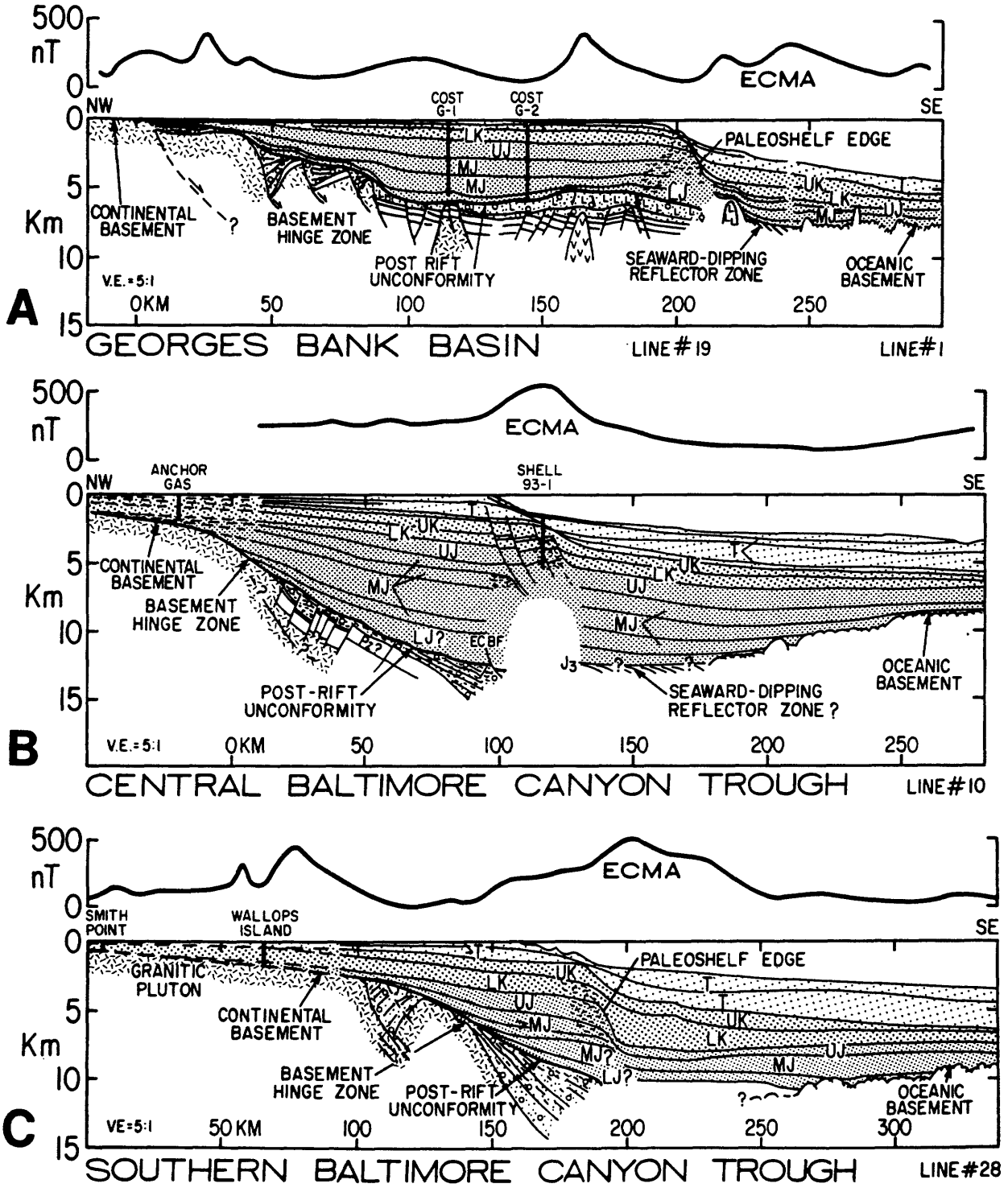
500
nT
0
ECMA
NW
SE
COST G-1
COST G-2
PALEOSHELF EDGE
LK
UJ
MJ
UK
LJ
CONTINENTAL BASEMENT
BASEMENT HINGE ZONE
POST RIFT UNCONFORMITY
SEAWARD-DIPPING REFLECTOR ZONE
OCEANIC BASEMENT
Km
V.E.=5:1
0KM
50
100
150
200
250
A
GEORGES BANK BASIN
LINE # 19
LINE#1
ANCHOR GAS
SHELL 93-1
ECBF
LJ?
J3
POST-RIFT UNCONFORMITY
SEAWARD-DIPPING REFLECTOR ZONE ?
B
CENTRAL BALTIMORE CANYON TROUGH
LINE#10
SMITH POINT
WALLOPS ISLAND
GRANITIC PLUTON
MJ?
LJ?
VE=5:1
50 KM
300
C
SOUTHERN BALTIMORE CANYON TROUGH
LINE#28

Figure 3

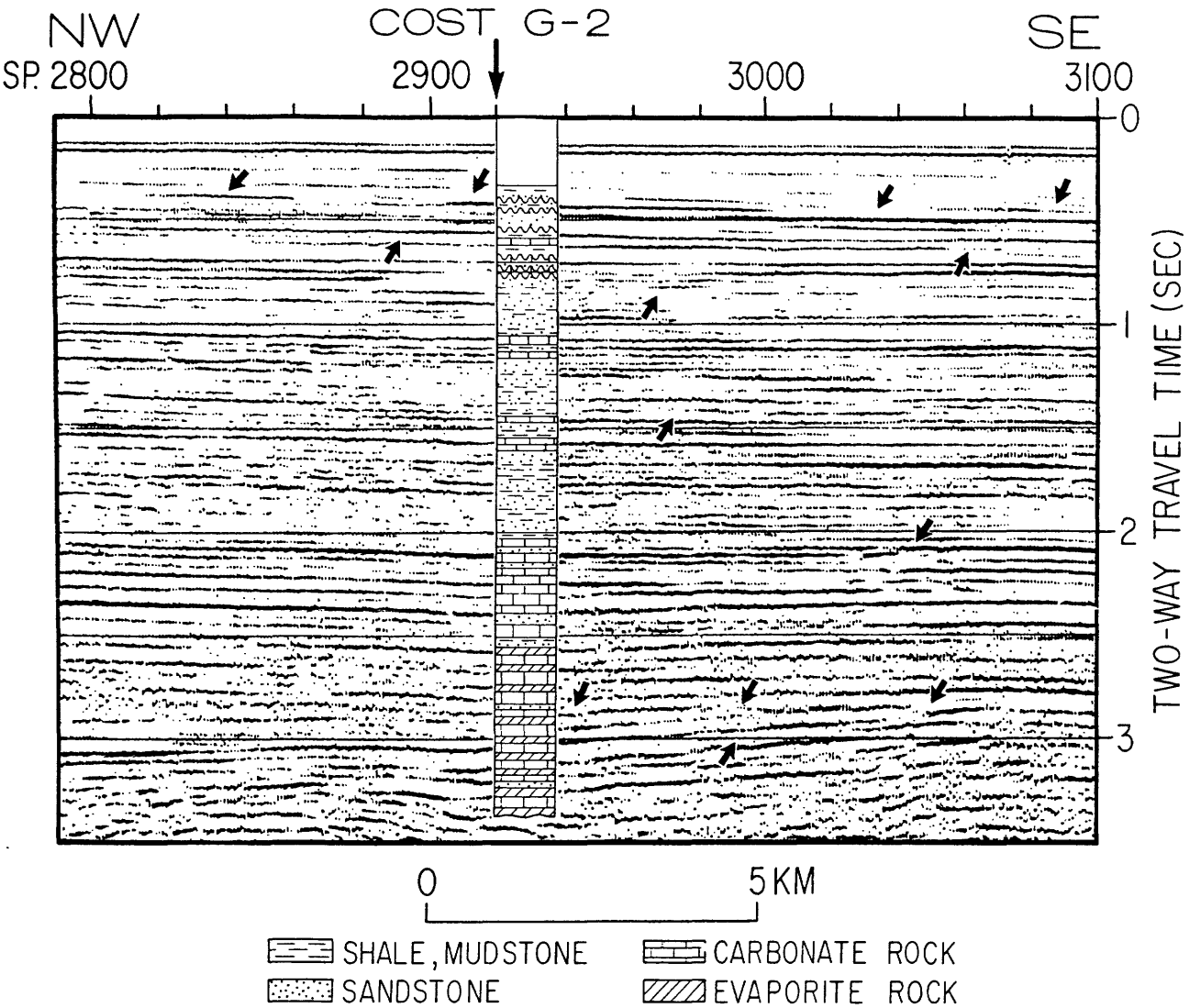
NW
SP. 2800
COST G-2
2900
3000
SE
3100
0
1
2
3
TWO-WAY TRAVEL TIME (SEC)
0
5 KM
SHALE, MUDSTONE
SANDSTONE
CARBONATE ROCK
EVAPORITE ROCK

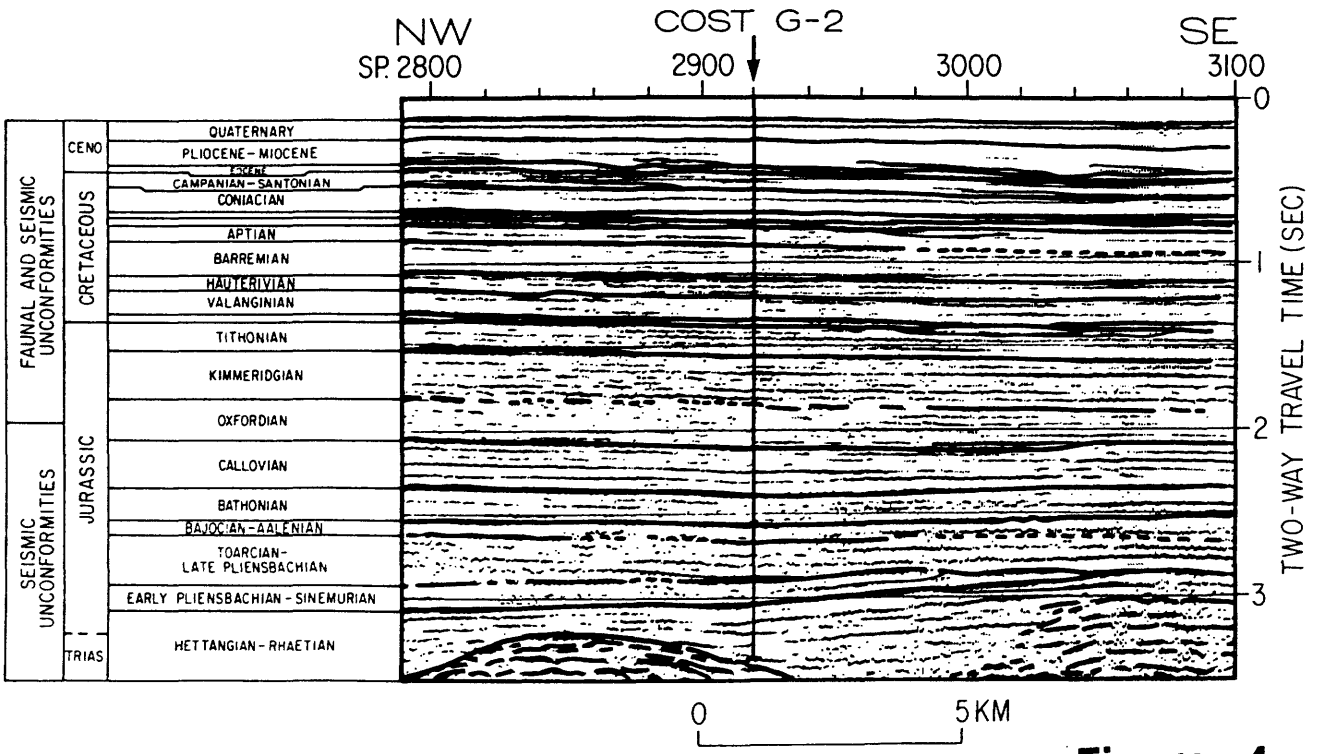
NW
SP. 2800
COST G-2
2900
3000
SE
3100
0
1
2
3
TWO-WAY TRAVEL TIME (SEC)
FAUNAL AND SEISMIC UNCONFORMITIES
SEISMIC UNCONFORMITIES
CENO
CRETACEOUS
JURASSIC
TRIAS
QUATERNARY
PLIOCENE-MIOCENE
EOCENE
CAMPANIAN-SANTONIAN
CONIACIAN
APTIAN
BARREMIAN
HAUTERIVIAN
VALANGINIAN
TITHONIAN
KIMMERIDGIAN
OXFORDIAN
CALLOVIAN
BATHONIAN
BAJOCIAN-AALENIAN
TOARCIAN-
LATE PLIENSBACHIAN
EARLY PLIENSBACHIAN-SINEMURIAN
HETTANGIAN-RHAETIAN
0
5 KM

Figure 4

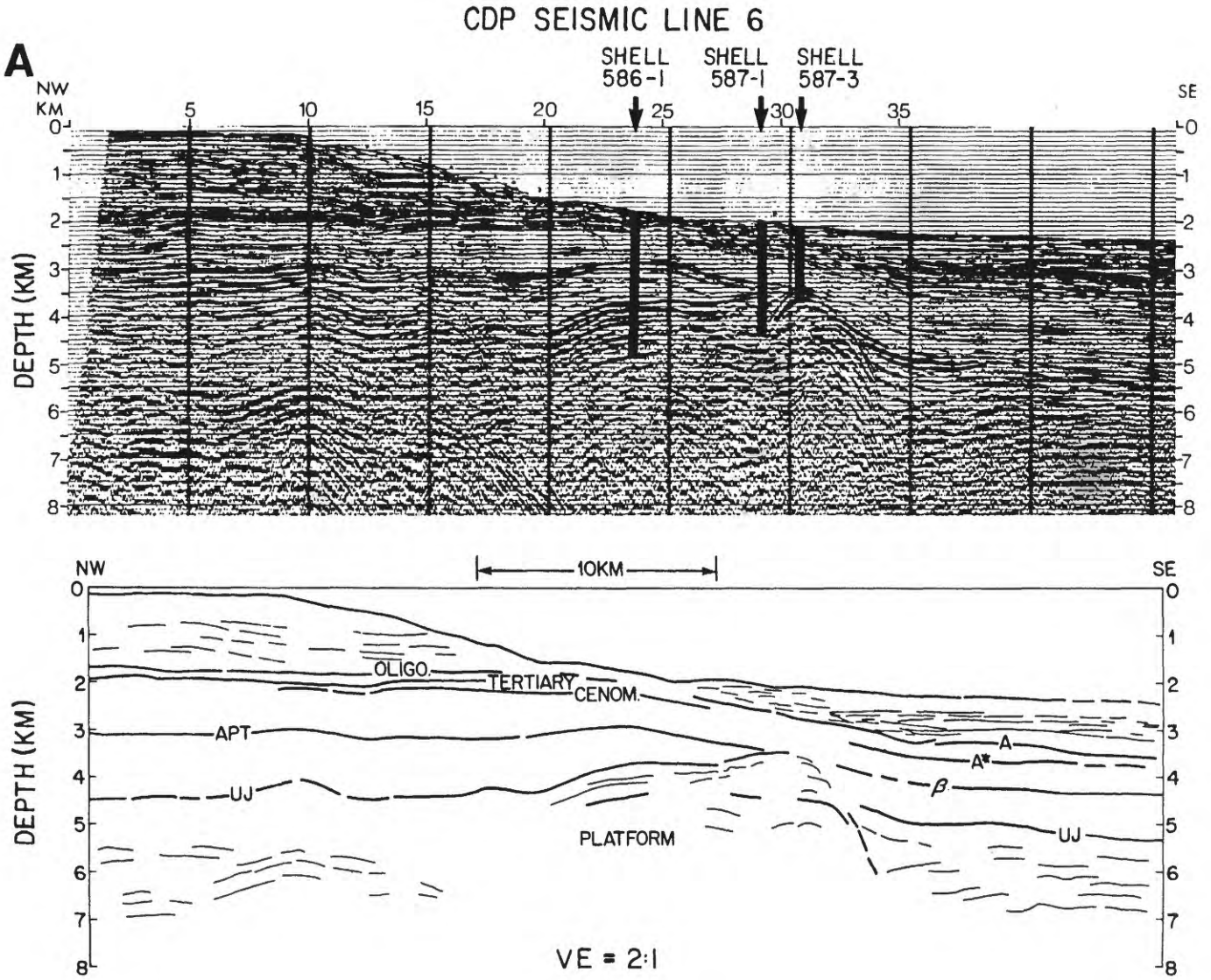
CDP SEISMIC LINE 6
A
NW
KM
SE
SHELL 586-1
SHELL 587-1
SHELL 587-3
5
10
15
20
25
30
35
DEPTH (KM)
0
1
2
3
4
5
6
7
8
NW
SE
10KM
OLIGO.
TERTIARY
CENOM.
APT
UJ
A
A*
β
UJ
PLATFORM
VE = 2:1

Figure 5

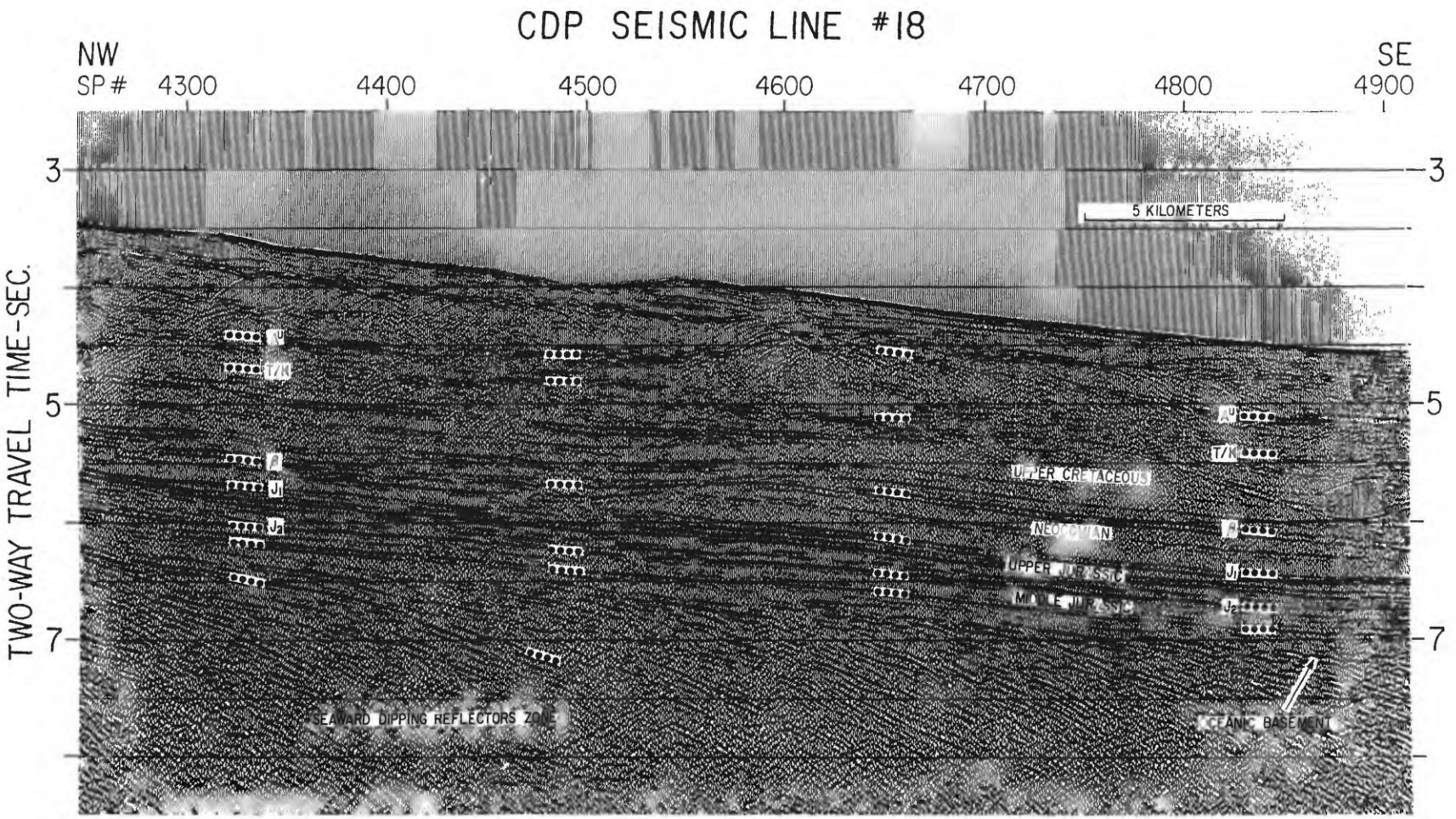
CDP SEISMIC LINE #18
NW
SE
SP #
4300
4400
4500
4600
4700
4800
4900
3
5
7
TWO-WAY TRAVEL TIME-SEC.
5 KILOMETERS
T/K
J1
J2
UPPER CRETACEOUS
NEOCOMIAN
UPPER JURASSIC
MIDDLE JURASSIC
SEAWARD DIPPING REFLECTORS ZONE
OCEANIC BASEMENT

Figure 6

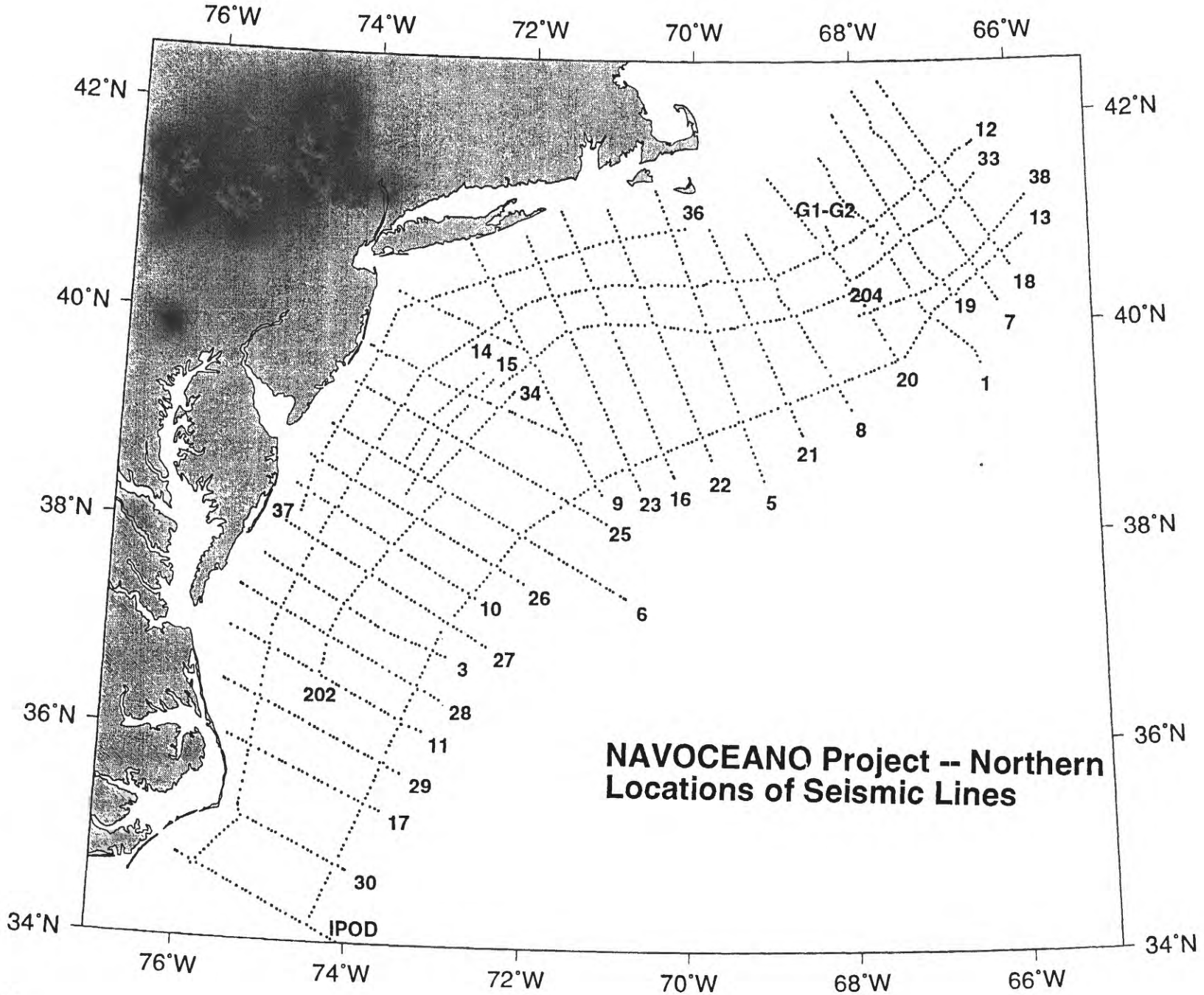
NAVOCEANO Project -- Northern
Locations of Seismic Lines
76°W
74°W
72°W
70°W
68°W
66°W
42°N
40°N
38°N
36°N
34°N
G1-G2
IPOD
12
33
38
13
18
7
19
1
204
20
8
21
5
22
16
23
9
25
6
26
10
27
3
28
11
29
17
30
202
37
14
15
34
36

Figure 7

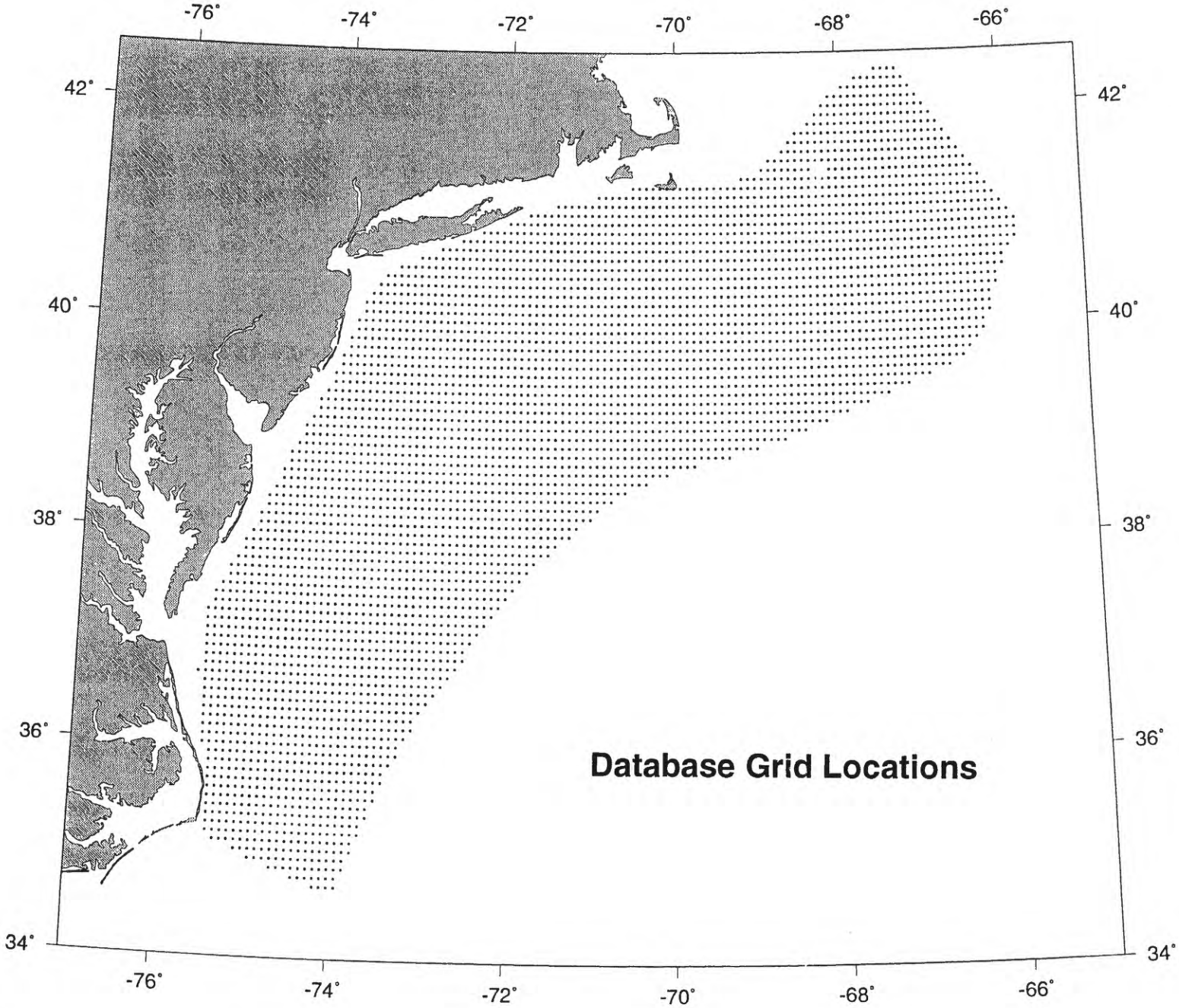

Figure 8

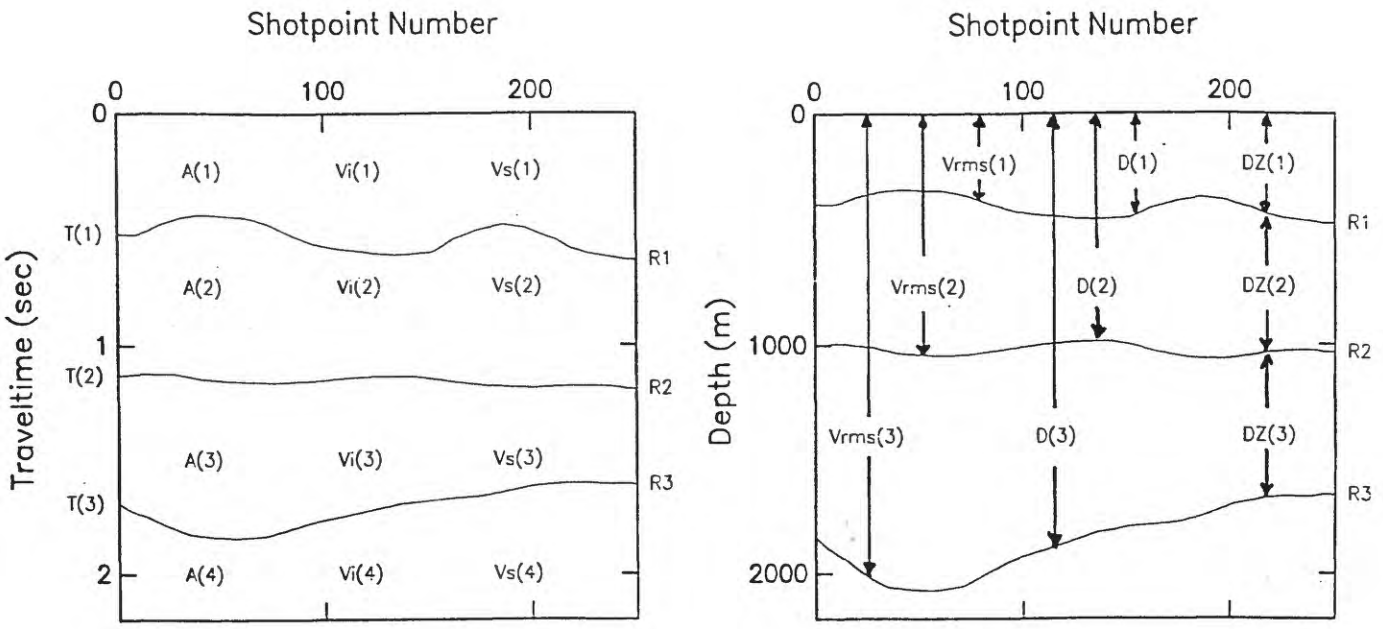

Figure 9

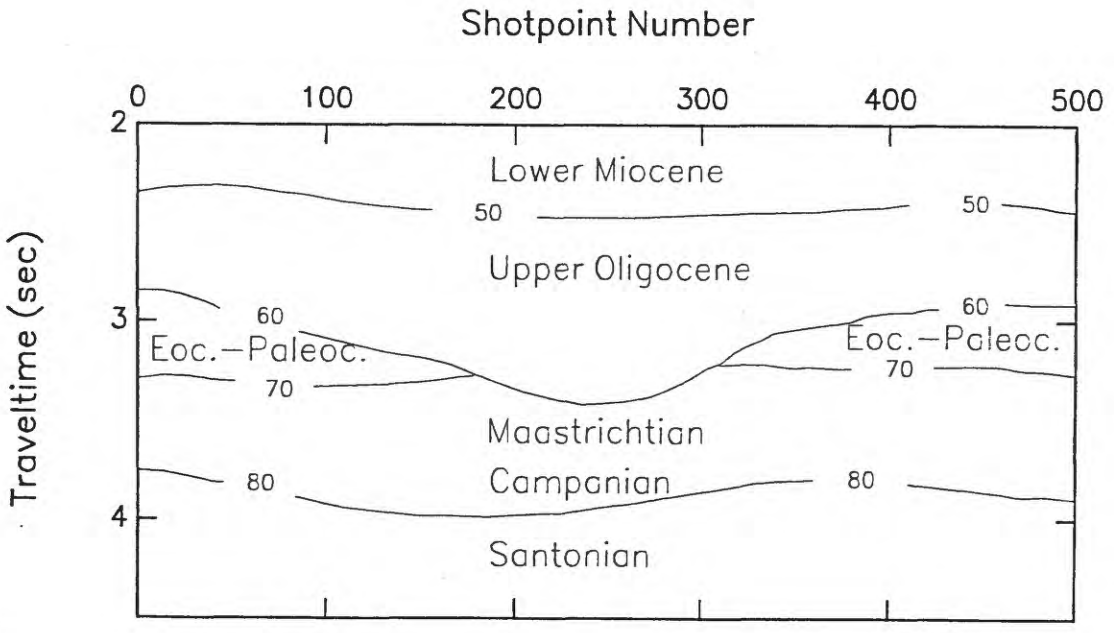

Figure 10

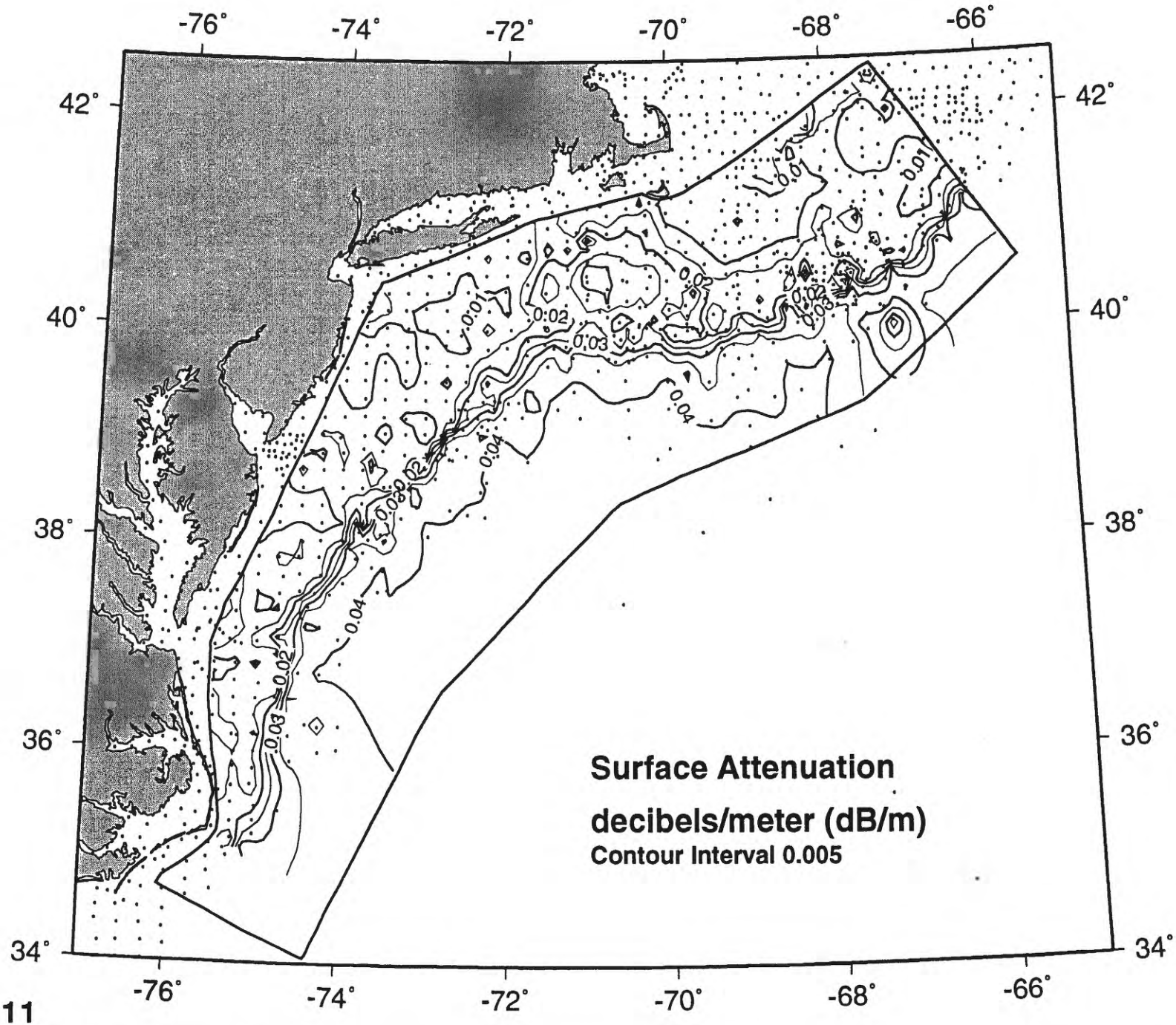
-76°
-74°
-72°
-70°
-68°
-66°
42°
40°
38°
36°
34°
0.0
0.01
0.02
0.03
0.04
Surface Attenuation
decibels/meter (dB/m)
Contour Interval 0.005

Figure 11

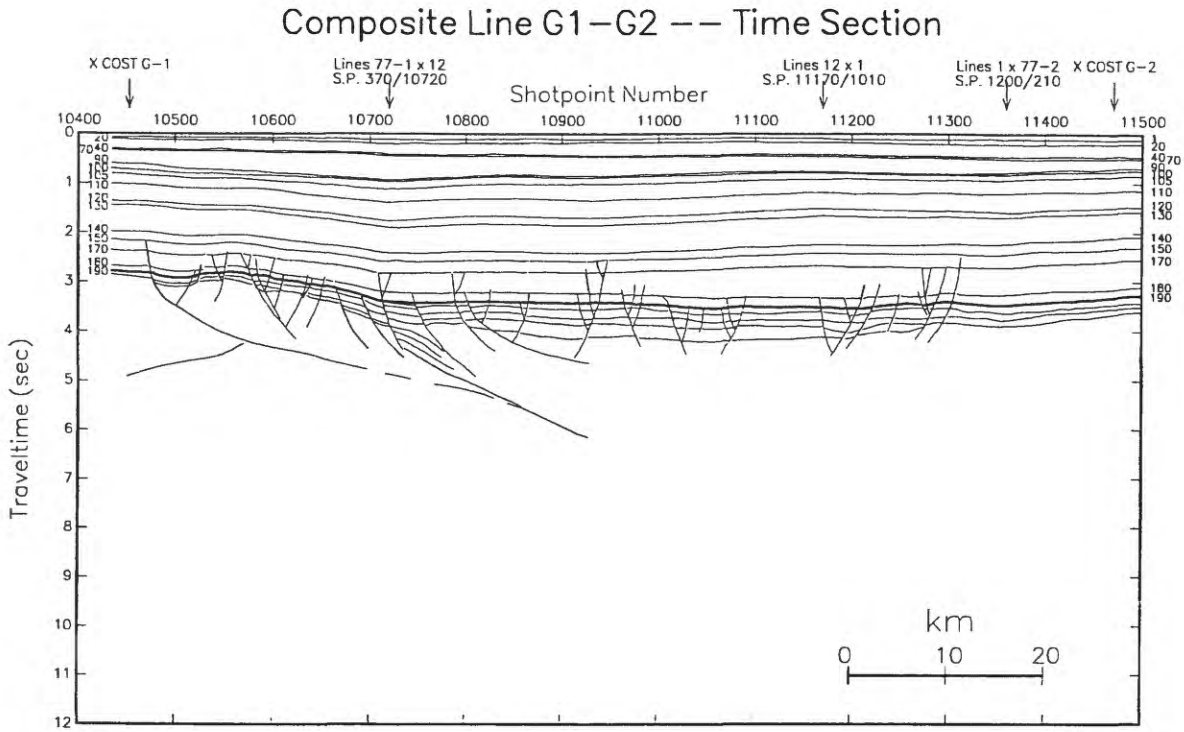
Composite Line G1–G2 -- Time Section
X COST G-1
Lines 77-1 x 12
S.P. 370/10720
Lines 12 x 1
S.P. 11170/1010
Lines 1 x 77-2
S.P. 1200/210
X COST G-2
Shotpoint Number
10400
10500
10600
10700
10800
10900
11000
11100
11200
11300
11400
11500
Traveltime (sec)
km
0
10
20

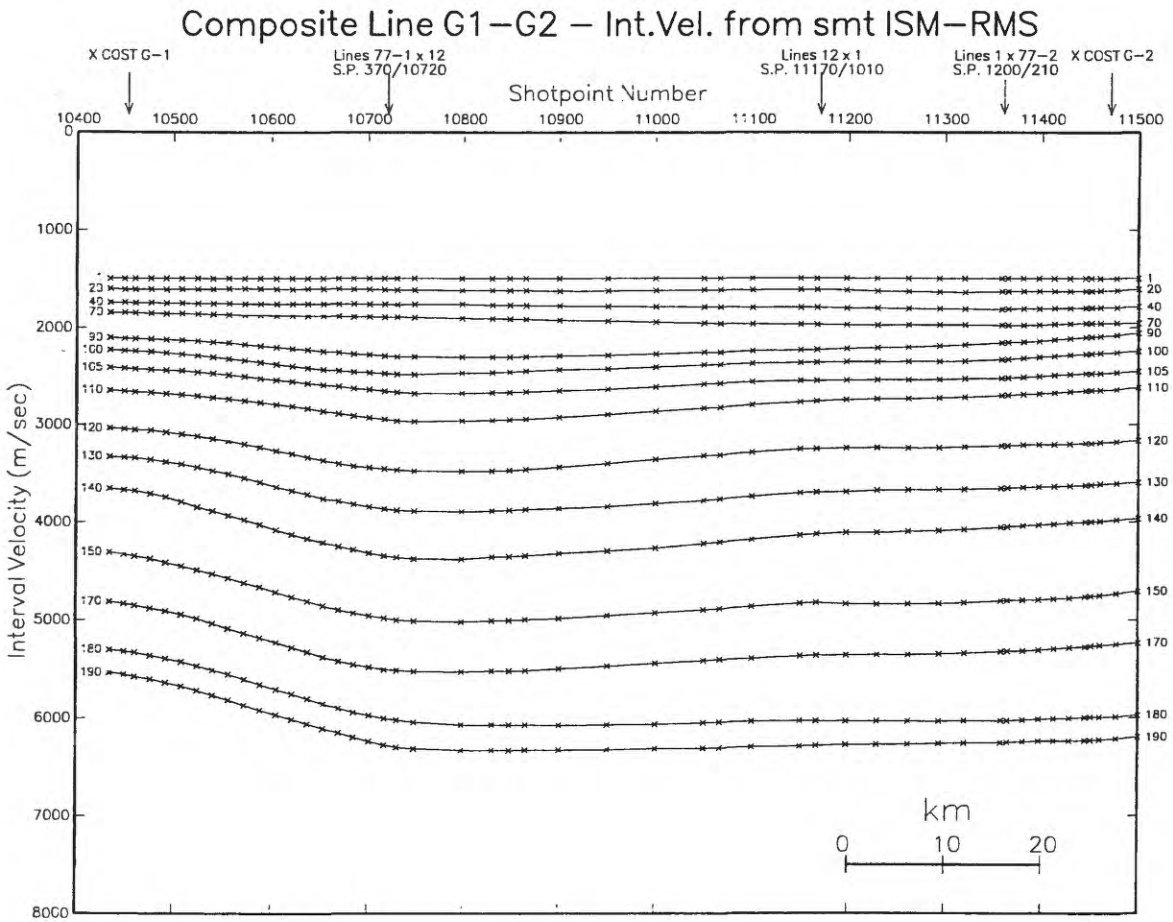
Composite Line G1–G2 – Int.Vel. from smt ISM–RMS
X COST G-1
Lines 77-1 x 12
S.P. 370/10720
Lines 12 x 1
S.P. 11170/1010
Lines 1 x 77-2
S.P. 1200/210
X COST G-2
Shotpoint Number
10400
10500
10600
10700
10800
10900
11000
11100
11200
11300
11400
11500
Interval Velocity (m/sec)
1000
2000
3000
4000
5000
6000
7000
8000
km
0
10
20

Figure 12

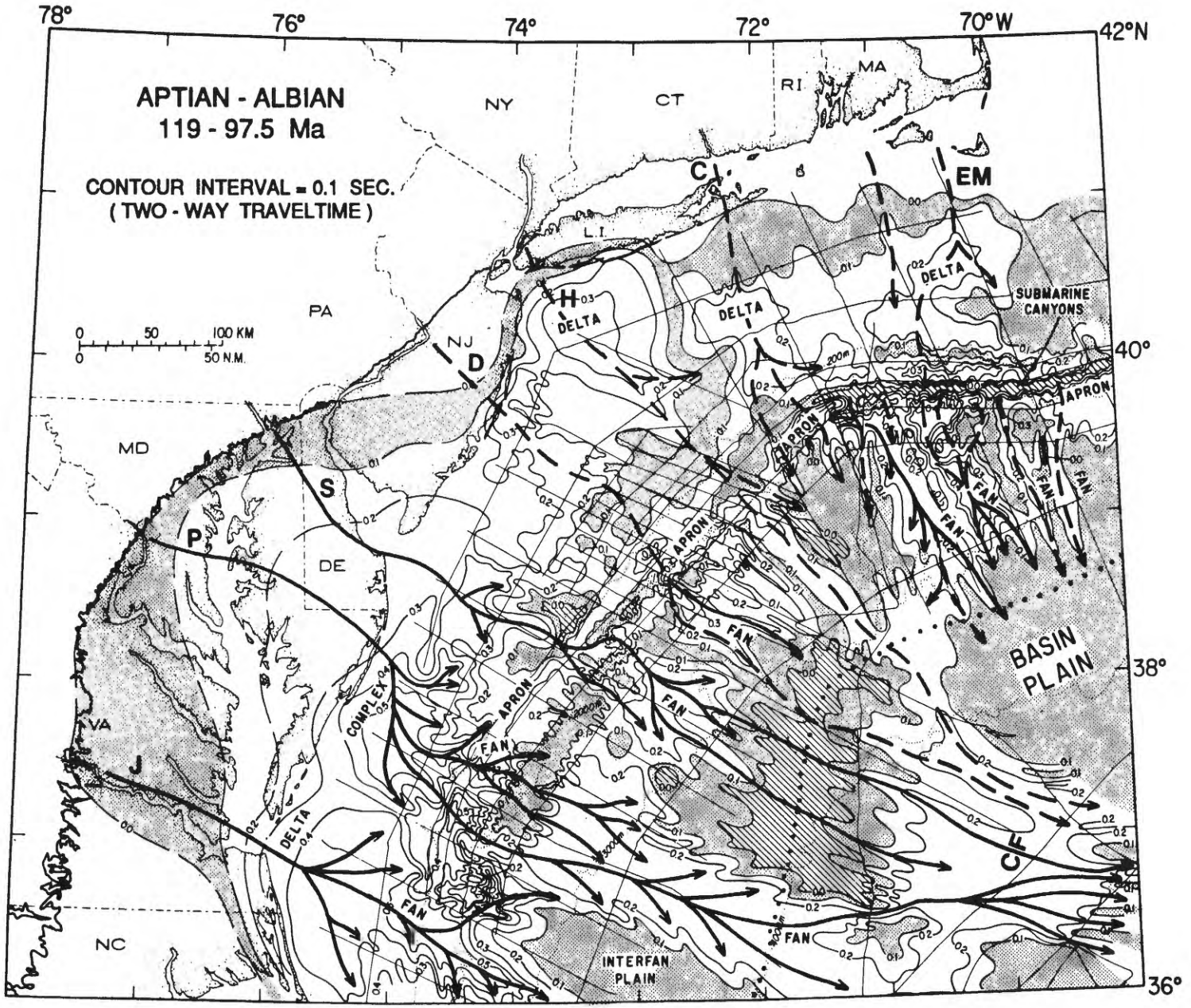
APTIAN - ALBIAN
119 - 97.5 Ma
CONTOUR INTERVAL = 0.1 SEC.
(TWO - WAY TRAVELTIME)
0 50 100 KM
0 50 N.M.
78°
76°
74°
72°
70°W
42°N
40°
38°
36°
NY
CT
RI
MA
L.I.
PA
NJ
MD
DE
VA
NC
C
EM
H
D
S
P
J
CF
DELTA
SUBMARINE CANYONS
APRON
FAN
COMPLEX
BASIN PLAIN
INTERFAN PLAIN

Figure 13

APPENDIX 1
U.S. Geological Survey CDP Lines

Seismic Line #	Shot Pts.	Shot Pt Spacing	Channels-Steamer-Source
Composite Line G1-G2	10435-11500	100m	48 - 3500 m - 1700 cu.in.
USGS CDP Line 1	100-2920	100m	24 - 2321 m - 1260 cu.in.
USGS CDP Line 2	100-2625	100m	24 - 2321 m - 1260 cu.in.
USGS CDP Line 3	130-2370	100m	24 - 2321 m - 1260 cu.in.
USGS CDP Line 5	100-3410	100m	36 - 3600 m - 1700 cu.in.
USGS CDP Line 6	200-3870	100m	36 - 3600 m - 1700 cu.in.
USGS CDP Line 7	70-2765	100m	36 - 3500 m - ?
USGS CDP Line 8c	140-2400	100m	36 - 3500 m - ?
USGS CDP Line 9	100-3135	100m	36 - 3600 m - 1700 cu.in.
USGS CDP Line 10	120-2780	100m	36 - 3600 m - 1700 cu.in.
USGS CDP Line 11	190-2540	100m	48 - 3600 m - 1700 cu.in.
USGS CDP Line 12a	100-1620	100m	48 - 3500 m - 1700 cu.in.
USGS CDP Line 12bc	1600-4100	100m	48 - 3500 m - 1700 cu.in.
USGS CDP Line 12de	4100-7400	100m	48 - 3500 m - 1700 cu.in.
USGS CDP Line 12fg	7400-9160	100m	48 - 3500 m - 1700 cu.in.
USGS CDP Line 12hi	9120-10720	100m	48 - 3500 m - 1700 cu.in.
USGS CDP Line 12j1	1072-12600	100m	48 - 3500 m - 1700 cu.in.
USGS CDP Line 13a	90-2000	100m	48 - 3500 m - 1700 cu.in.
USGS CDP Line 13b	2000-4000	100m	48 - 3500 m - 1700 cu.in.
USGS CDP Line 13cd	4000-6040	100m	48 - 3500 m - 1700 cu.in.
USGS CDP Line 13ef	6040-8600	100m	48 - 3500 m - 1700 cu.in.
USGS CDP Line 13gh	8580-11270	100m	48 - 3500 m - 1700 cu.in.
USGS CDP Line IPOD	100-2170	100m	36 - 3600 m - 1700 cu.in.
USGS CDP Line 14a	1000-2260	50m	48 - 3500 m - 1700 cu.in.
USGS CDP Line 14b	1000-2480	50m	48 - 3500 m - ?
USGS CDP Line 15a	520-2200	50m	48 - 3550 m - ?
USGS CDP Line 15b	1000-2425	50m	48 - 3550 m - ?
USGS CDP Line 16	1-6200	50m	48 - 3550 m - ?
USGS CDP Line 17	1290-4370	50m	24 - 3600 m - 2160 cu.in
USGS CDP Line 18	100-4900	50m	48 - 2400 m - 2000 cu.in.
USGS CDP Line 19	100-4895	50m	48 - 2400 m - 2000 cu.in.
USGS CDP Line 20	4870- 100	50m	48 - 2400 m - 2000 cu.in.
USGS CDP Line 21	210-5035	50m	48 - 3600 m - 2000 cu.in.
USGS CDP Line 22	915-6700	50m	48 - 3600 m - 2000 cu.in.
USGS CDP Line 23	360-6260	50m	48 - 3600 m - 2000 cu.in.
USGS CDP Line 24	490-3560	50m	48 - 3600 m - 2000 cu.in.
USGS CDP Line 25a	430-2870	50m	48 - 3600 m - 2000 cu.in.
USGS CDP Line 25b	2845-6570	50m	48 - 3600 m - 2000 cu.in.
USGS CDP Line 26	100-5470	50m	48 - 3600 m - 2000 cu.in.
USGS CDP Line 27	240-5350	50m	48 - 3600 m - 2000 cu.in.
USGS CDP Line 28	365-5315	50m	48 - 3600 m - 2000 cu.in.
USGS CDP Line 29	640-4940	50m	48 - 3600 m - 2000 cu.in.
USGS CDP Line 30	470-3060	50m	48 - 3600 m - 2000 cu.in.
USGS CDP Line 33	85-3840	50m	48 - 2400 m - 2000 cu.in.
USGS CDP Line 34	100-2820	50m	48 - 3600 m - 2000 cu.in.
USGS CDP Line 36	100-6500	50m	48 - 3600 m - 2000 cu.in.
USGS CDP Line 37	100-4865	50m	48 - 3600 m - 2000 cu.in.
USGS CDP Line 38	100-4600	50m	48 - 3600 m - 2000 cu.in.
BGR 79-202	1-4880	50m	24 - 2400 m - 23.45 liters
BGR 79-204	7500-15650	50m	24 - 2400 m - 23.45 liters

Line crossing and well crossing shot point numbers

Seismic Line#	Shot Pt. #	Crossing Line# or Well	Shot Pt. #
2	125	AMCOR 6011 (on line)	
2	940	Mobil 544-1 (2 km NE of line)	
2	1060	Conoco 590-1 (3 km NE of line)	
5	1770	ASP 17/18 (10 km NE of line)	
6	1060	Shell 273-1 (5 km SW of line)	
6	1415	Shell 586-1 (5 km SW of line)	
6	1470	Shell 587-1 (5 km SW of line)	
8a	800	20	3900
9	1400	24	3560
9	2450	2	2495
10	1140	Shell 93-1 (on line)	
11	190	USCGLT-CH1-2	
12ab	160	IPOD	320
12ab	900	30	470
12ab	1598	17	1835
12ab	2117	29	1480
12ab	2672	11	680
12c	3095	28	1420
12c	3470	3	565
12c	3900	27	1060
12d	4298	10	603
12d	4650	26	1189
12d	5050	6	704
12d	5565	25	1510
12d	5850	AMCOR 6020 (17 km NW of line)	
12d	6000	2	735
12e	6785	24	2565
12e	7095	9	945
12fg	7620	23	1740
12fg	8060	16	1780
12fg	8550	22	2660
12fg	9110	5	1150
12hi	9570	21	1440
12hi	9965	8	680
12hi	10630	20	2850
12hi	10720	77-1	370
12j1	11170	1	1010
12j1	11430	19	2480
12j1	11815	7	1280
12j1	12115	18	2360
12j1	12410	4	1090
13ad	170	IPOD	1709
13ad	825	30	2800
13ad	1548	17	4370
13ad	2000	29	4410
13ad	2485	11	2300
13ad	2890	28	4700
13ad	3300	3	2200
13ad	3645	27	4360
13ad	4030	10	2325
13ad	4435	26	4700
13ad	4815	6	2540
13ad	5490	25	5580
13ad	5840	9	2980
13eh	6250	23	5690
13eh	6640	16	5580
13eh	7080	22	6155
13eh	7540	5	2705
13eh	8065	21	4250
13eh	8615	8	2040
13eh	9335	20	120
13eh	9930	1	2160
13eh	10280	19	4730
13eh	10620	7	2390
13eh	10940	18	4590
13eh	11260	4	2205

14a	1050	6	1060
14a	1240	Shell 272-1 (8 km NW of line)	
14a	1350	Shell 273-1 (2 km NW of line)	
14a	2100	25	2195
14a	2260	14b	1000
14b	1790	2	1198
14b	2035	COST B-2 (on line)	
15a	930	Tenneco 495-1 (on line)	
15a	1050	6	1250
15a	2115	25	2550
15a	2185	Mobil 17-2 (2 km NW of line)	
15a	2200	15b	1010
15b	1380	HOM 855-1 (5 km NW of line)	
15b	1460	Gulf 857-1 (1 km SE of line)	
15b	1900	2	1360
15b	1905	Exxon 728-1 (1 km SE of line)	
15b	1950	Exxon 684-2 (1 km NW of line)	
15b	2010	Exxon 648-1 (2 km NE of line)	
15b	2220	Tenneco 642-2 (5 km SE of line)	
15b	2250	Texaco 598-2 (NW of line)	
15b	2300	Texaco 598-3 (on line)	
19	365	AMCOR 6019	
20	4150	AMCOR 6016	
25	570	37	3095
25	1424	LASE ESP-1	
25	1510	12d	5565
25	2068	LASE ESP-2	
25	2195	14a	2100
25	2428	LASE ESP-3	
25	2550	15a	2115
25	2720	204	5990
25	2880	ASP-17	
25	3050	DSDP 612 (on line)	
25	3060	34	1270
25	3143	LASE ESP-4	
25	3390	DSDP 605 (on line)	
25	3500	DSDP 604 (on line)	
25	3650	DSDP 107 (on line)	
25	3710	LASE ESP-5	
25	5580	13	5490
26	2340	Shell 586-1 (on line)	
26	2440	Shell 587-1 (on line)	
28	1905	ASP 10	
28	2100	ASP 22	
30	470	USCG-LT DS-1/2	
33	238	20	2082
33	1220	1	1345
33	1750	19	3160
33	2590	7	1680
33	3230	18	3030
33	3845	4	1390
34	190	6	1400
34	1170	ASP 15	
34	1270	25	3060
34	1450	COST B-3 (Proj.)	
34	2325	2	1640
36	640	24	1075
36	2130	9	527
36	3230	23	1000
36	4120	16	910
36	5040	22	1659
36	6130	5	550

37	4871	36	101
37	3900	2	240
37	3095	25	570
37	2105	6	260
37	1300	26	340
37	600	10	250
38	355	20	1328
38	1390	1	1880
38	2045	19	4370
38	2760	7	2250
38	3460	18	4180
38	4090	4	1960
77-1	105	COST G-1	
77-1	370	12	10720
77-2	210	1	1200
77-2	105	COST G-2	
202	0001	11	1320
202	865	28	2560
202	1595	3	1140
202	2445	27	2365
202	3240	10	1327
202	4000	26	2750
202	4880	6	1600
204	0005	11	1020
204	900	28	1920
204	900	ASP 10	
204	1650	3	810
204	2530	27	1675
204	3340	10	990
204	4070	26	2050
204	4900	6	1220
204	5990	25	2720
204	7010	2	1440
204	8350	9	1490
204	9370	23	2600
204	9725	AMCOR 6012	
204	10250	16	2300
204	11250	22	3605
204	12380	5	1685
204	13310	21	2400
204	14230	8	1190
204	15660	20	1840
204	16600	1	1635

Appendix 2

U.S. Atlantic Margin Industry Wells Used to Calibrate Database.

Industry wells with both velocity and bio-/lithostratigraphic information used in this database (Klitgord and Schneider, 1994).

Basin	Co.	WELL NO.	LATITUDE	LONGITUDE	W.D.	T.D.	Sonic	Ckshot
GBB		COST G-1	40°55.87'N	68°18.32'W	47.9m	4821m	yes	yes
GBB		COST G-2	40°50.26'N	67°30.49'W	81.7m	6554m	yes	yes
BCT		COST B-2	39°22.53'N	72°44.06'W	90.8m	4863m	yes	yes
BCT	SHELL	SH-273-1	38d42.974'N	73d27.341'W	72m	5237m	yes	yes
BCT	SHELL	SH-587-1	38d22.92'N	73d09.85'W	2042m	4420m	no	yes
BCT	SHELL	SH-586-1	38d24.34'N	73d13.05'W	1794m	3076m	no	yes
BCT	SHELL	SH-93-1	37d53.58'N	73d44.16'W	1529m	5407m	yes	yes
BCT	GULF	Gu-857-1	39d06.318'N	72d49.457'W	102m	5527m	no	yes
BCT	TEXACO	TX-598-2	39d22.316'N	72d31.859'W	128m	5244m	no	yes
BCT	MOBIL	MO-17-2	38d58.067'N	73d02.943'W	79m	4160m	yes	yes
BCT	MOBIL	MO-544-1	39d25.47'N	73d04.60'W	66m	2543m	no	yes
BCT	EXXON	EX-684-2	39d16.731'N	72d39.133'W	126m	4969m	yes	yes
BCT	TENNECO	TN-495-1	38d27.981'N	73d22.698'W	108m	5443m	yes	yes

Industry wells with bio-/lithoiostratigraphic information incorporated into the stratigraphic analyses as indicated in the reports by Poag (1982, 1985b, 1987, 1991, 1992), Poag and Valentine (1988) and Poag and Wade (1993).

Basin	Co.	WELL NO.	LATITUDE	LONGITUDE	W.D.	T.D.
GBB	EXXON	EX-133-1	40d49.08'N	67d56.046'W	69m	4303m
GBB	EXXON	EX-975-1	41d00.90'N	67d37.35'W	64m	4361m
GBB	SHELL	SH-410-1	40d34.39'N	67d12.54'W	136m	4587m
GBB	MOBIL	MO-312-1	40d39.10'N	67d46.90'W	84m	6096m
GBB	MOBIL	MO-187-1	40d46.25'N	67d23.32'W	94m	5407m
GBB	GULF	GU-145-1	40d50.73'N	67d17.57'W	91m	4302m
GBB	MOBIL	MO-273-1	40d41.08'N	67d30.21'W	98m	4624m
GBB	SHELL	SH-357-1	40d37.57'N	67d44.77'W	82m	5818m
BCT		COST B-3	38°55.10'N	72°46.38'W	819m	3991m
BCT	CONOCO	CO-590-1	39d22.560'N	72d58.040'W	70m	3562m
BCT	SHELL	SH-632-1	39d20.999'N	73d06.320'W	64m	4180m
BCT	TEXACO	TX-598-1	39d22.319'N	72d30.328'W	130m	4423m
BCT	HOUSTON	HO-676-1	39d17.217'N	73d06.383'W	67m	3713m
BCT	EXXON	EX-684-1	39d18.163'N	72d38.499'W	12m	5226m
BCT	MOBIL	MO-17-1	38d58.080'N	73d02.950'W	85m	261m
BCT	HOUSTON	HO-855-1	39d06.347'N	72d54.840'W	89m	5217m
BCT	SHELL	SH-272-1	38d42.070'N	73d32.430'W	66m	4024m
BCT	GULF	GU-718-1	39d15.657'N	73d09.957'W	58m	3825m
BCT	EXXON	EX-902-1	39d04.239'N	72d45.246'W	132m	4713m
BCT	TENNECO	TN-642-2	39d20.597'N	72d29.650'W	139m	5447m
BCT	EXXON	EX-500-1	39d26.920'N	73d06.100'W	62m	3647m
BCT	TEXACO	TX-642-1	39d20.865'N	72d30.878'W	139m	5264m
BCT	MURPHY	MU-106-1	38d51.238'N	72d57.304'W	125m	4908m
BCT	TENNECO	TN-642-3	39d20.262'N	72d31.736'W	137m	4861m
BCT	EXXON	EX-599-1	39d21.88'N	72d29.15'W	135m	5058m
BCT	TEXACO	TX-598-4	39d21.70'N	72d30.35'W	129m	4724m
BCT	EXXON	EX-816-1	39d10.05'N	72d38.10'W	143m	5257m
BCT	EXXON	EX-728-1	39d15.22'N	72d39.15'W	132m	4477m
BCT	SHELL	SH-372-1	38d36.02'N	72d52.23'W	2119m	3545m

Appendix 3

Stratigraphic Time Sections and Layer Interval Velocity Sections

The upper profile (time section) for each line is the seismostratigraphic base displayed in terms of two-way travel time (in seconds) vs distance along track (shot points). Each numbered surface corresponds to one of the seismostratigraphic units listed in Table 4. The upper most surface is the sea floor (reflector 1). Un-numbered lines crossing diagonally through the sedimentary section are interpreted faults. Un-numbered lines beneath the numbered stratigraphic section are basement structures or synrift strata. They are provided as a guide to the general nature of geologic features beneath the geologic units in the data base, but they are not included in the gridded database.

The lower profile for each line displays the interval velocity for the stratigraphic units shown in the upper profile. These velocities are the final, smoothed functions derived from the ISM smoothed RMS velocity data. Velocities increase going down the page, with highest velocities at the bottom. Average water velocity has been assumed 1500 m/sec. Note the general increase in velocities in the seaward direction across the shelf. This change is primarily associated with the greater depth of burial of the units. Each velocity curve is numbered and corresponds to the unit directly above the same numbered surface listed in Table 4 and show in the upper profile. The x's indicate the locations of velocity analyses.

Composite Line G1–G2 -- Time Section

Shotpoint Number

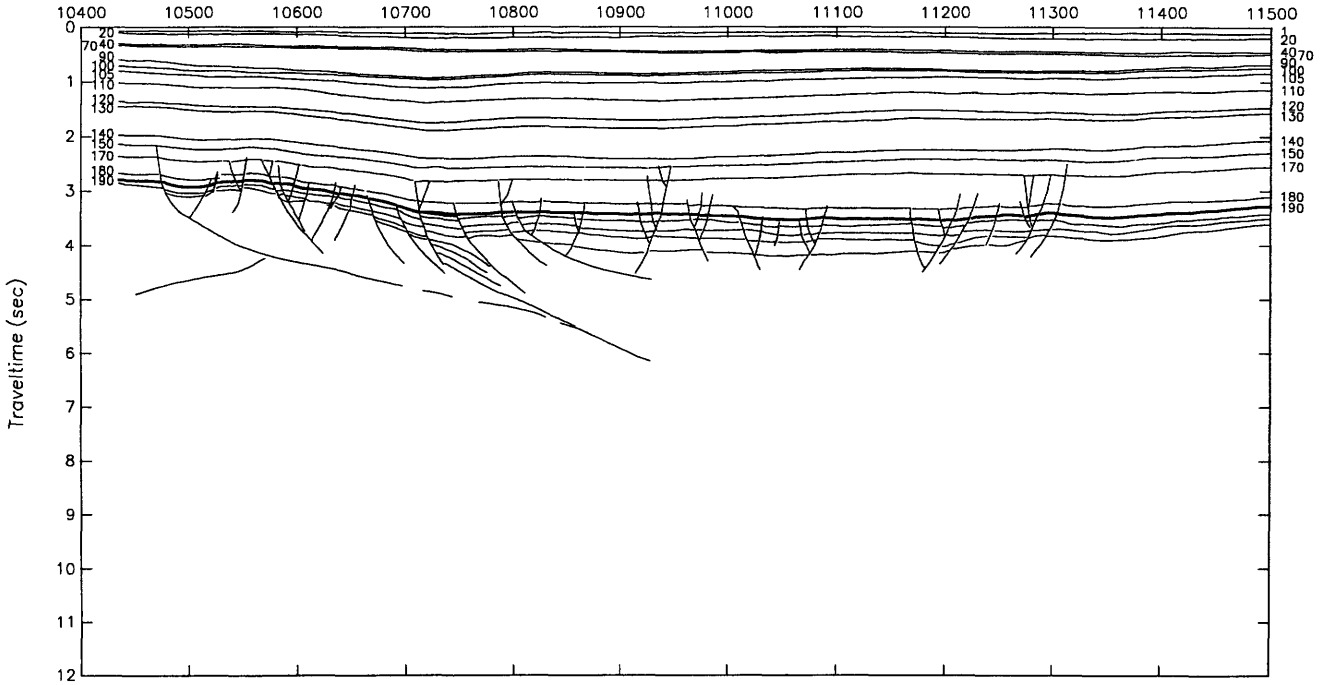

Composite Line G1–G2 – Int.Vel. from smt ISM–RMS

Shotpoint Number

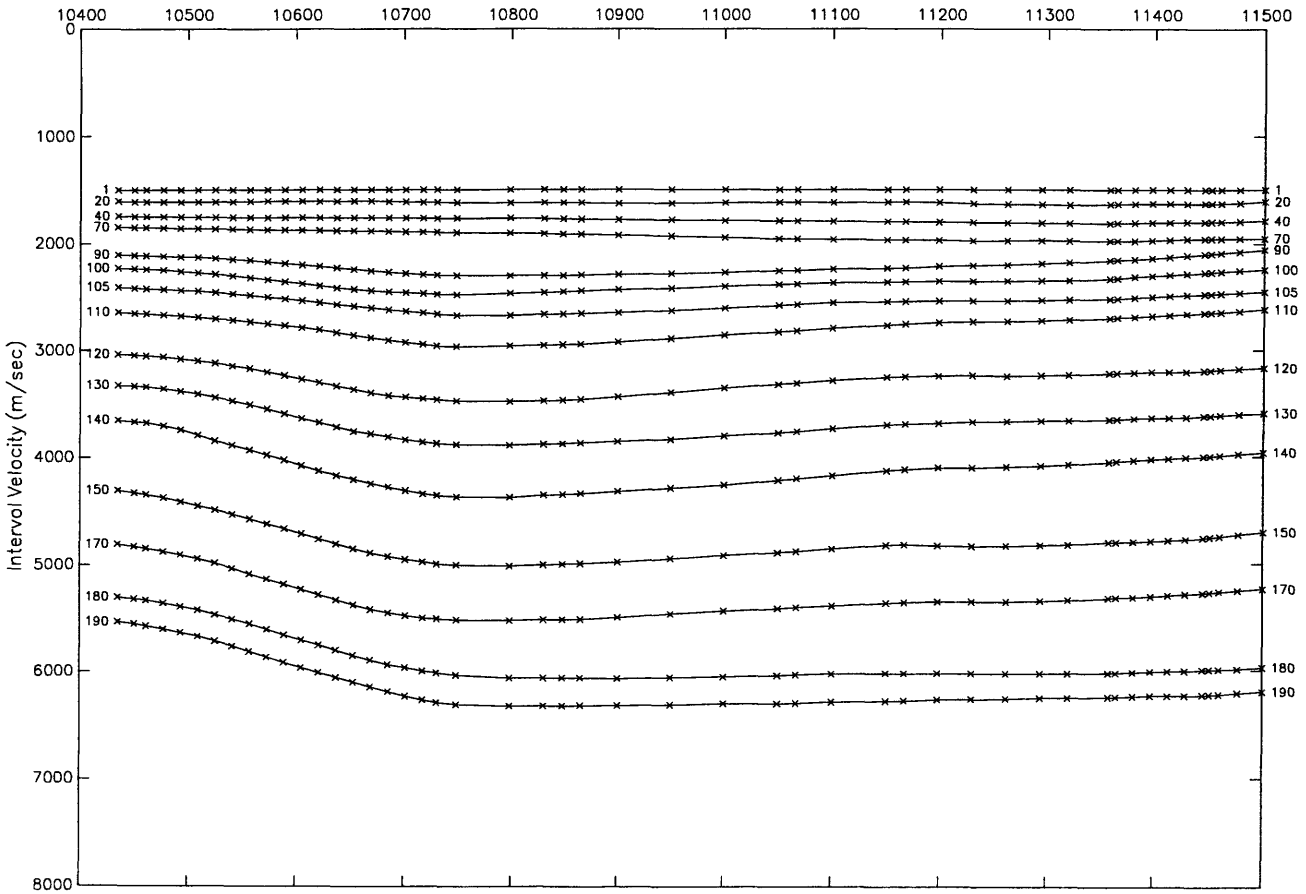

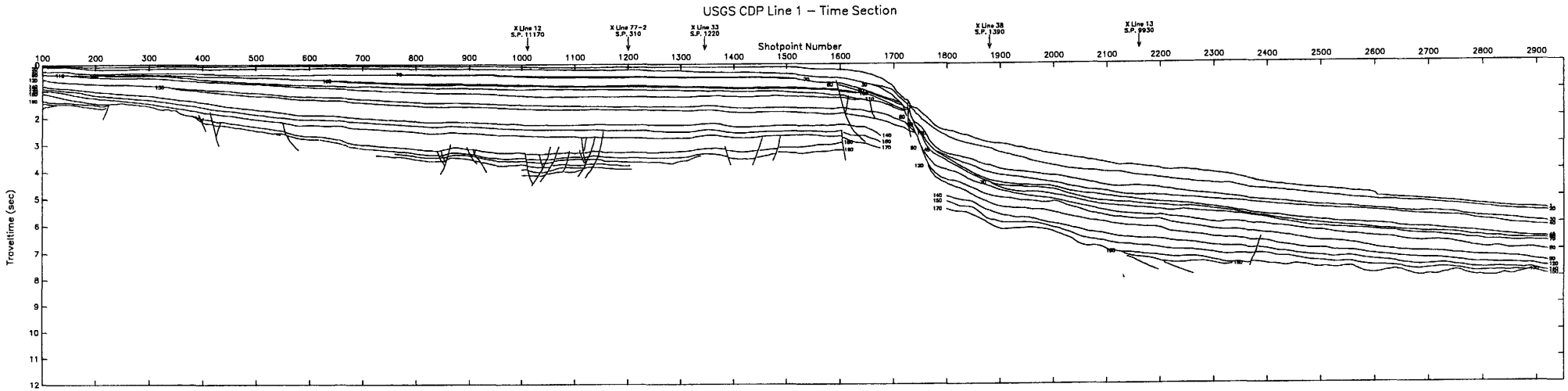
USGS CDP Line 1 -- Time Section
X Line 12 S.P. 11170
X Line 77-2 S.P. 310
X Line 33 S.P. 1220
X Line 38 S.P. 1390
X Line 13 S.P. 9930
Shotpoint Number
Traveltime (sec)

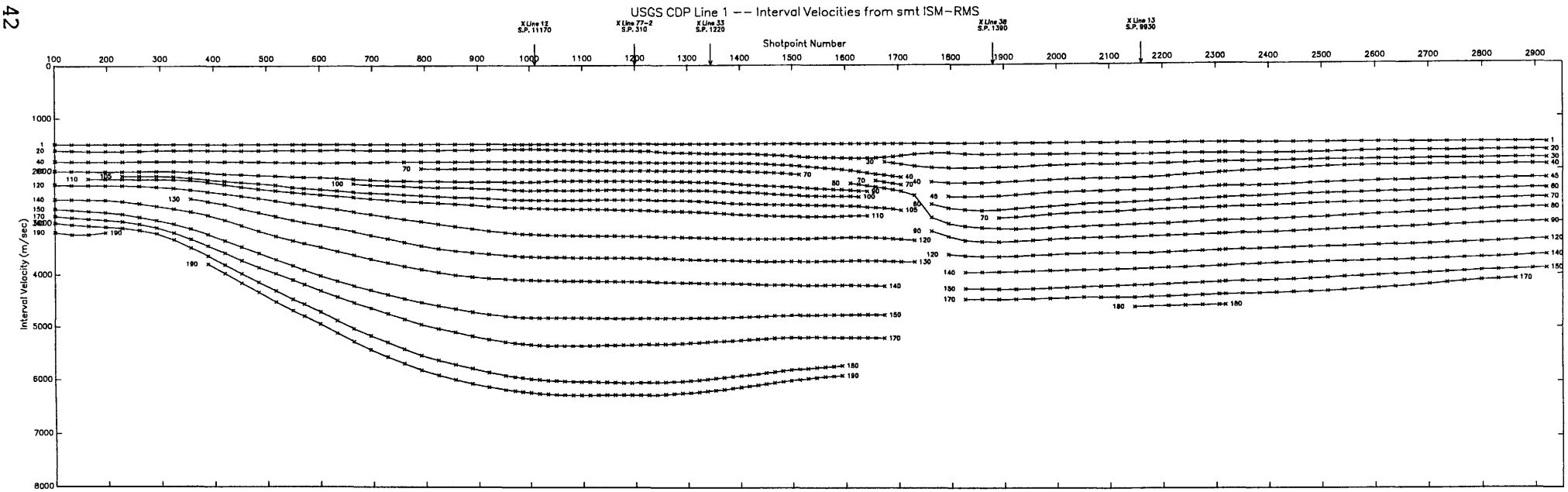
USGS CDP Line 1 -- Interval Velocities from smt ISM-RMS
X Line 12 S.P. 11170
X Line 77-2 S.P. 310
X Line 33 S.P. 1220
X Line 38 S.P. 1390
X Line 13 S.P. 9930
Shotpoint Number
Interval Velocity (m/sec)

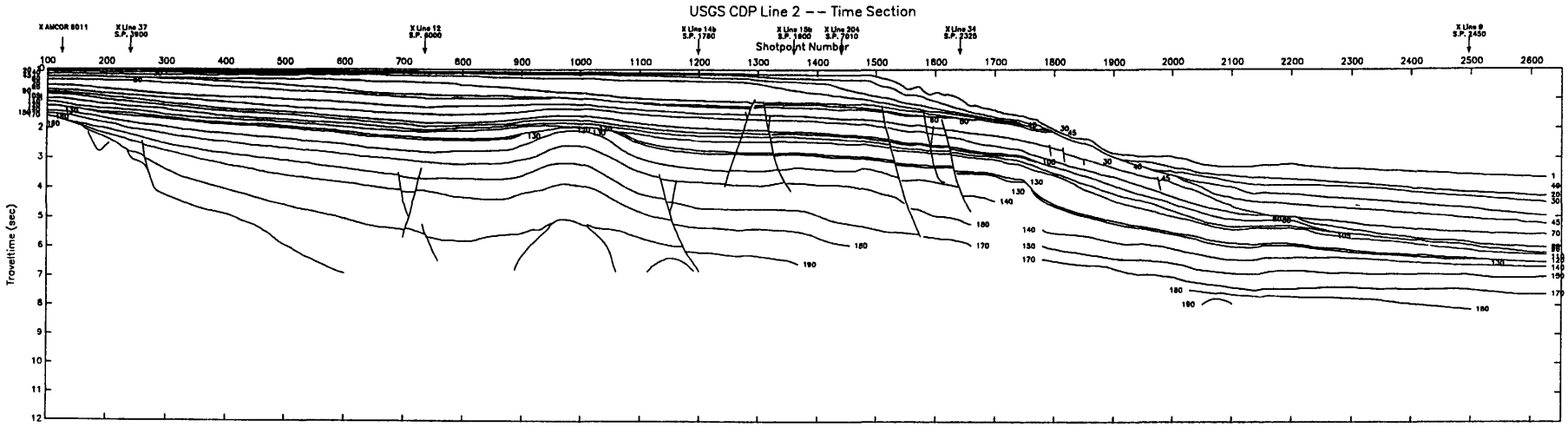
USGS CDP Line 2 -- Time Section
X AMCOR 8011
X Line 37 S.P. 3900
X Line 12 S.P. 6000
X Line 14b S.P. 1780
X Line 15b S.P. 1900
X Line 204 S.P. 7010
X Line 34 S.P. 2325
X Line 9 S.P. 2450
Shotpoint Number
Traveltime (sec)

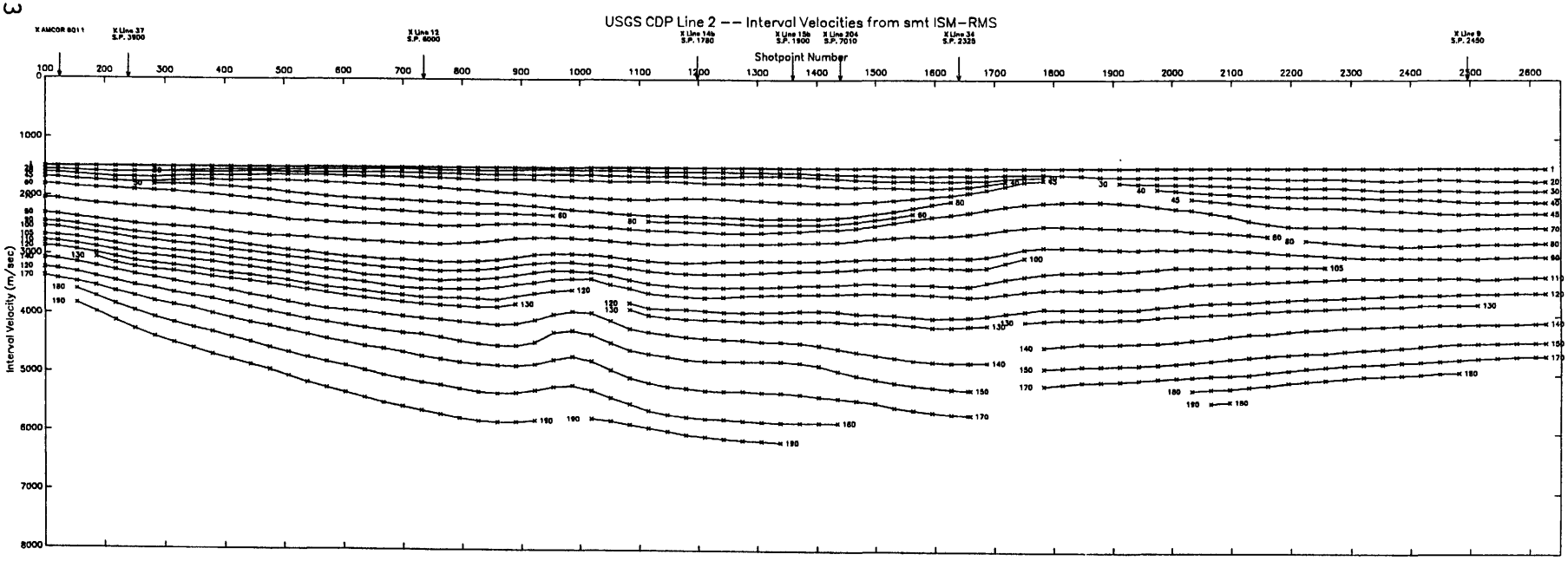
USGS CDP Line 2 -- Interval Velocities from smt ISM-RMS
X AMCOR 8011
X Line 37 S.P. 3900
X Line 12 S.P. 6000
X Line 14b S.P. 1780
X Line 15b S.P. 1900
X Line 204 S.P. 7010
X Line 34 S.P. 2325
X Line 9 S.P. 2450
Shotpoint Number
Interval Velocity (m/sec)

USGS CDP Line 3 -- Time Section

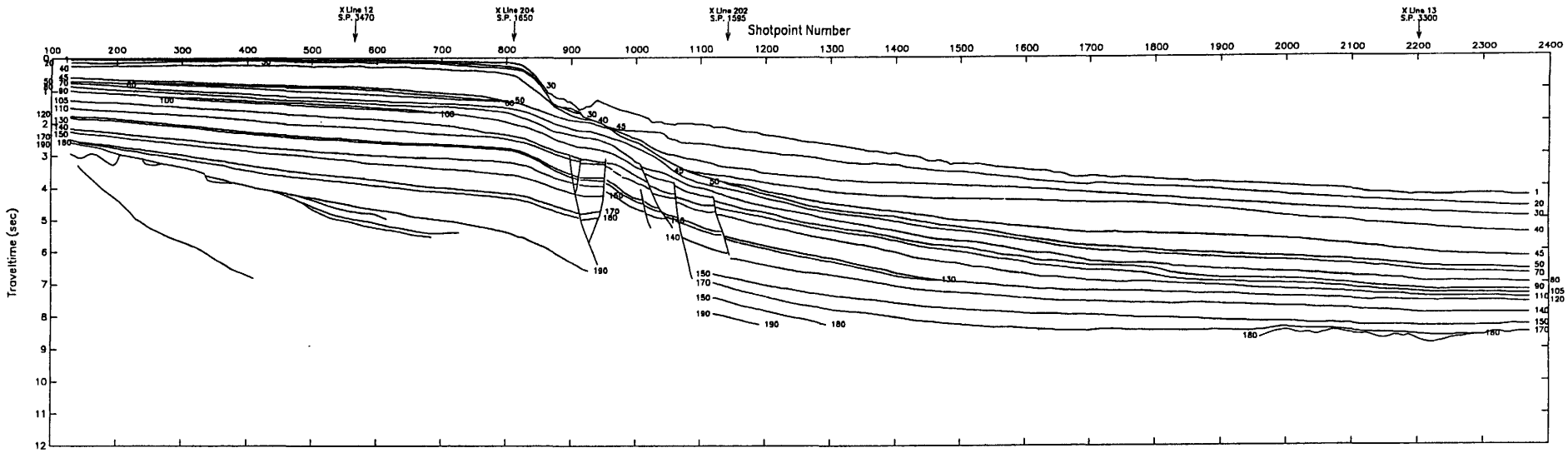

USGS CDP Line 3 -- Interval Velocities from smt ISM-RMS

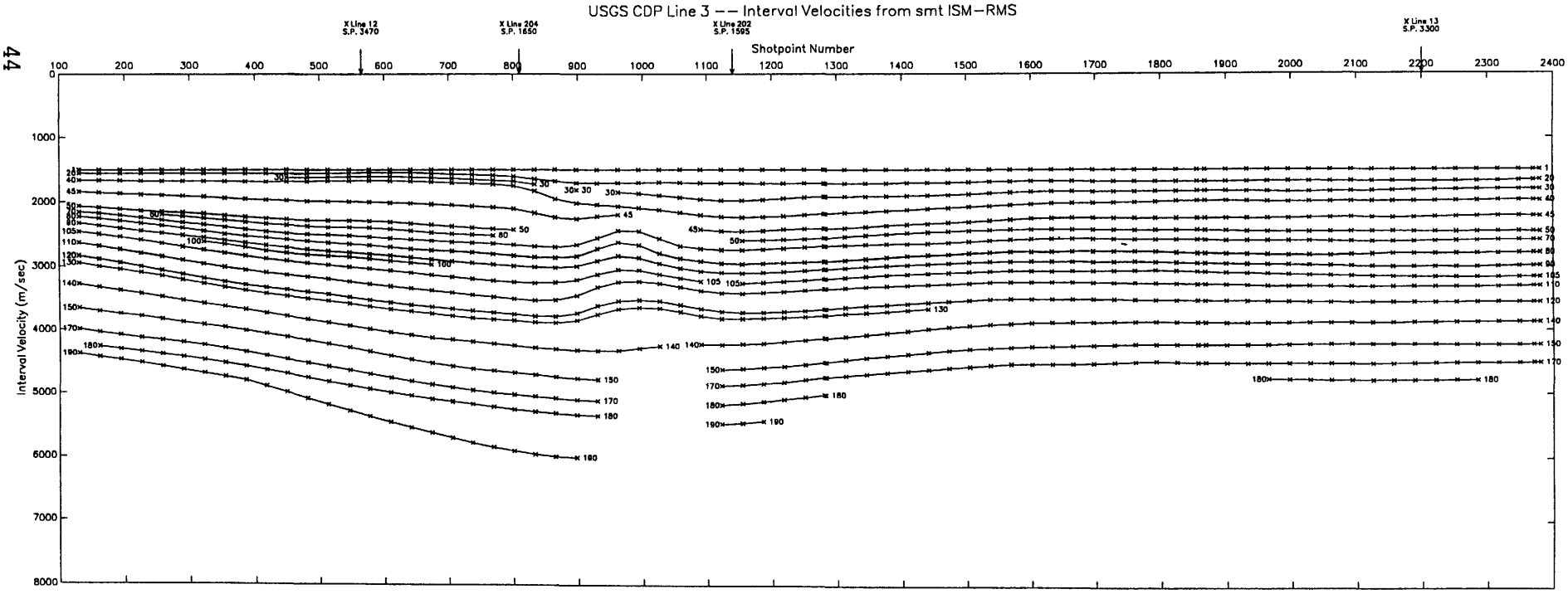

USGS CDP Line 5 -- Time Section

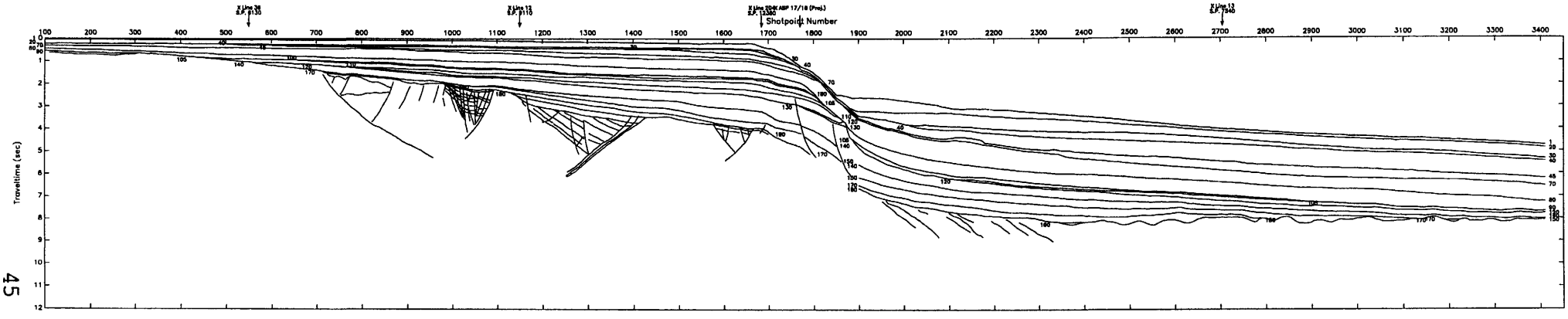

USGS CDP Line 5 -- Interval Velocities from smt ISM-RMS

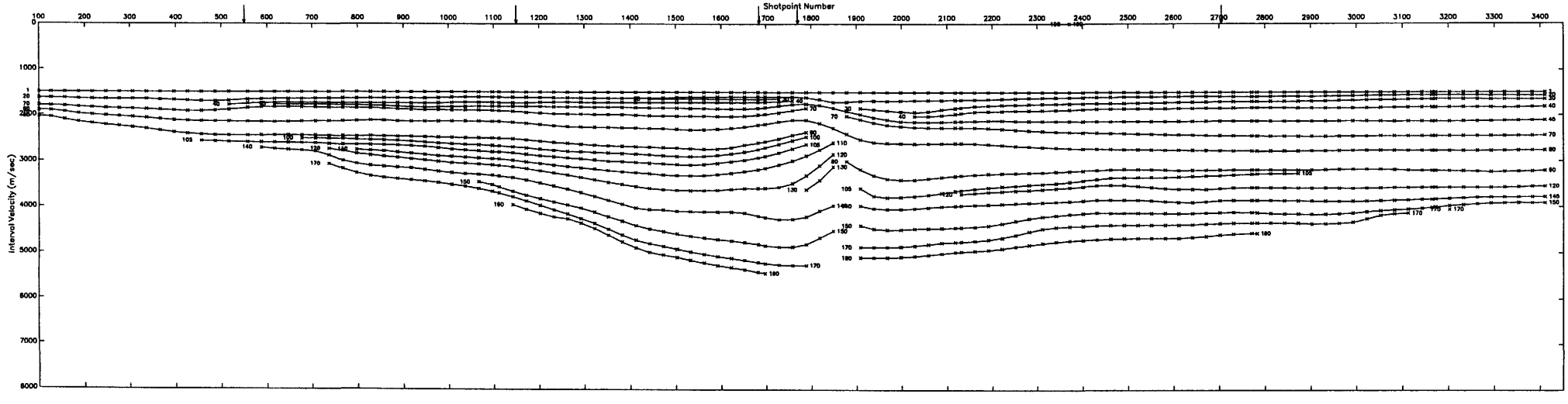

USGS CDP Line 6 -- Time Section

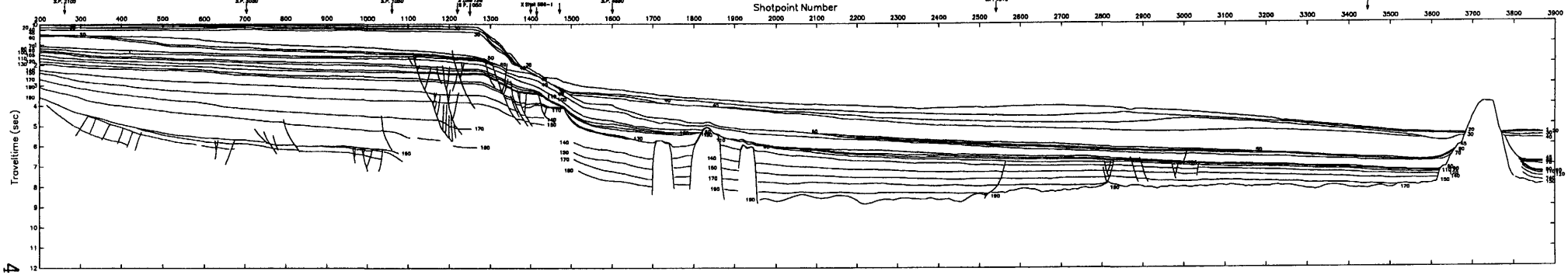

USGS CDP Line 6 -- Interval Velocities from smt ISM-RMS

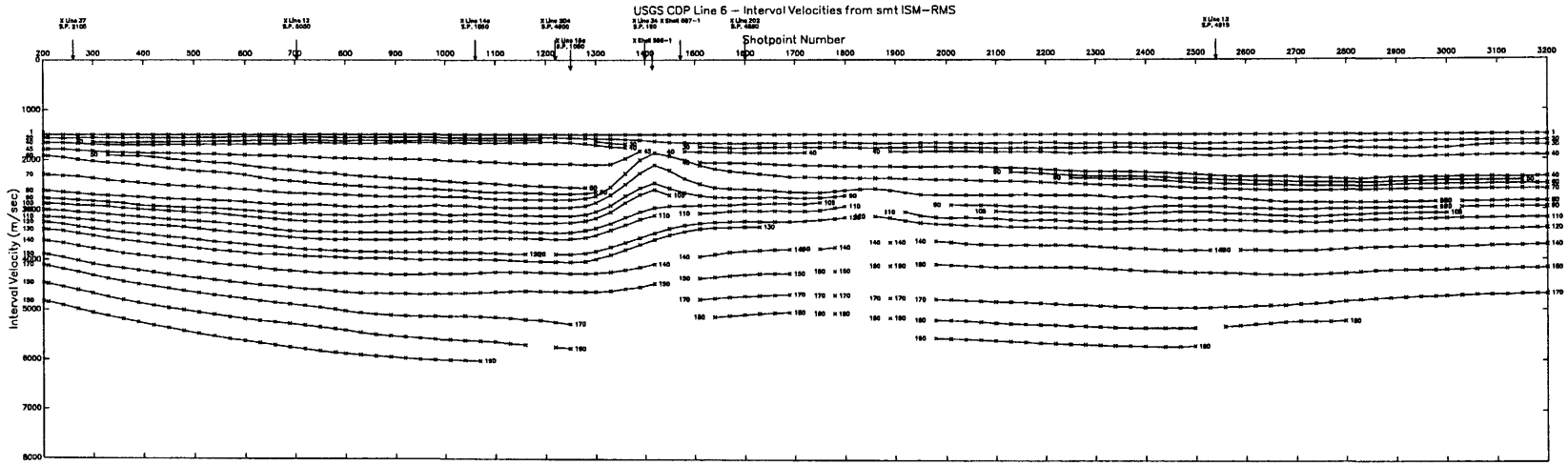

USGS CDP Line 7 – Time Section

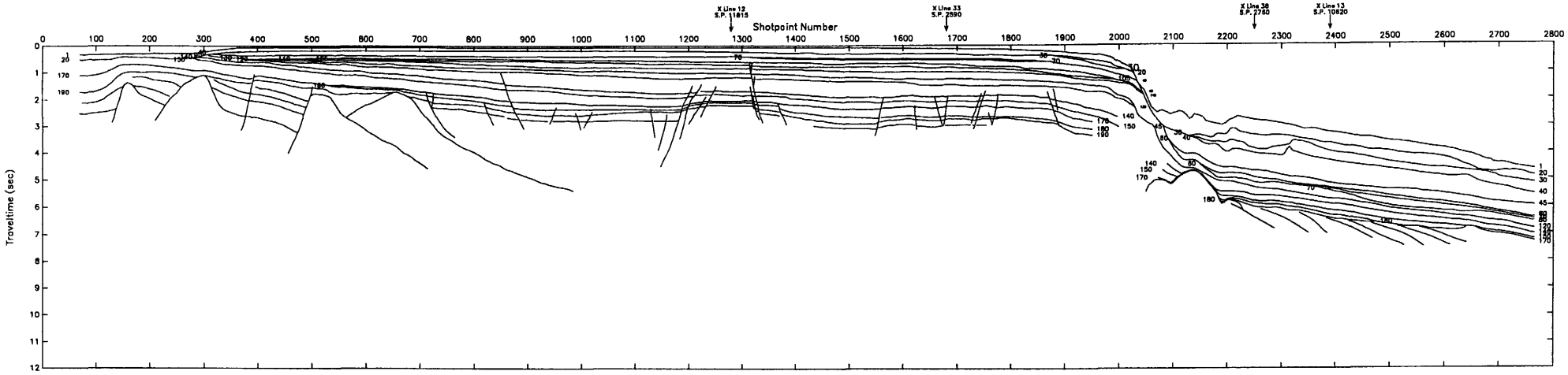

USGS CDP Line 7 -- Interval Velocities from smt ISM-RMS

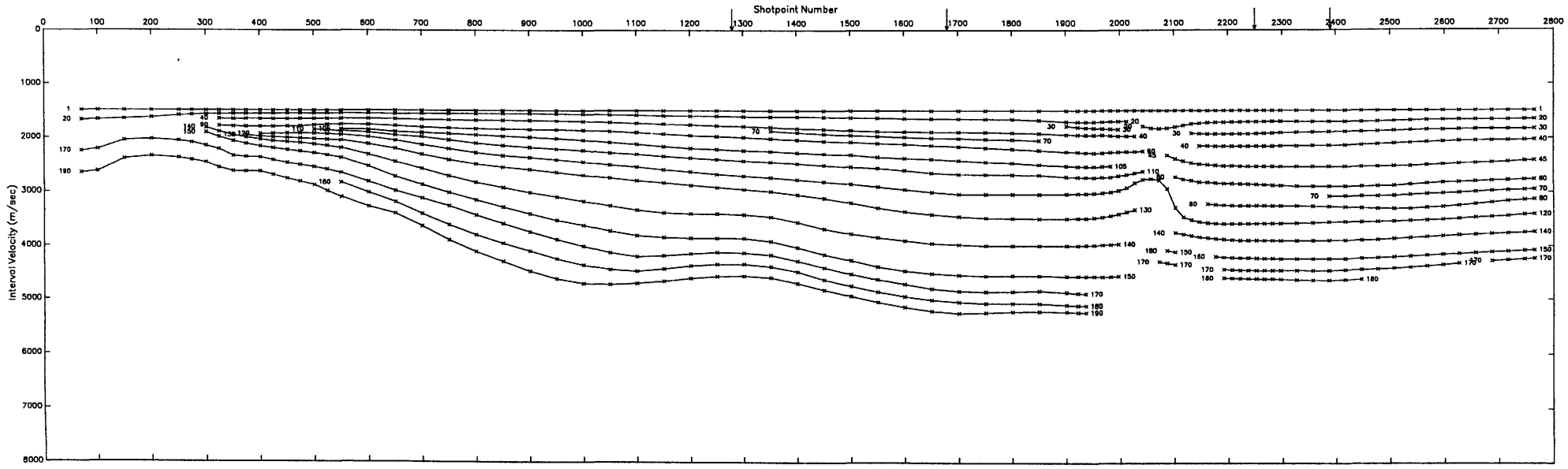

USGS CDP Line 8 -- Time Section

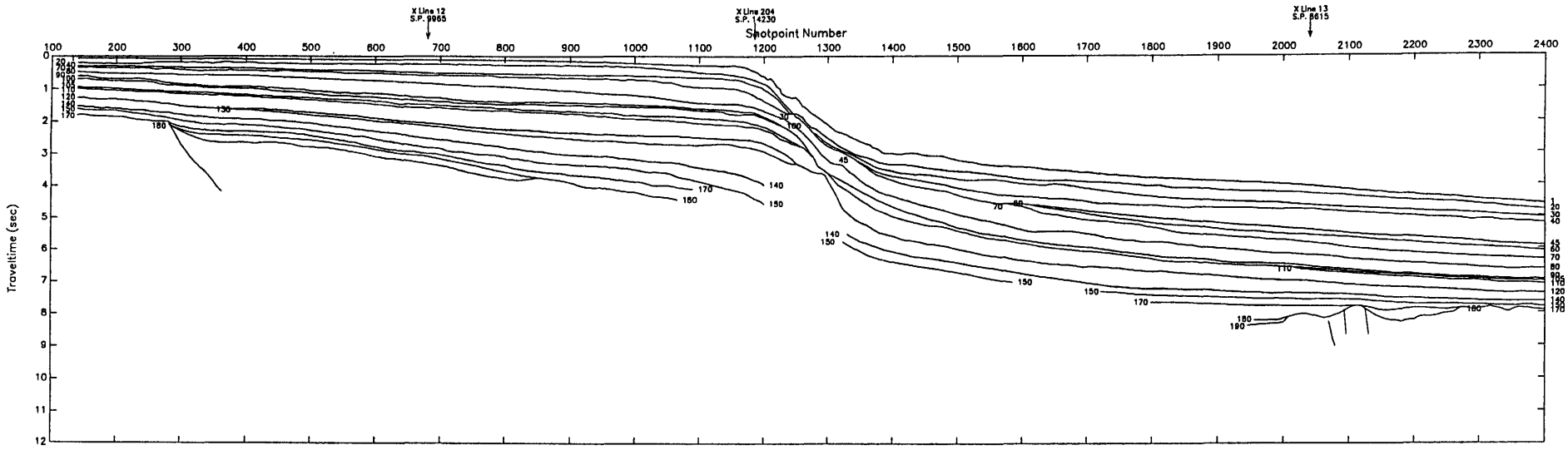

USGS CDP Line 8 -- Interval Velocities from smt ISM-RMS

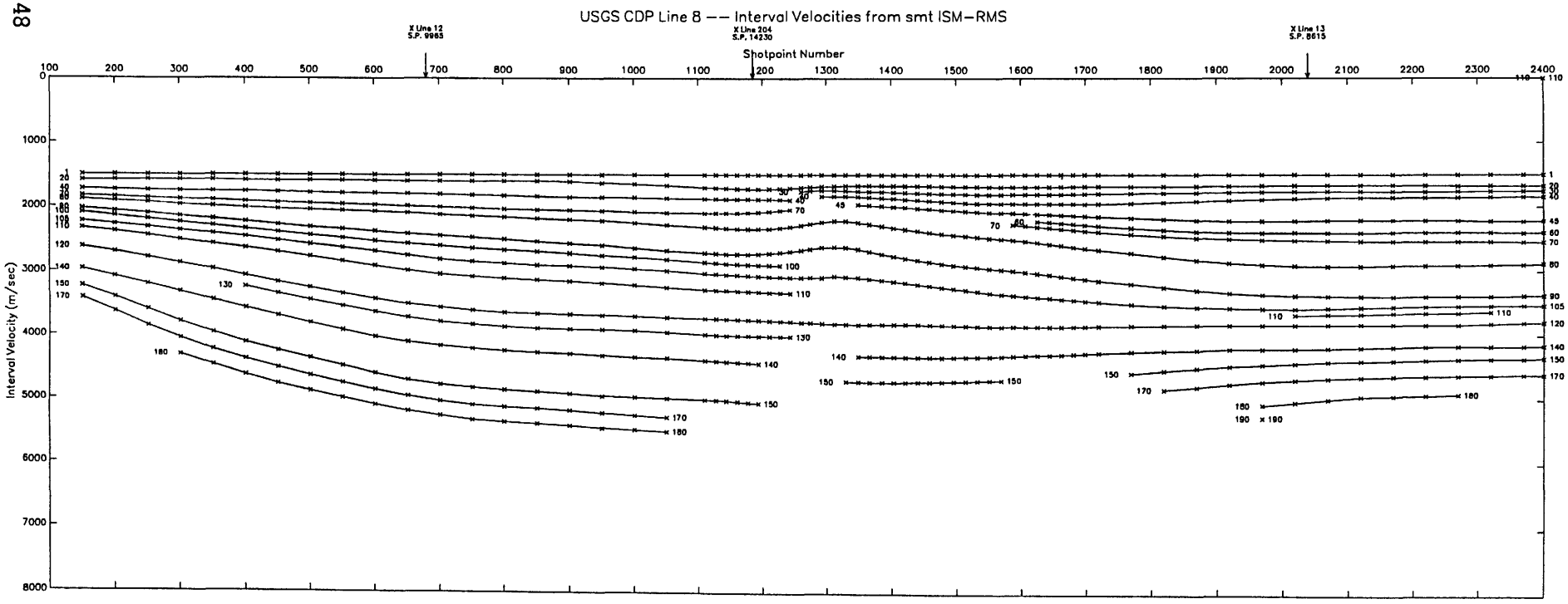

USGS CDP Line 9 -- Time Section

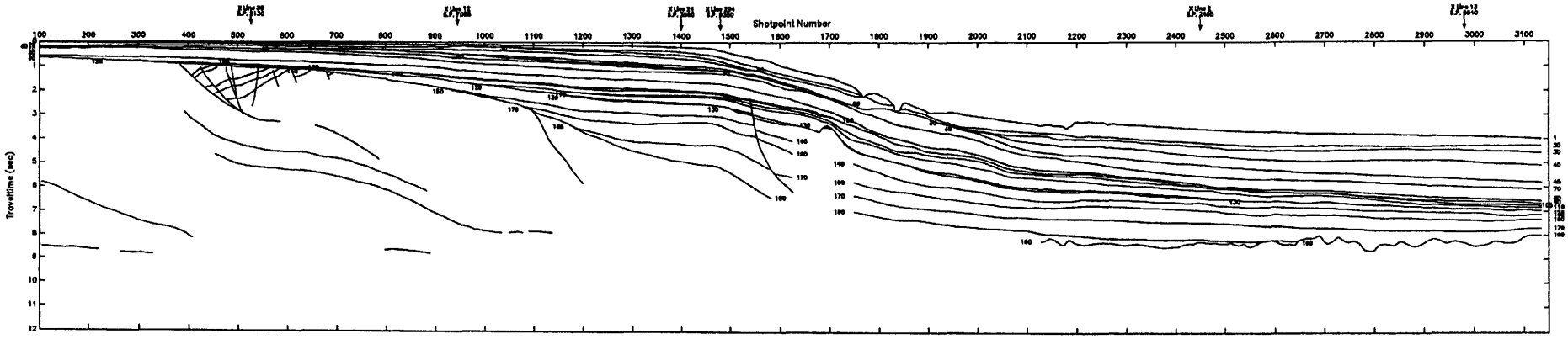

USGS CDP Line 9 -- Interval Velocities from smt ISM-RMS

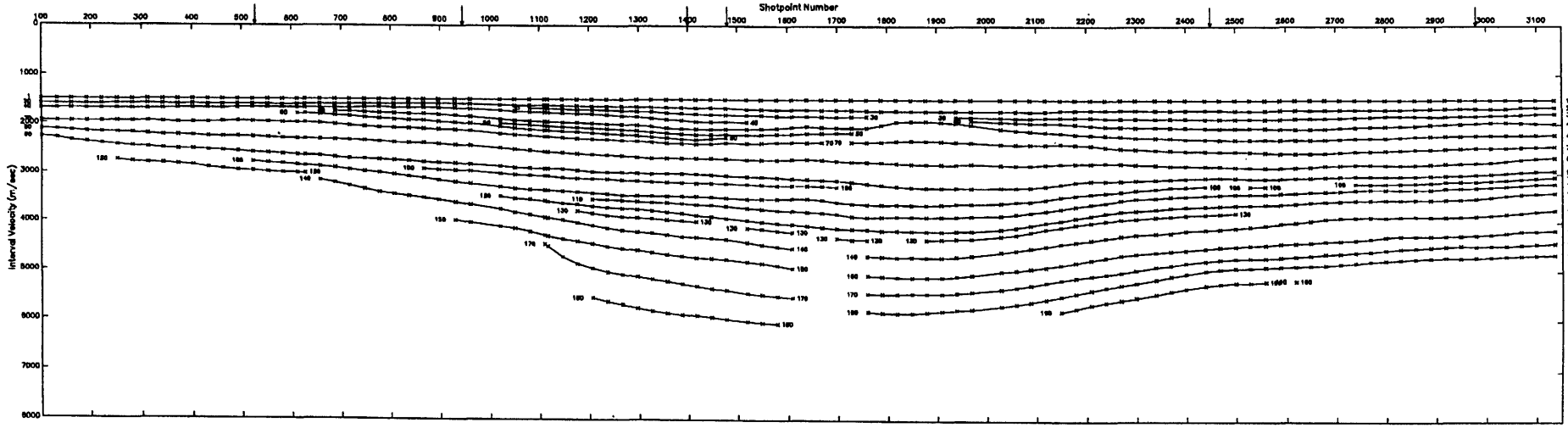

USGS CDP Line 10 -- Time Section

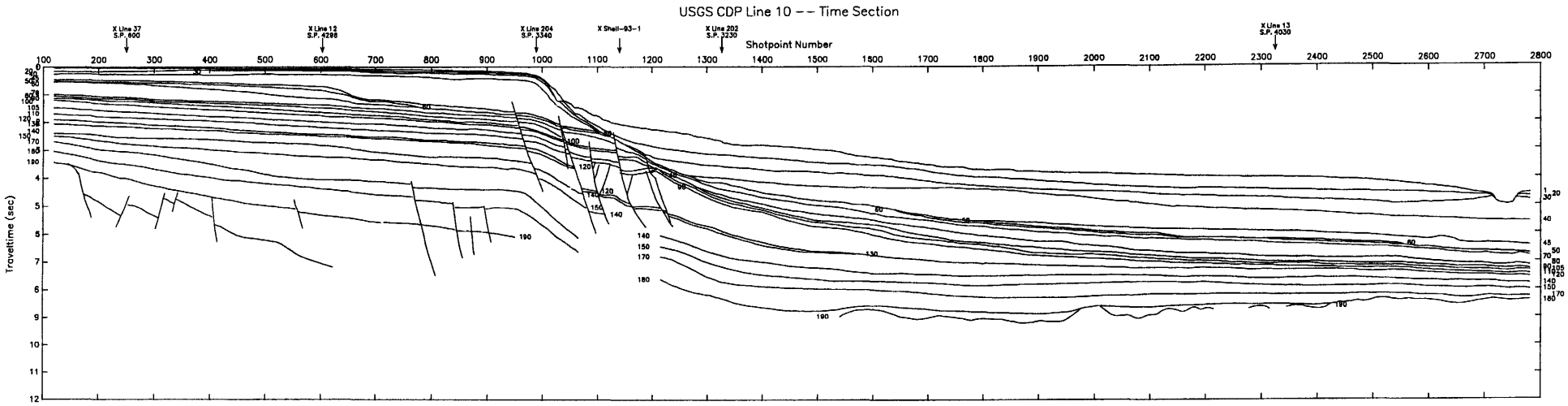

USGS CDP Line 10 – Intervol Velocities from smt ISM–RMS

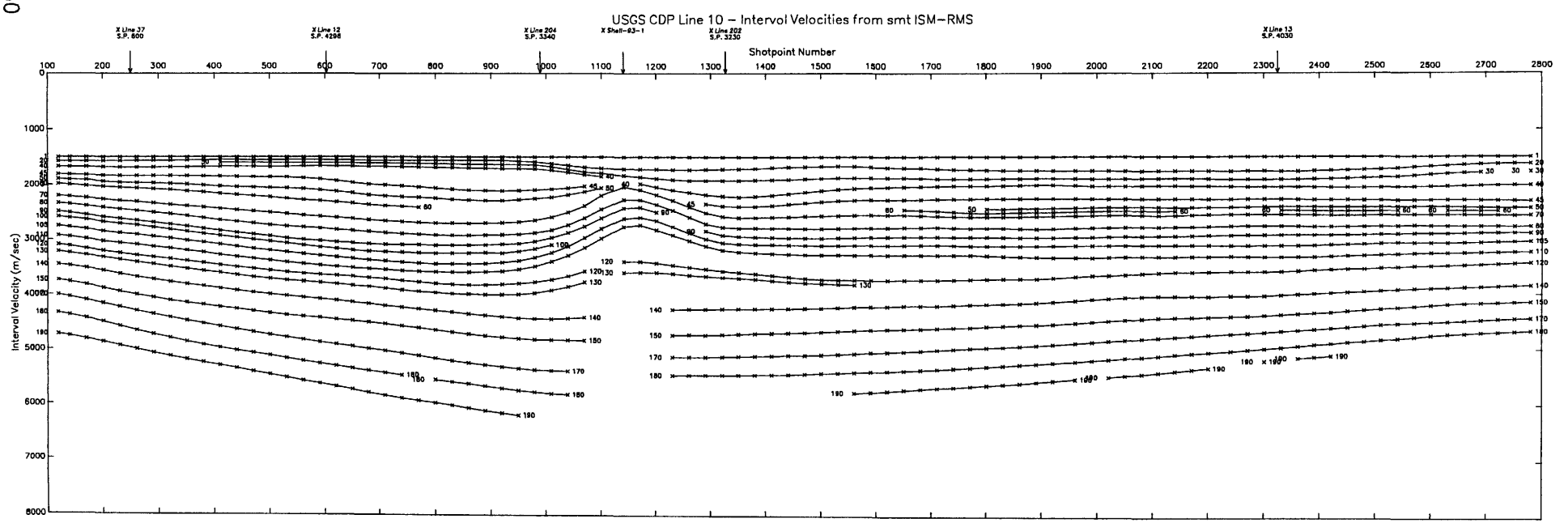

USGS CDP Line 11 -- Time Section

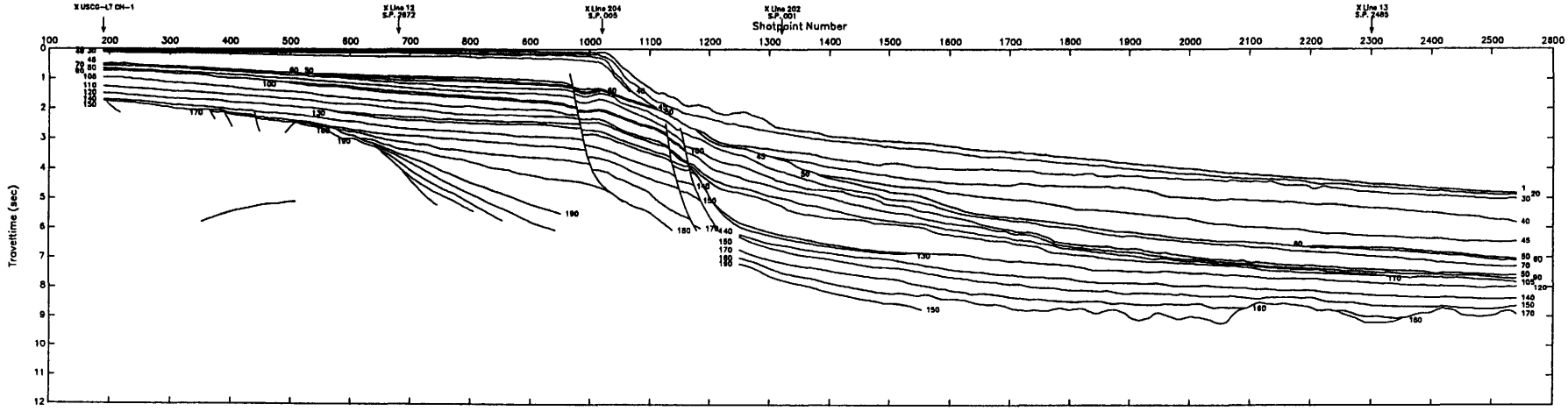

USGS CDP Line 11 -- Interval Velocities from smt ISM-RMS

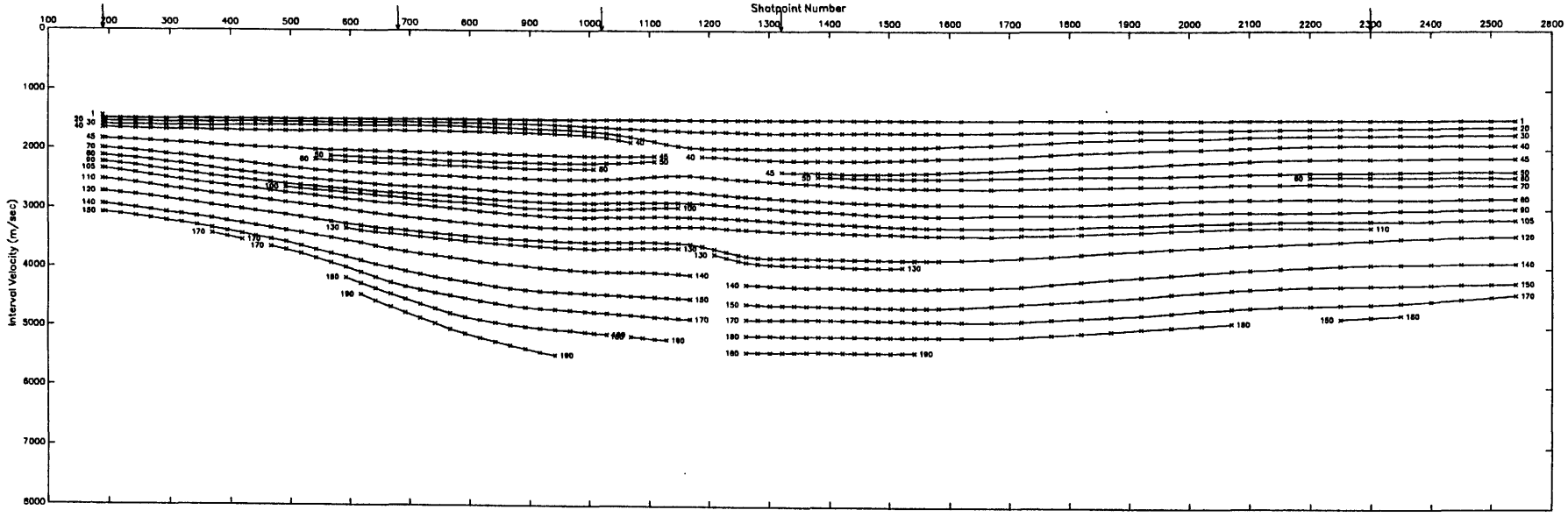

USGS CDP Line 12a -- Time Section

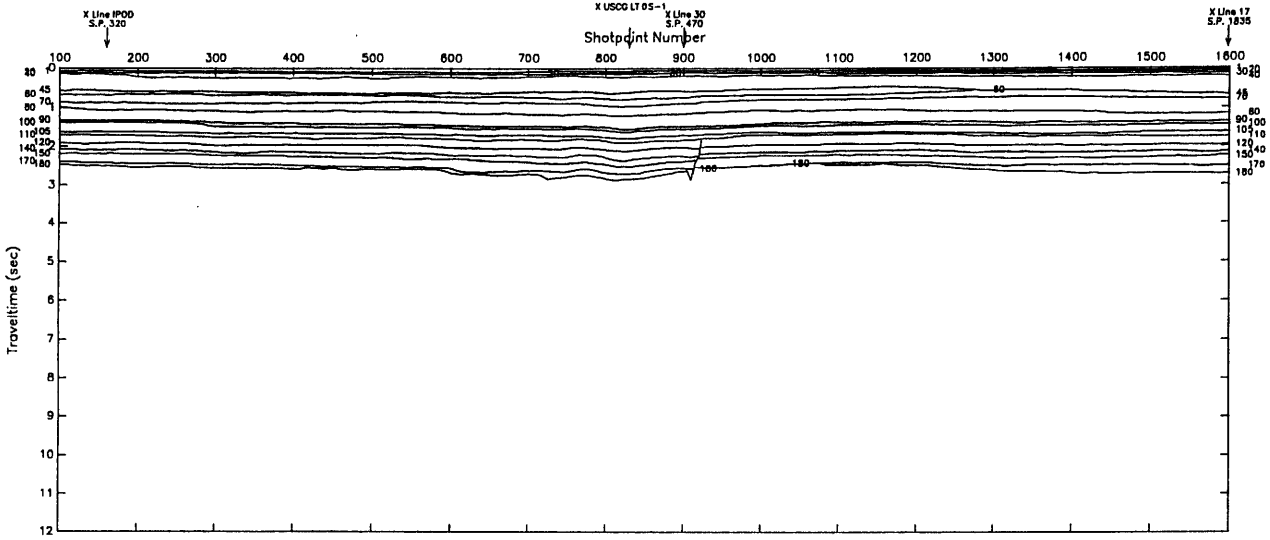

USGS CDP Line 12a -- Interval Velocities from smt ISM-RMS

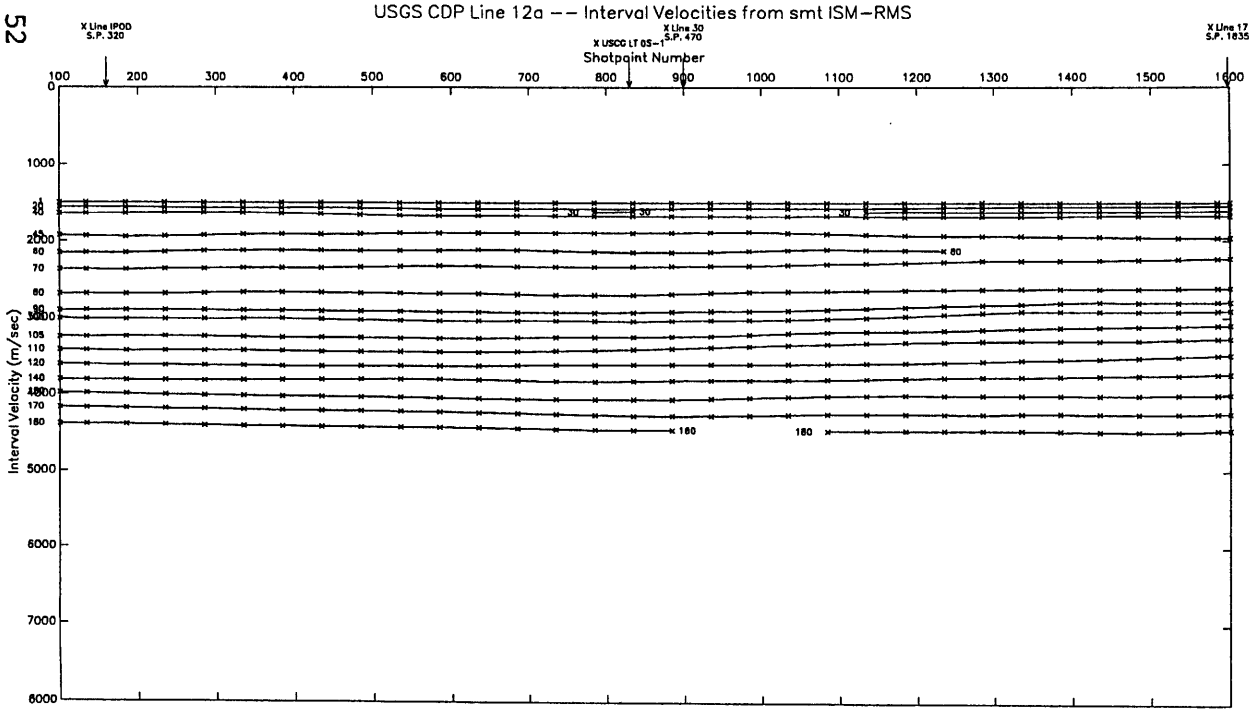

USGS CDP Line 12bc -- Time Section

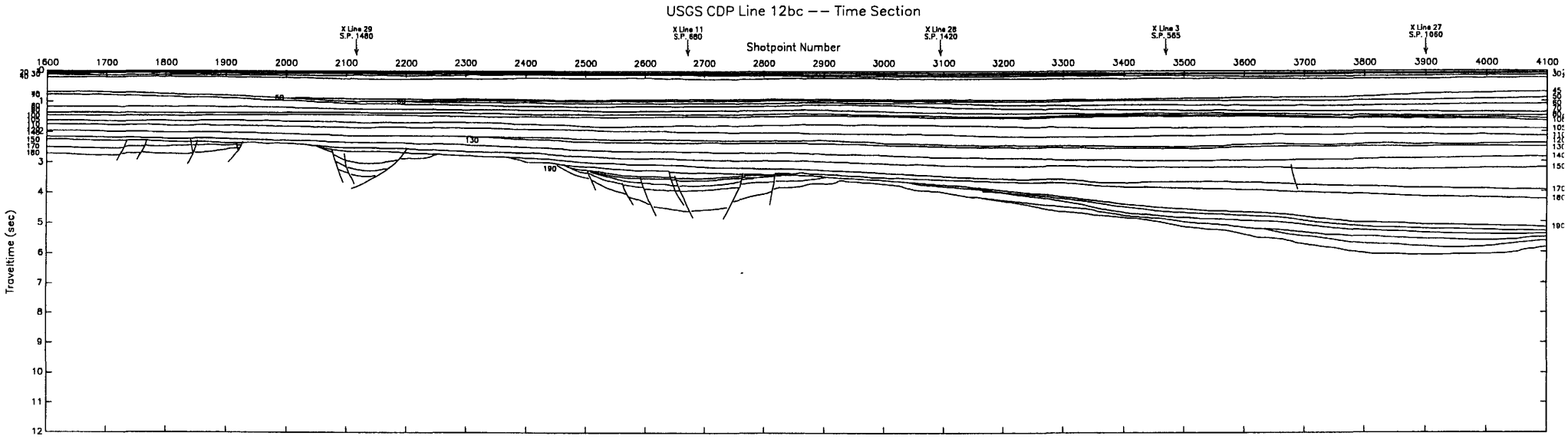

USGS CDP Line 12bc -- Interval Velocities from smt ISM-RMS

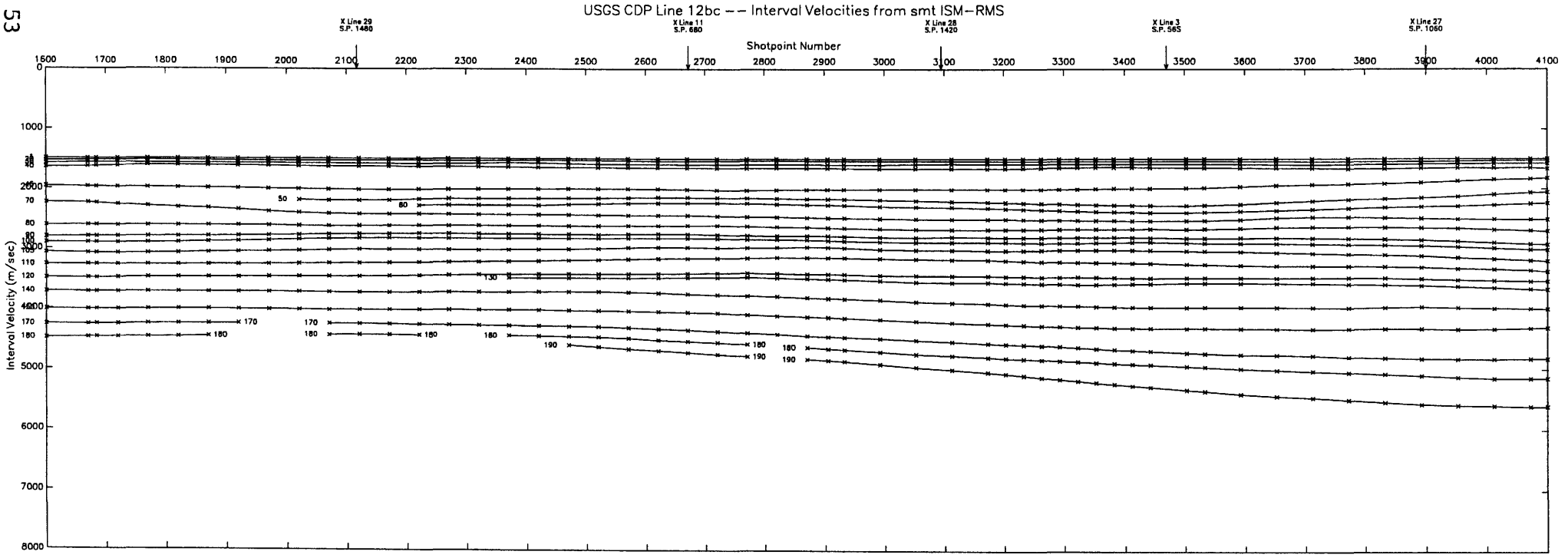

USGS CDP Line 12de -- Time Section

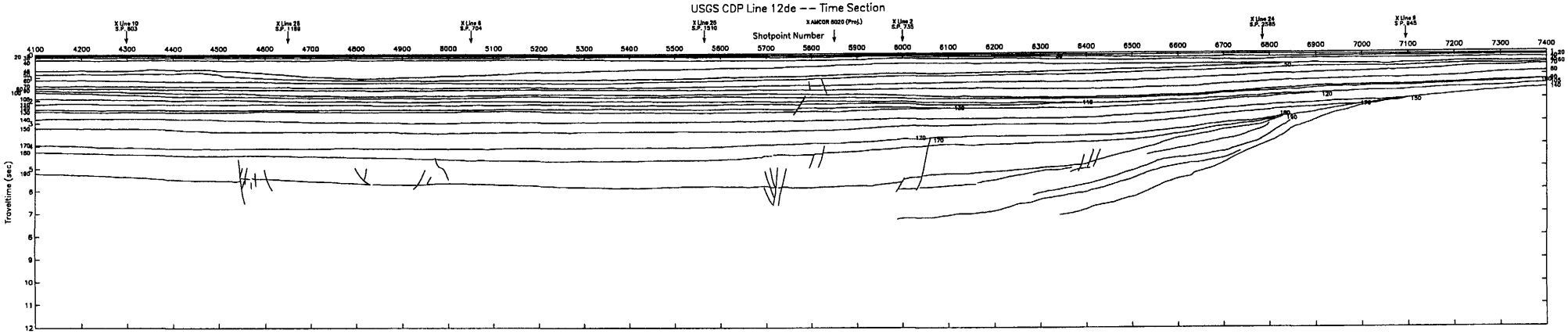

USGS CDP Line 12de -- Interval Velocities from smt ISM-RMS

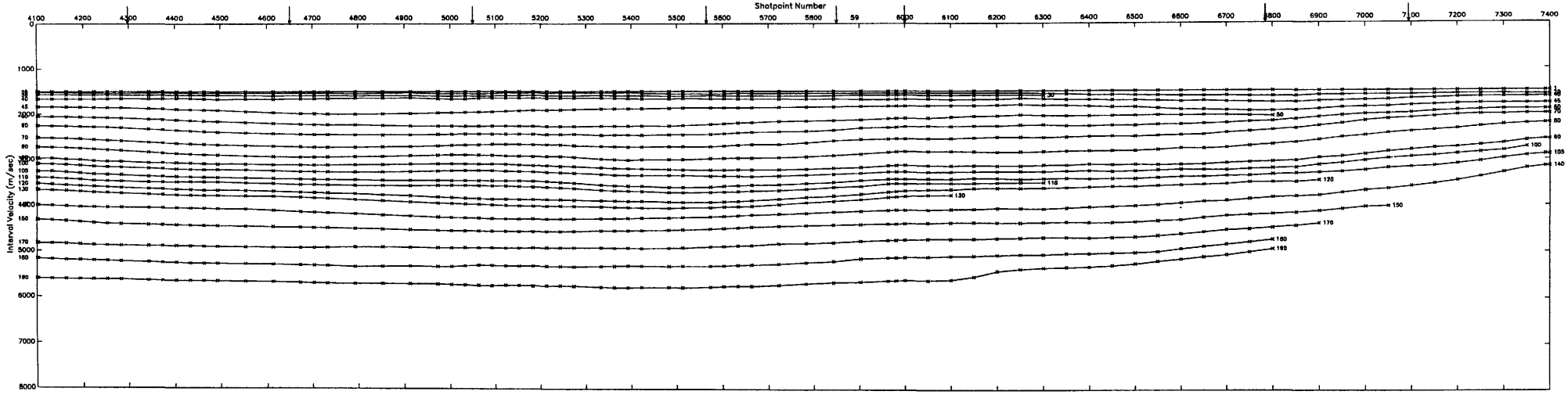

USGS CDP Line 12fg -- Time Section

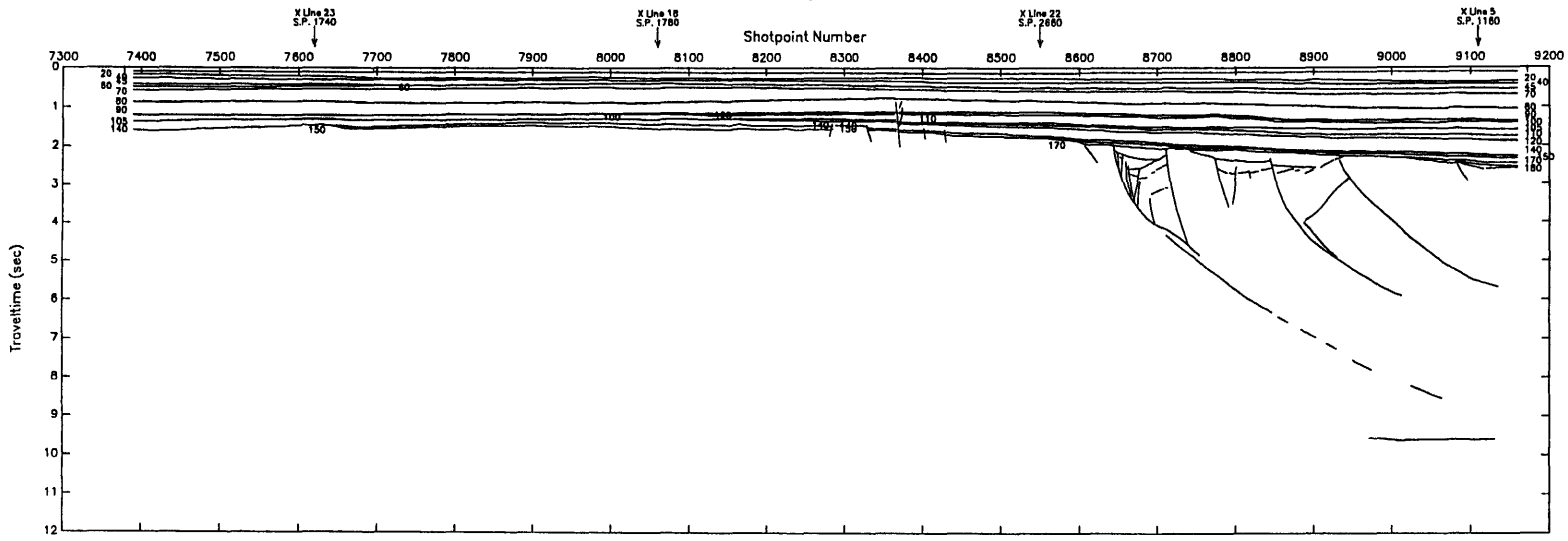

USGS CDP Line 12fg -- Interval Velocities from smt ISM-RMS

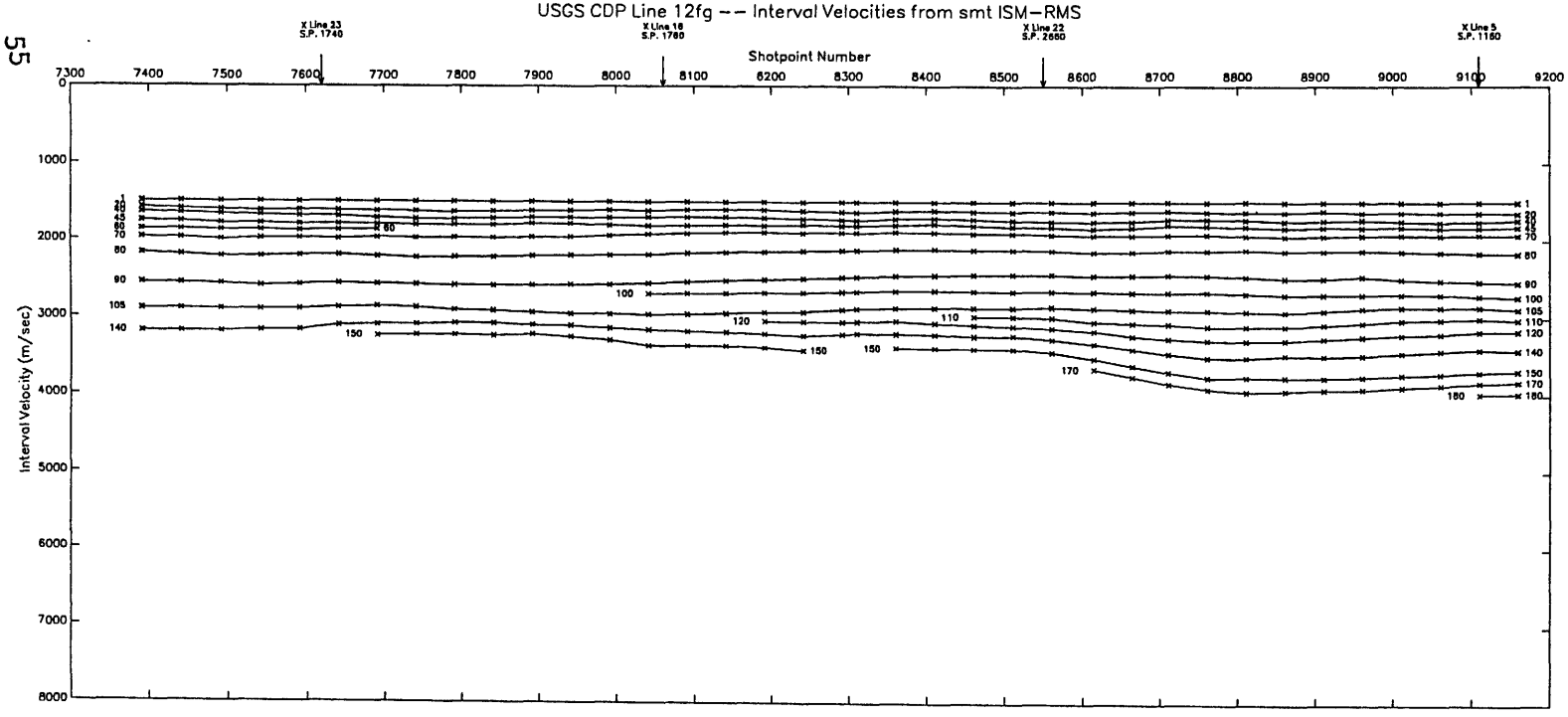

USGS CDP Line 12hi – Time Section

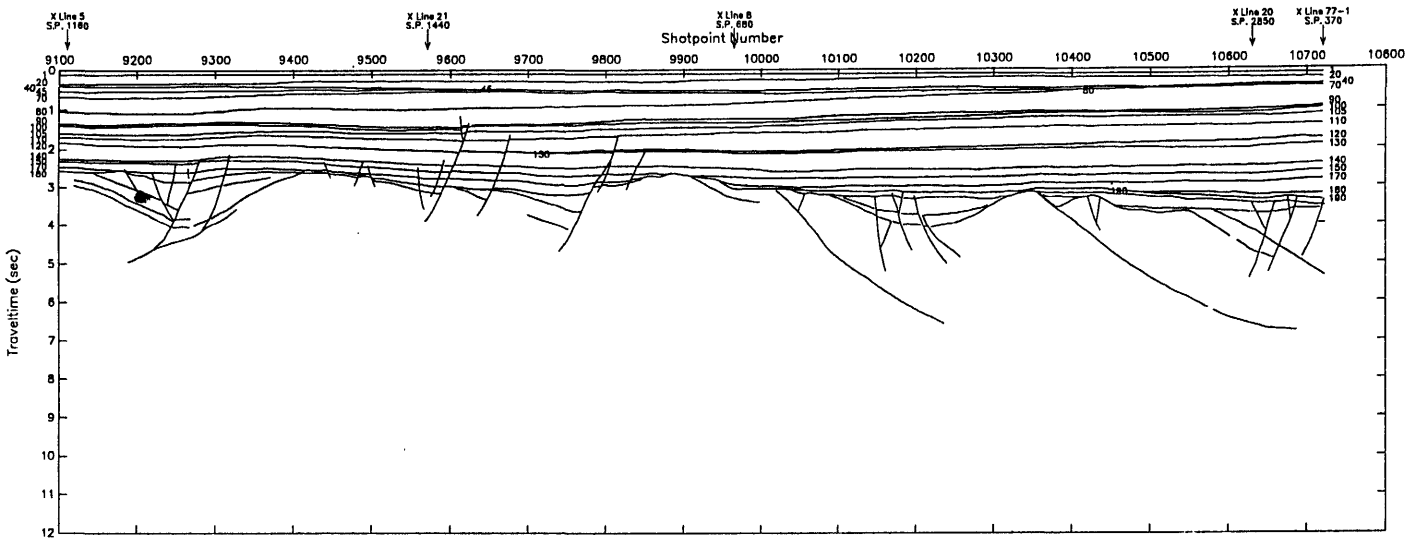

USGS CDP Line 12hi – Interval Velocities from smt ISM–RMS

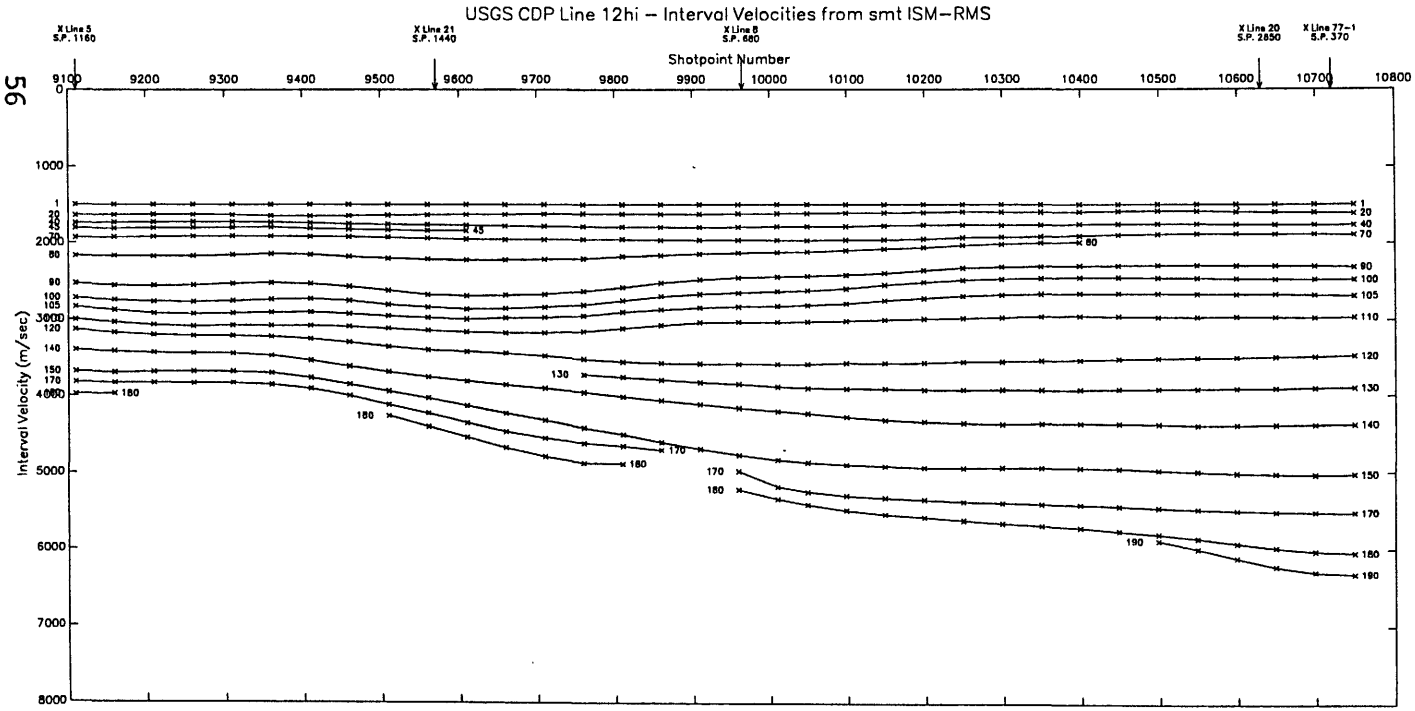

USGS CDP Line 12j1 -- Time Section

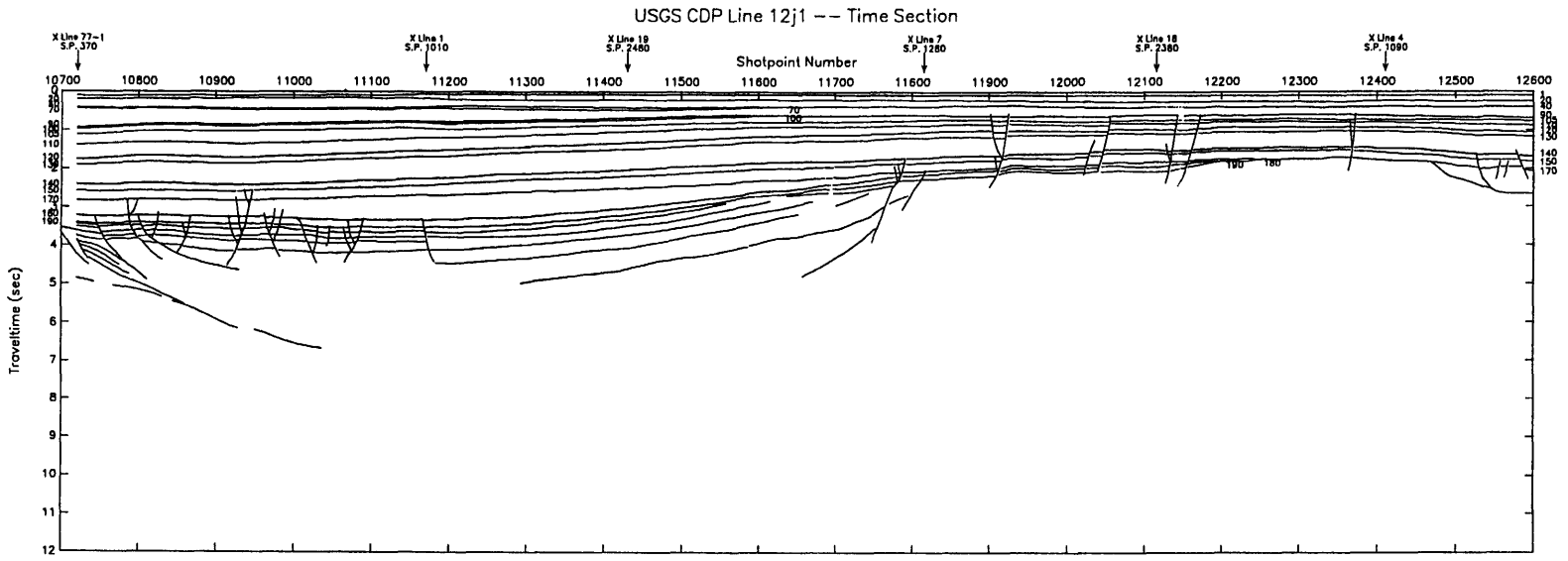

USGS CDP Line 12j1 – Interval Velocity from smt ISM–RMS

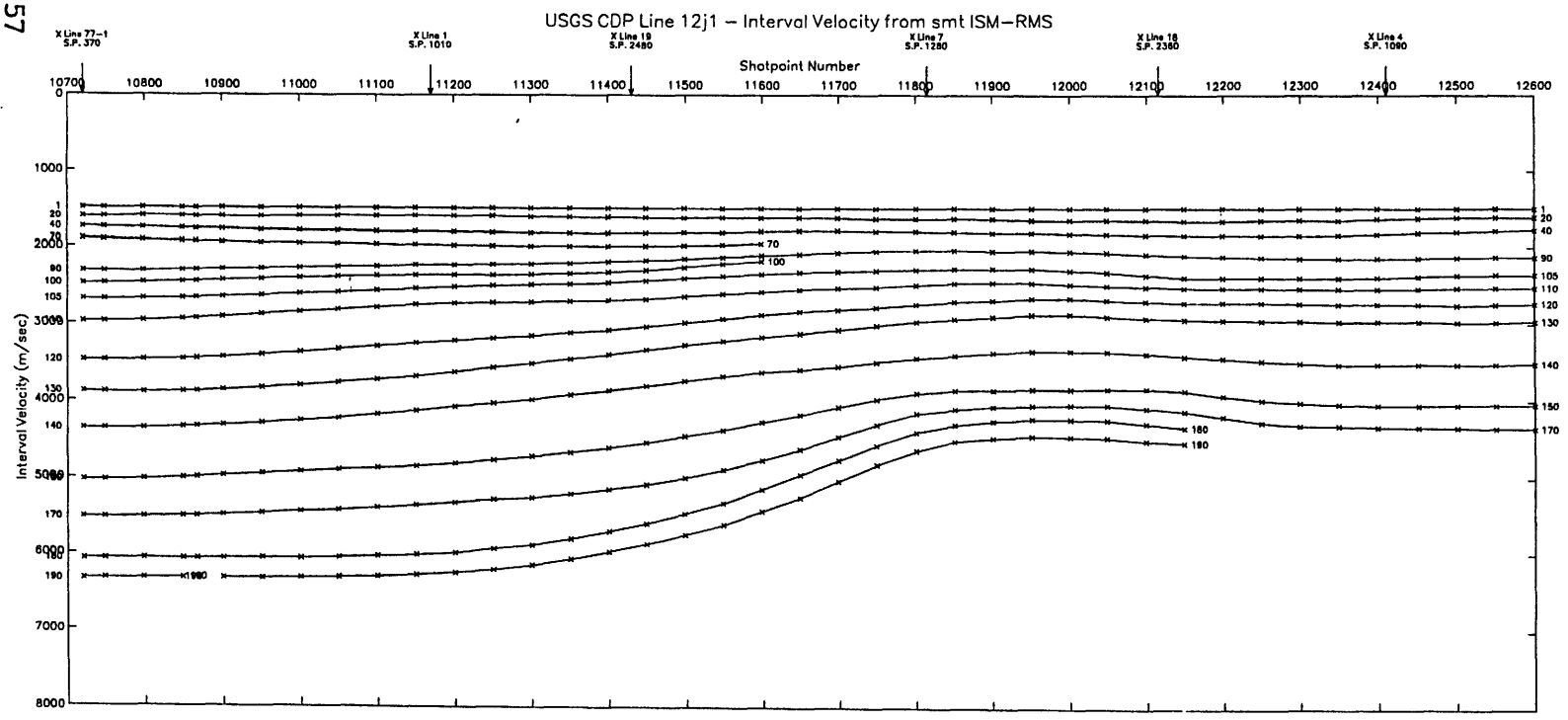

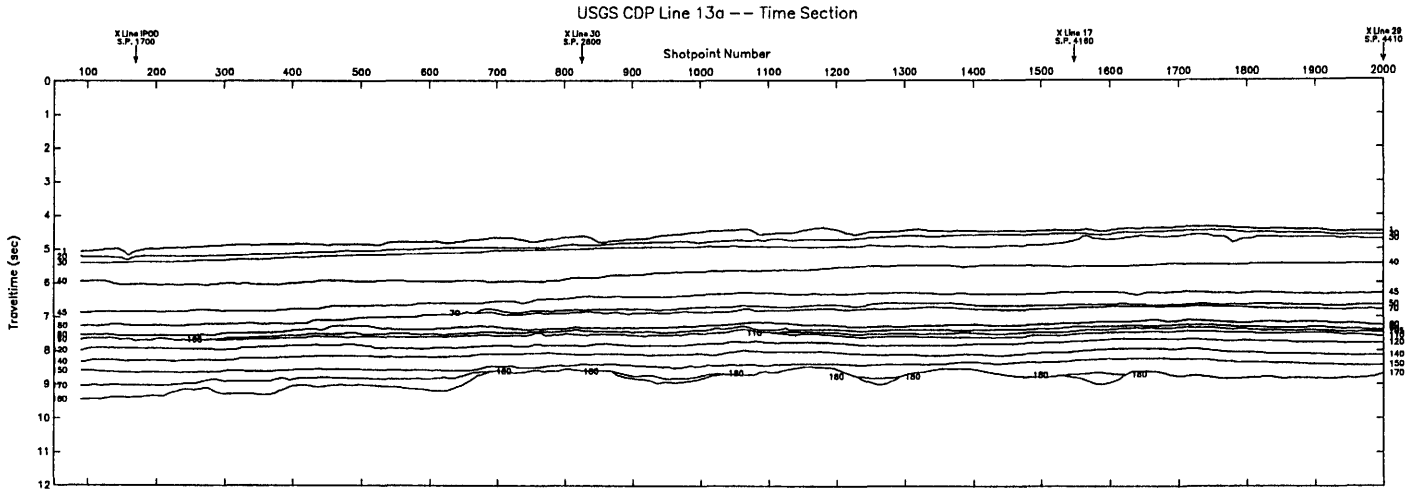
USGS CDP Line 13a -- Time Section
X Line 1POD S.P. 1700
X Line 30 S.P. 2800
X Line 17 S.P. 4180
X Line 29 S.P. 4410
Shotpoint Number
Traveltime (sec)

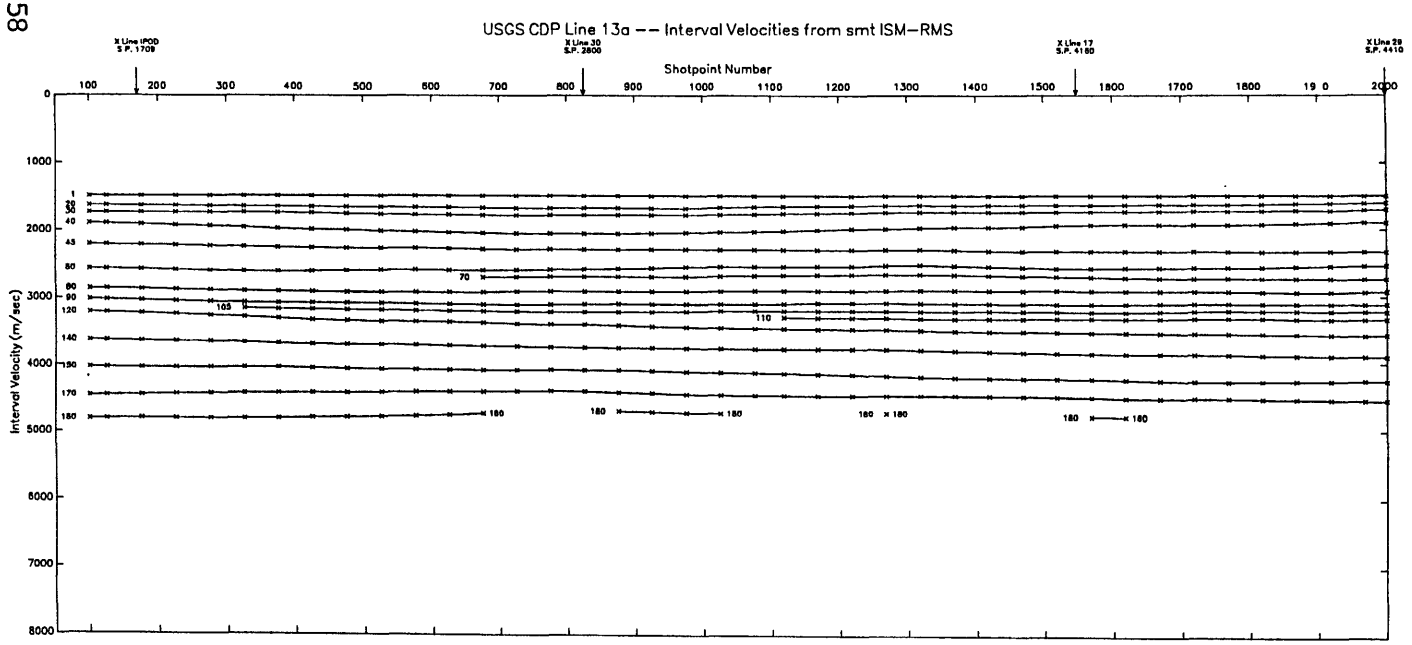
USGS CDP Line 13a -- Interval Velocities from smt ISM-RMS
X Line 1POD S.P. 1709
X Line 30 S.P. 2800
X Line 17 S.P. 4180
X Line 29 S.P. 4410
Shotpoint Number
Interval Velocity (m/sec)

USGS CDP Line 13b -- Time Section

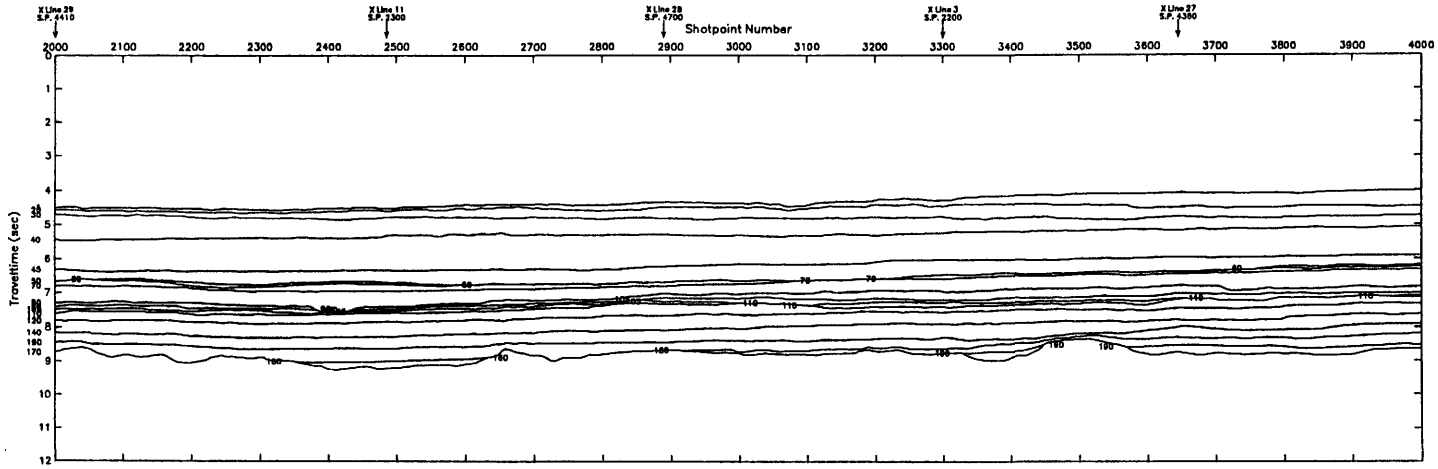

USGS CDP Line 13b -- Interval Velocities from smt ISM-RMS

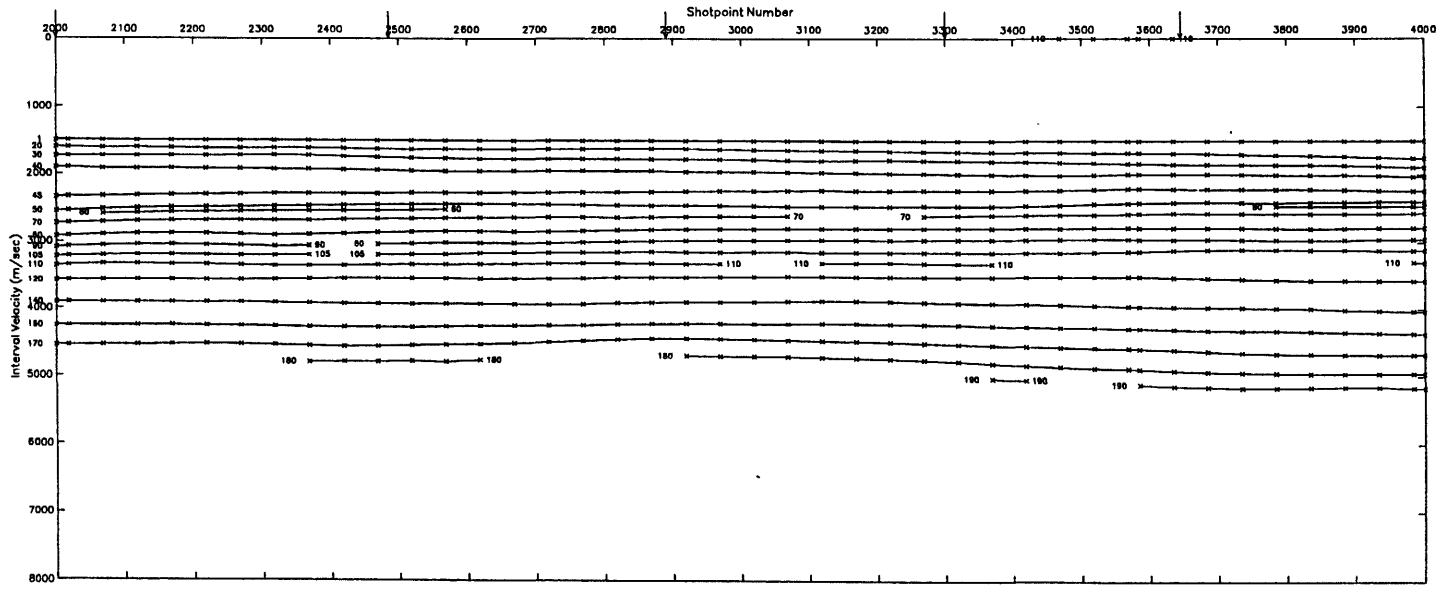

USGS CDP Line 13cd -- Time Section

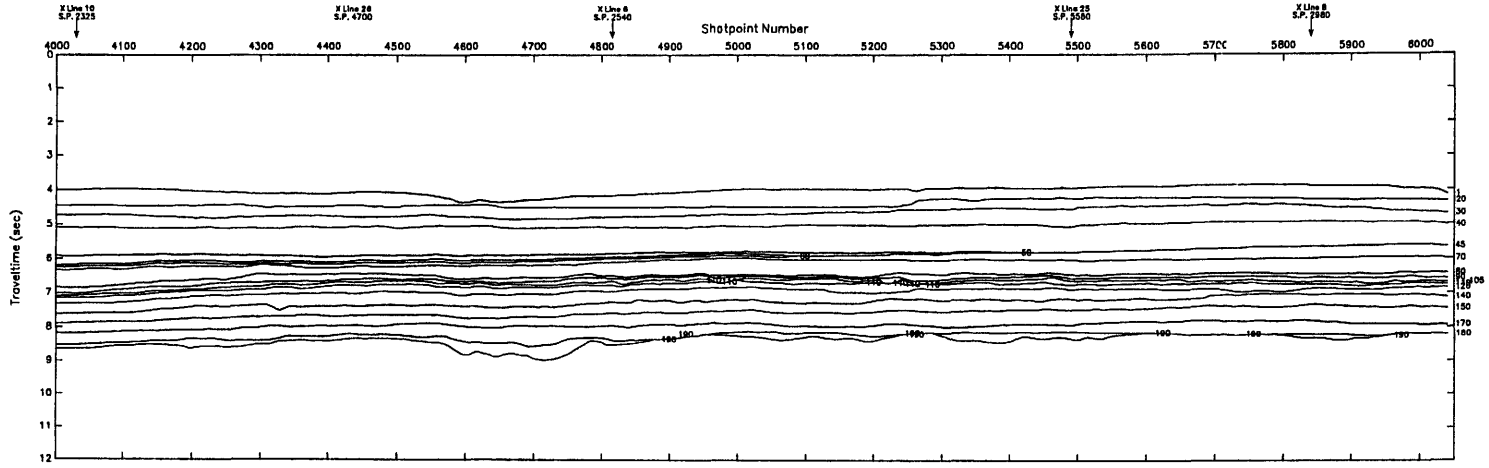

USGS CDP Line 13cd -- Interval Velocities from smt ISM-RMS

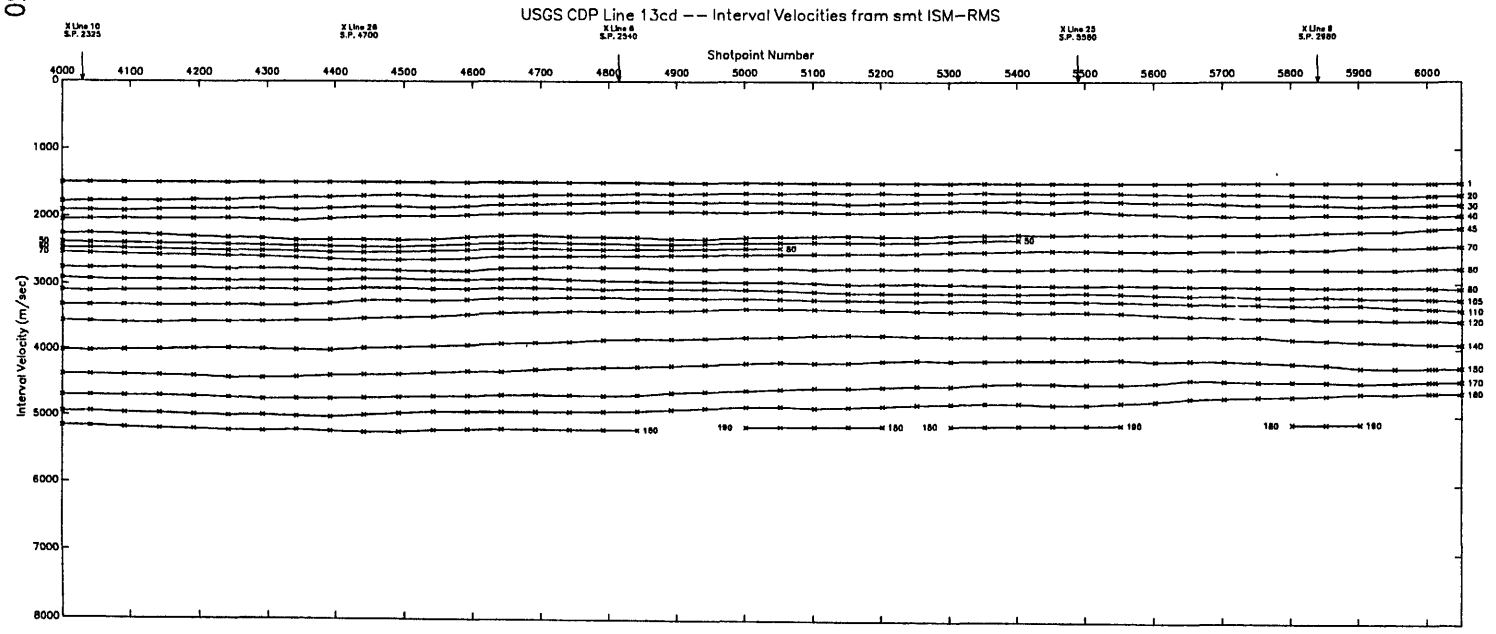

USGS CDP Line 13ef -- Time Section

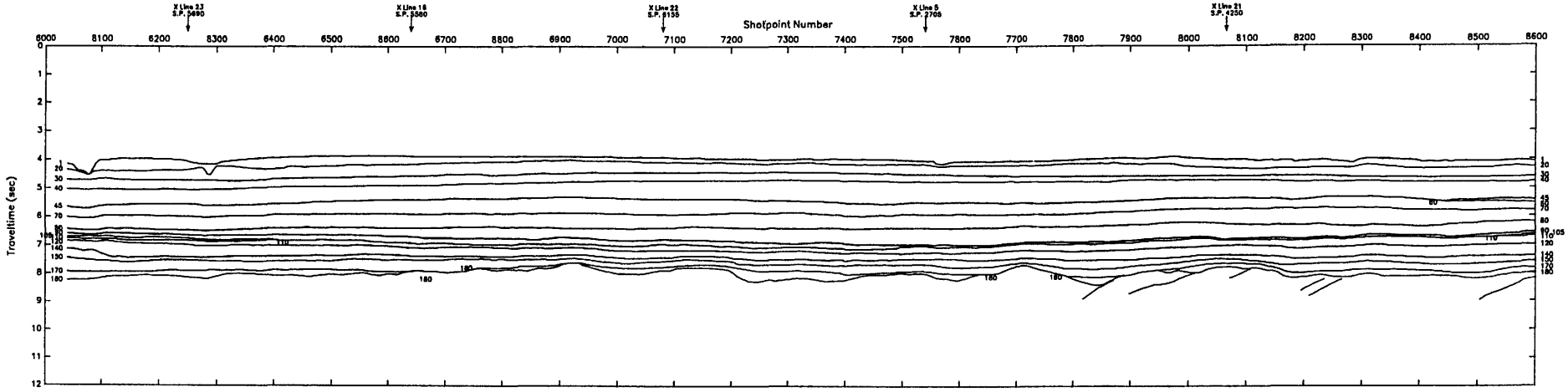

USGS CDP Line 13ef – Interval Velocities from smt ISM–RMS

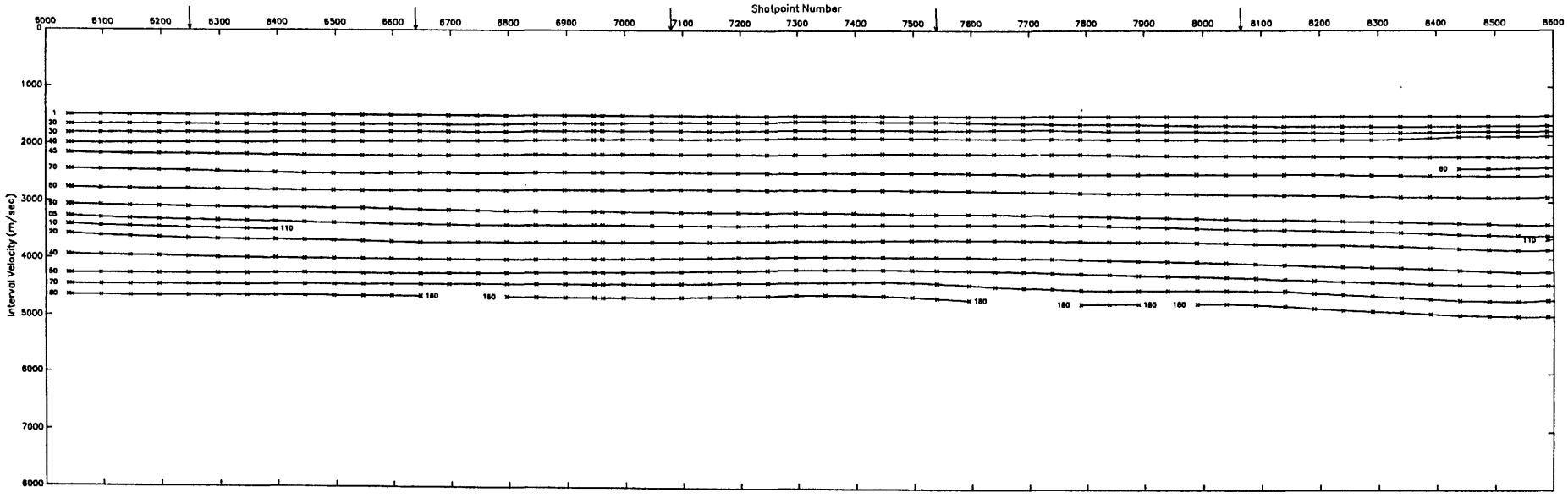

USGS CDP Line 13gh -- Time Section

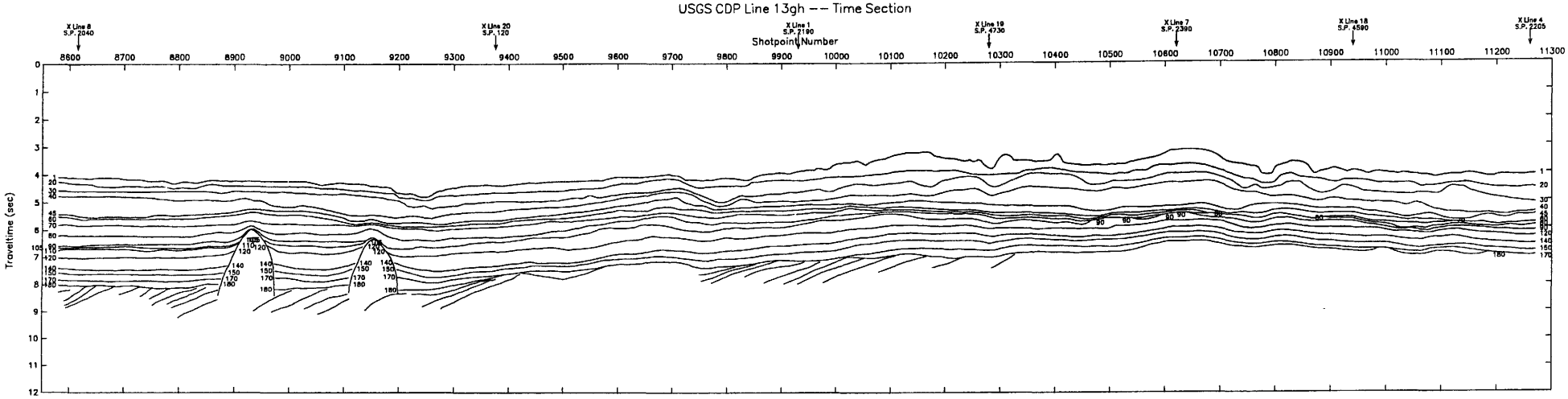

USGS CDP Line 13gh -- Interval Velocities from smt ISM-RMS

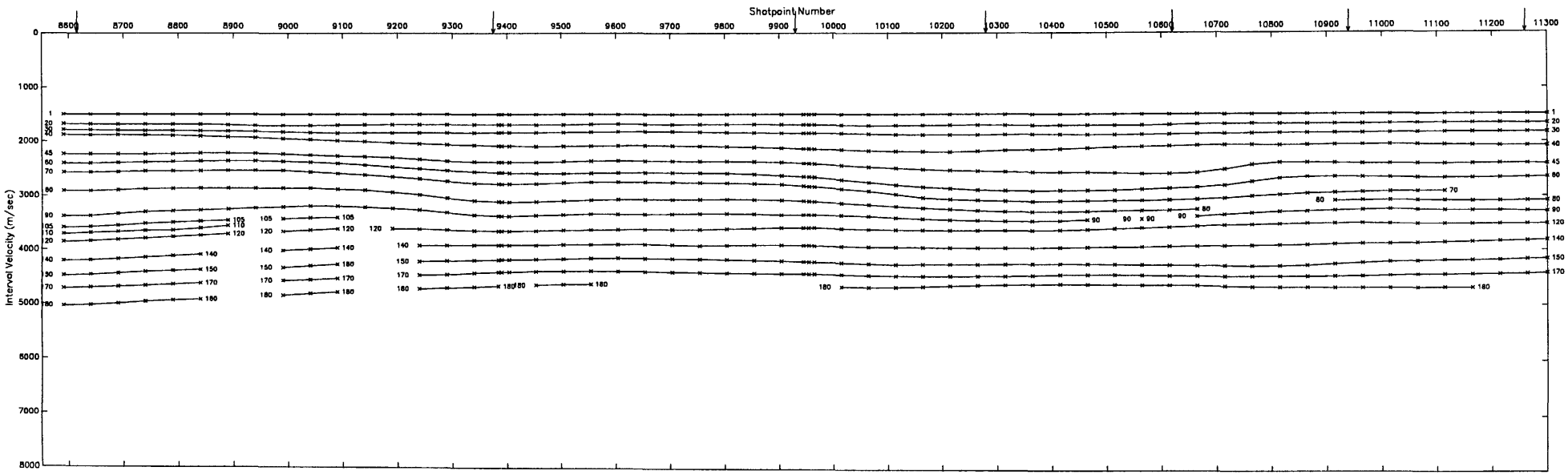

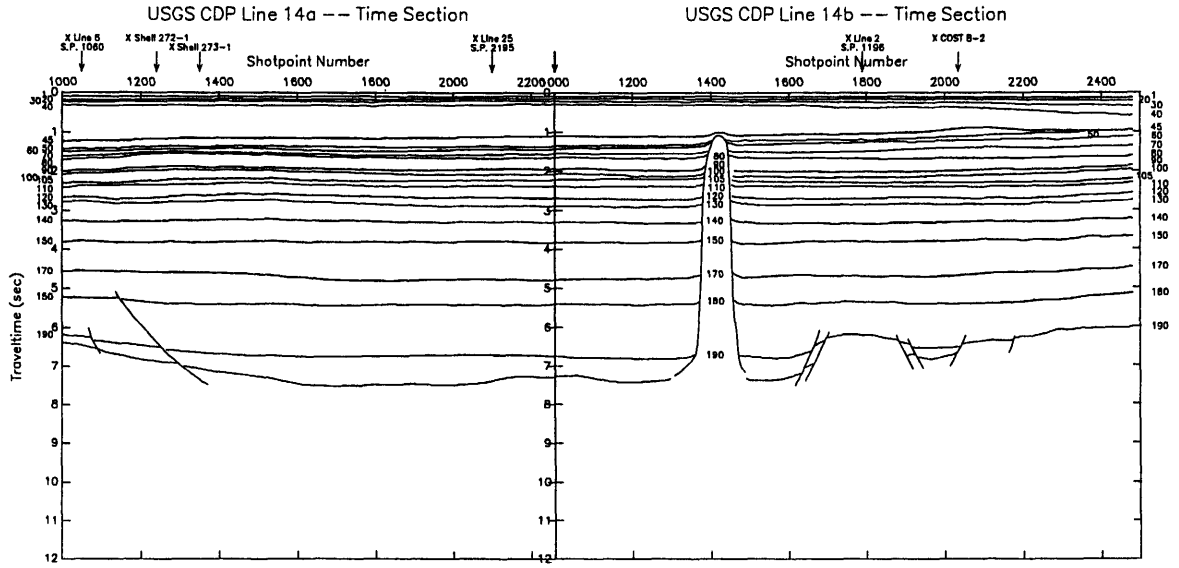
USGS CDP Line 14a -- Time Section
USGS CDP Line 14b -- Time Section
X Line 5 S.P. 1060
X Shell 272-1
X Shell 273-1
X Line 25 S.P. 2195
X Line 2 S.P. 1196
X COST B-2
Shotpoint Number
Traveltime (sec)

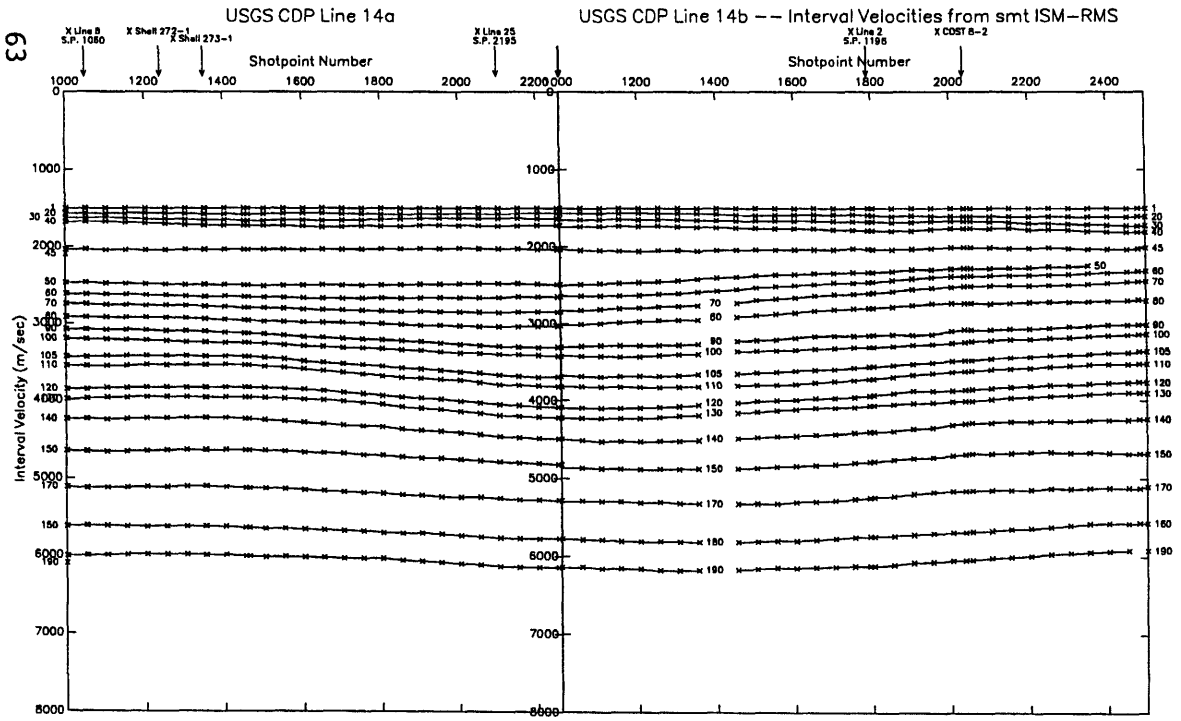
USGS CDP Line 14a
USGS CDP Line 14b -- Interval Velocities from smt ISM-RMS
X Line 5 S.P. 1060
X Shell 272-1
X Shell 273-1
X Line 25 S.P. 2195
X Line 2 S.P. 1196
X COST B-2
Shotpoint Number
Interval Velocity (m/sec)

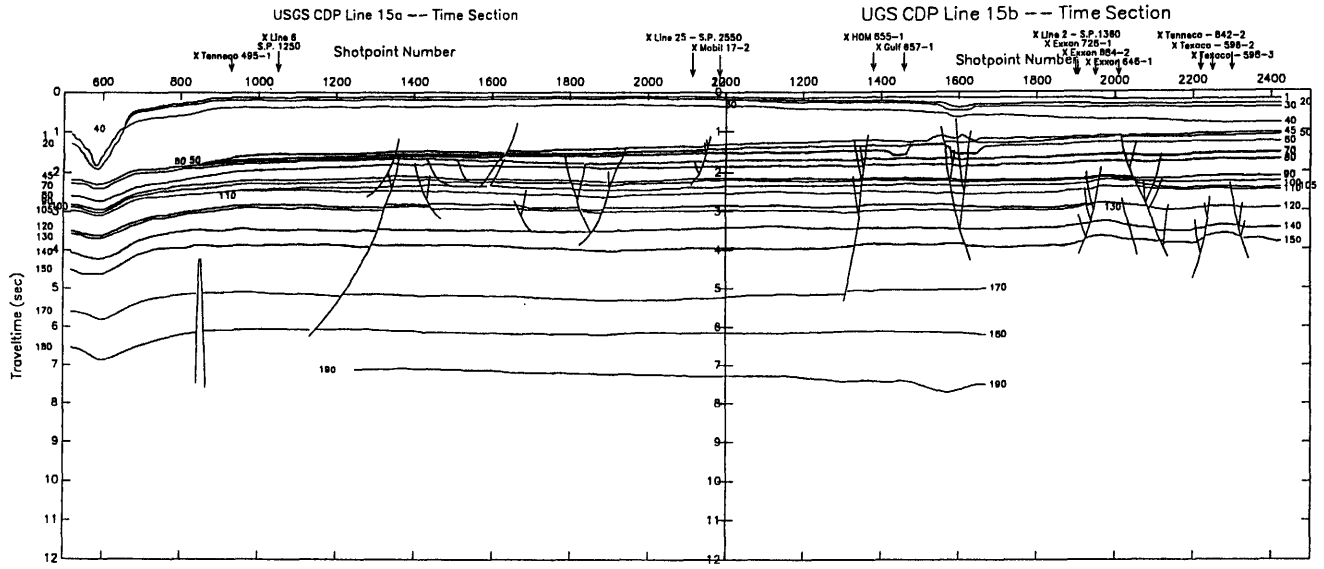
USGS CDP Line 15a -- Time Section
UGS CDP Line 15b -- Time Section
Shotpoint Number
Traveltime (sec)
X Tenneco 495-1
X Line 6 S.P. 1250
X Line 25 - S.P. 2550
X Mobil 17-2
X HOM 655-1
X Gulf 657-1
X Line 2 - S.P.1380
X Exxon 728-1
X Exxon 884-2
X Exxon 646-1
X Tenneco - 842-2
X Texaco - 596-2
X Texaco - 596-3

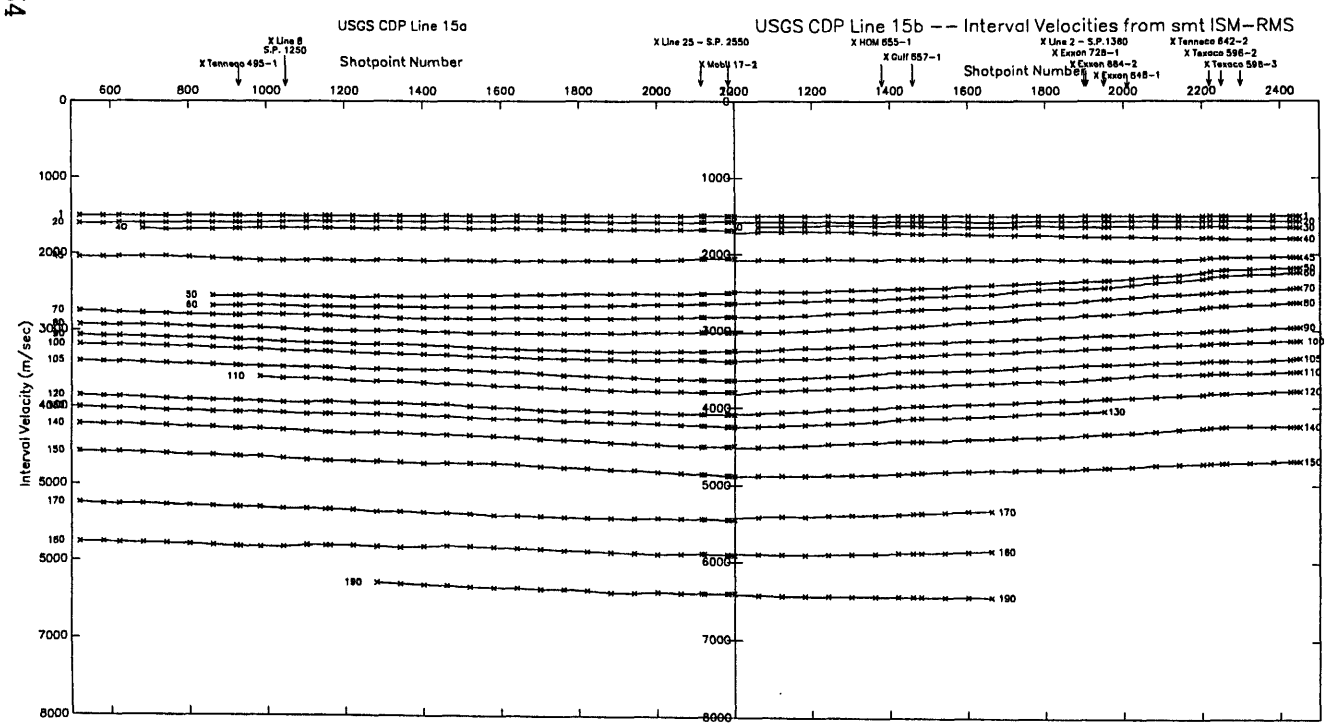
USGS CDP Line 15a
USGS CDP Line 15b -- Interval Velocities from smt ISM-RMS
Shotpoint Number
Interval Velocity (m/sec)
X Tenneco 495-1
X Line 6 S.P. 1250
X Line 25 - S.P. 2550
X Mobil 17-2
X HOM 655-1
X Gulf 657-1
X Line 2 - S.P.1380
X Exxon 728-1
X Exxon 884-2
X Exxon 646-1
X Tenneco 842-2
X Texaco 596-2
X Texaco 596-3

USGS CDP Line 16 -- Time Section

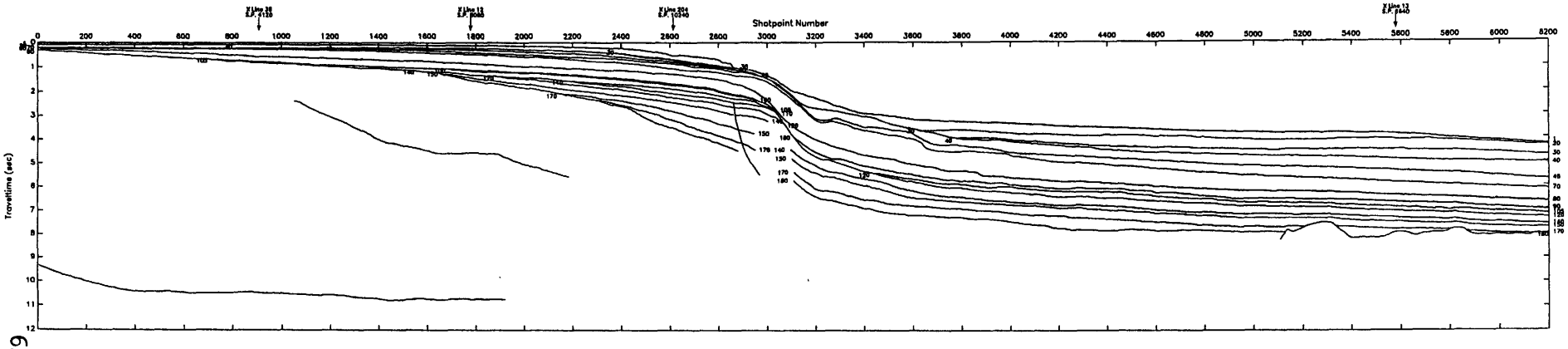

USGS CDP Line 16 -- Interval Velocities from smt ISM-RMS

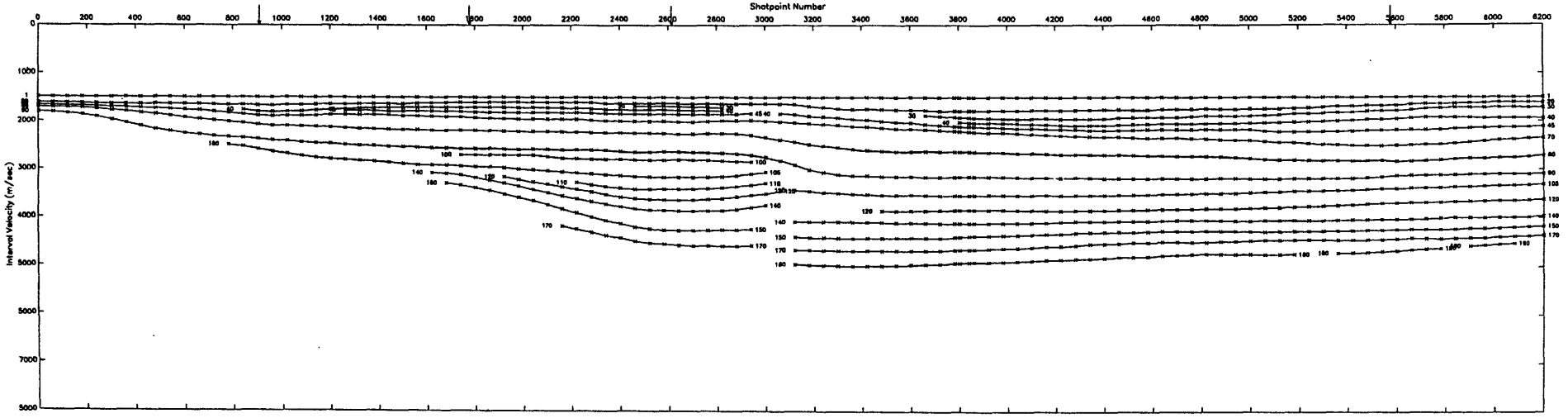

USGS CDP Line 17 -- Time Section

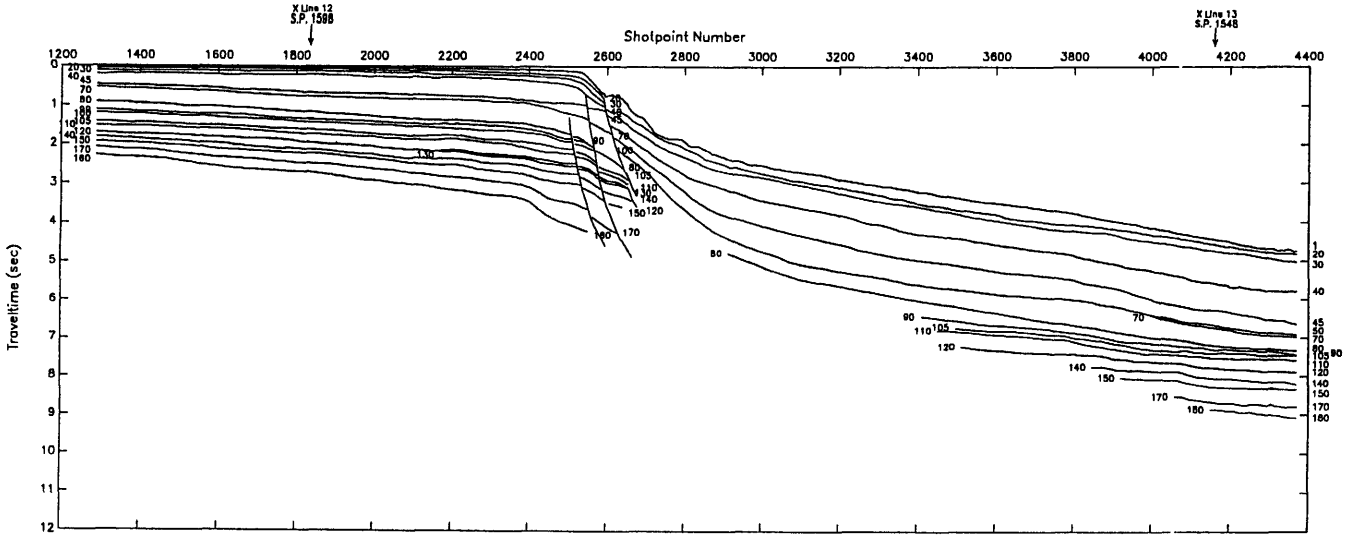

USGS CDP Line 17 – Interval Velocities from smt ISM–RMS

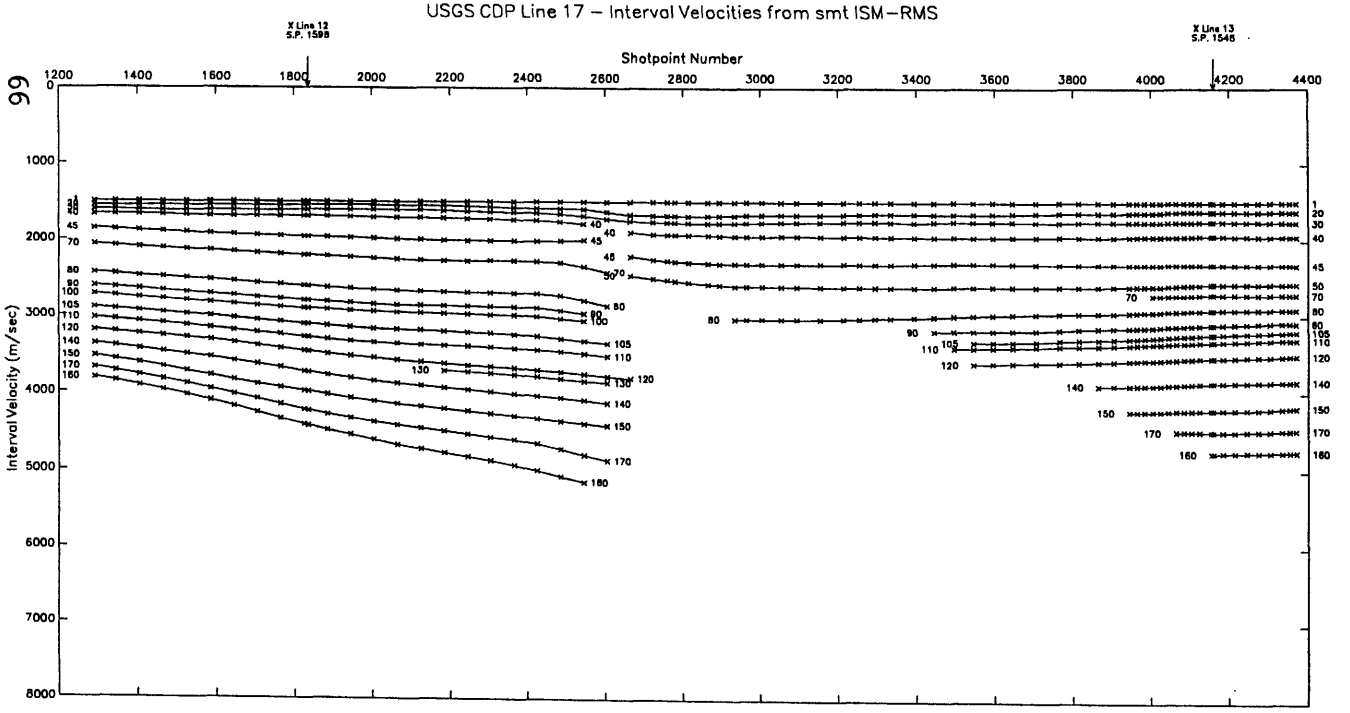

USGS CDP Line 18 – Time Section

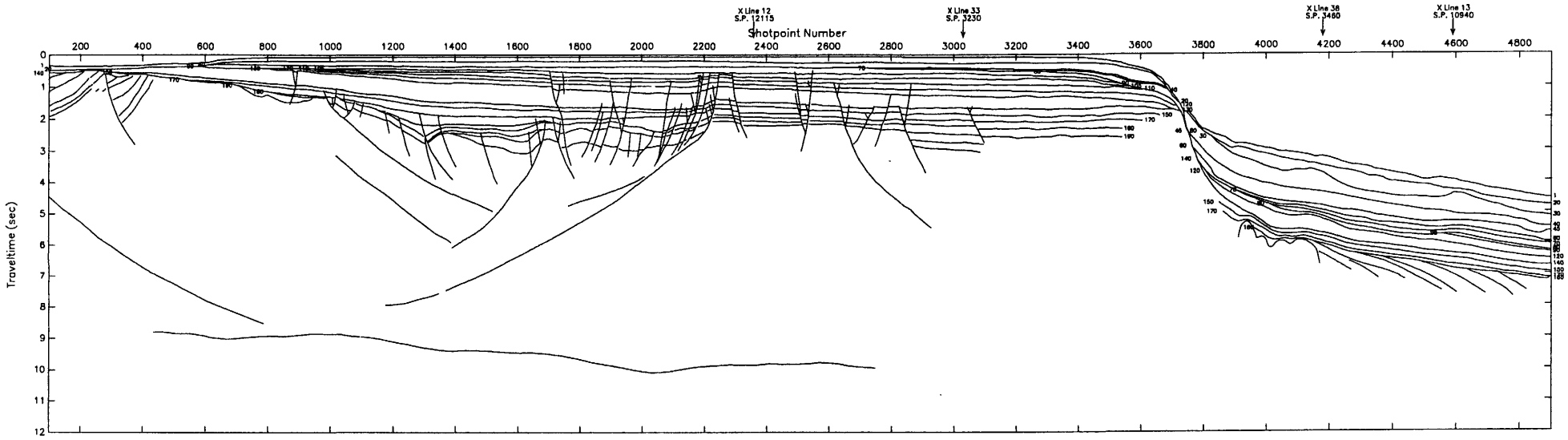

USGS CDP Line 18 -- Interval Velocities from smt ISM–RMS

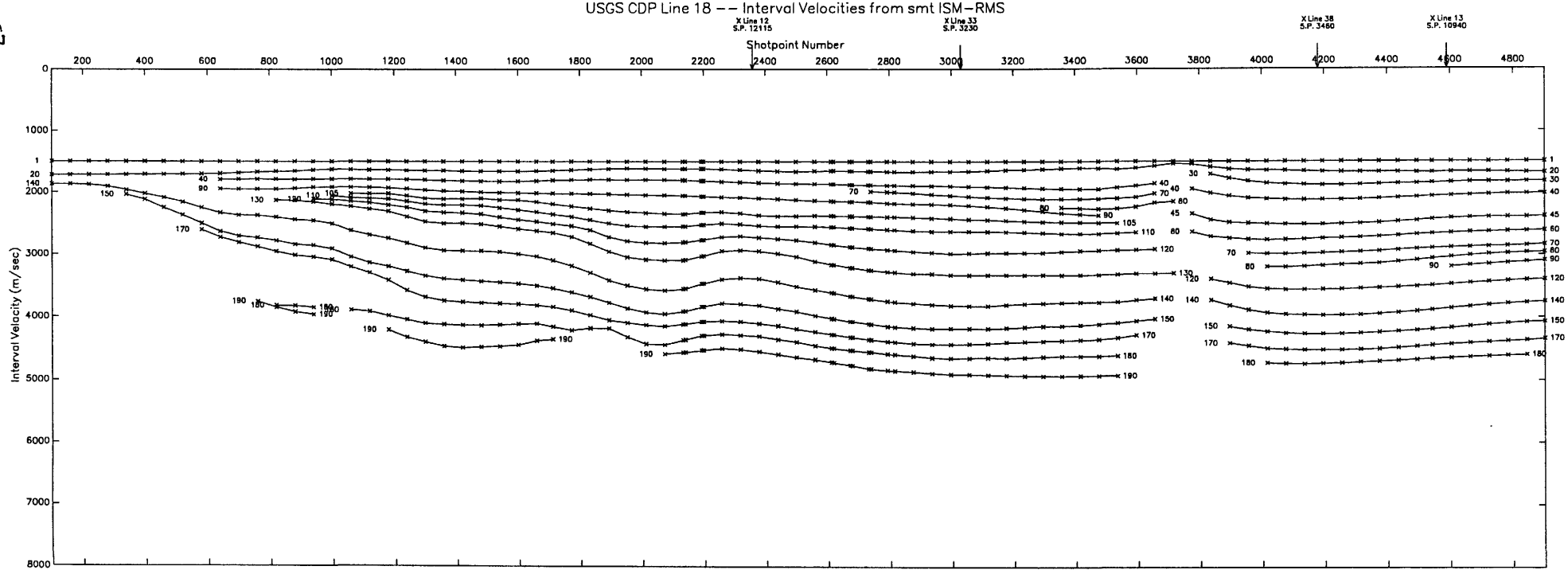

USGS CDP Line 19 — Time Section

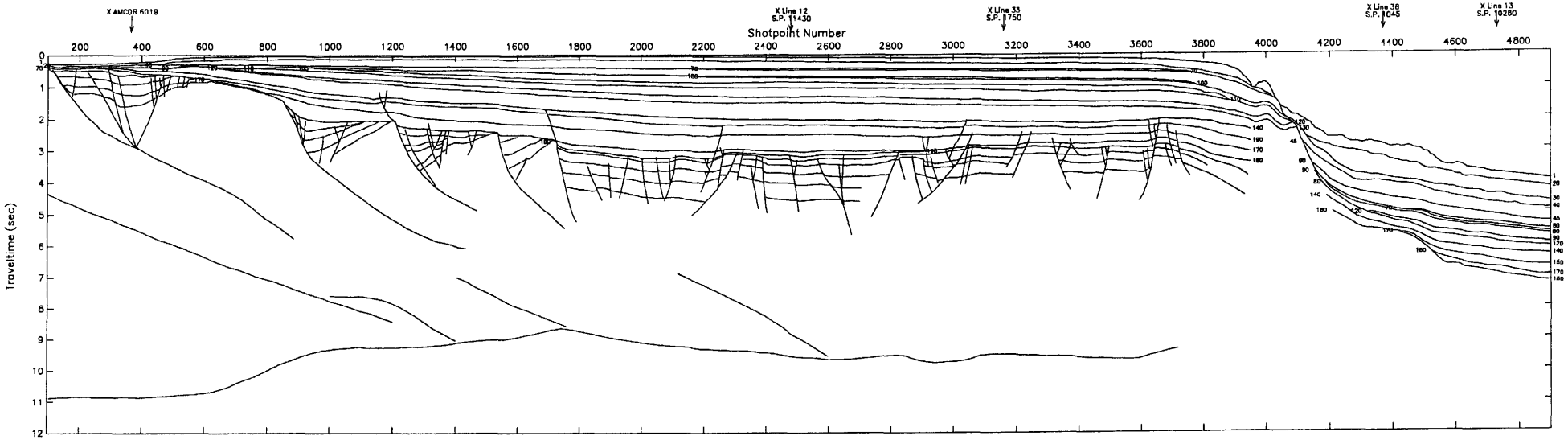

USGS CDP Line 19 -- Interval Velocities from smt ISM-RMS

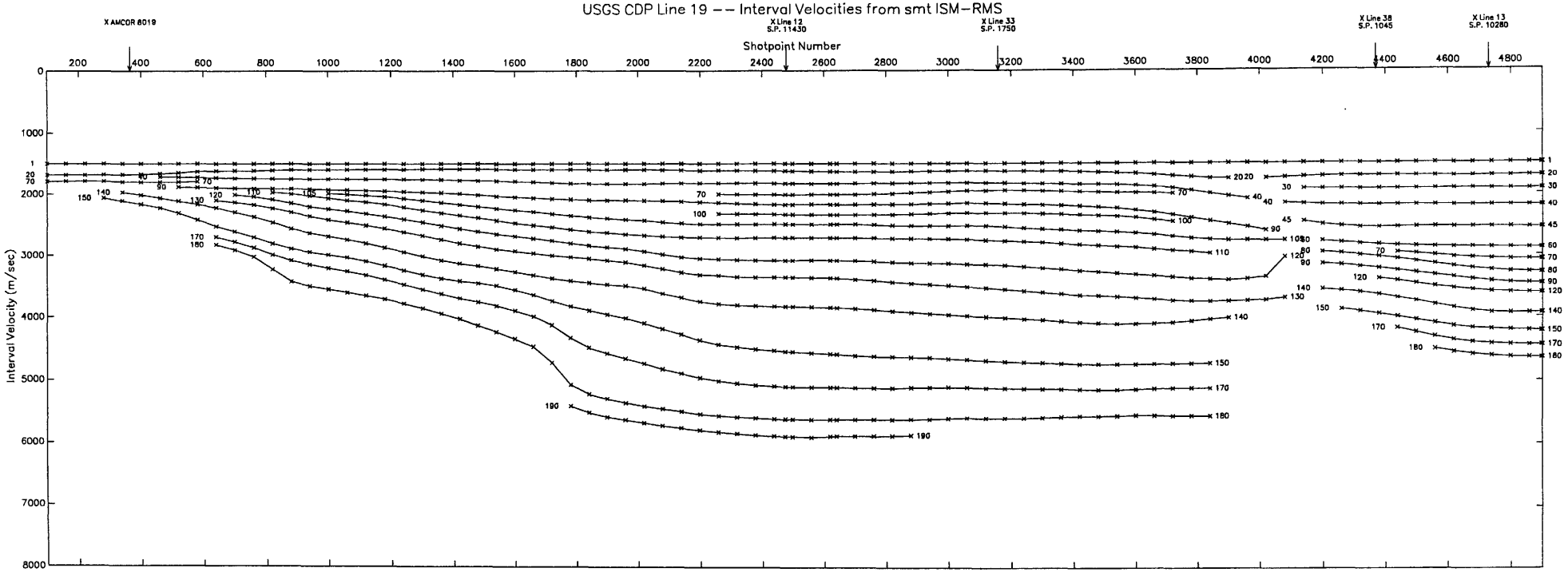

USGS CDP Line 20 – Time Section

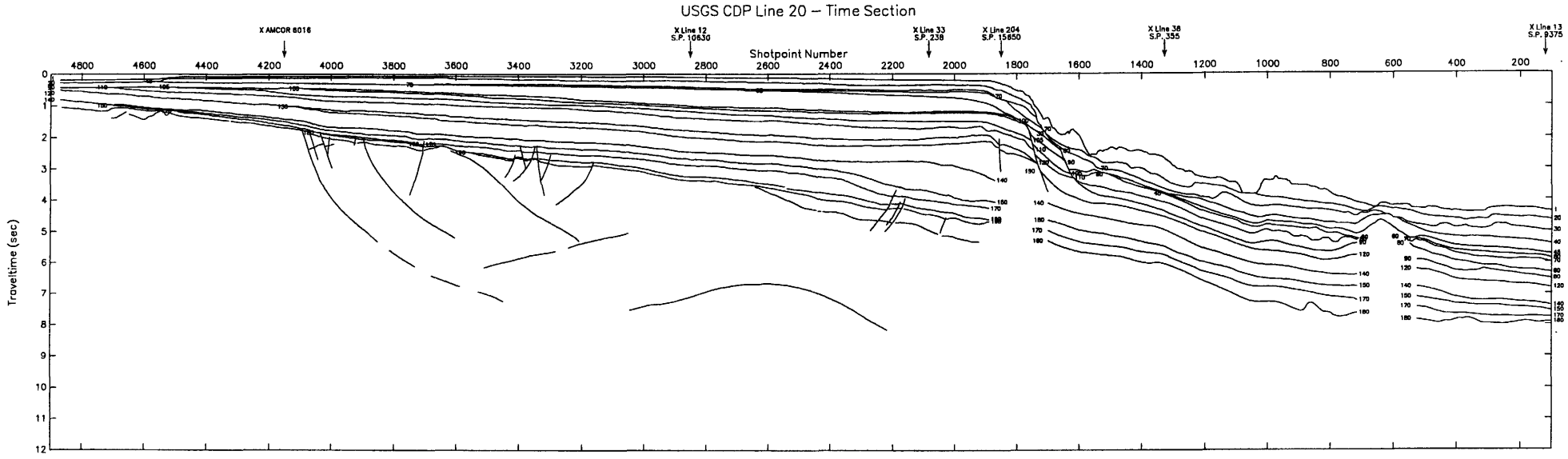

USGS CDP Line 20 -- Interval Velocities from smt ISM–RMS

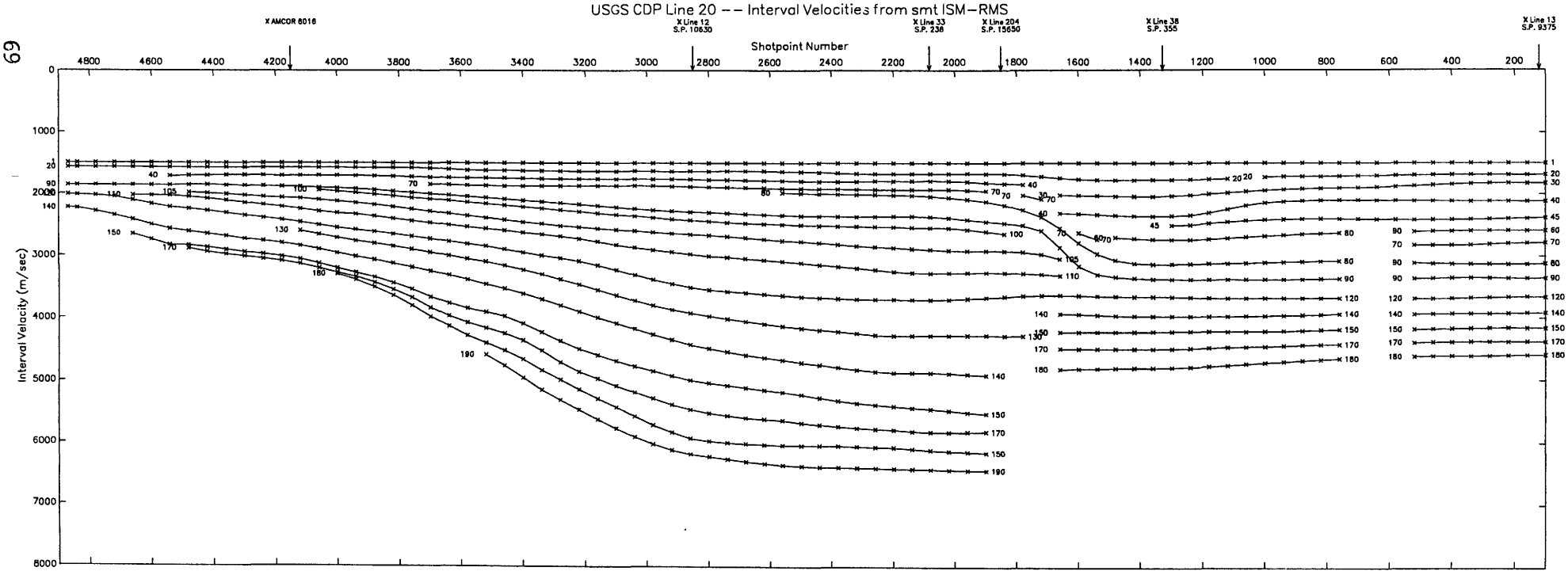

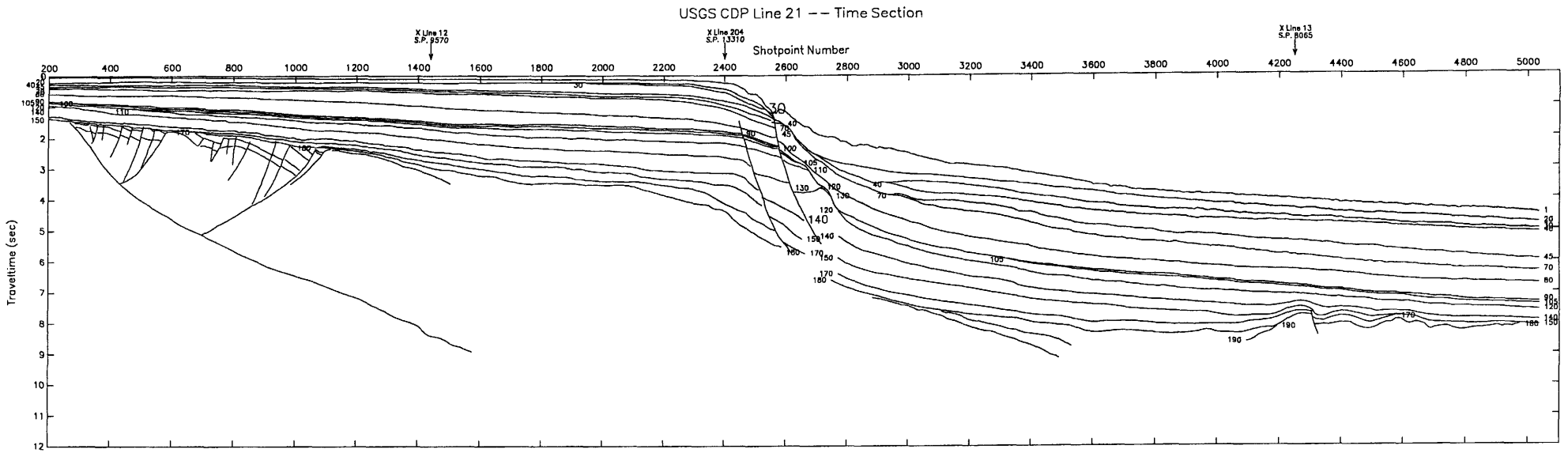
USGS CDP Line 21 -- Time Section
X Line 12
S.P. 9570
X Line 204
S.P. 13310
X Line 13
S.P. 8065
Shotpoint Number
Traveltime (sec)

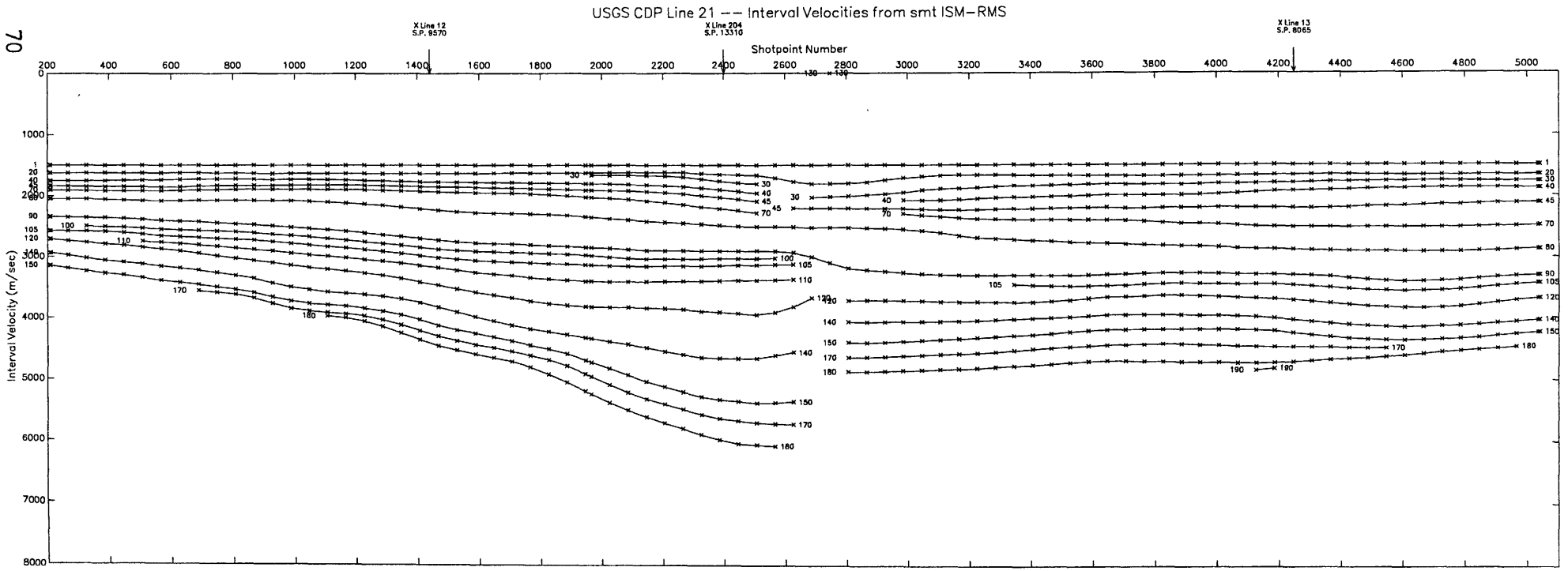
USGS CDP Line 21 -- Interval Velocities from smt ISM-RMS
X Line 12
S.P. 9570
X Line 204
S.P. 13310
X Line 13
S.P. 8065
Shotpoint Number
Interval Velocity (m/sec)

USGS CDP Line 22 – Time Section

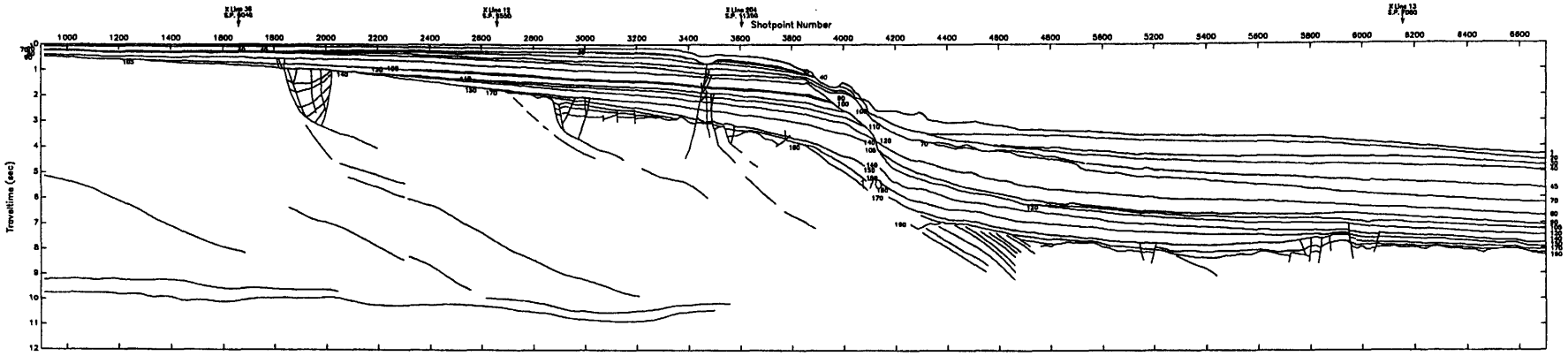

USGS CDP Line 22 – Interval Velocities from smt ISM–RMS

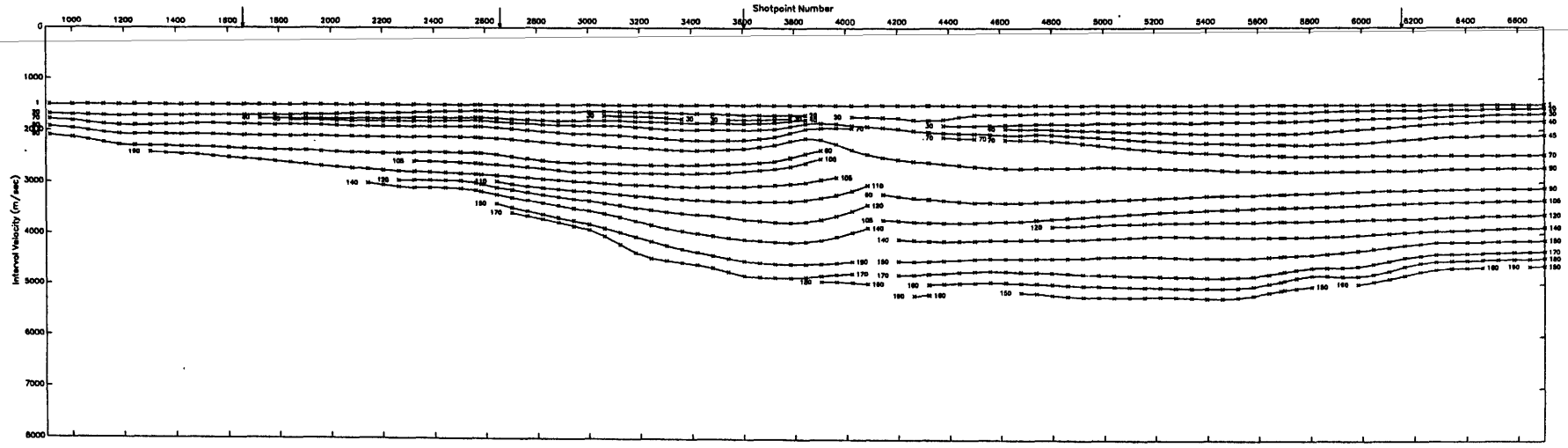

USGS CDP Line 23 -- Time Section

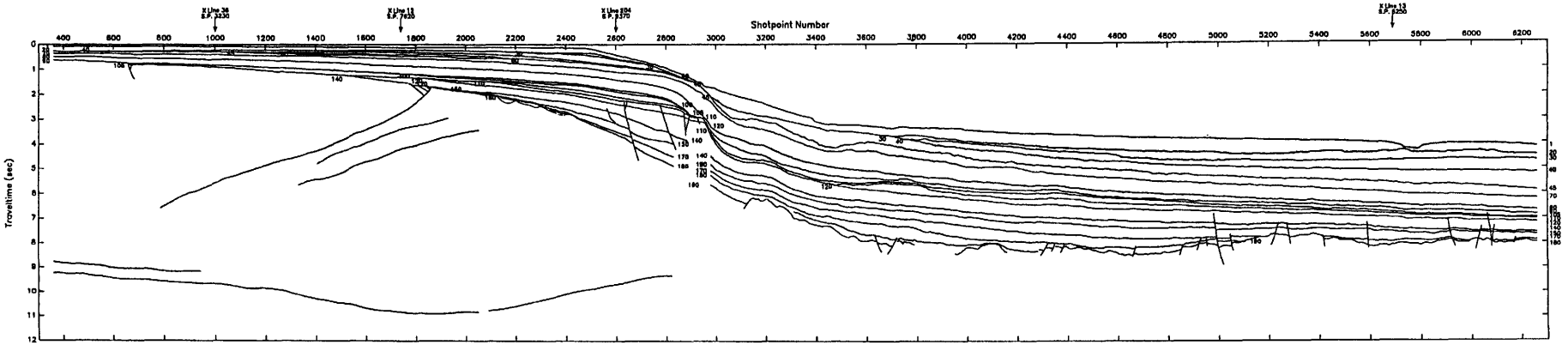

USGS CDP Line 23 -- Interval Velocities from smt ISM-RMS

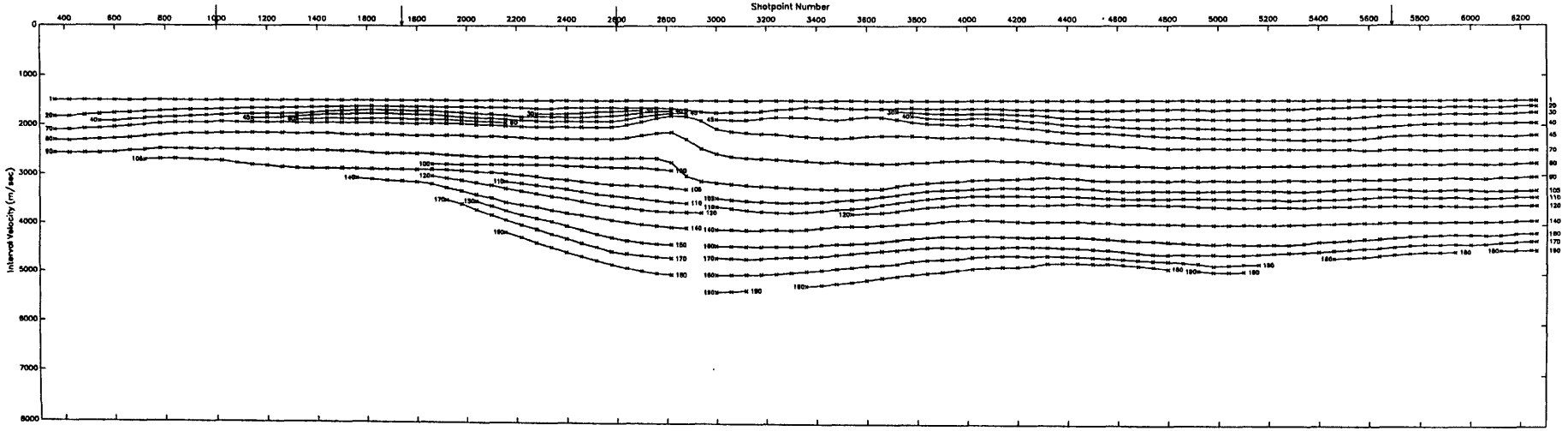

USGS CDP Line 24 -- Time Section

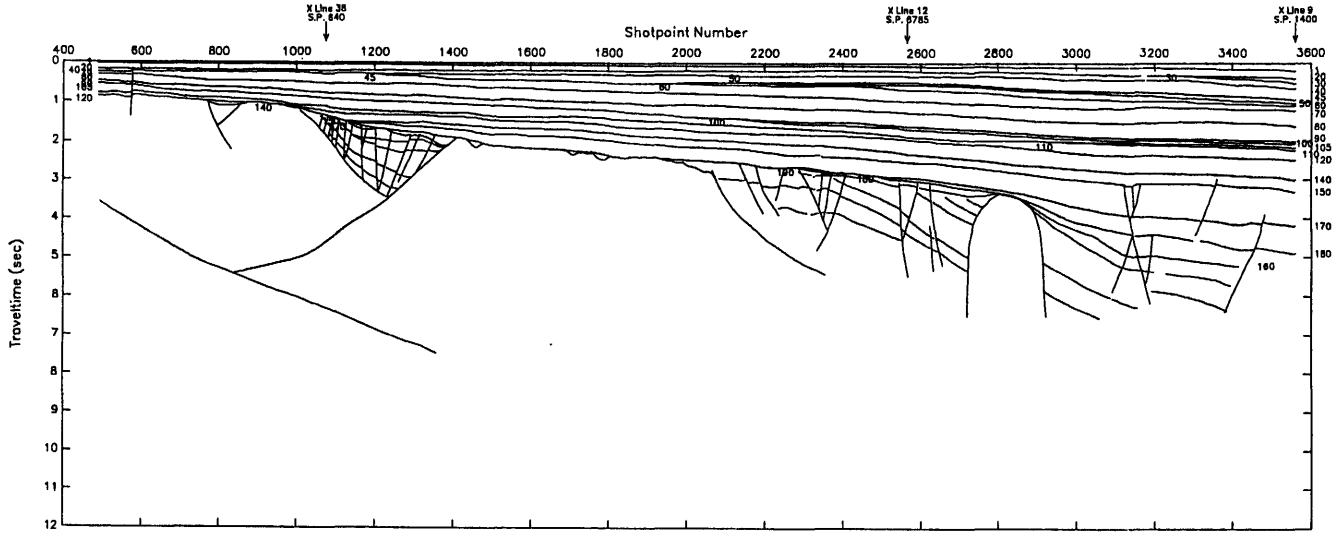

USGS CDP Line 24 -- Interval Velocities from smt ISM-RMS

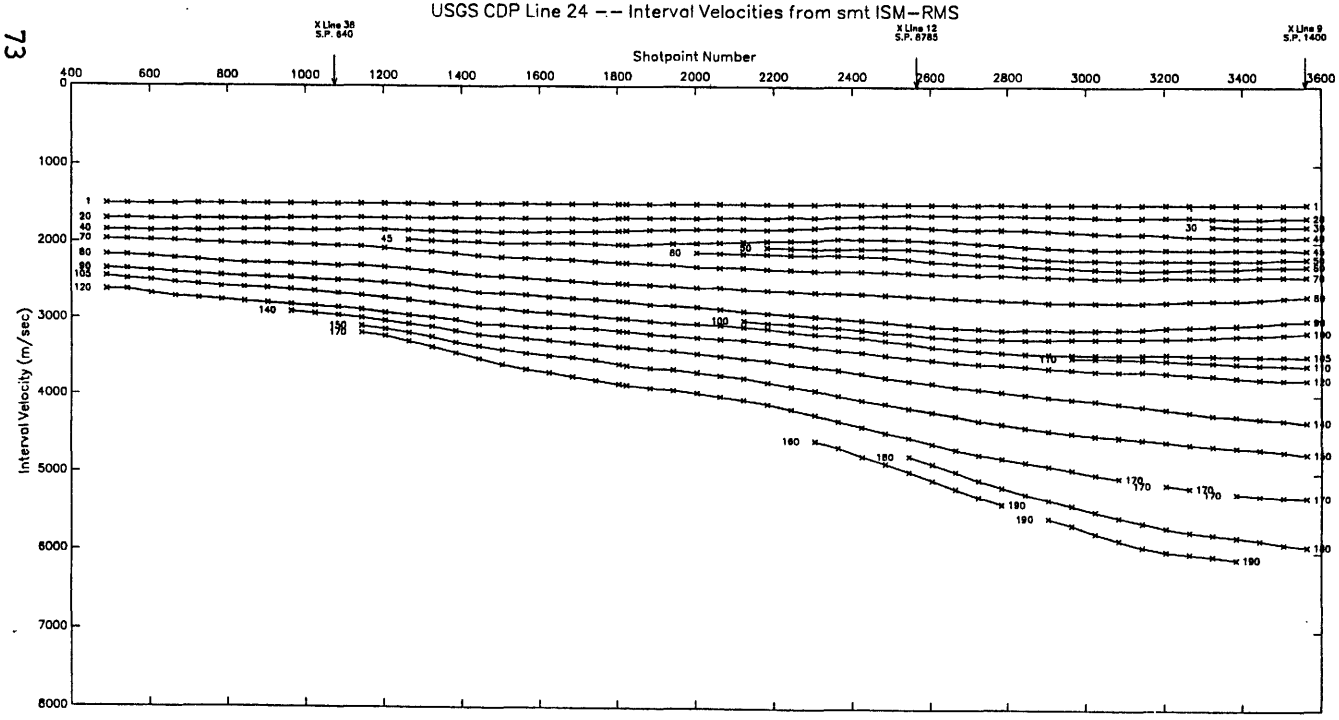

USGS CDP Line 25a -- Time Section

USGS CDP Line 25b -- Time Section

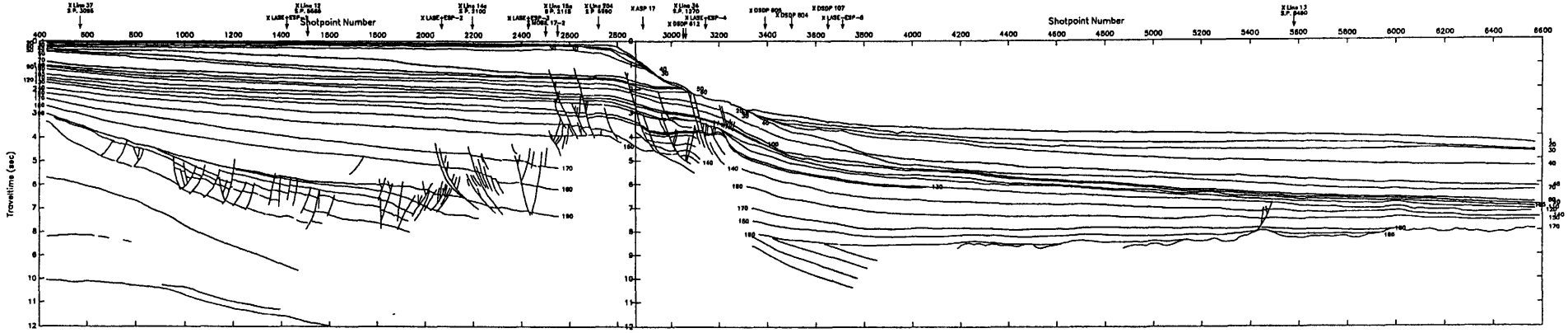

USGS CDP Line 25a -- Interval Velocities from smt ISM-RMS

USGS CDP Line 25b - - Interval Velocities from smt ISM-RMS

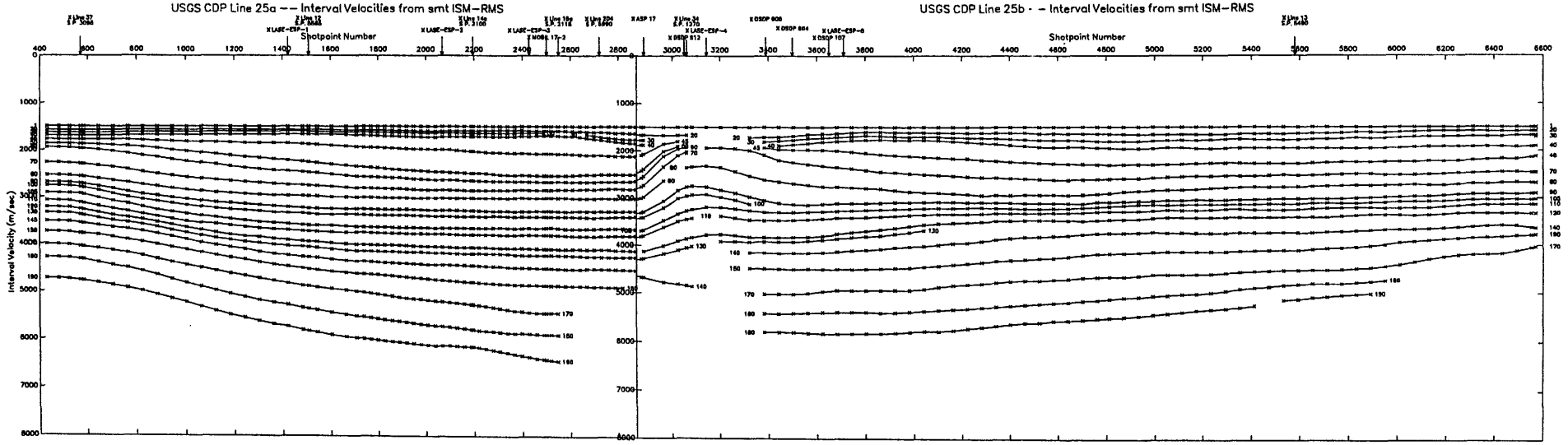

USGS CDP Line 26 — Time Section

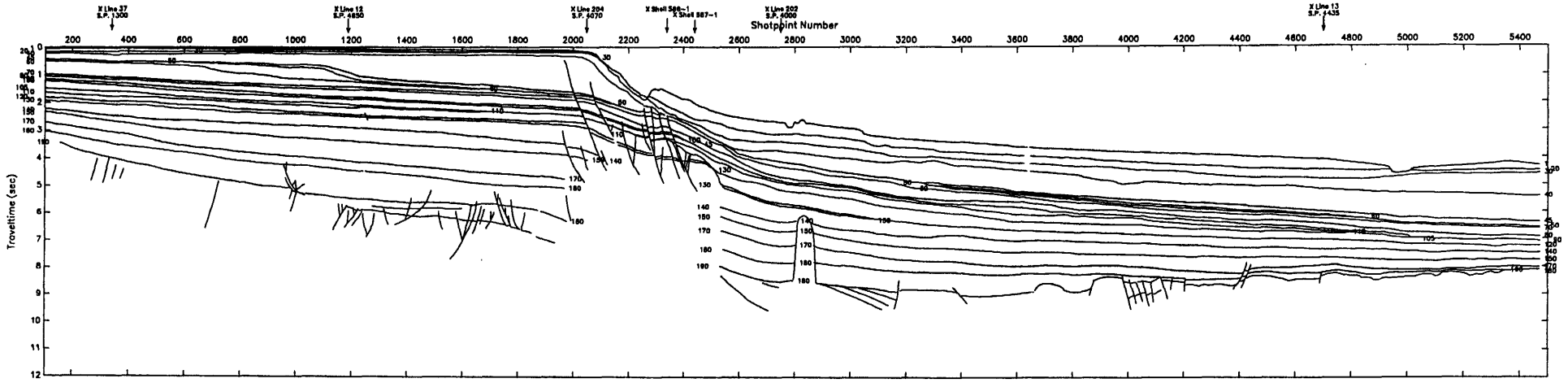

USGS CDP Line 26 -- Interval Velocities from smt ISM-RMS

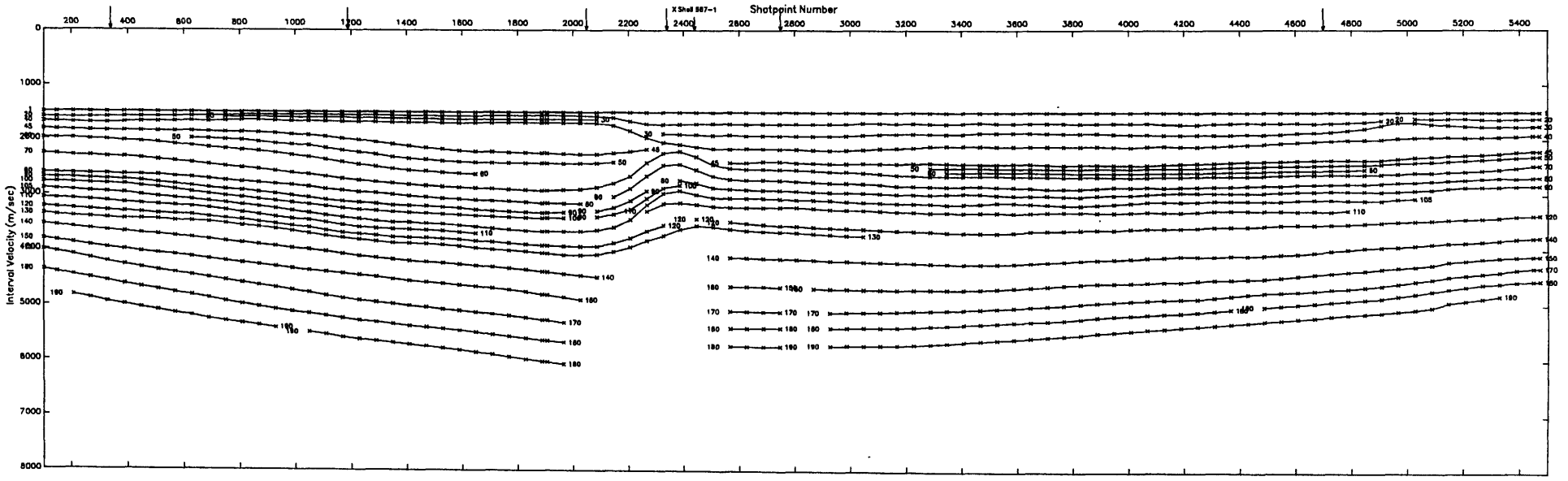

USGS CDP Line 27 -- Time Section

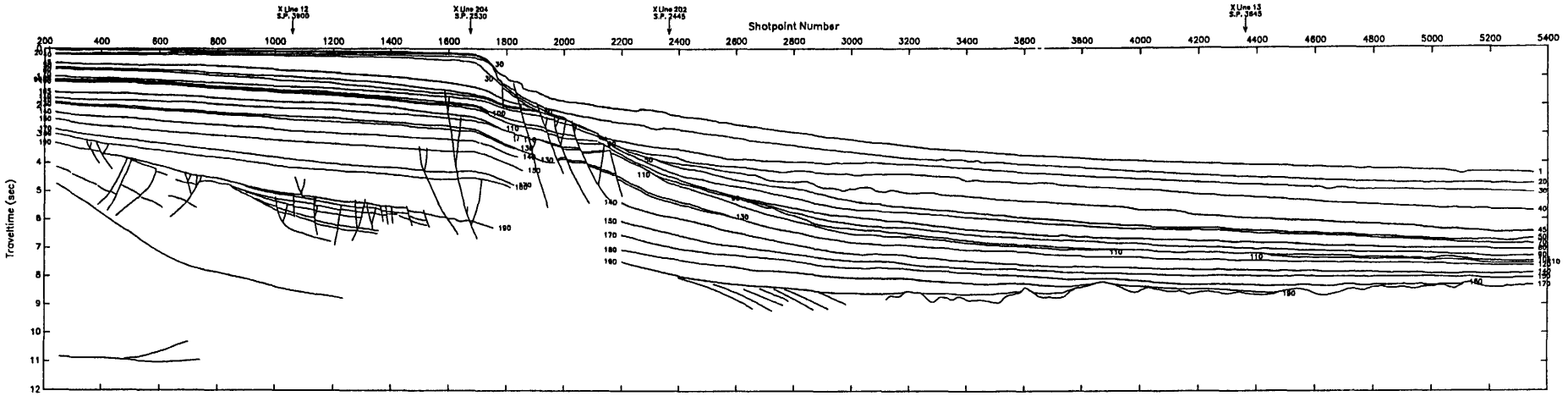

USGS CDP Line 27 -- Interval Velocities from smt ISM-RMS

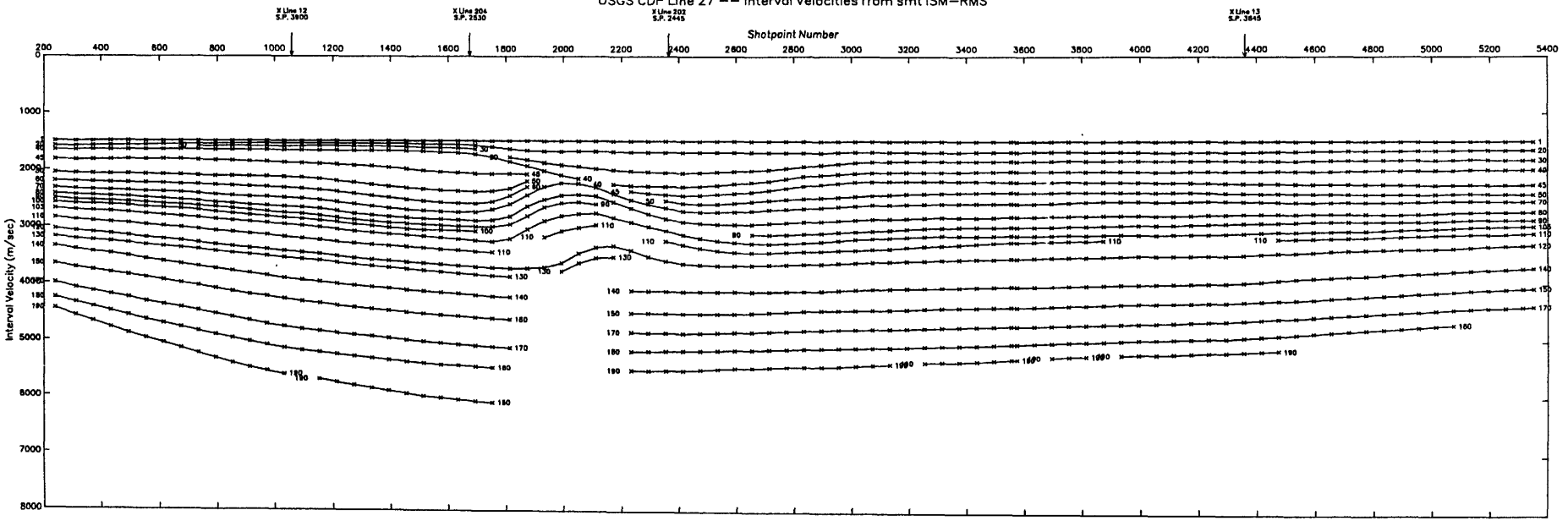

USGS CDP Line 28 -- Time Section

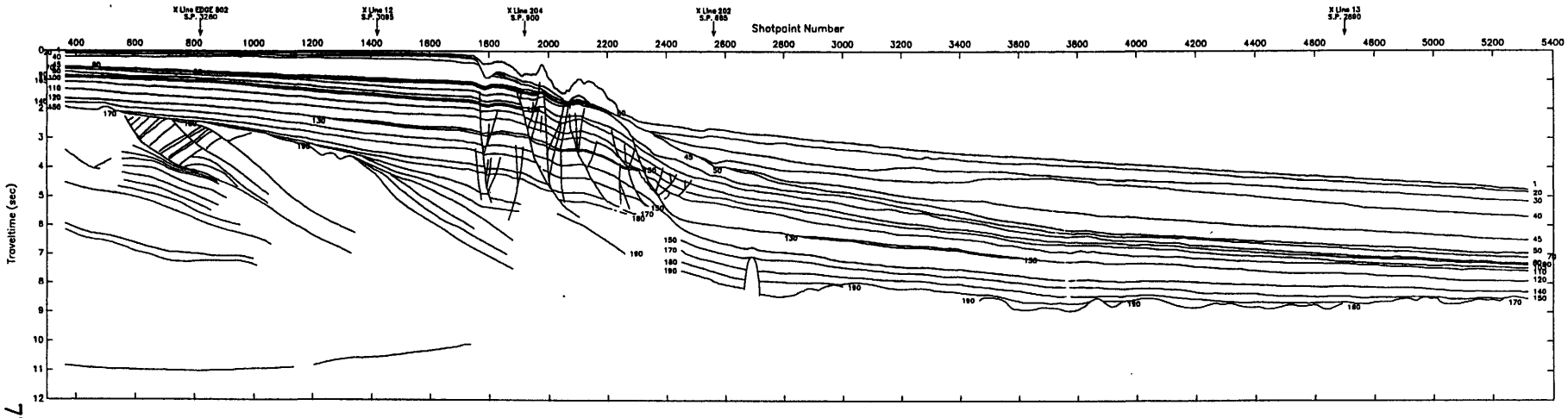

USGS CDP Line 28 – Interval Velocities from smt ISM–RMS

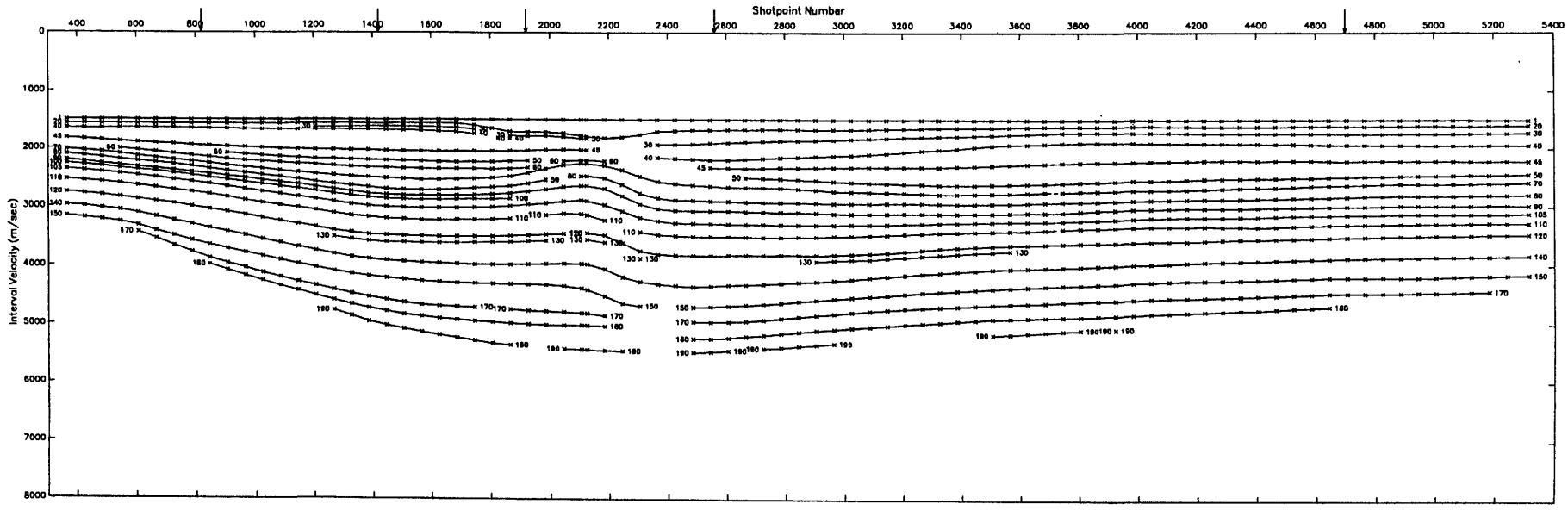

USGS CDP Line 29 -- Time Section

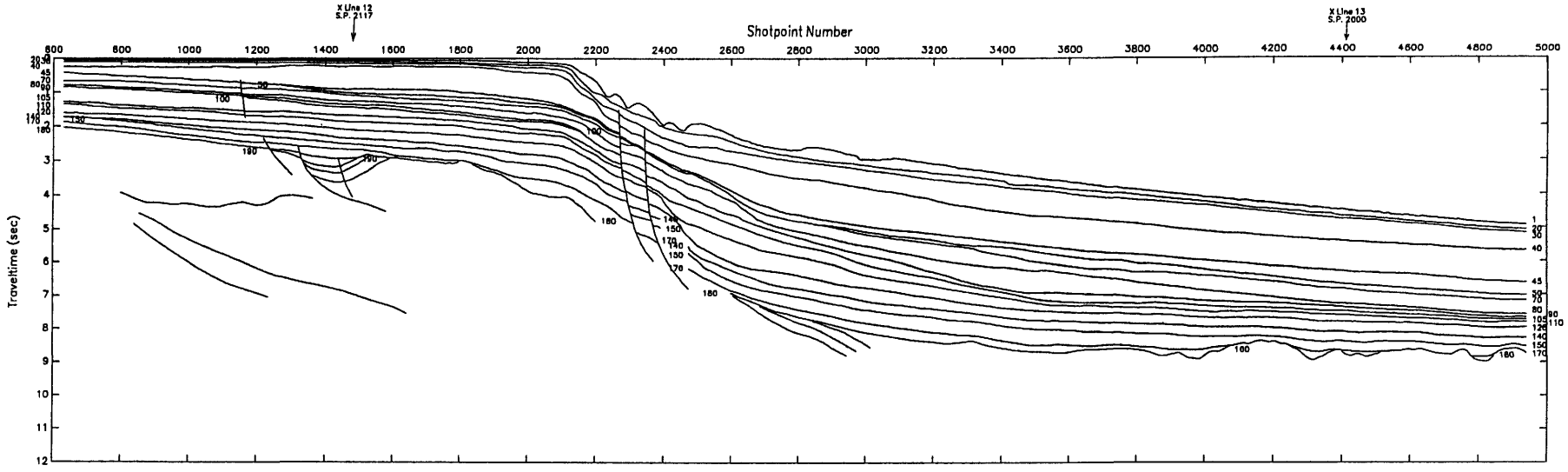

USGS CDP Line 29 – Interval Velocities from smt ISM–RMS

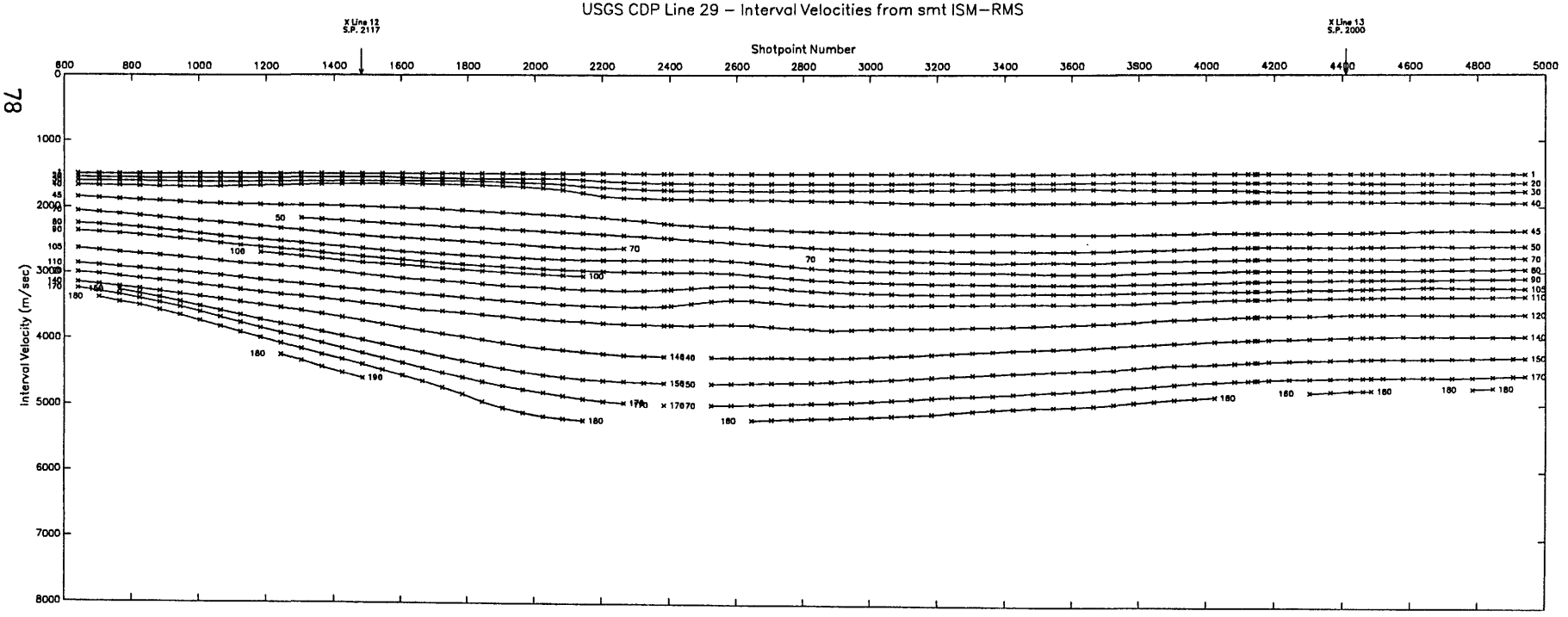

USGS CDP Line 30 -- Time Section

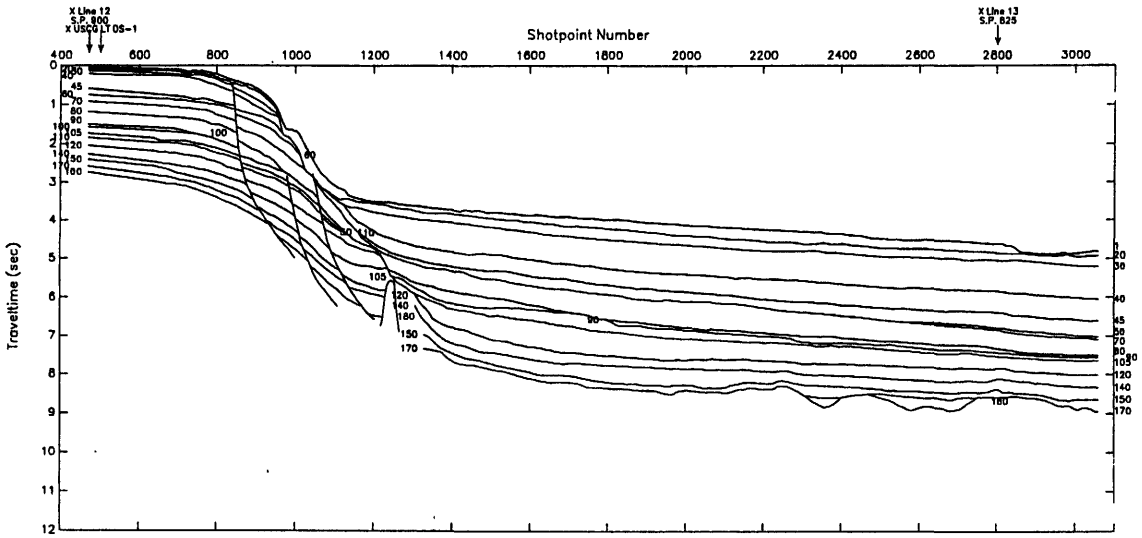

USGS CDP Line 30 – Interval Velocities from smt ISM–RMS

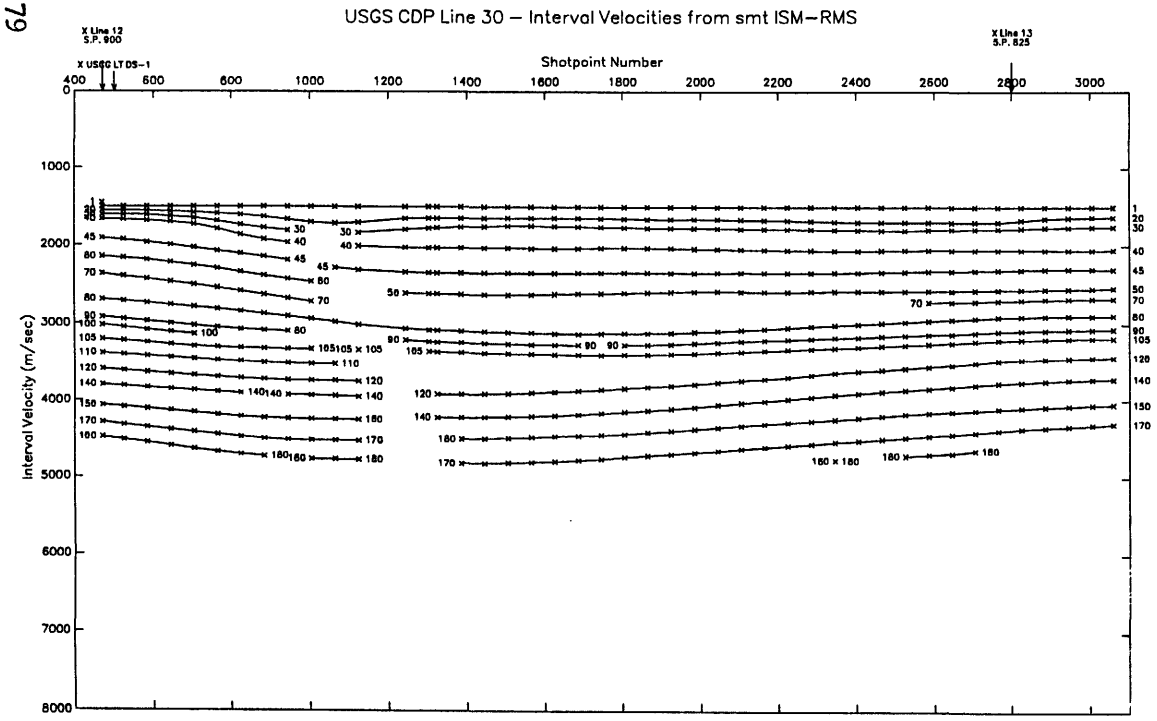

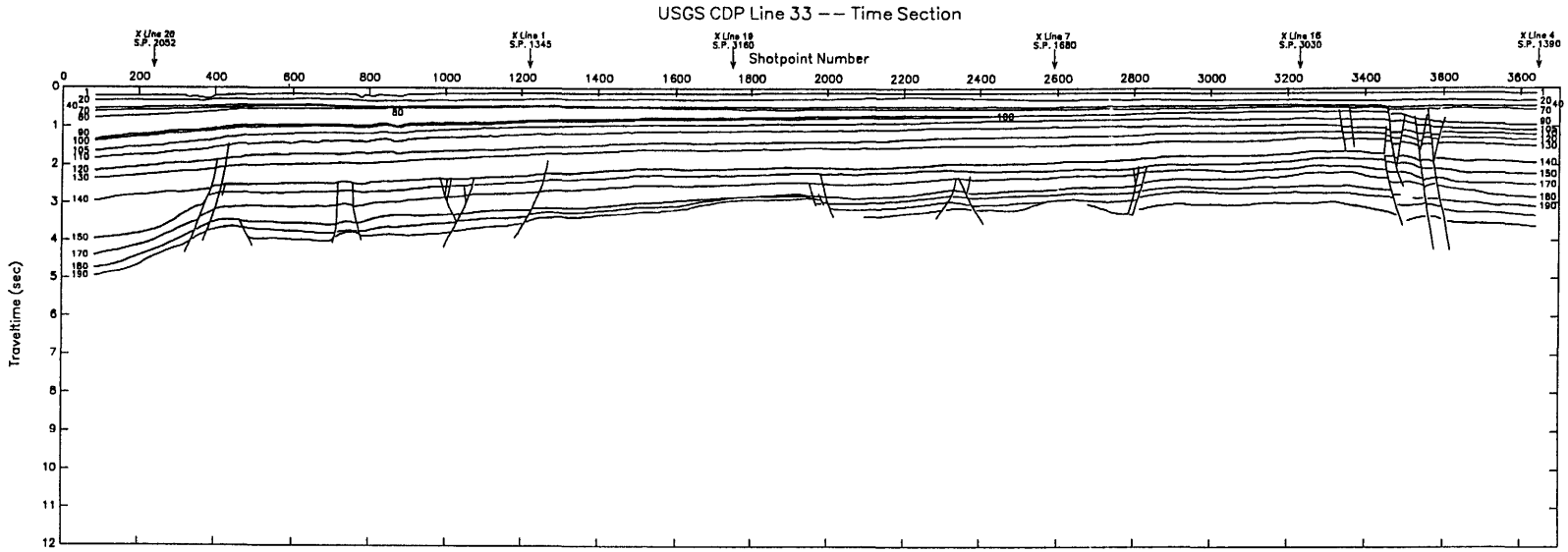
USGS CDP Line 33 -- Time Section
X Line 20 S.P. 2082
X Line 1 S.P. 1345
X Line 19 S.P. 3160
X Line 7 S.P. 1680
X Line 18 S.P. 3030
X Line 4 S.P. 1390
Shotpoint Number
Traveltime (sec)

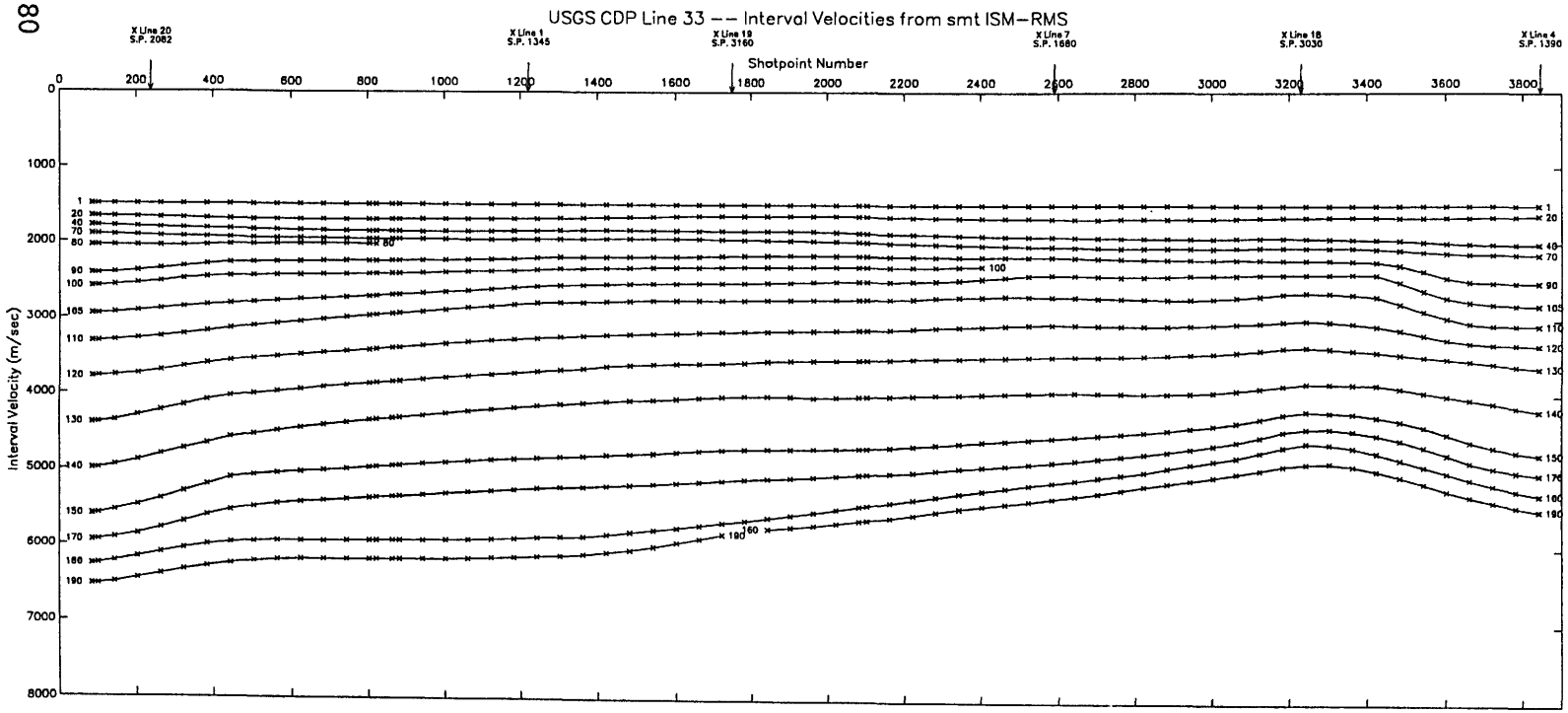
USGS CDP Line 33 -- Interval Velocities from smt ISM-RMS
X Line 20 S.P. 2082
X Line 1 S.P. 1345
X Line 19 S.P. 3160
X Line 7 S.P. 1680
X Line 18 S.P. 3030
X Line 4 S.P. 1390
Shotpoint Number
Interval Velocity (m/sec)

USGS CDP Line 34 -- Time Section

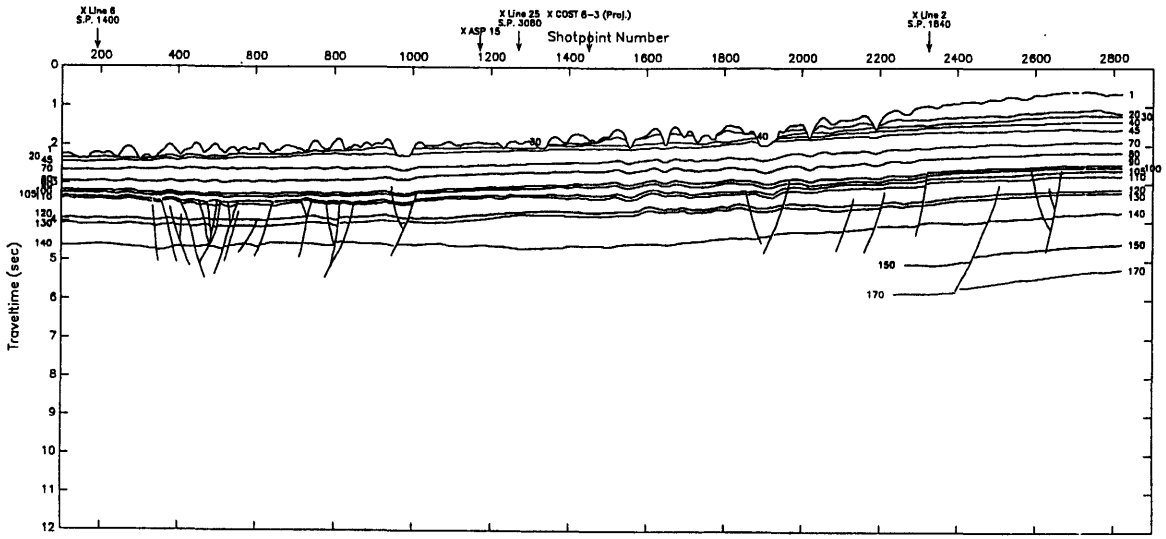

USGS CDP Line 34 -- Interval Velocities from smt ISM-RMS

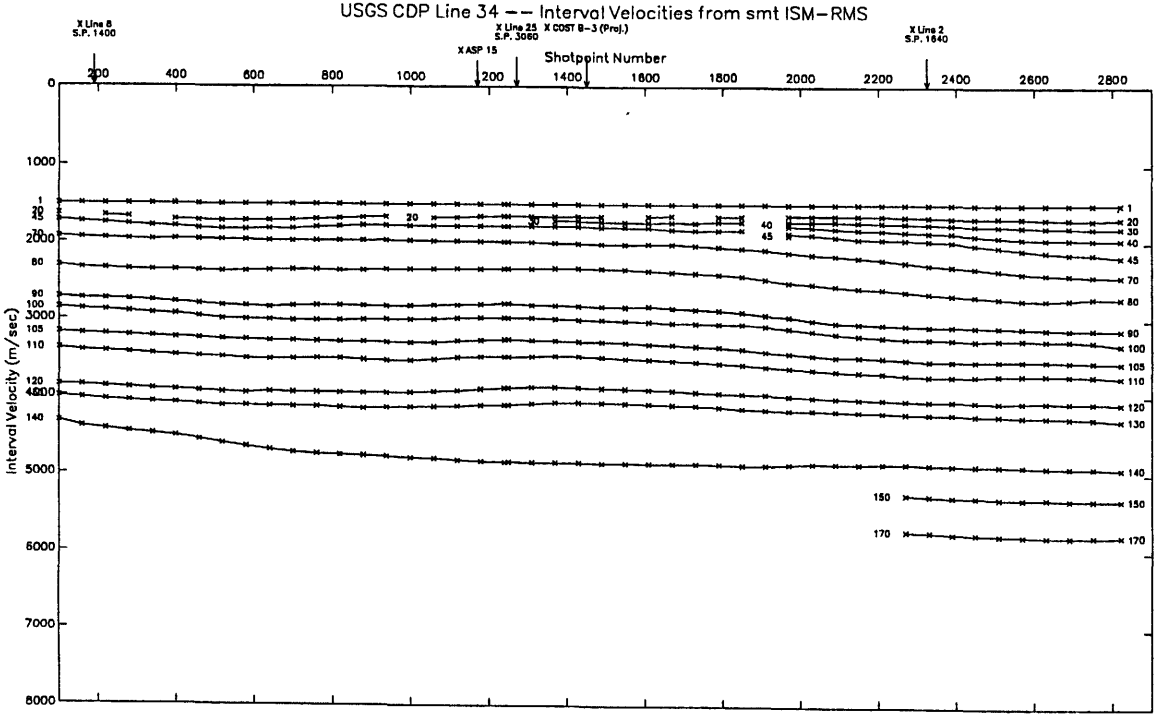

USGS CDP Line 36 -- Time Section

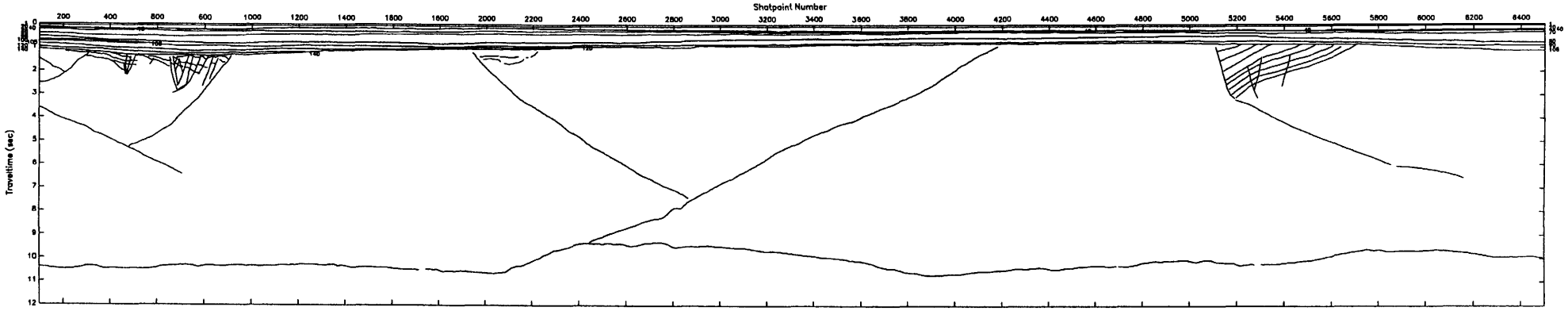

USGS CDP Line 36 -- Interval Velocities from smt ISM-RMS

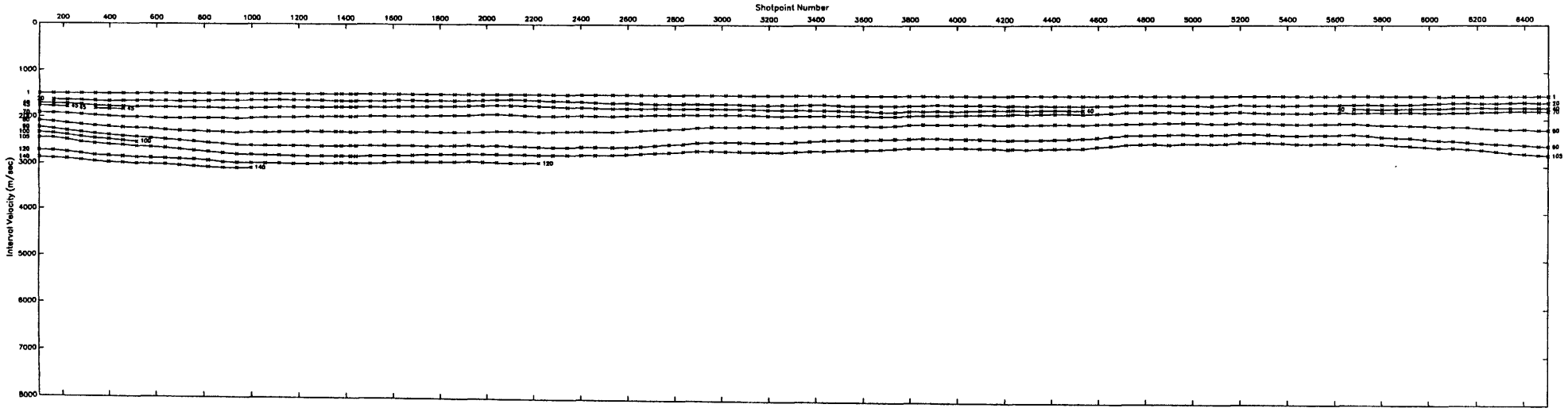

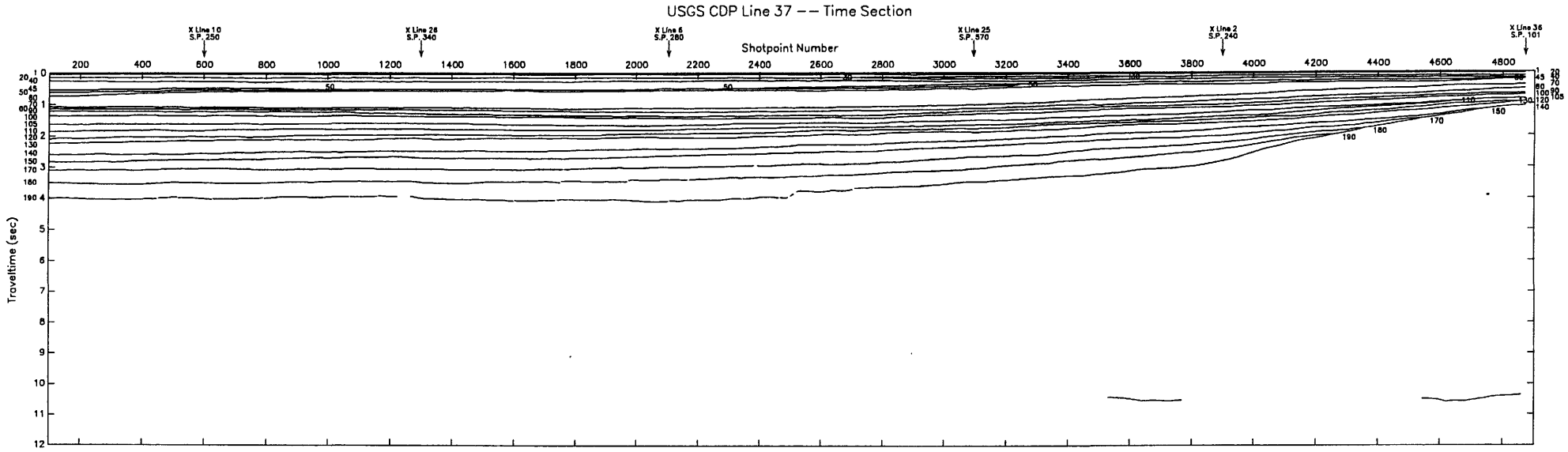
USGS CDP Line 37 -- Time Section
X Line 10 S.P. 250
X Line 26 S.P. 340
X Line 6 S.P. 260
X Line 25 S.P. 370
X Line 2 S.P. 240
X Line 36 S.P. 101
Shotpoint Number
Traveltime (sec)

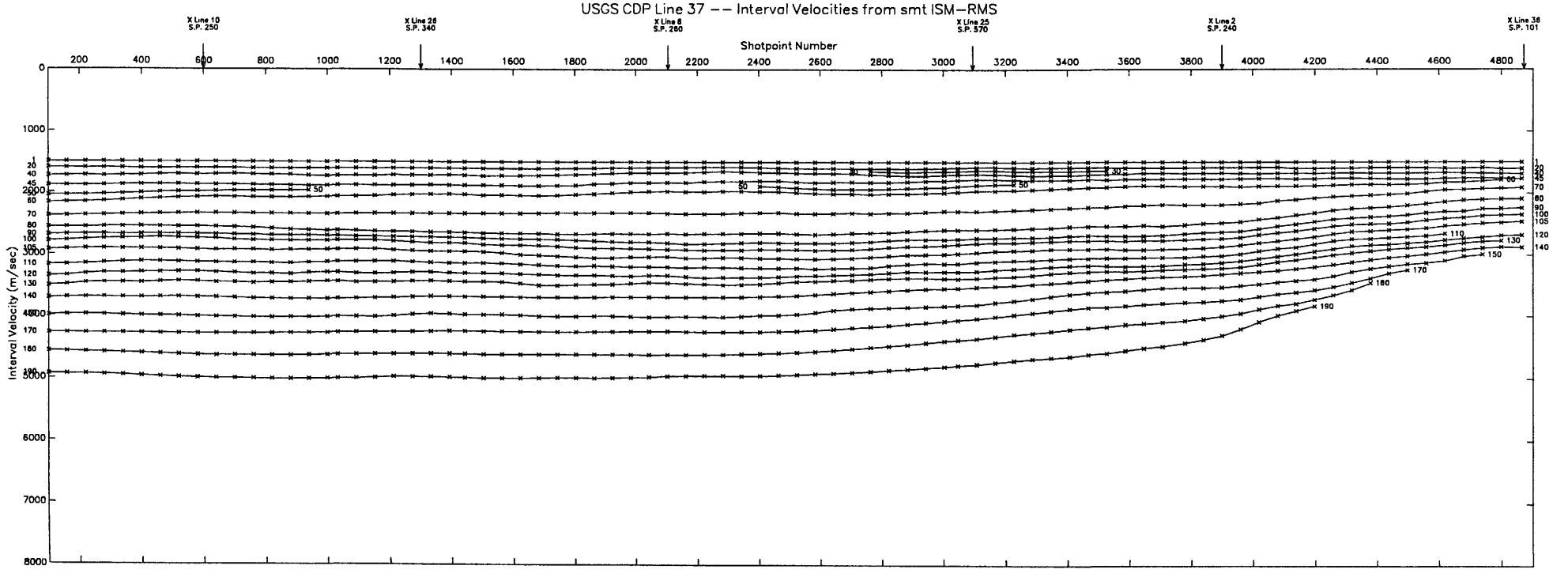
USGS CDP Line 37 -- Interval Velocities from smt ISM-RMS
X Line 10 S.P. 250
X Line 26 S.P. 340
X Line 6 S.P. 260
X Line 25 S.P. 370
X Line 2 S.P. 240
X Line 36 S.P. 101
Shotpoint Number
Interval Velocity (m/sec)

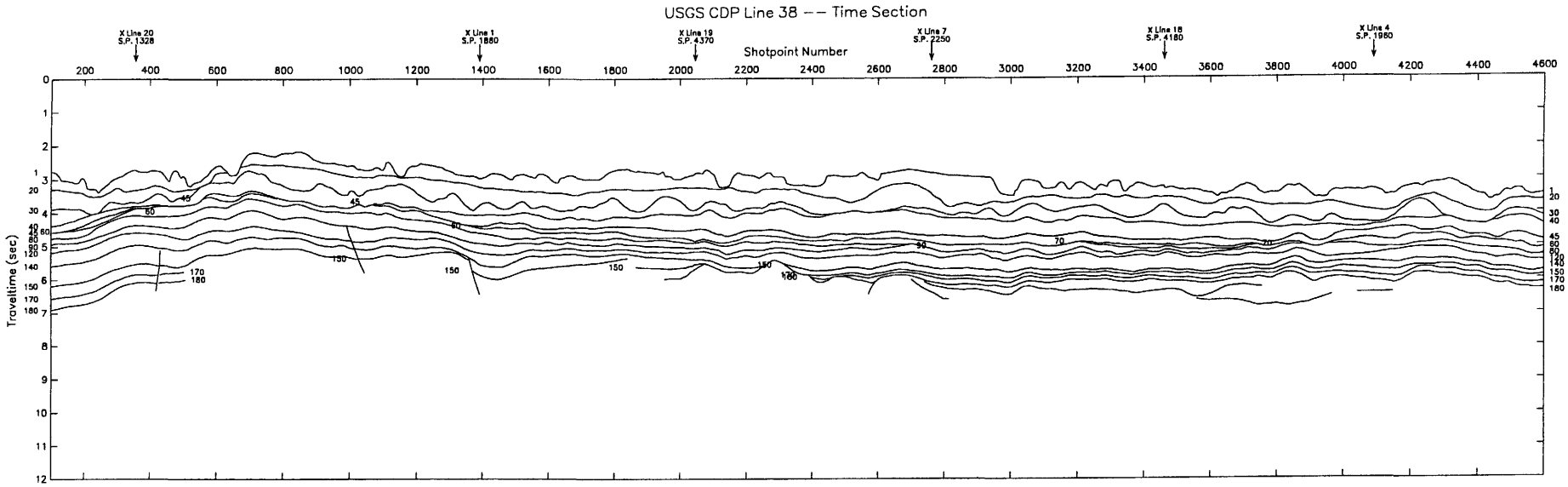
USGS CDP Line 38 -- Time Section
X Line 20 S.P. 1328
X Line 1 S.P. 1880
X Line 19 S.P. 4370
X Line 7 S.P. 2250
X Line 18 S.P. 4180
X Line 4 S.P. 1960
Shotpoint Number
Traveltime (sec)

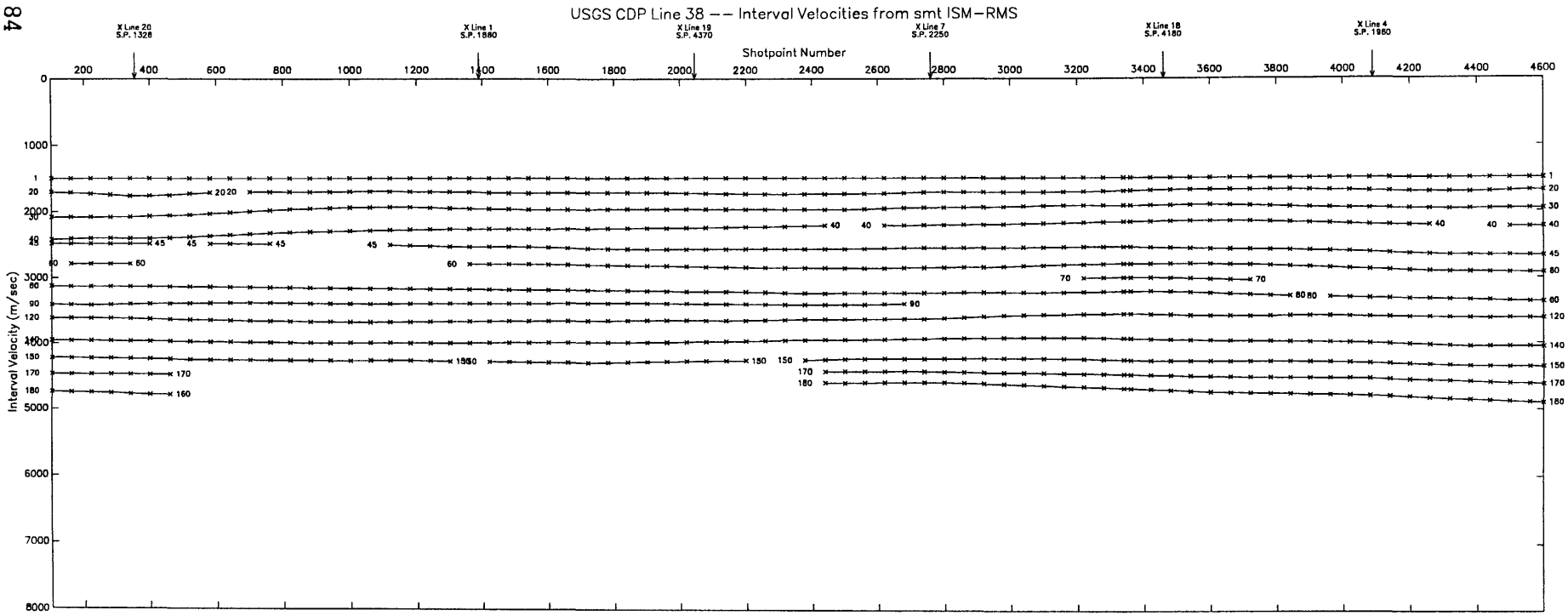
USGS CDP Line 38 -- Interval Velocities from smt ISM-RMS
X Line 20 S.P. 1328
X Line 1 S.P. 1880
X Line 19 S.P. 4370
X Line 7 S.P. 2250
X Line 18 S.P. 4180
X Line 4 S.P. 1960
Shotpoint Number
Interval Velocity (m/sec)

BGR Line 79-202 -- Time Section

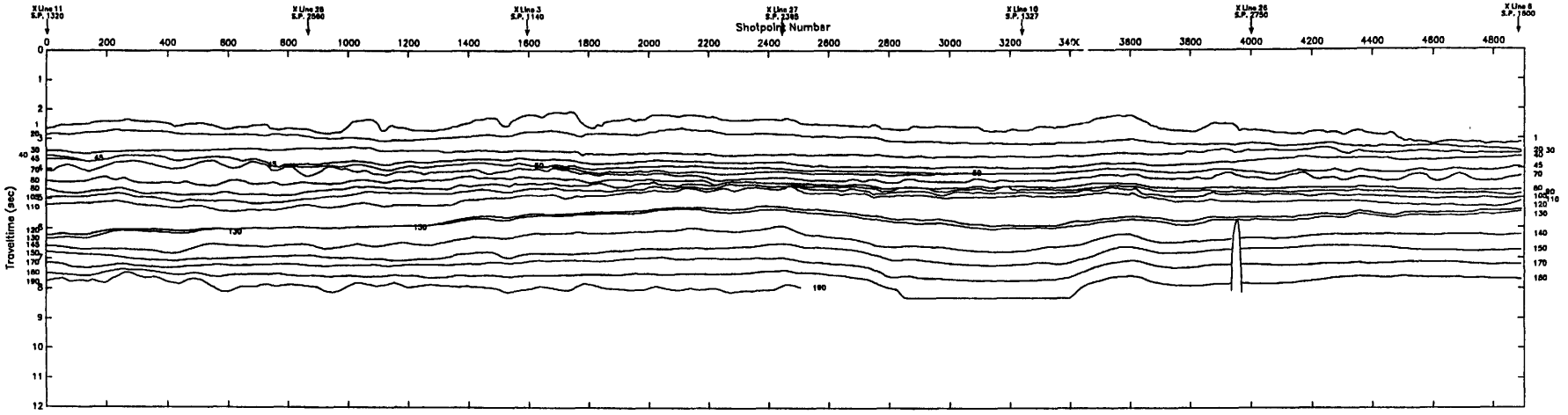

BGR Line 79-202 -- Interval Velocities from smt ISM-RMS

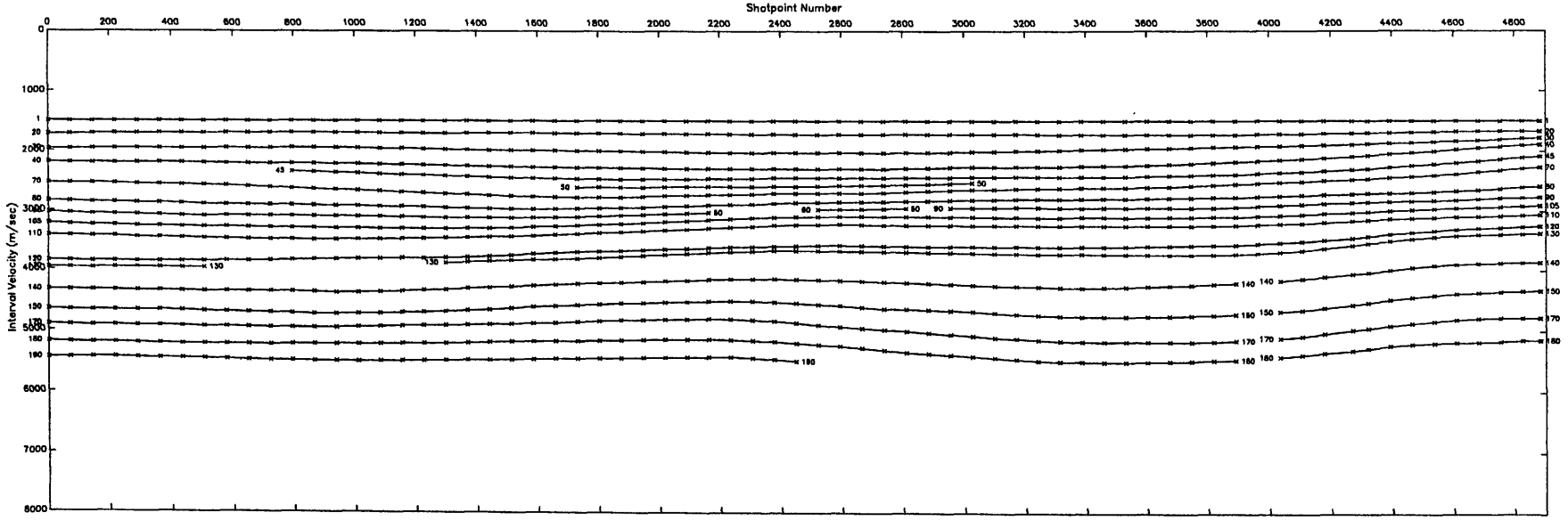

BGR Line 79-204 -- Time Section

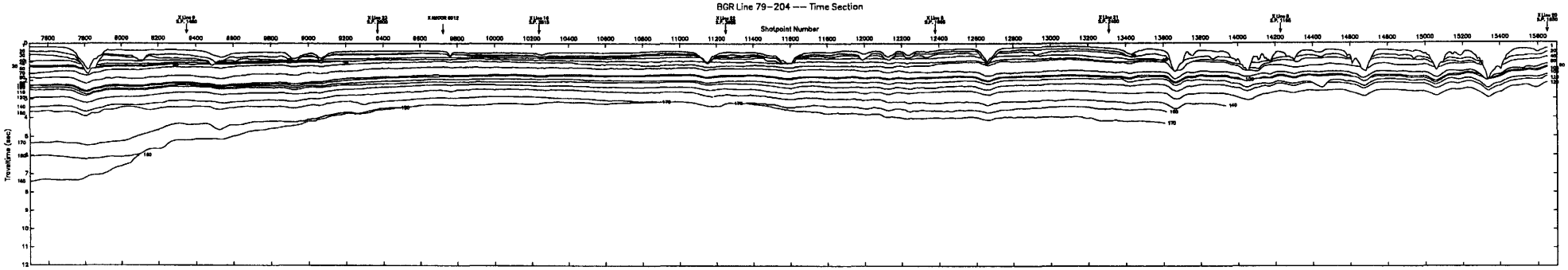

BGR Line 79-204 -- Interval Velocities from smt ISM-RMS

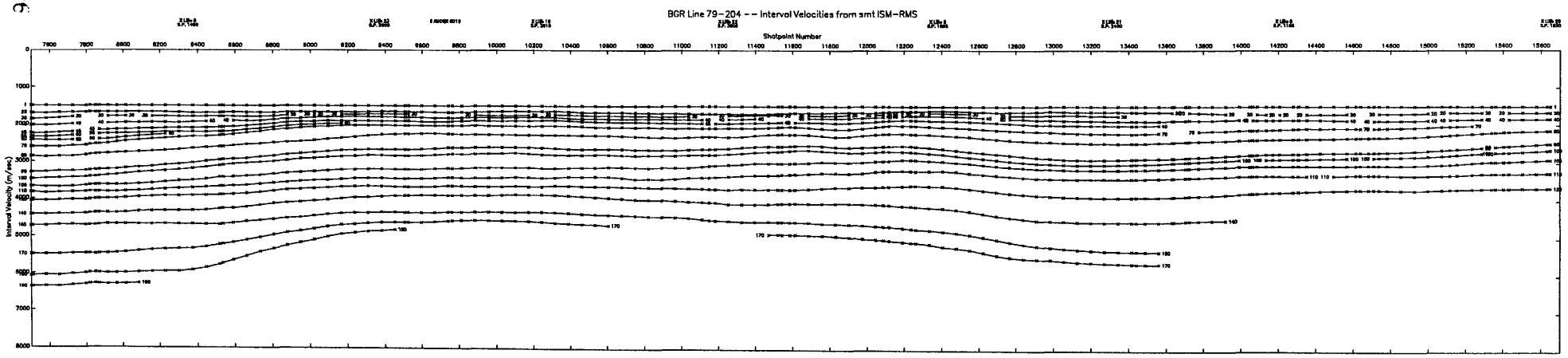

USGS–IPOD CDP Line –– Time Section

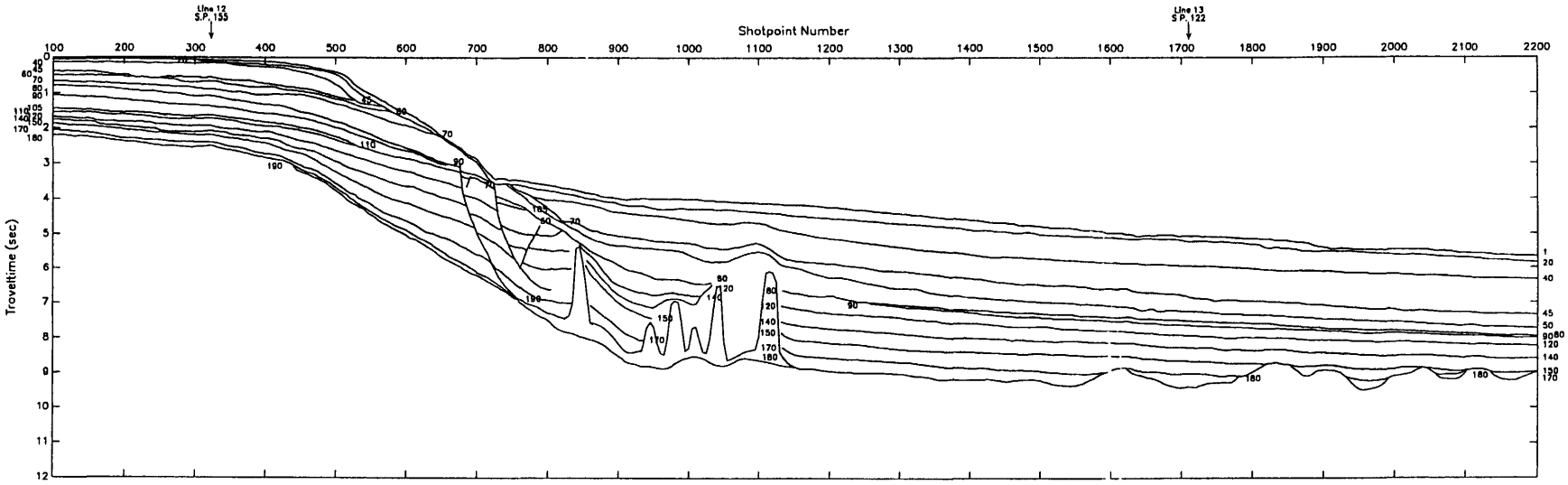

USGS–IPOD CDP Line – Interval Velocities from smt ISM–RMS

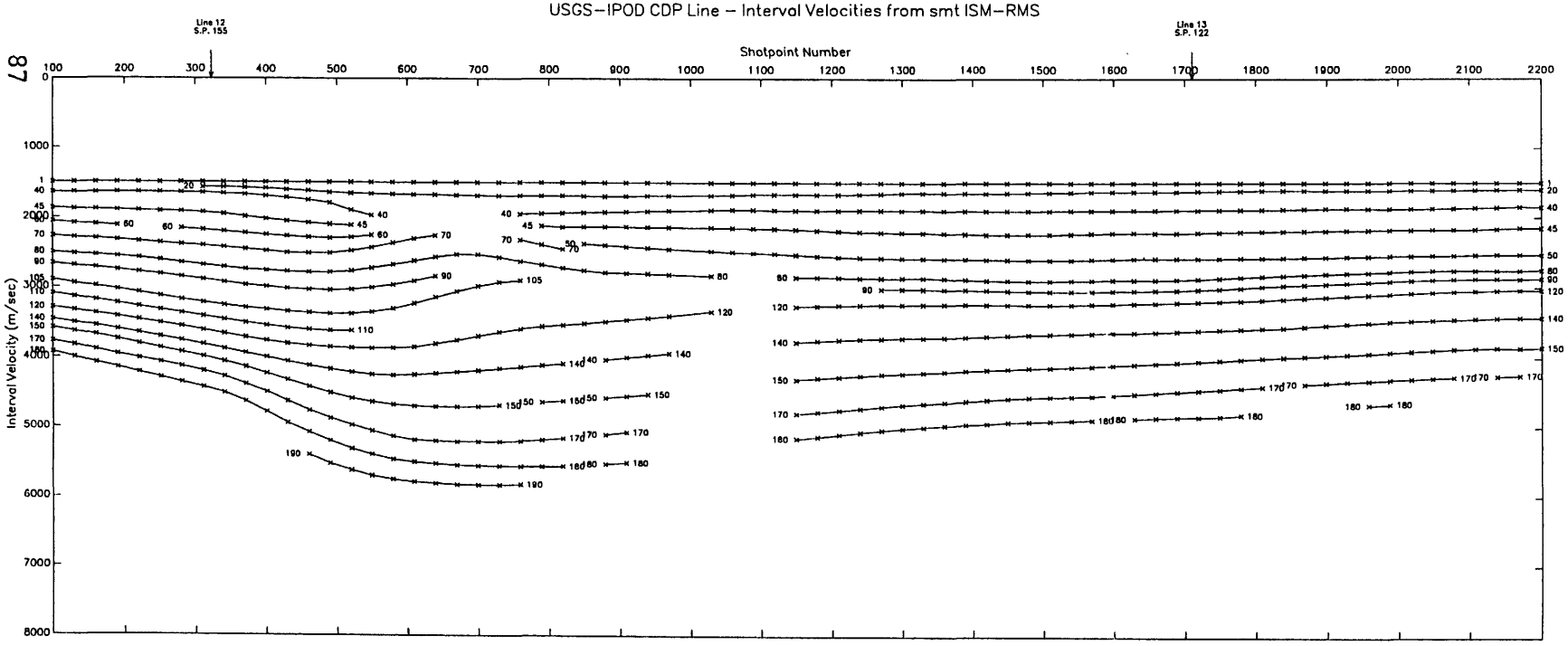

Appendix 4

Time Depth Contour Maps for the Base of Acoustic Units in Digital Database

Surface contour maps of the two-way travel times to the base of each acoustic unit in this geoacoustic database. The dotted lines represent the seismic line control used to construct each surface. See Figure 8 for the 5-minute grid point map, based on these seismic lines, used to construct the contour map. Shaded masks indicate the regions where a particular surface has been eroded into by an overlying surface. Narrow blank zones in the shelf-edge region are where deeper units are obscured by the Jurassic carbonate bank. Contour interval is 0.2 sec in two-way travel times.

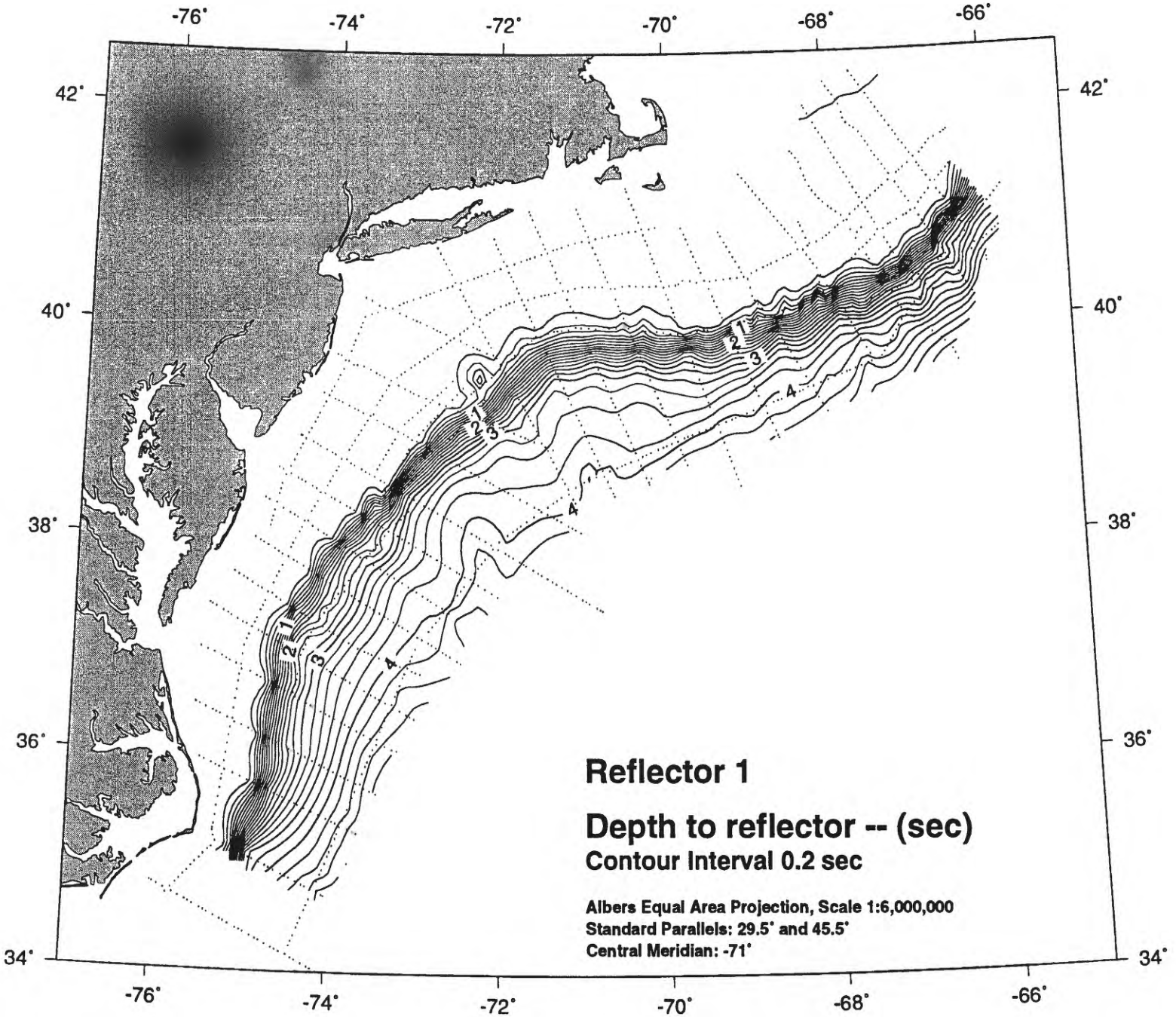
-76°
-74°
-72°
-70°
-68°
-66°
42°
40°
38°
36°
34°
1
2
3
4
Reflector 1
Depth to reflector -- (sec)
Contour Interval 0.2 sec
Albers Equal Area Projection, Scale 1:6,000,000
Standard Parallels: 29.5° and 45.5°
Central Meridian: -71°

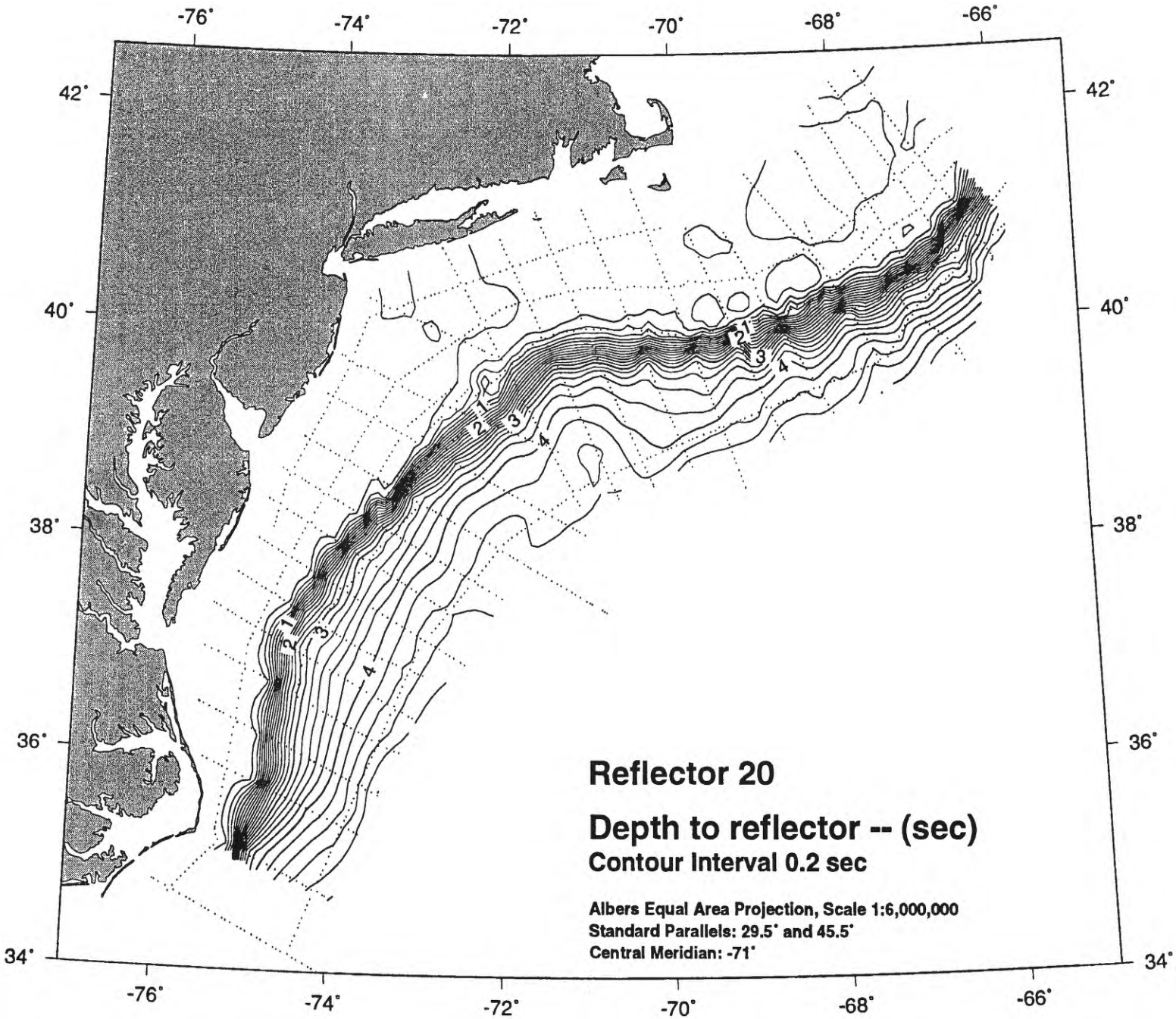
-76°
-74°
-72°
-70°
-68°
-66°
42°
40°
38°
36°
34°
1
2
3
4
Reflector 20
Depth to reflector -- (sec)
Contour Interval 0.2 sec
Albers Equal Area Projection, Scale 1:6,000,000
Standard Parallels: 29.5° and 45.5°
Central Meridian: -71°

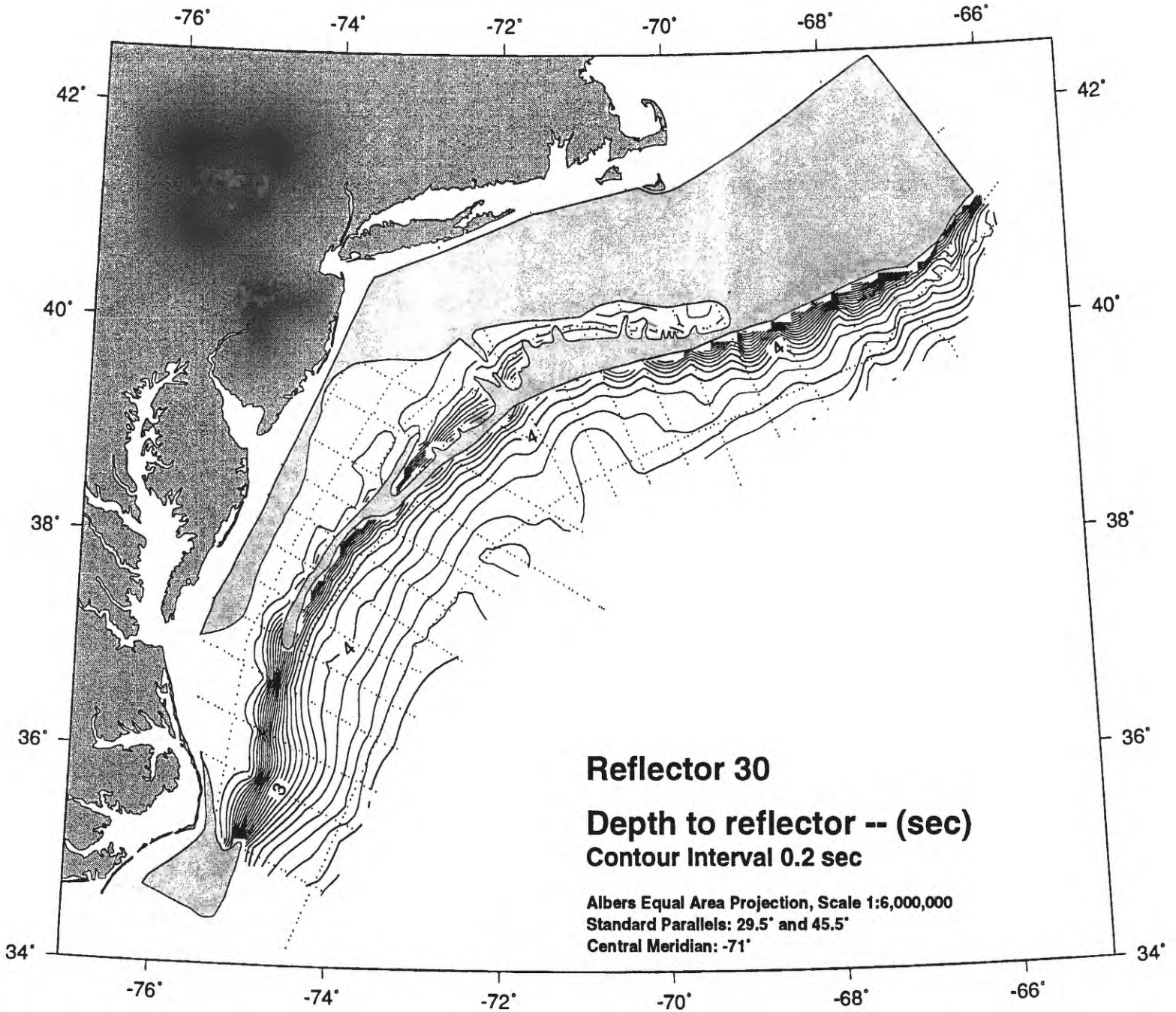
-76°
-74°
-72°
-70°
-68°
-66°
42°
40°
38°
36°
34°
4
3
Reflector 30
Depth to reflector -- (sec)
Contour Interval 0.2 sec
Albers Equal Area Projection, Scale 1:6,000,000
Standard Parallels: 29.5° and 45.5°
Central Meridian: -71°

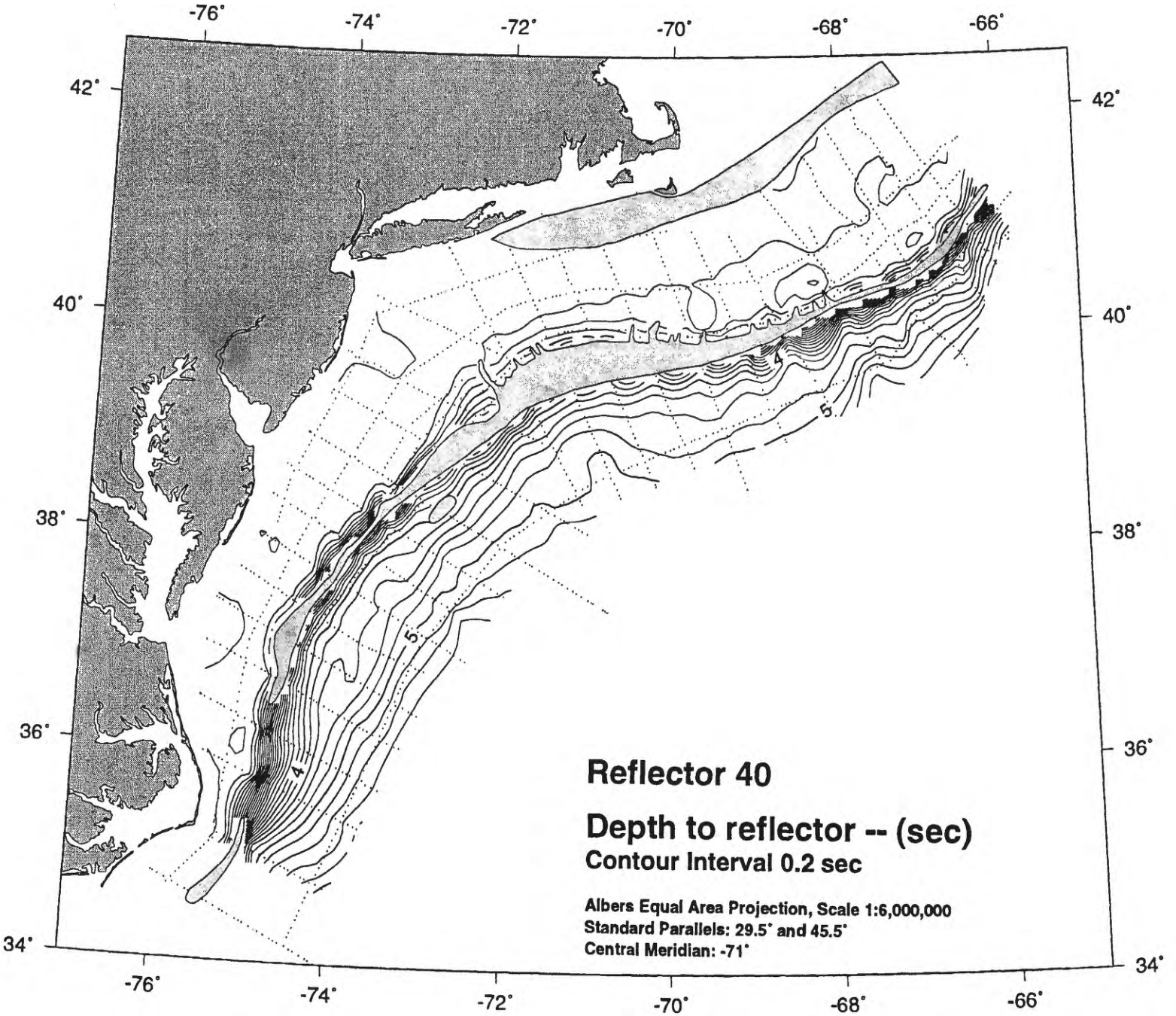
-76°
-74°
-72°
-70°
-68°
-66°
42°
40°
38°
36°
34°
4
5
Reflector 40
Depth to reflector -- (sec)
Contour Interval 0.2 sec
Albers Equal Area Projection, Scale 1:6,000,000
Standard Parallels: 29.5° and 45.5°
Central Meridian: -71°

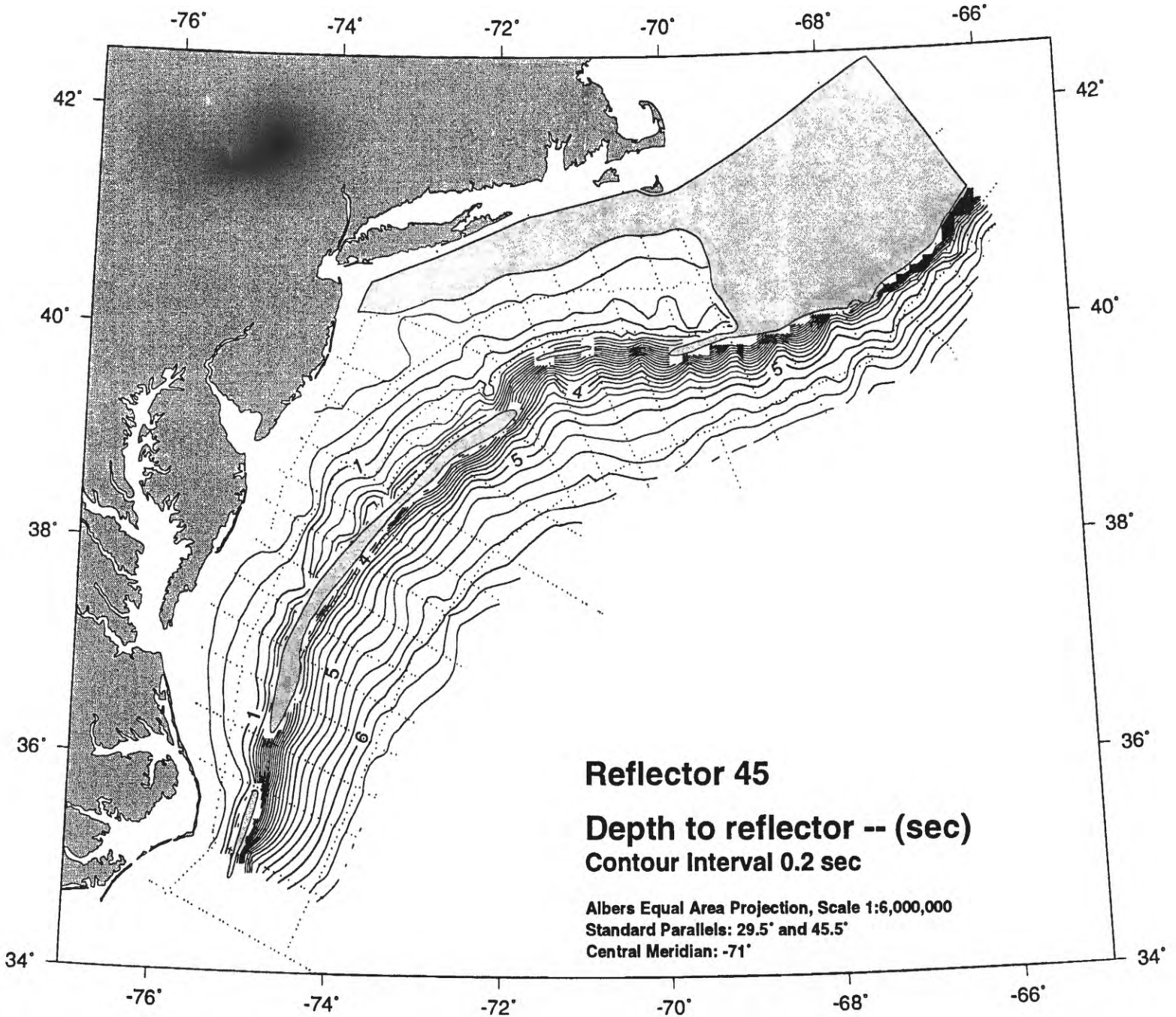
-76°
-74°
-72°
-70°
-68°
-66°
42°
40°
38°
36°
34°
1
4
5
6
Reflector 45
Depth to reflector -- (sec)
Contour Interval 0.2 sec
Albers Equal Area Projection, Scale 1:6,000,000
Standard Parallels: 29.5° and 45.5°
Central Meridian: -71°

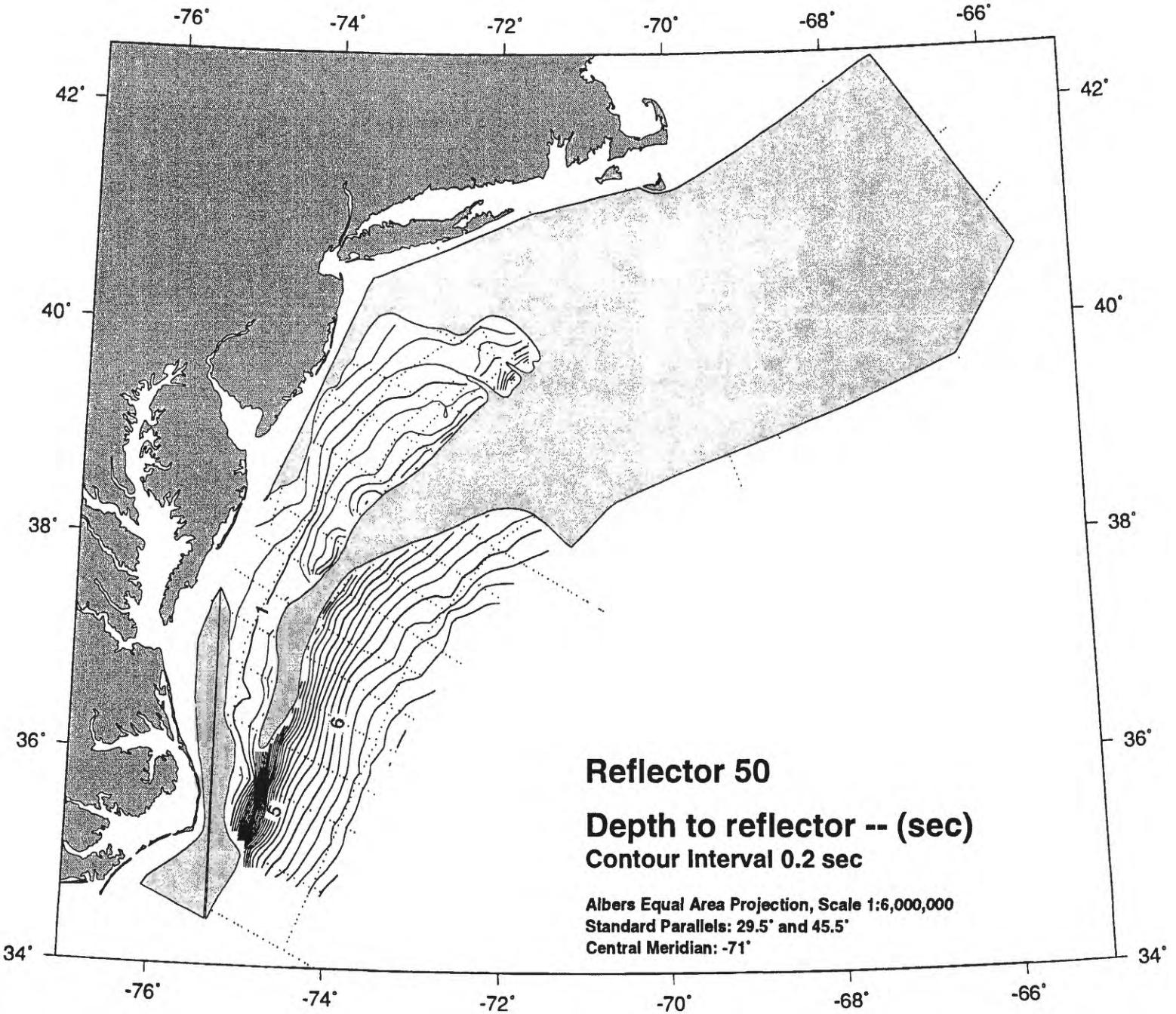
-76°
-74°
-72°
-70°
-68°
-66°
42°
40°
38°
36°
34°
1
5
6
Reflector 50
Depth to reflector -- (sec)
Contour Interval 0.2 sec
Albers Equal Area Projection, Scale 1:6,000,000
Standard Parallels: 29.5° and 45.5°
Central Meridian: -71°

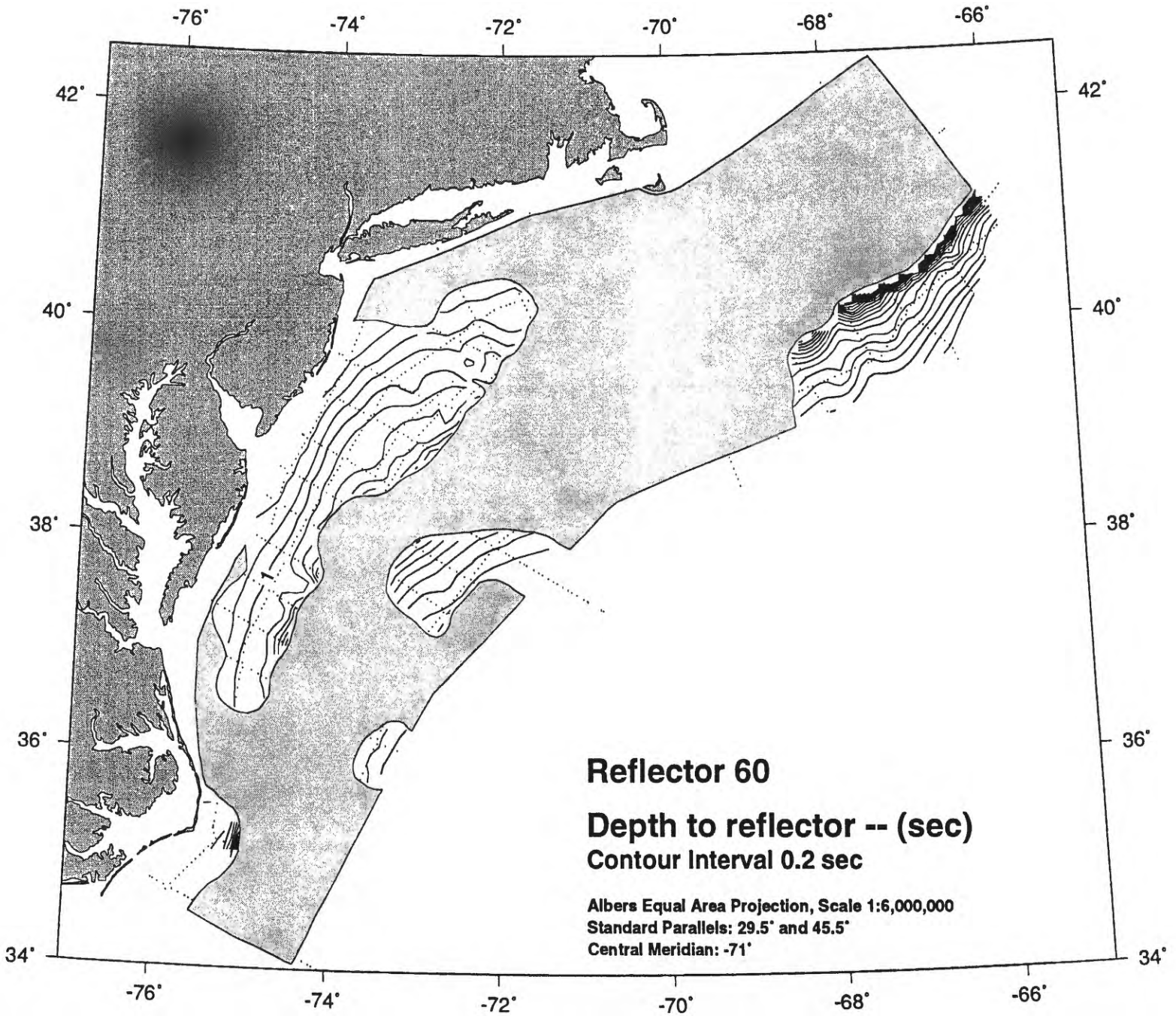
-76°
-74°
-72°
-70°
-68°
-66°
42°
40°
38°
36°
34°
Reflector 60
Depth to reflector -- (sec)
Contour Interval 0.2 sec
Albers Equal Area Projection, Scale 1:6,000,000
Standard Parallels: 29.5° and 45.5°
Central Meridian: -71°

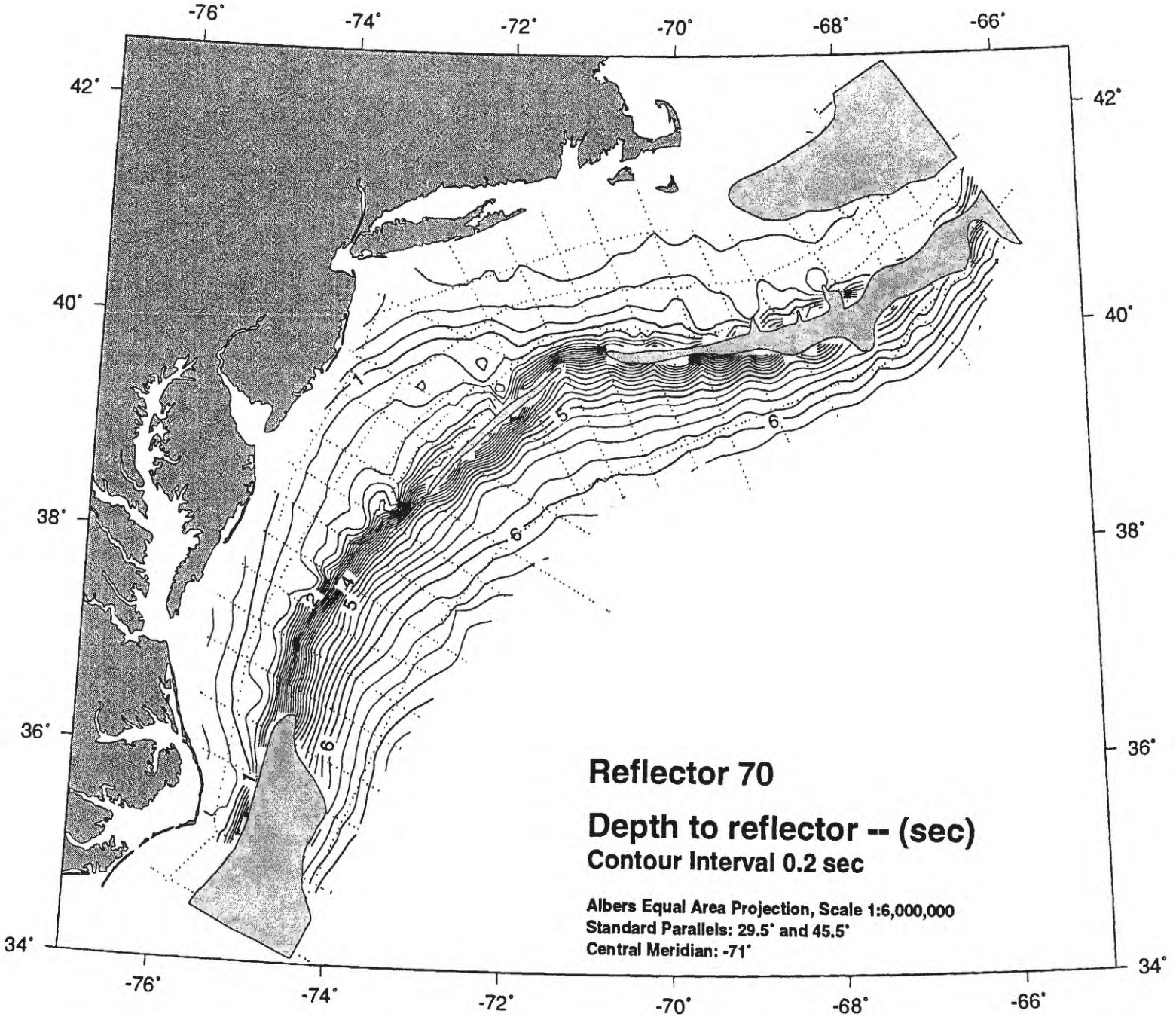
-76°
-74°
-72°
-70°
-68°
-66°
42°
40°
38°
36°
34°
1
2
3
4
5
6
Reflector 70
Depth to reflector -- (sec)
Contour Interval 0.2 sec
Albers Equal Area Projection, Scale 1:6,000,000
Standard Parallels: 29.5° and 45.5°
Central Meridian: -71°

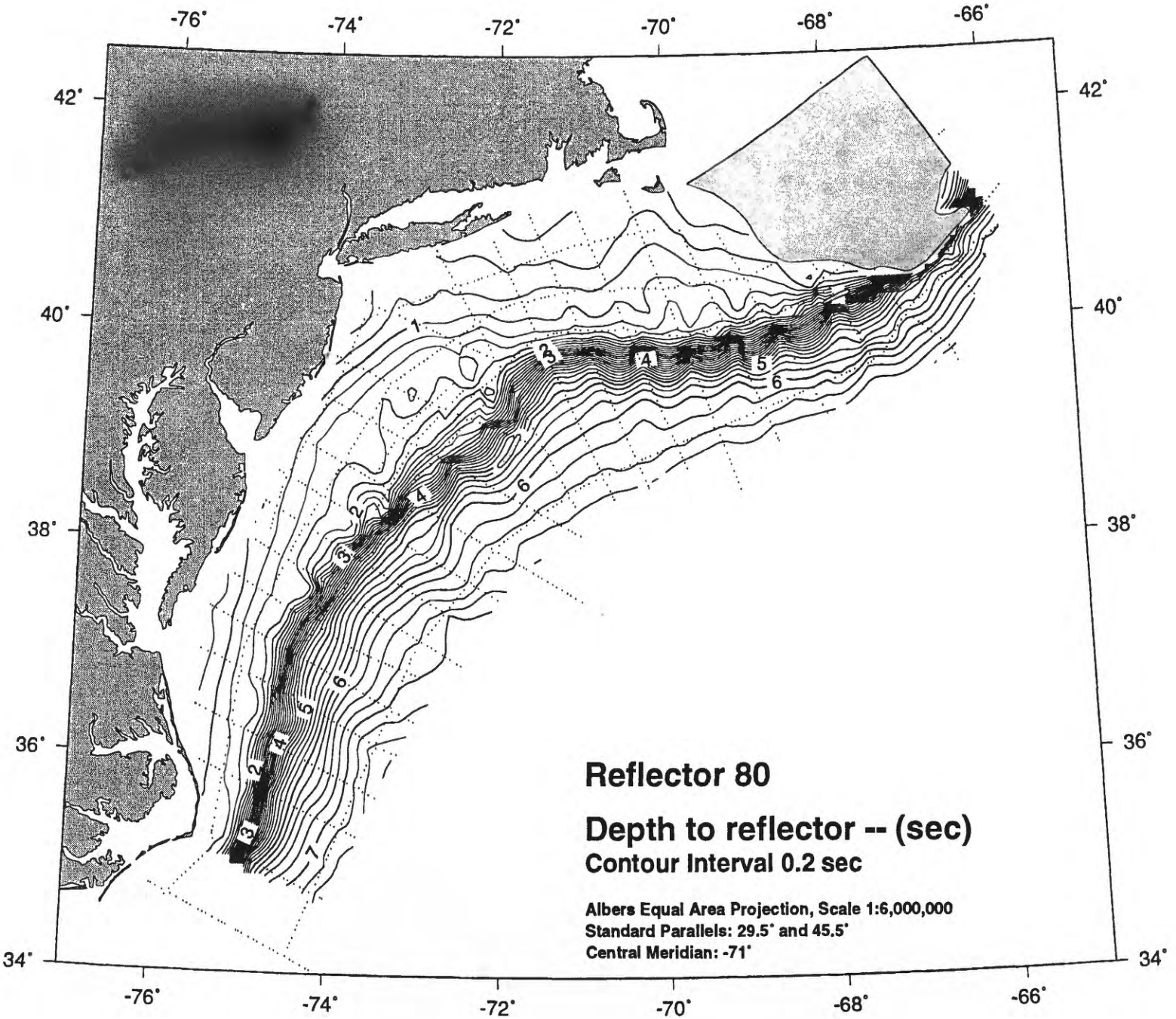
-76°
-74°
-72°
-70°
-68°
-66°
42°
40°
38°
36°
34°
Reflector 80
Depth to reflector -- (sec)
Contour Interval 0.2 sec
Albers Equal Area Projection, Scale 1:6,000,000
Standard Parallels: 29.5° and 45.5°
Central Meridian: -71°

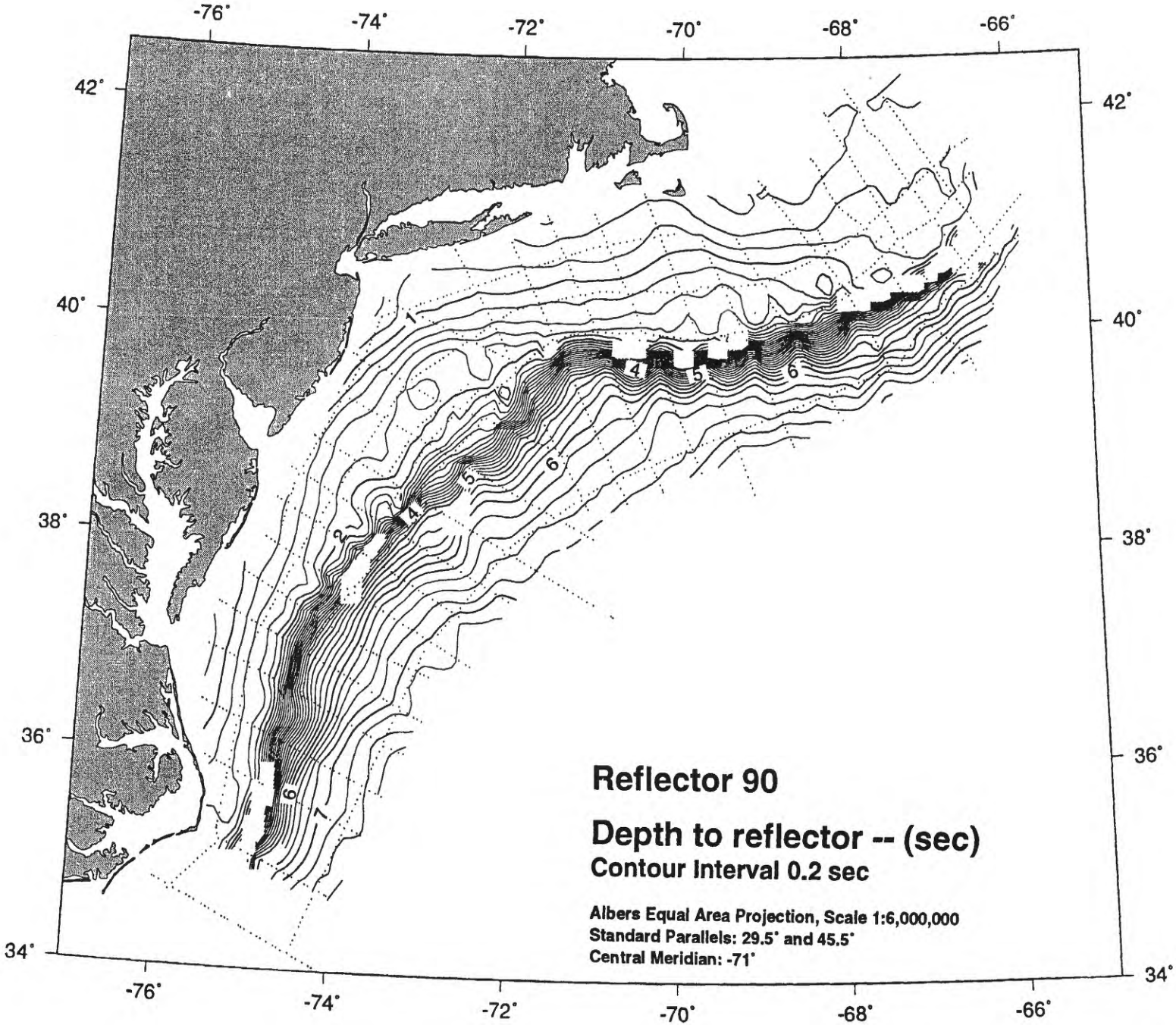
-76°
-74°
-72°
-70°
-68°
-66°
42°
40°
38°
36°
34°
1
2
4
5
6
7
Reflector 90
Depth to reflector -- (sec)
Contour Interval 0.2 sec
Albers Equal Area Projection, Scale 1:6,000,000
Standard Parallels: 29.5° and 45.5°
Central Meridian: -71°

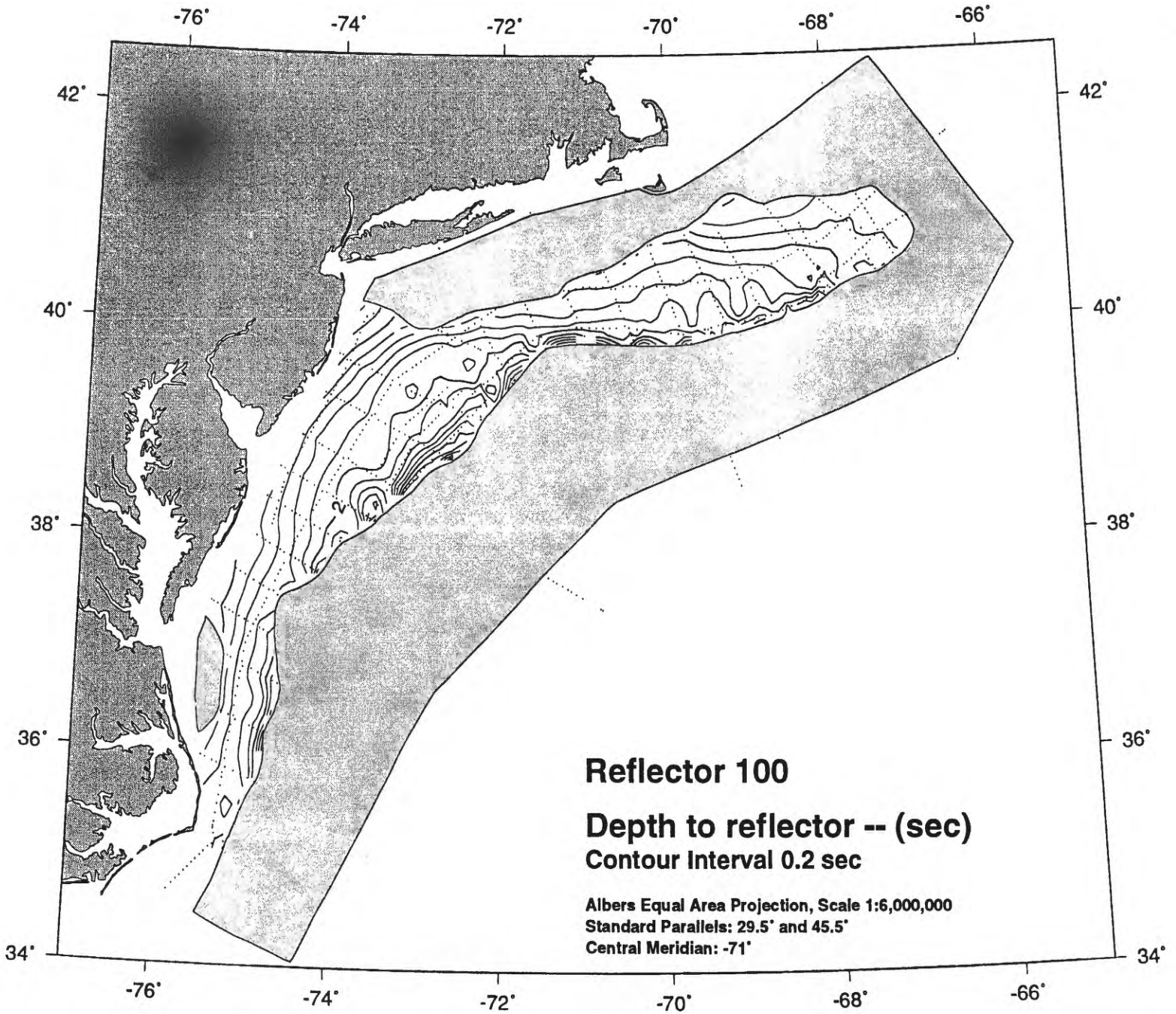
-76°
-74°
-72°
-70°
-68°
-66°
42°
40°
38°
36°
34°
Reflector 100
Depth to reflector -- (sec)
Contour Interval 0.2 sec
Albers Equal Area Projection, Scale 1:6,000,000
Standard Parallels: 29.5° and 45.5°
Central Meridian: -71°

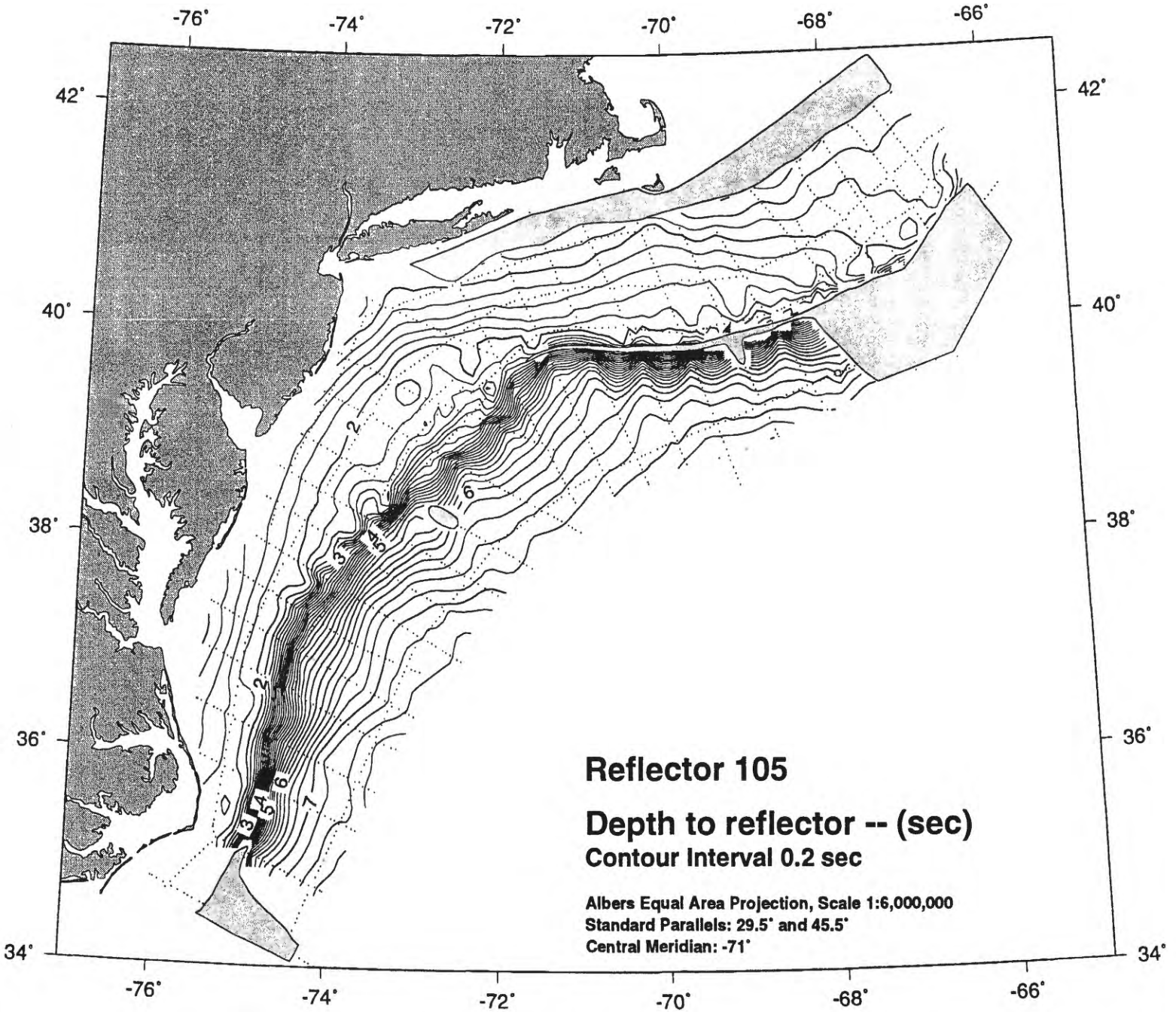
-76°
-74°
-72°
-70°
-68°
-66°
42°
40°
38°
36°
34°
Reflector 105
Depth to reflector -- (sec)
Contour Interval 0.2 sec
Albers Equal Area Projection, Scale 1:6,000,000
Standard Parallels: 29.5° and 45.5°
Central Meridian: -71°

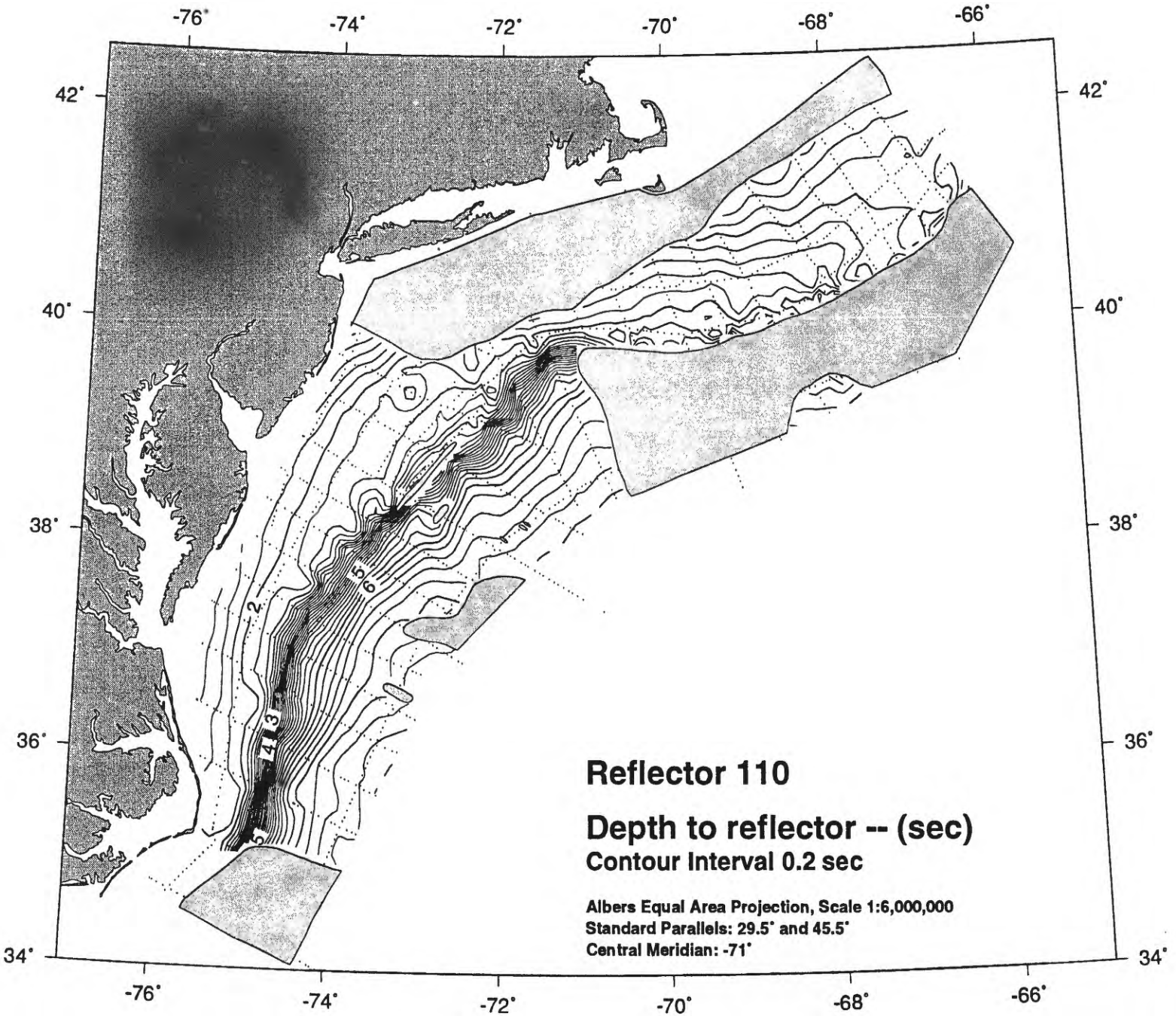
-76°
-74°
-72°
-70°
-68°
-66°
42°
40°
38°
36°
34°
2
5
6
4
3
1
Reflector 110
Depth to reflector -- (sec)
Contour Interval 0.2 sec
Albers Equal Area Projection, Scale 1:6,000,000
Standard Parallels: 29.5° and 45.5°
Central Meridian: -71°

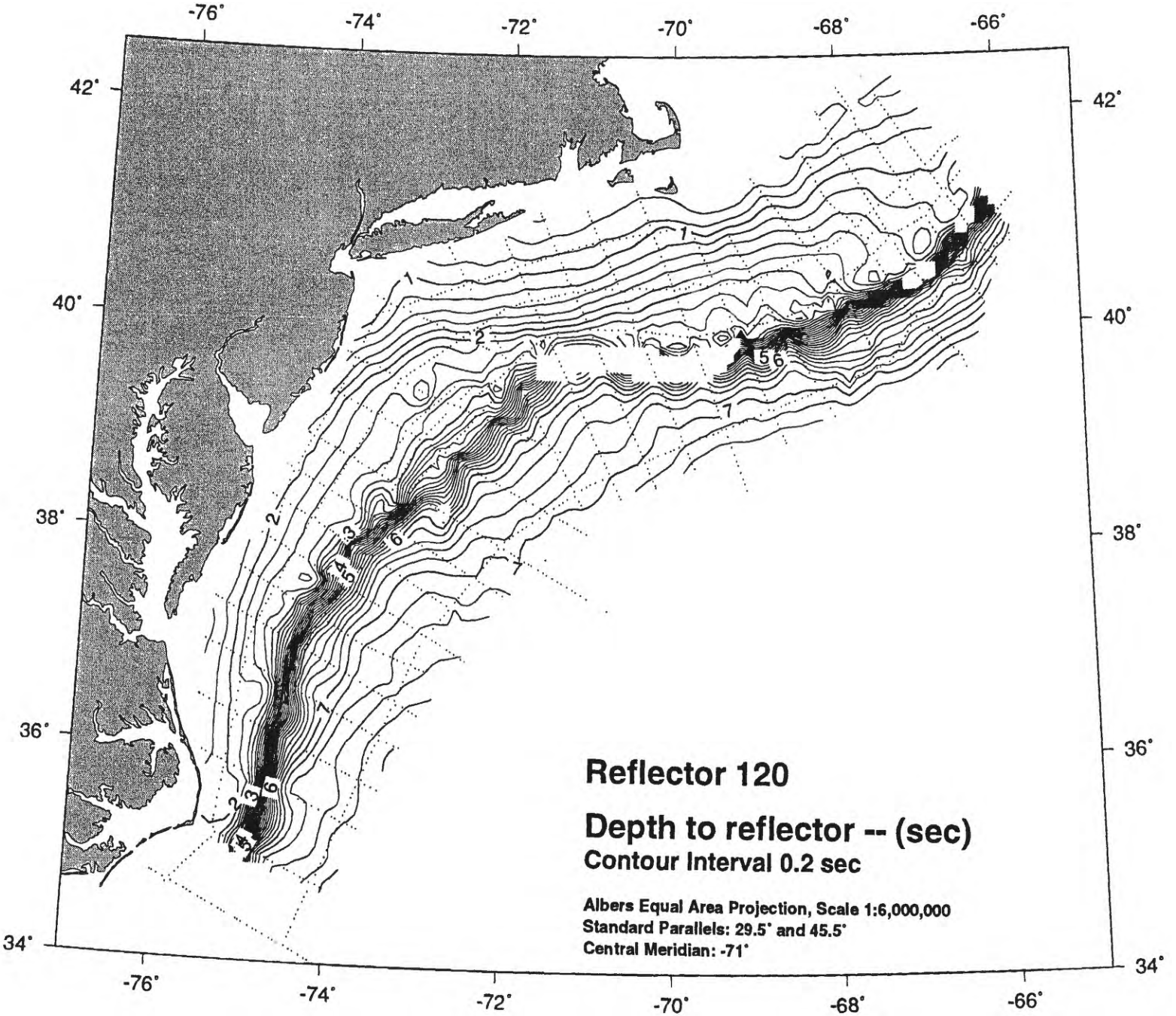
Reflector 120
Depth to reflector -- (sec)
Contour Interval 0.2 sec
Albers Equal Area Projection, Scale 1:6,000,000
Standard Parallels: 29.5° and 45.5°
Central Meridian: -71°
-76°
-74°
-72°
-70°
-68°
-66°
42°
40°
38°
36°
34°

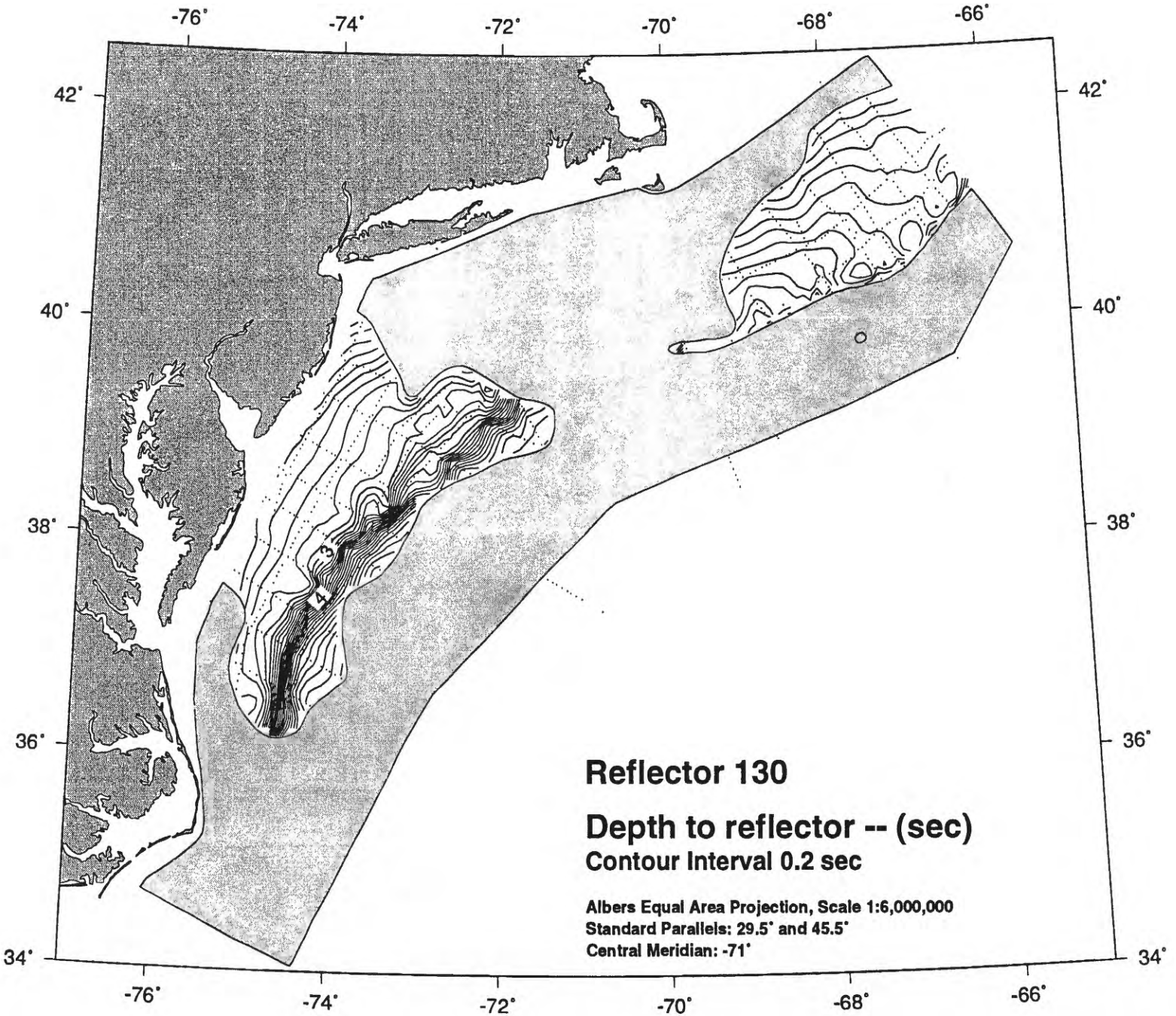
-76°
-74°
-72°
-70°
-68°
-66°
42°
40°
38°
36°
34°
3
4
Reflector 130
Depth to reflector -- (sec)
Contour Interval 0.2 sec
Albers Equal Area Projection, Scale 1:6,000,000
Standard Parallels: 29.5° and 45.5°
Central Meridian: -71°

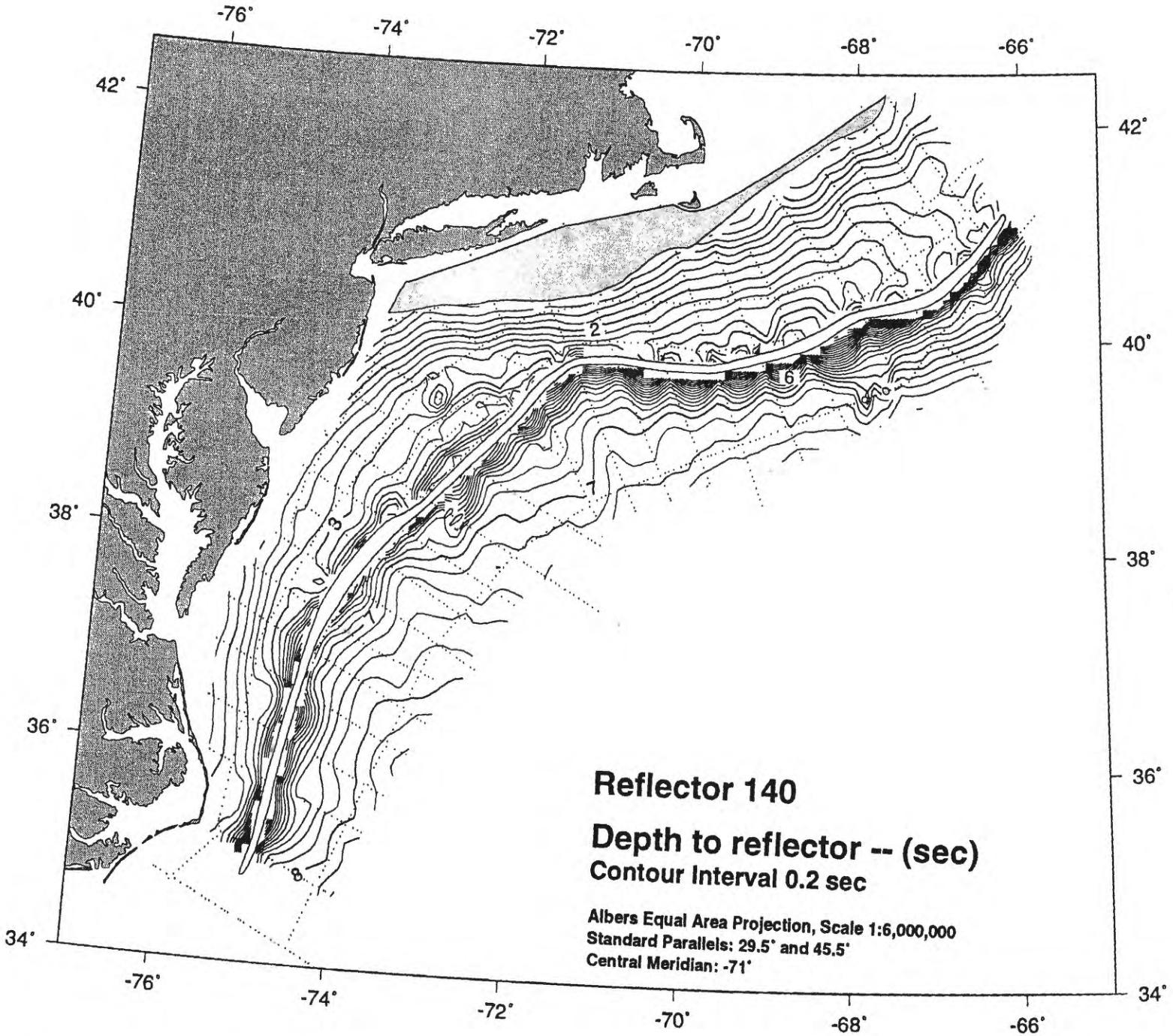
-76°
-74°
-72°
-70°
-68°
-66°
42°
40°
38°
36°
34°
2
3
4
6
8
Reflector 140
Depth to reflector -- (sec)
Contour Interval 0.2 sec
Albers Equal Area Projection, Scale 1:6,000,000
Standard Parallels: 29.5° and 45.5°
Central Meridian: -71°

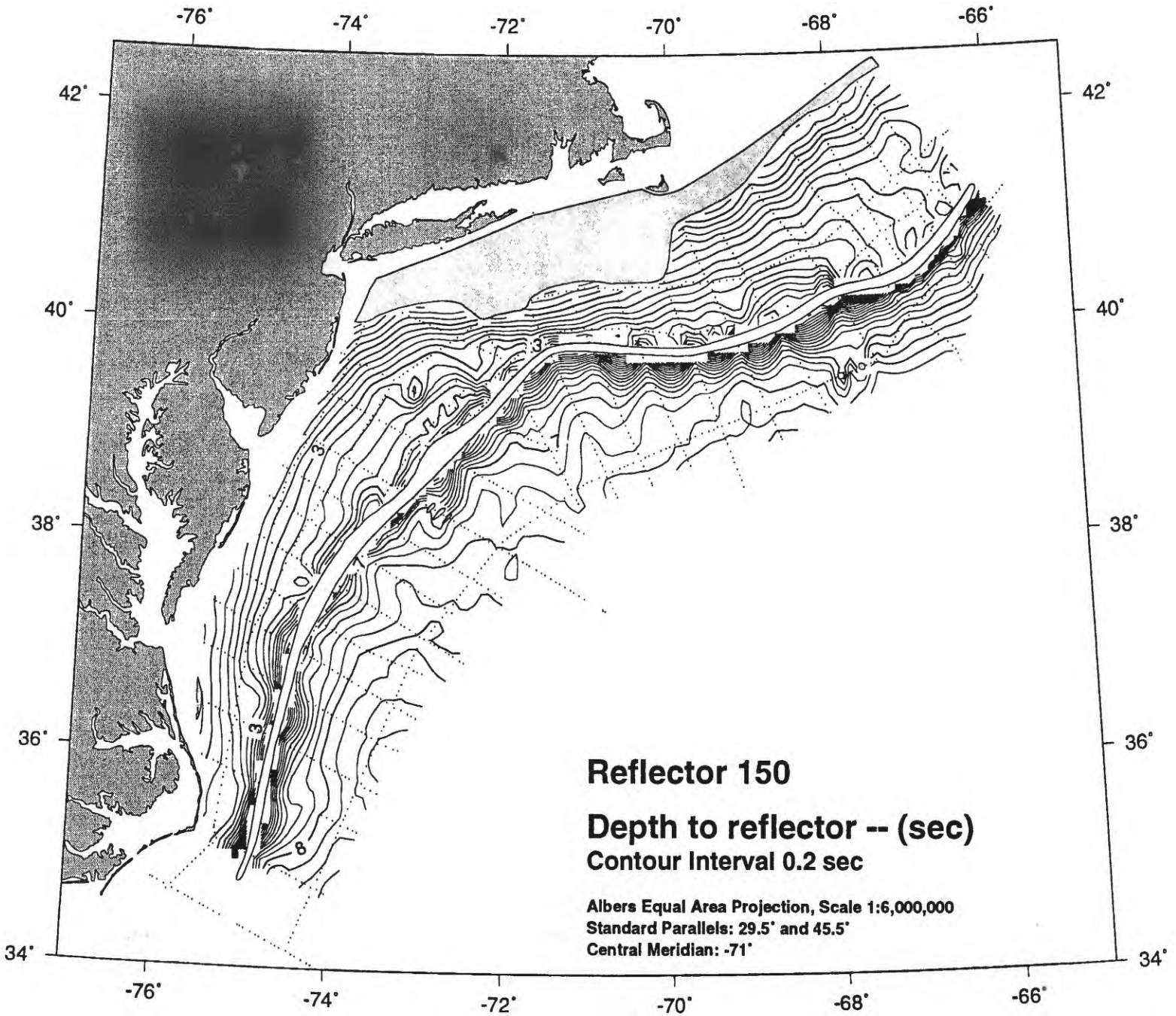
-76°
-74°
-72°
-70°
-68°
-66°
42°
40°
38°
36°
34°
Reflector 150
Depth to reflector -- (sec)
Contour Interval 0.2 sec
Albers Equal Area Projection, Scale 1:6,000,000
Standard Parallels: 29.5° and 45.5°
Central Meridian: -71°

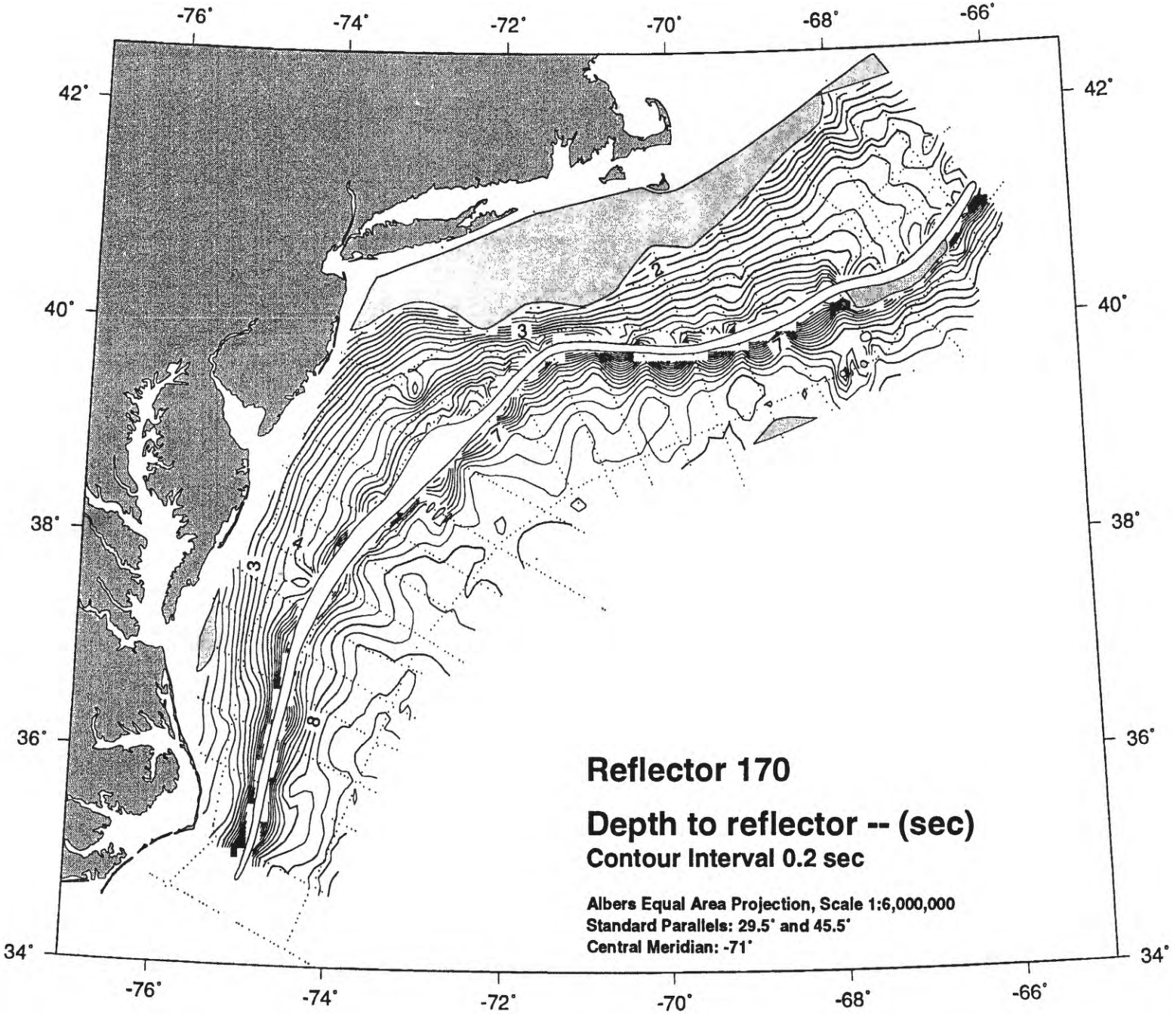
-76°
-74°
-72°
-70°
-68°
-66°
42°
40°
38°
36°
34°
Reflector 170
Depth to reflector -- (sec)
Contour Interval 0.2 sec
Albers Equal Area Projection, Scale 1:6,000,000
Standard Parallels: 29.5° and 45.5°
Central Meridian: -71°

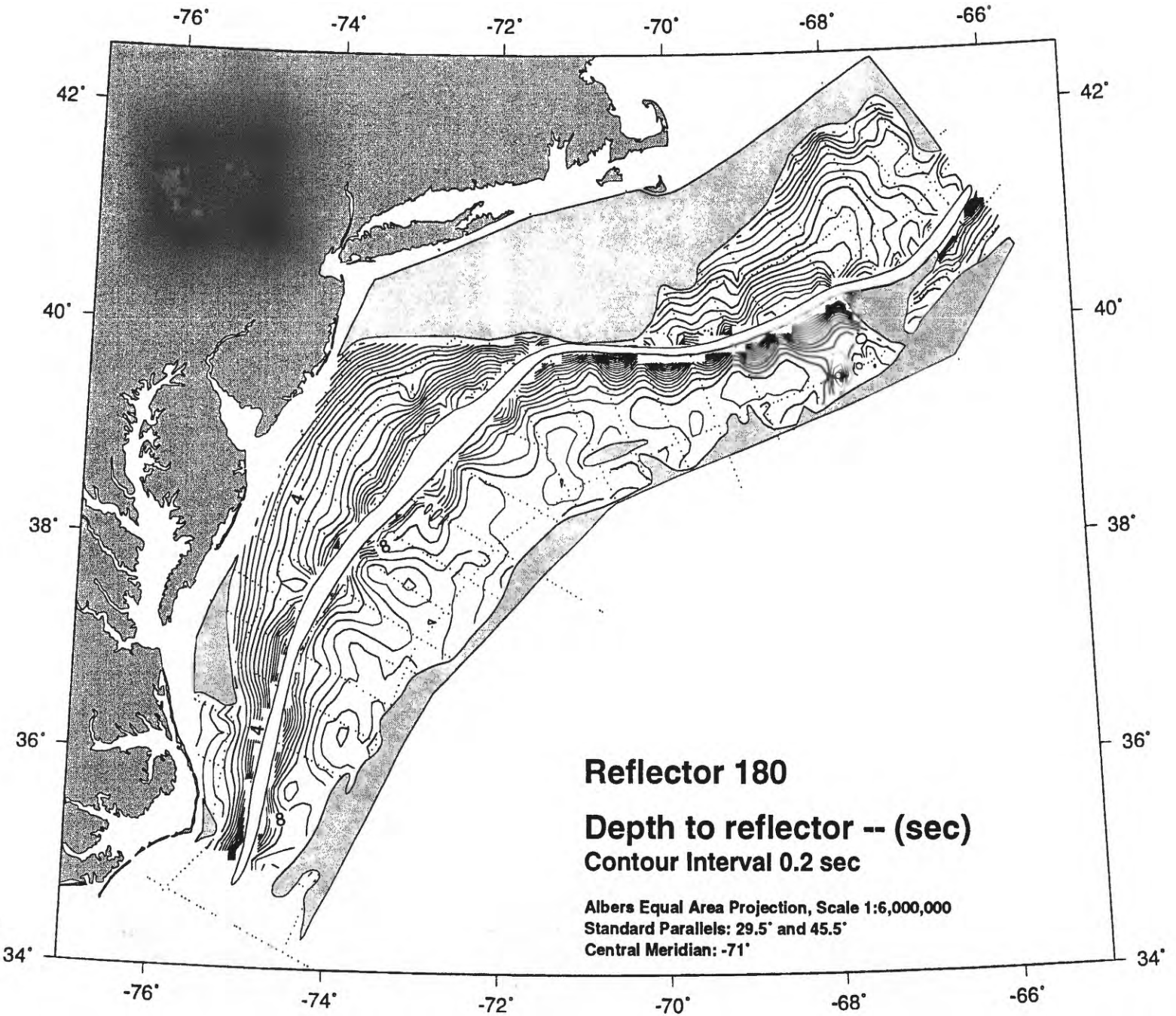
-76°
-74°
-72°
-70°
-68°
-66°
42°
40°
38°
36°
34°
4
8
Reflector 180
Depth to reflector -- (sec)
Contour Interval 0.2 sec
Albers Equal Area Projection, Scale 1:6,000,000
Standard Parallels: 29.5° and 45.5°
Central Meridian: -71°

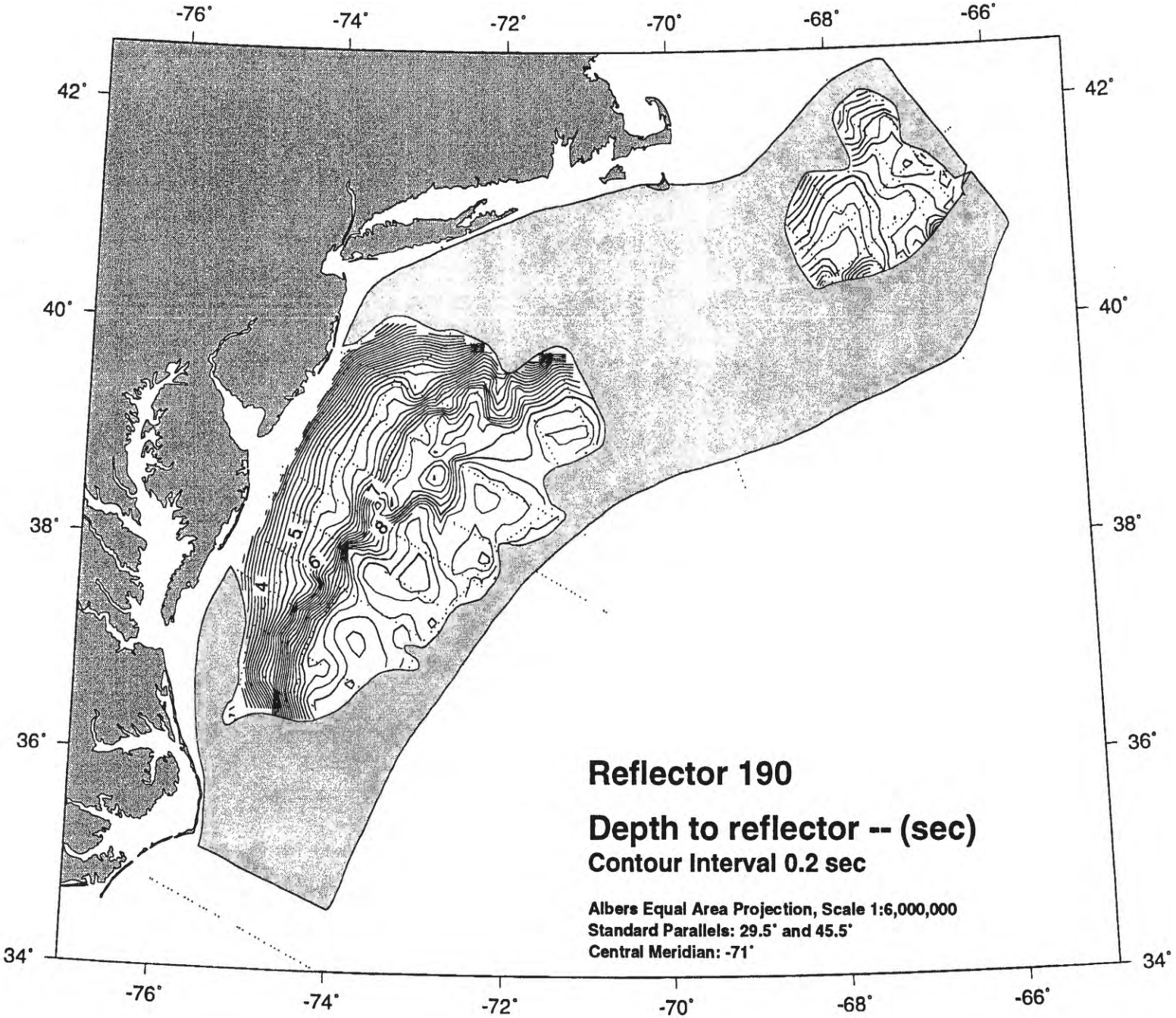
-76°
-74°
-72°
-70°
-68°
-66°
42°
40°
38°
36°
34°
4
5
6
7
8
Reflector 190
Depth to reflector -- (sec)
Contour Interval 0.2 sec
Albers Equal Area Projection, Scale 1:6,000,000
Standard Parallels: 29.5° and 45.5°
Central Meridian: -71°

Appendix 5

Depth (in meters) Contour Maps for the Base of Acoustic Units in Digital Database

Surface contour maps of the depth in meters to the base of each acoustic unit in this geoacoustic database. The dotted lines represent the seismic line control used to construct each surface. See Figure 8 for the 5-minute grid point map, based on these seismic lines, used to construct the contour map. Shaded masks indicate the regions where a particular surface has been eroded into by an overlying surface. Narrow blank zones in the shelf edge region are where deeper units are obscured by the Jurassic carbonate bank. Contour interval is 500 m.

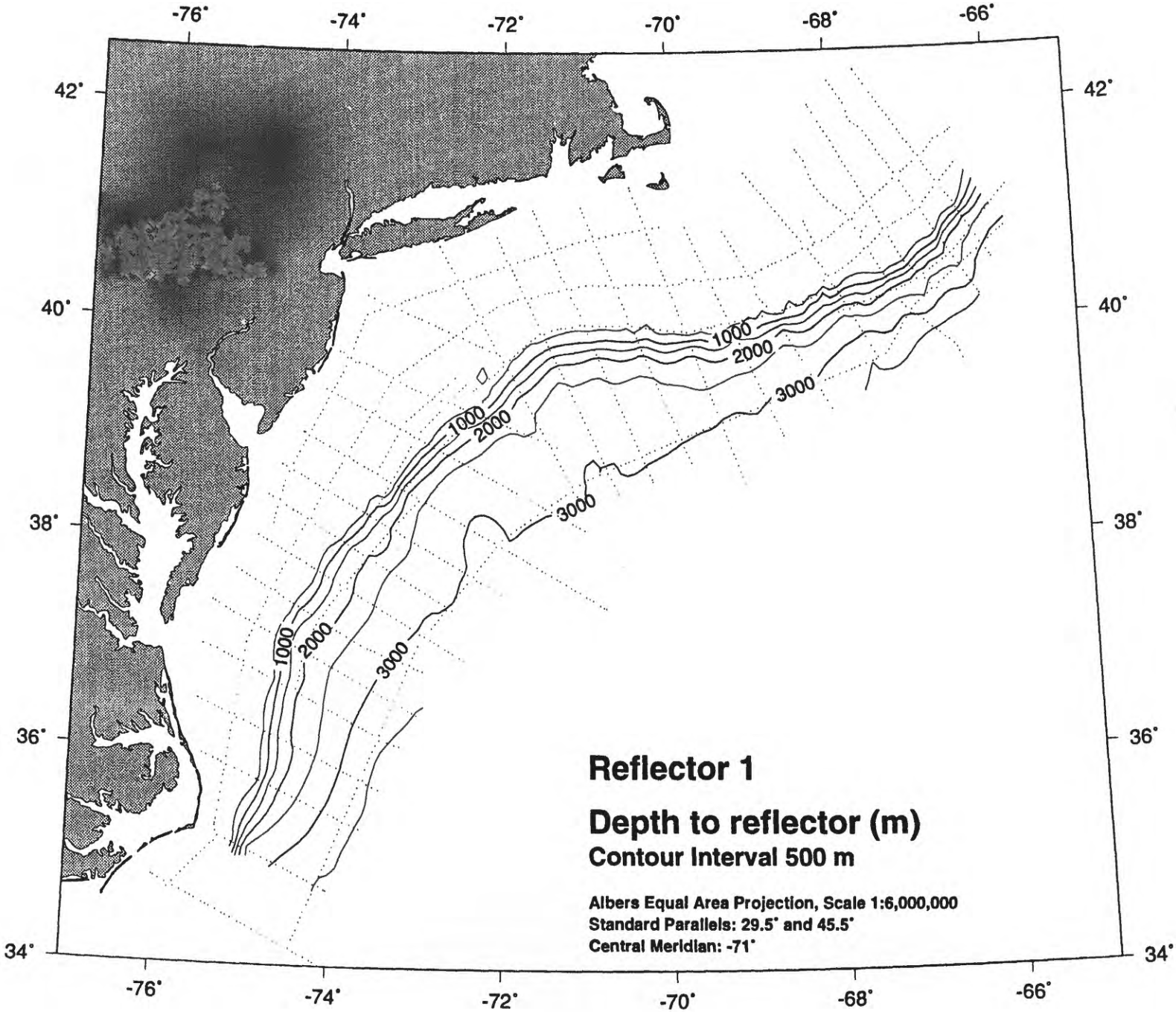
-76°
-74°
-72°
-70°
-68°
-66°
42°
40°
38°
36°
34°
1000
2000
3000
Reflector 1
Depth to reflector (m)
Contour Interval 500 m
Albers Equal Area Projection, Scale 1:6,000,000
Standard Parallels: 29.5° and 45.5°
Central Meridian: -71°

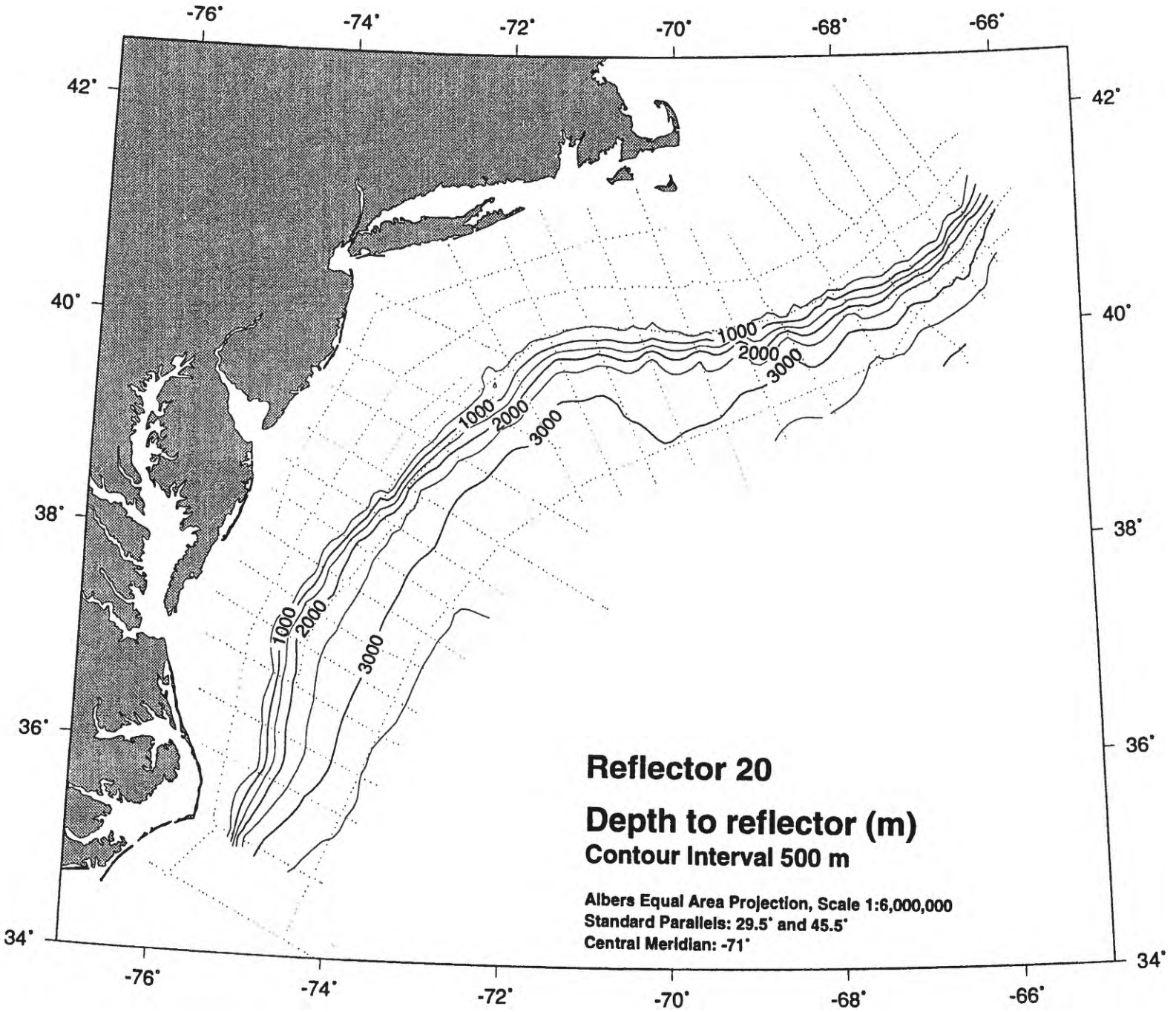
-76°
-74°
-72°
-70°
-68°
-66°
42°
40°
38°
36°
34°
1000
2000
3000
Reflector 20
Depth to reflector (m)
Contour Interval 500 m
Albers Equal Area Projection, Scale 1:6,000,000
Standard Parallels: 29.5° and 45.5°
Central Meridian: -71°

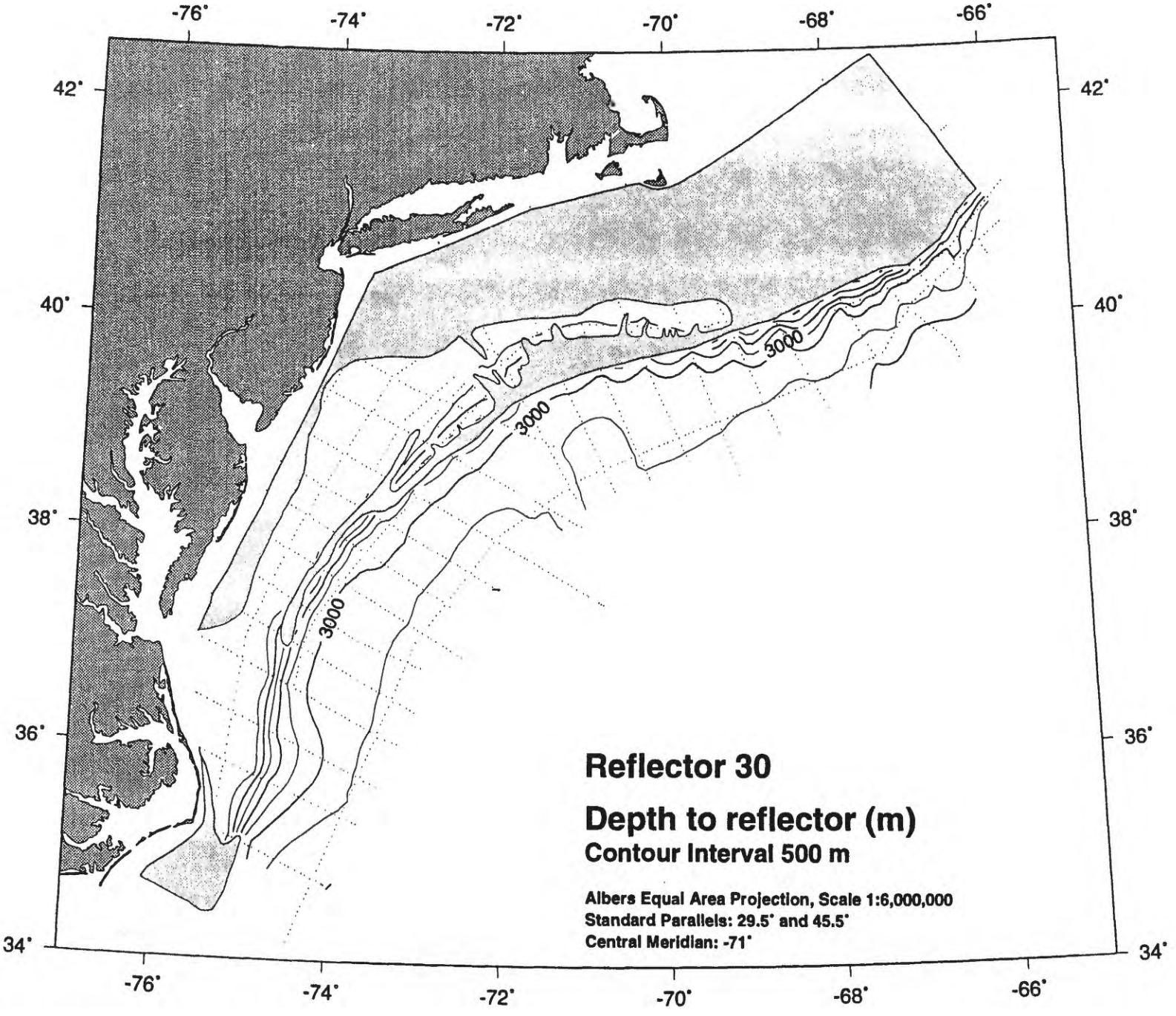
-76°
-74°
-72°
-70°
-68°
-66°
42°
40°
38°
36°
34°
3000
3000
3000
Reflector 30
Depth to reflector (m)
Contour Interval 500 m
Albers Equal Area Projection, Scale 1:6,000,000
Standard Parallels: 29.5° and 45.5°
Central Meridian: -71°

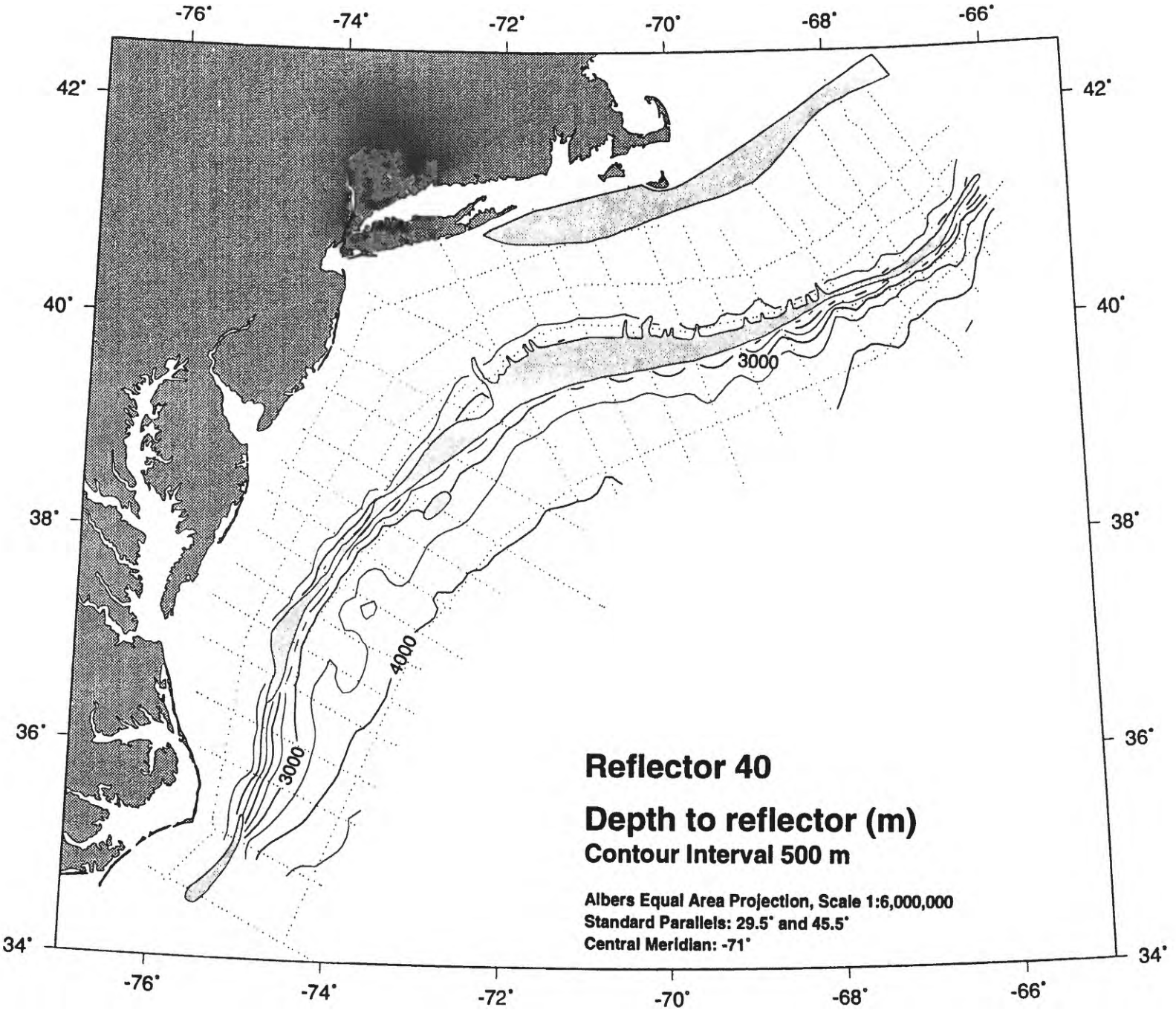
-76°
-74°
-72°
-70°
-68°
-66°
42°
40°
38°
36°
34°
3000
4000
3000
Reflector 40
Depth to reflector (m)
Contour Interval 500 m
Albers Equal Area Projection, Scale 1:6,000,000
Standard Parallels: 29.5° and 45.5°
Central Meridian: -71°

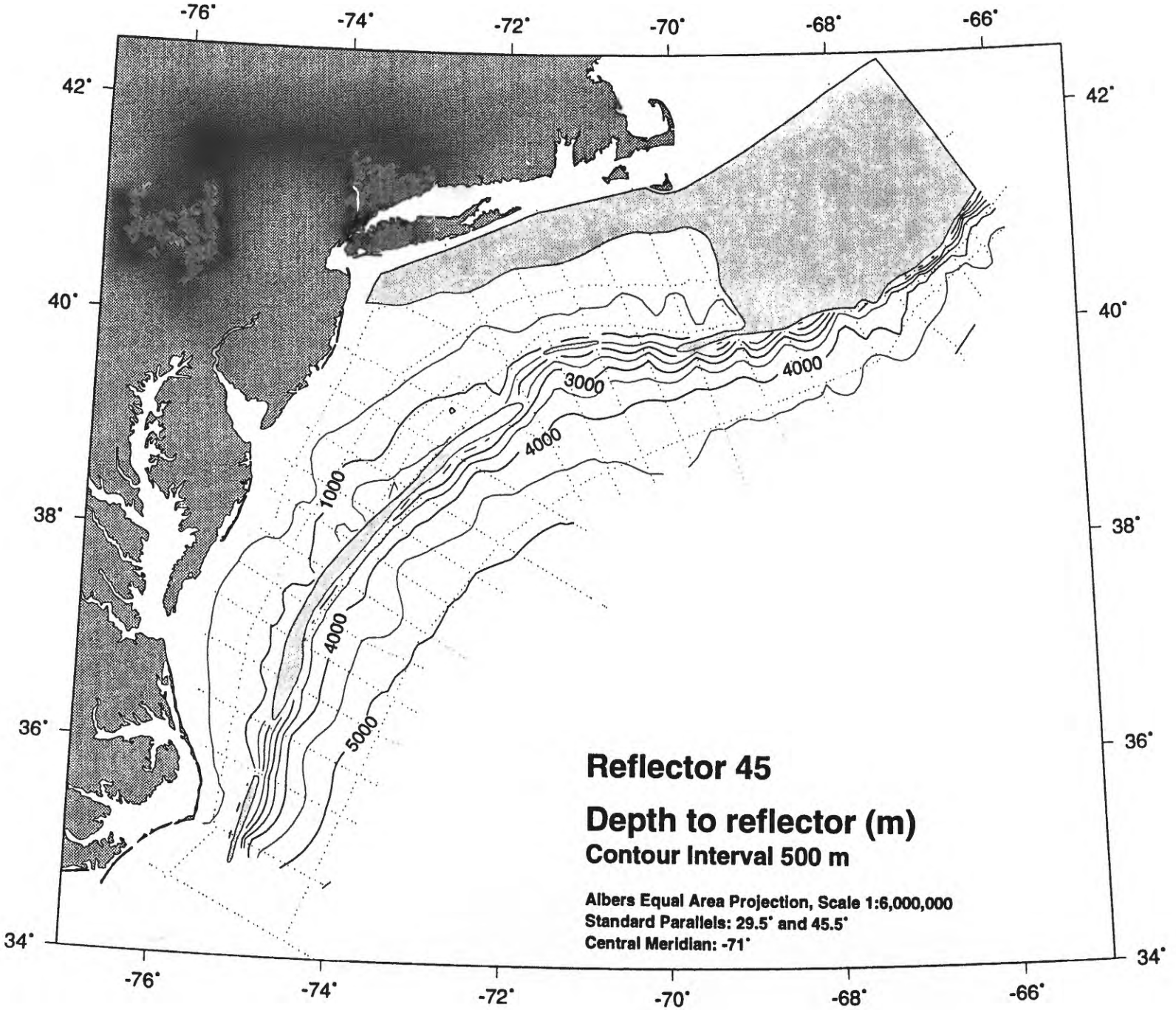
-76°
-74°
-72°
-70°
-68°
-66°
42°
40°
38°
36°
34°
1000
3000
4000
4000
4000
5000
Reflector 45
Depth to reflector (m)
Contour Interval 500 m
Albers Equal Area Projection, Scale 1:6,000,000
Standard Parallels: 29.5° and 45.5°
Central Meridian: -71°

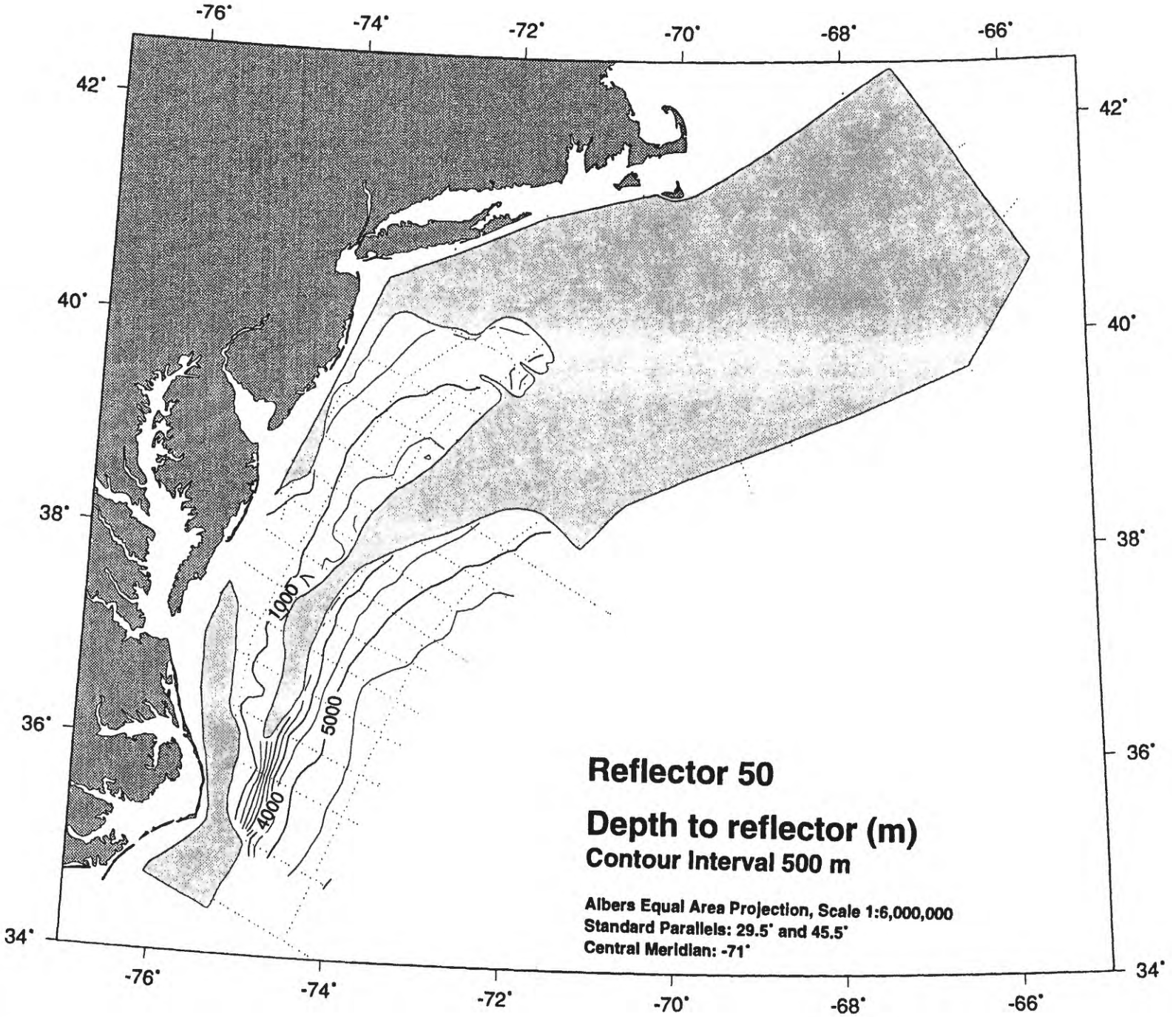
-76°
-74°
-72°
-70°
-68°
-66°
42°
40°
38°
36°
34°
1000
4000
5000
Reflector 50
Depth to reflector (m)
Contour Interval 500 m
Albers Equal Area Projection, Scale 1:6,000,000
Standard Parallels: 29.5° and 45.5°
Central Meridian: -71°

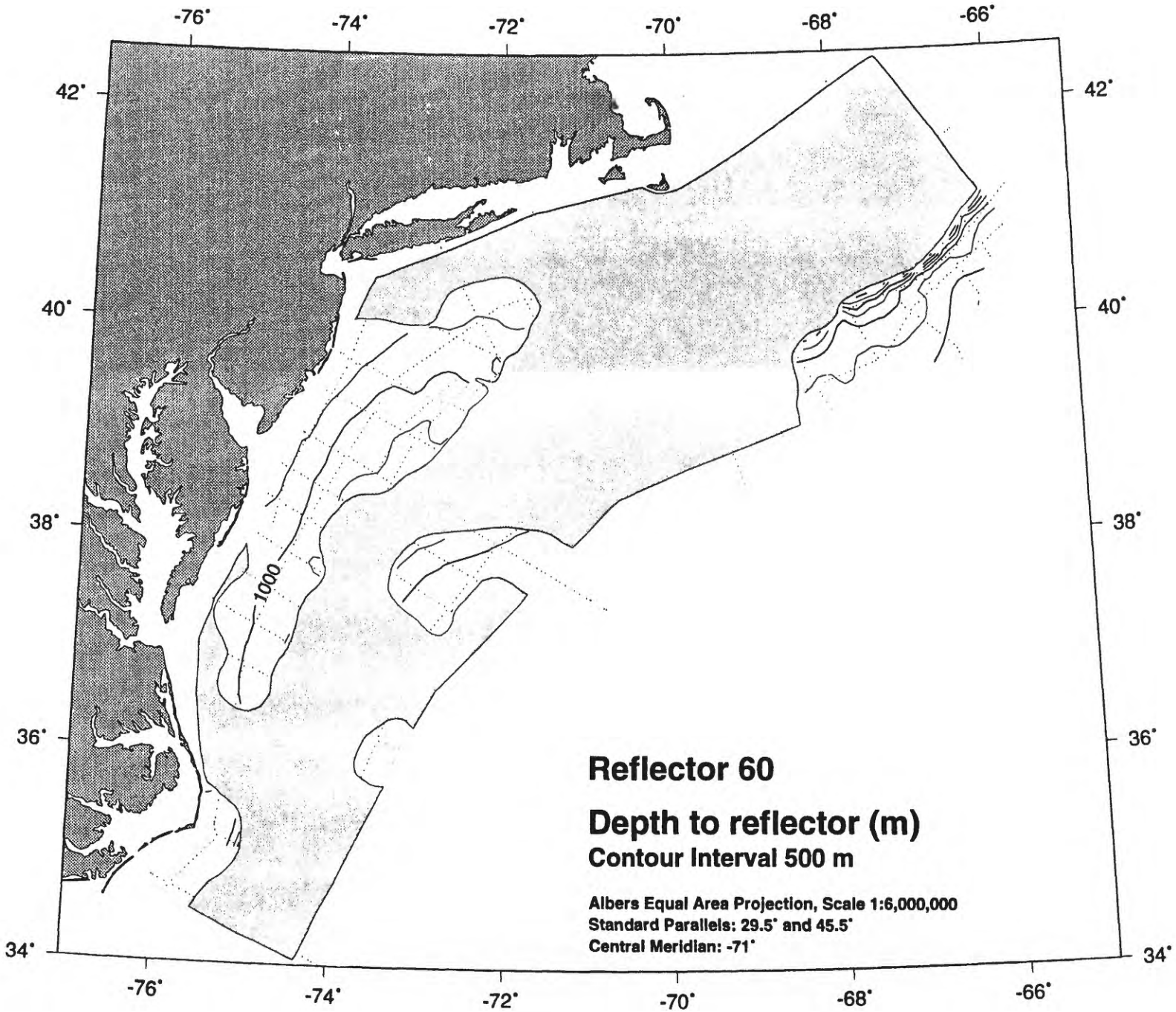
-76°
-74°
-72°
-70°
-68°
-66°
42°
40°
38°
36°
34°
1000
Reflector 60
Depth to reflector (m)
Contour Interval 500 m
Albers Equal Area Projection, Scale 1:6,000,000
Standard Parallels: 29.5° and 45.5°
Central Meridian: -71°

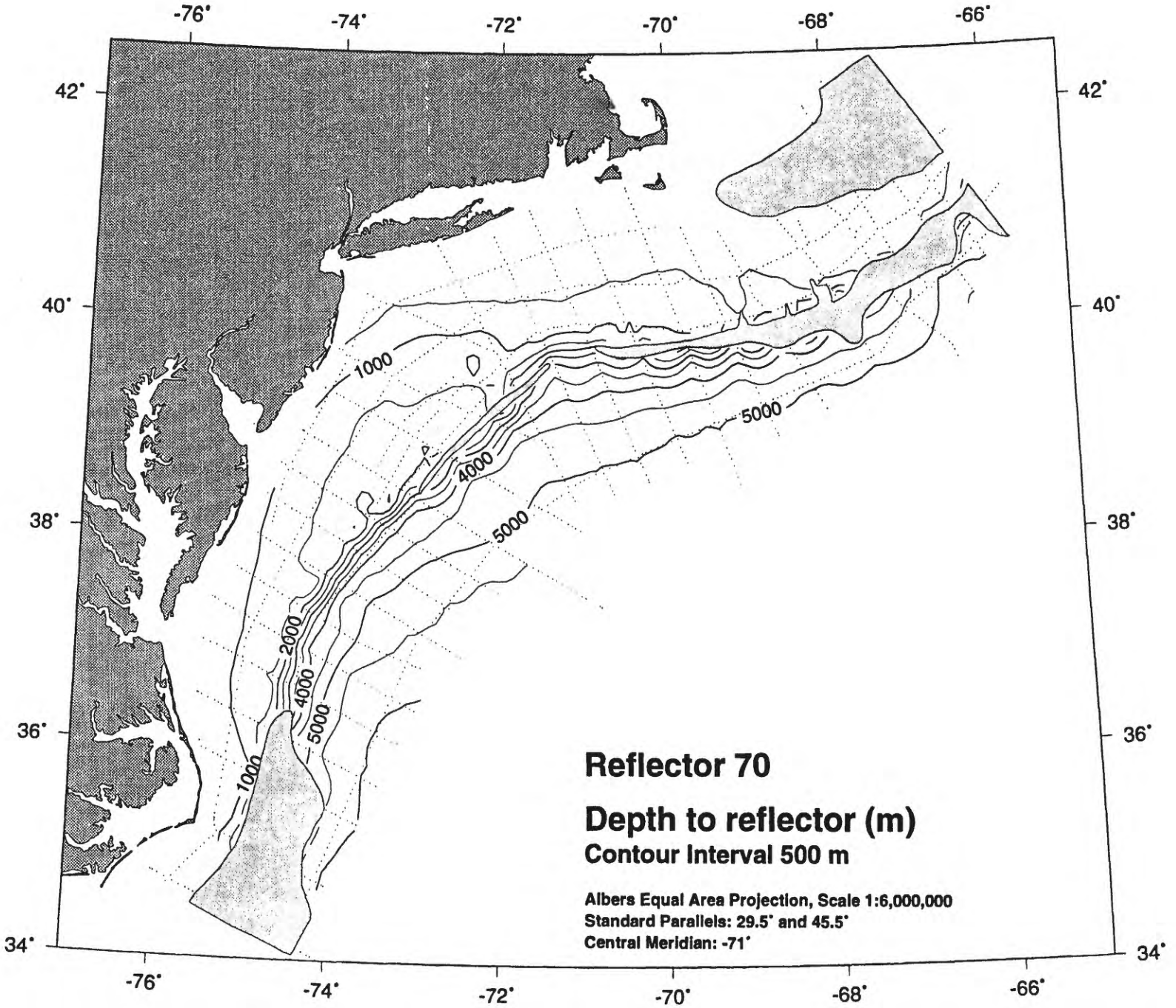
-76°
-74°
-72°
-70°
-68°
-66°
42°
40°
38°
36°
34°
1000
5000
4000
5000
2000
4000
5000
1000
Reflector 70
Depth to reflector (m)
Contour Interval 500 m
Albers Equal Area Projection, Scale 1:6,000,000
Standard Parallels: 29.5° and 45.5°
Central Meridian: -71°

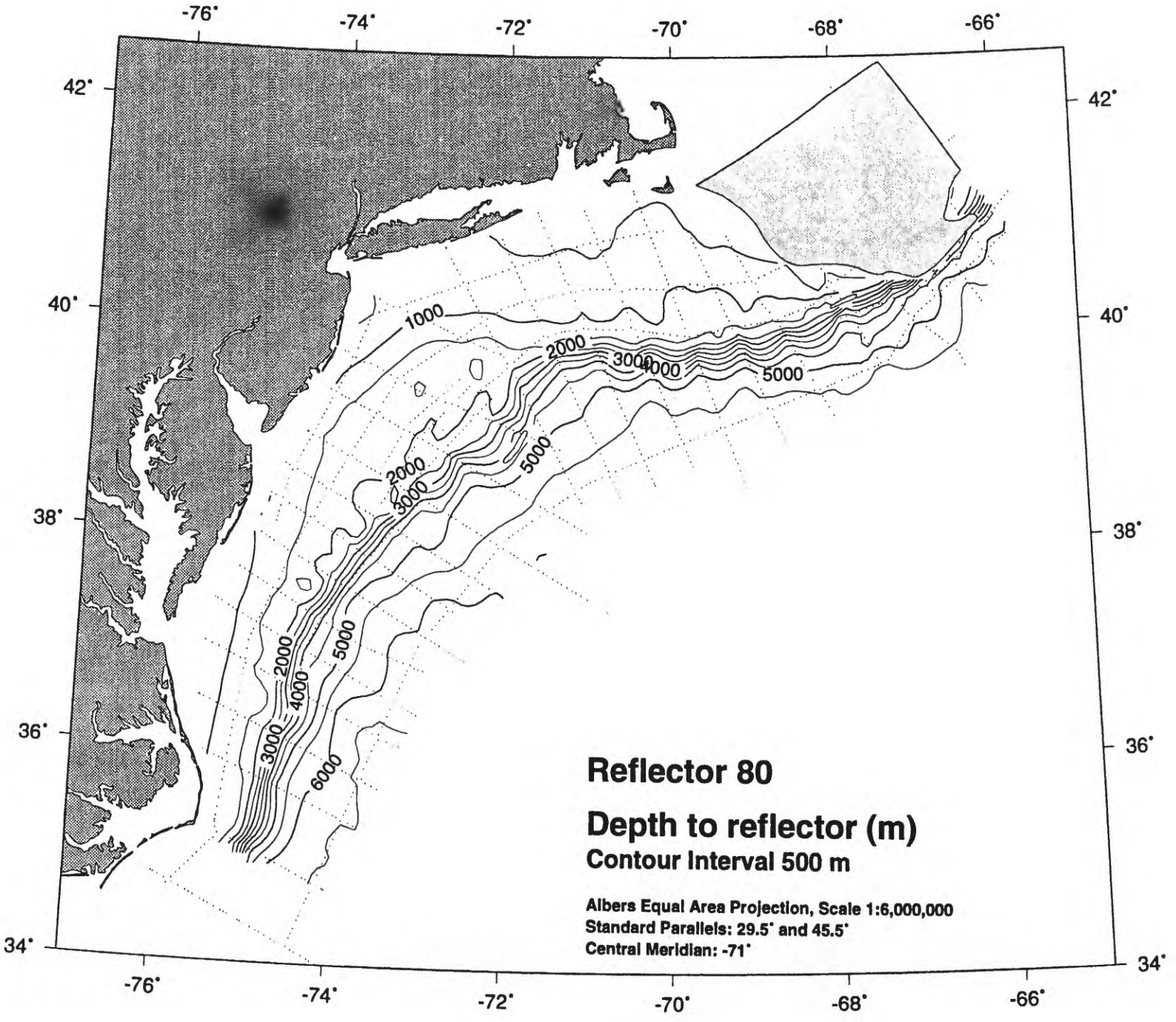
-76°
-74°
-72°
-70°
-68°
-66°
42°
40°
38°
36°
34°
1000
2000
3000
4000
5000
6000
Reflector 80
Depth to reflector (m)
Contour Interval 500 m
Albers Equal Area Projection, Scale 1:6,000,000
Standard Parallels: 29.5° and 45.5°
Central Meridian: -71°

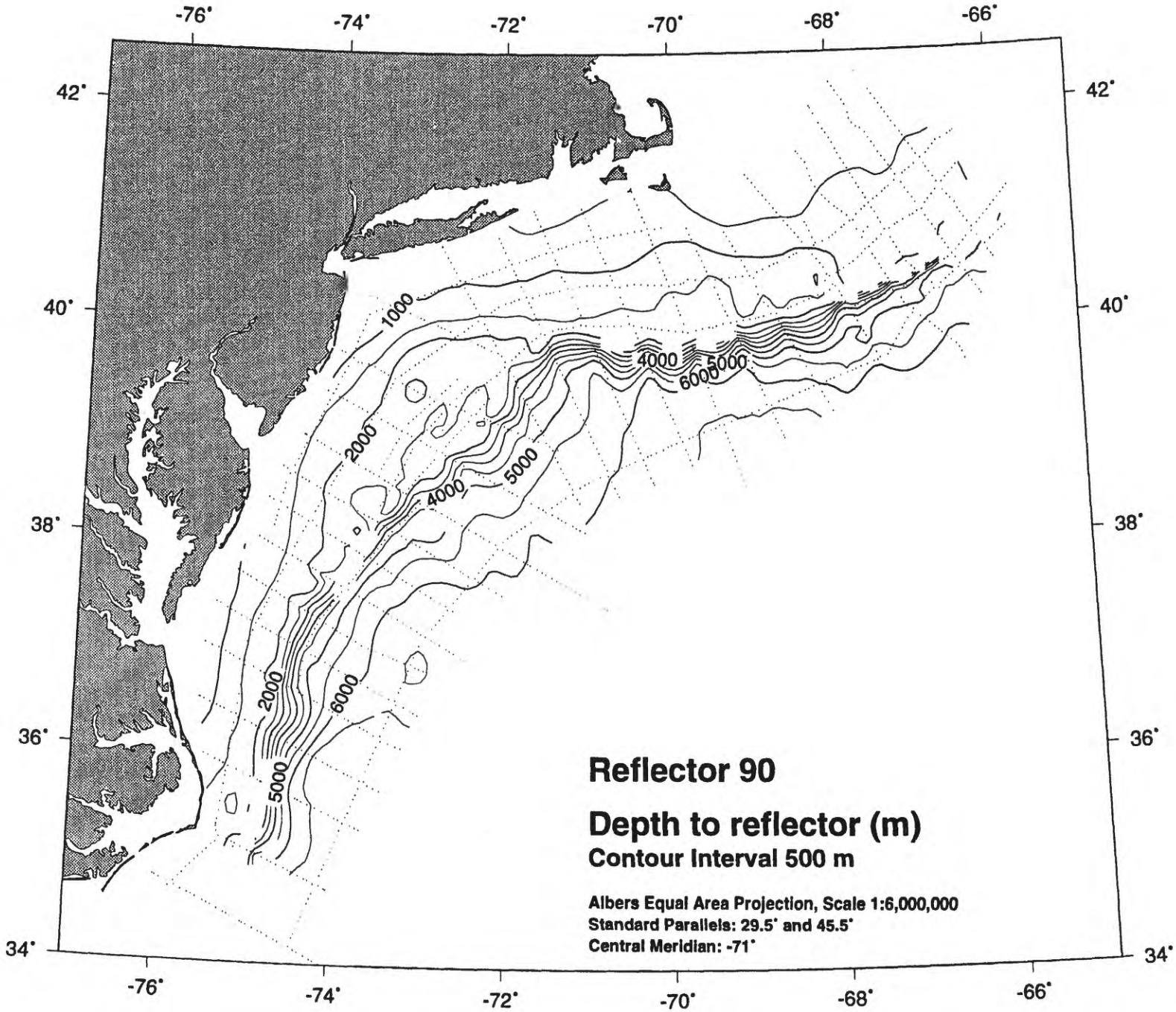
-76°
-74°
-72°
-70°
-68°
-66°
42°
40°
38°
36°
34°
1000
2000
4000
5000
6000
Reflector 90
Depth to reflector (m)
Contour Interval 500 m
Albers Equal Area Projection, Scale 1:6,000,000
Standard Parallels: 29.5° and 45.5°
Central Meridian: -71°

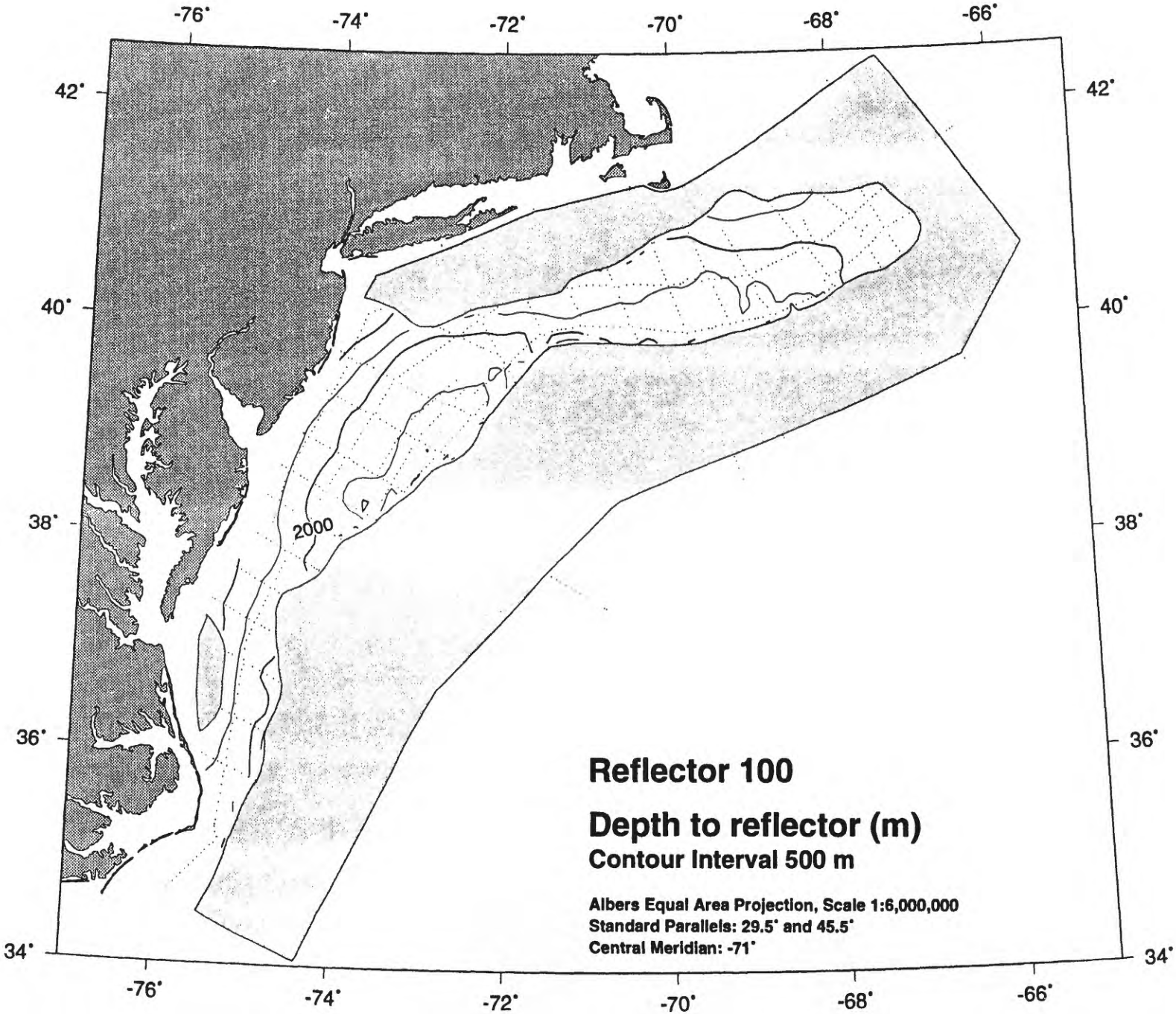
-76°
-74°
-72°
-70°
-68°
-66°
42°
40°
38°
36°
34°
2000
Reflector 100
Depth to reflector (m)
Contour Interval 500 m
Albers Equal Area Projection, Scale 1:6,000,000
Standard Parallels: 29.5° and 45.5°
Central Meridian: -71°

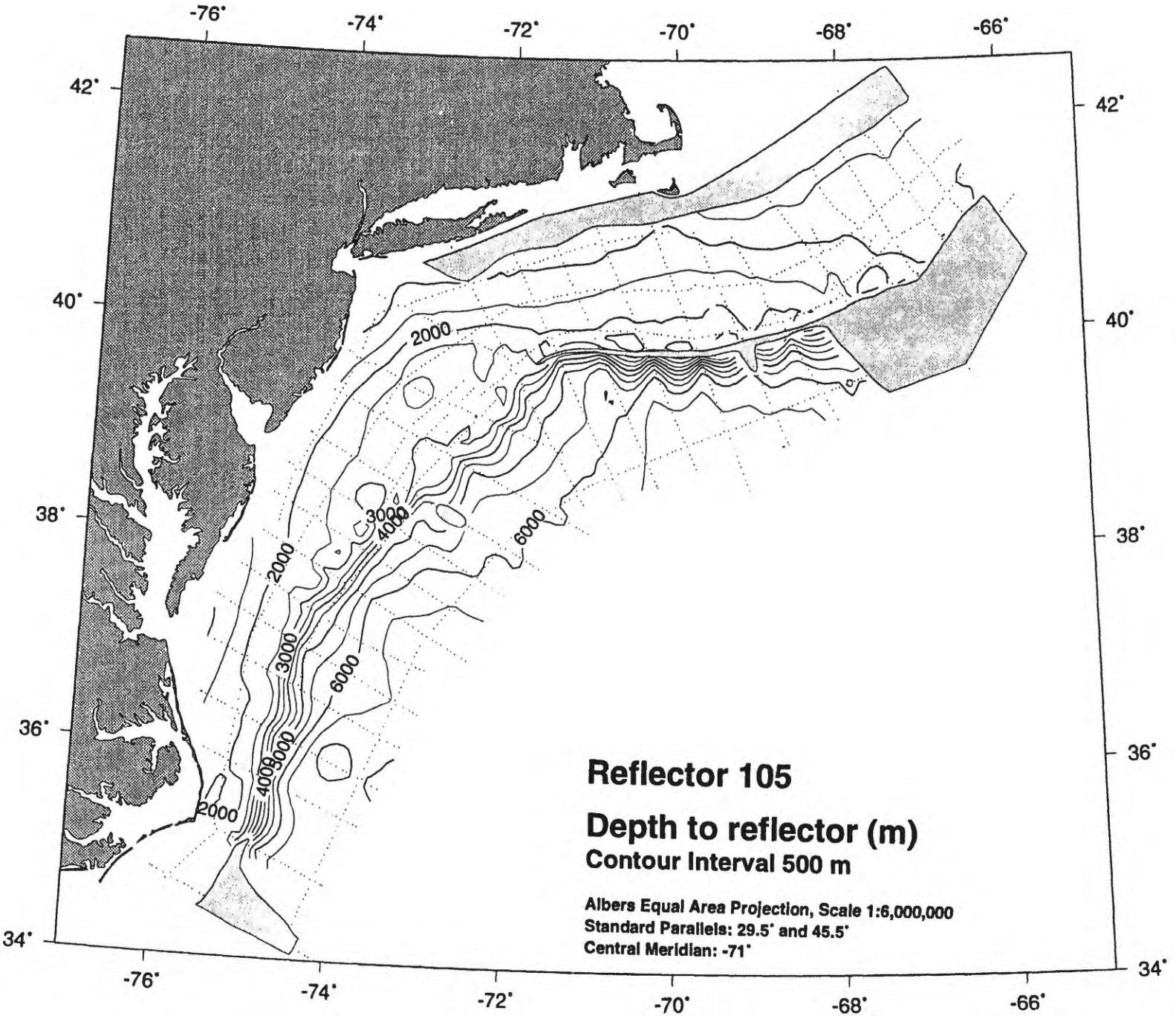
-76°
-74°
-72°
-70°
-68°
-66°
42°
40°
38°
36°
34°
2000
3000
4000
6000
Reflector 105
Depth to reflector (m)
Contour Interval 500 m
Albers Equal Area Projection, Scale 1:6,000,000
Standard Parallels: 29.5° and 45.5°
Central Meridian: -71°

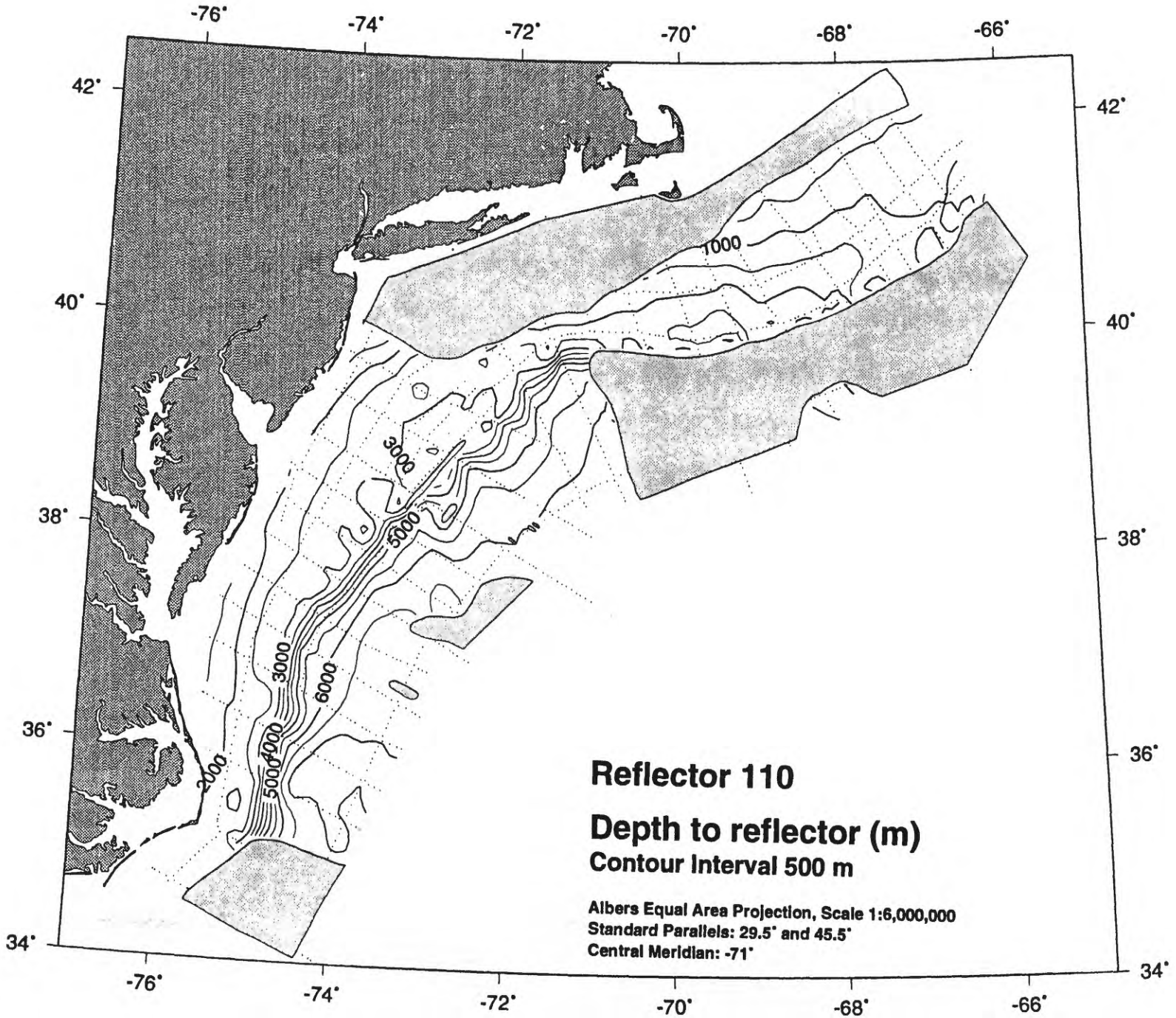
-76°
-74°
-72°
-70°
-68°
-66°
42°
40°
38°
36°
34°
1000
2000
3000
4000
5000
6000
Reflector 110
Depth to reflector (m)
Contour Interval 500 m
Albers Equal Area Projection, Scale 1:6,000,000
Standard Parallels: 29.5° and 45.5°
Central Meridian: -71°

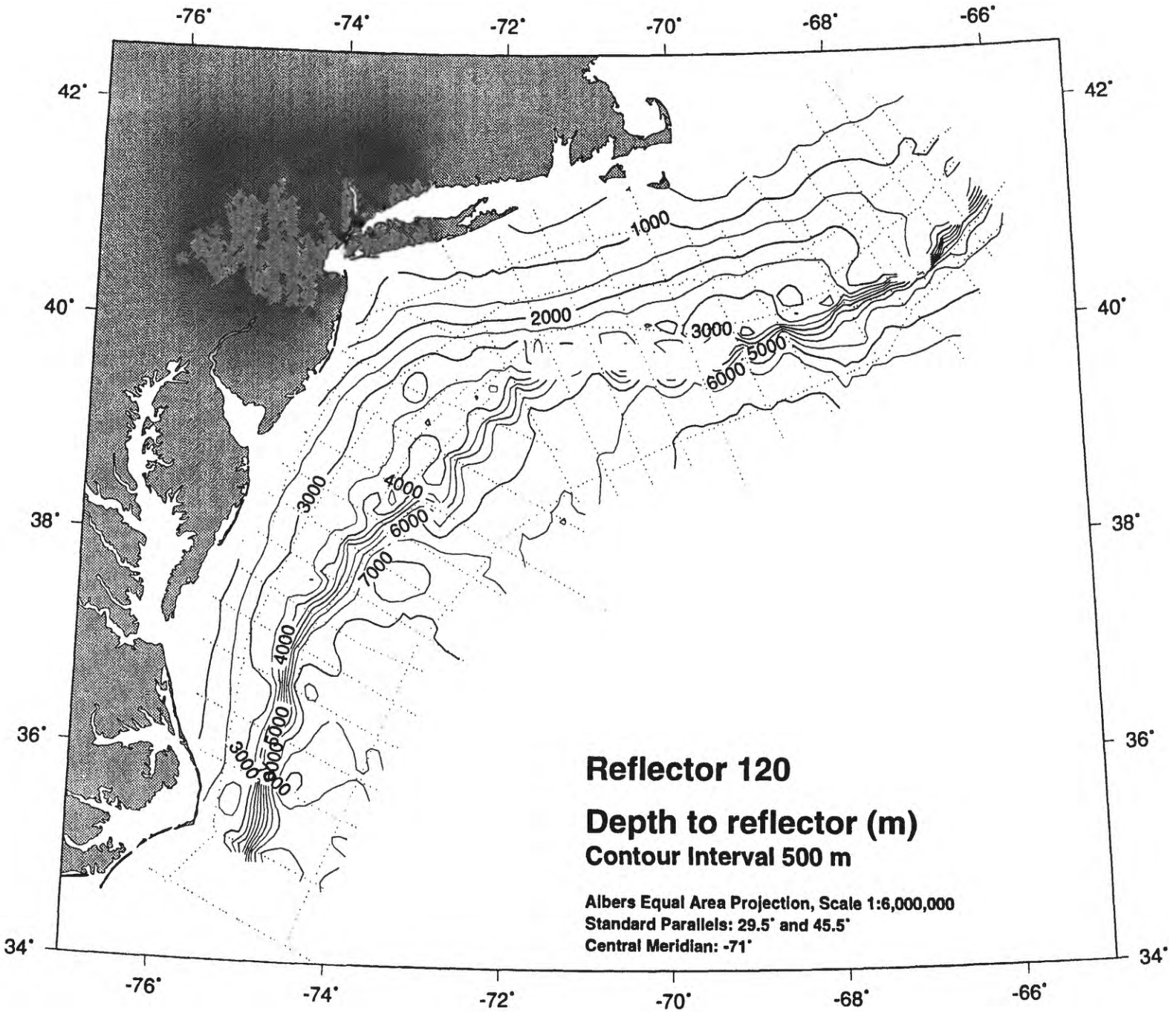
-76°
-74°
-72°
-70°
-68°
-66°
42°
40°
38°
36°
34°
1000
2000
3000
4000
5000
6000
7000
Reflector 120
Depth to reflector (m)
Contour Interval 500 m
Albers Equal Area Projection, Scale 1:6,000,000
Standard Parallels: 29.5° and 45.5°
Central Meridian: -71°

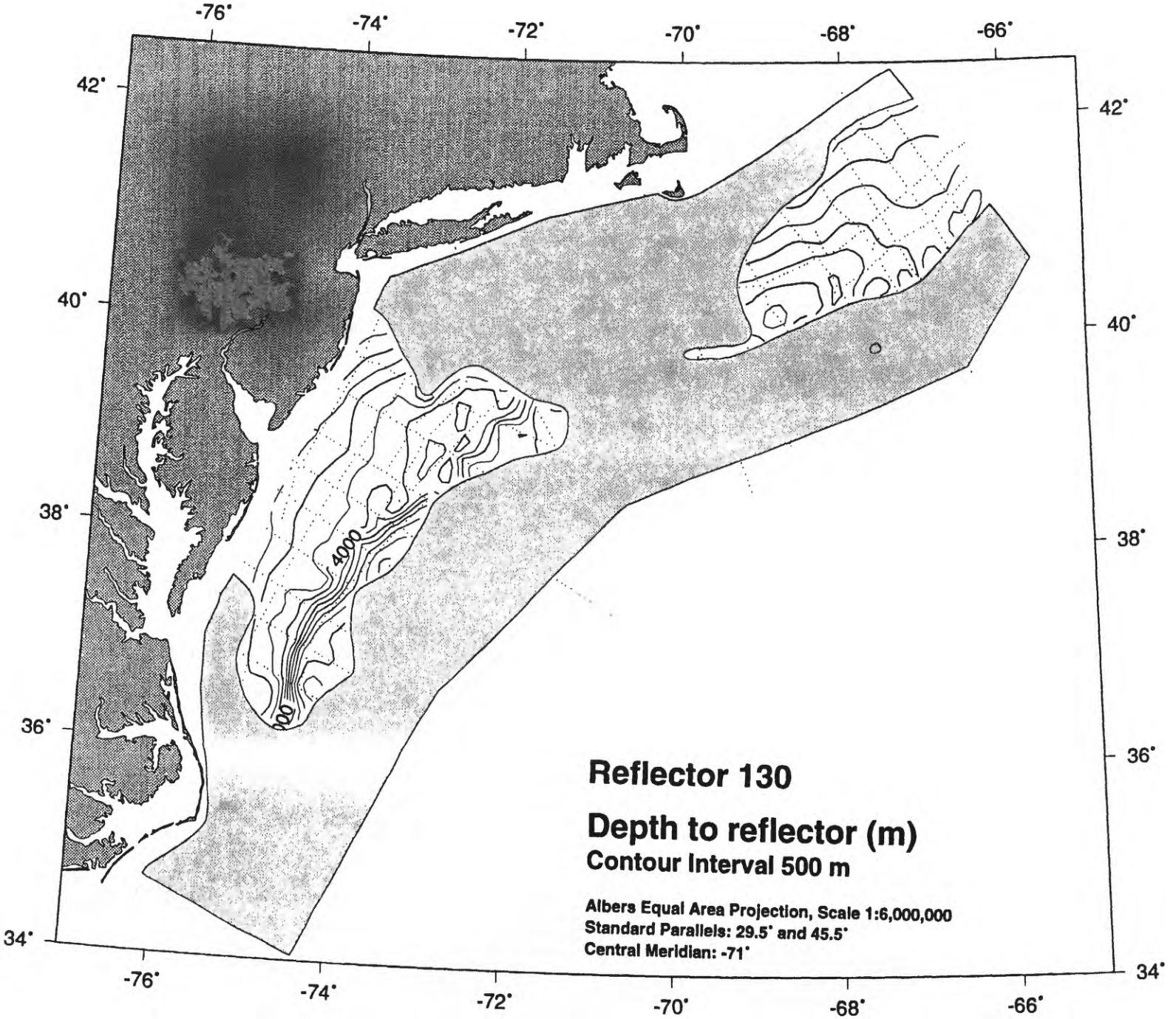
-76°
-74°
-72°
-70°
-68°
-66°
42°
40°
38°
36°
34°
4000
Reflector 130
Depth to reflector (m)
Contour Interval 500 m
Albers Equal Area Projection, Scale 1:6,000,000
Standard Parallels: 29.5° and 45.5°
Central Meridian: -71°

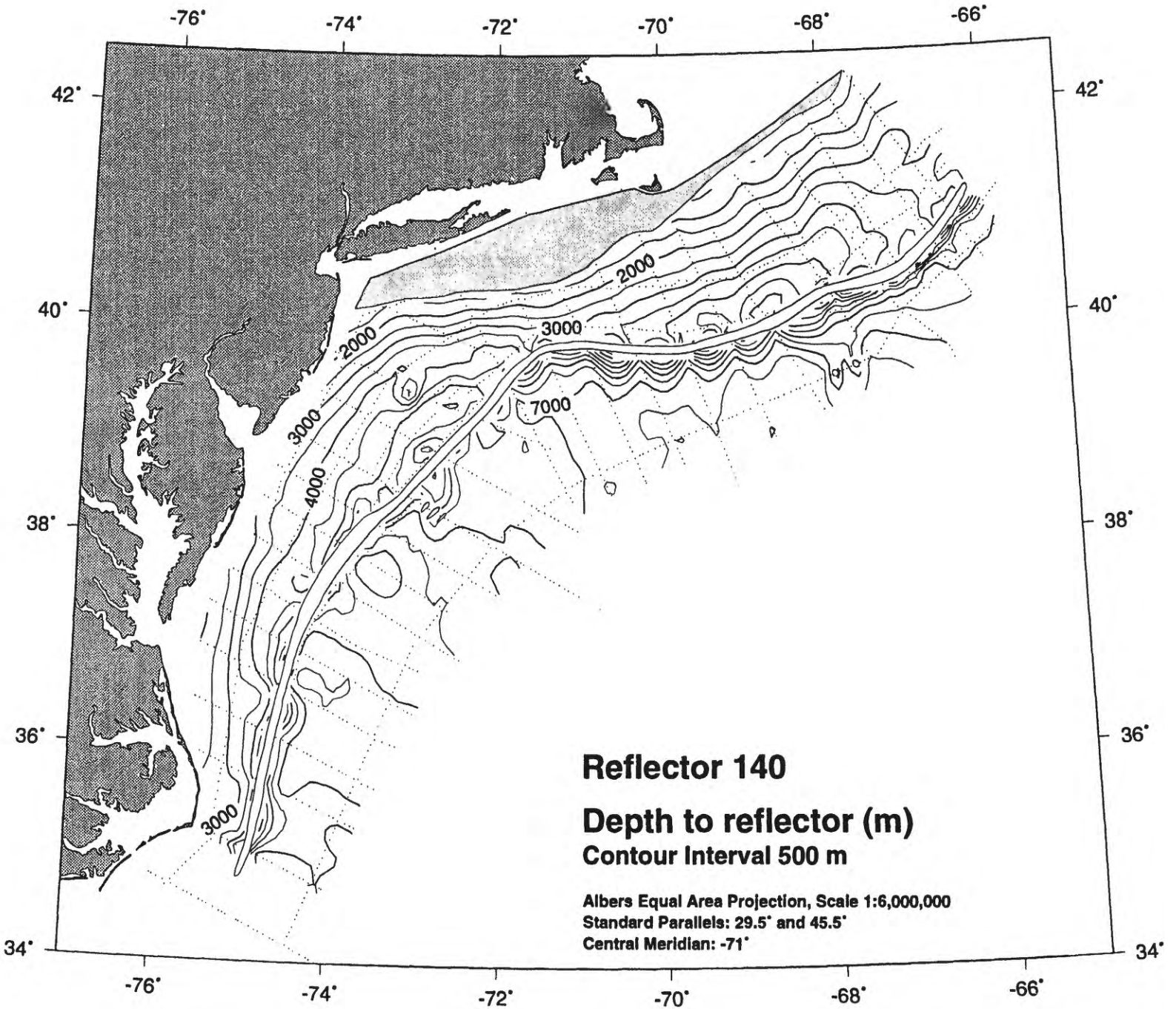
-76°
-74°
-72°
-70°
-68°
-66°
42°
40°
38°
36°
34°
2000
3000
7000
4000
Reflector 140
Depth to reflector (m)
Contour Interval 500 m
Albers Equal Area Projection, Scale 1:6,000,000
Standard Parallels: 29.5° and 45.5°
Central Meridian: -71°

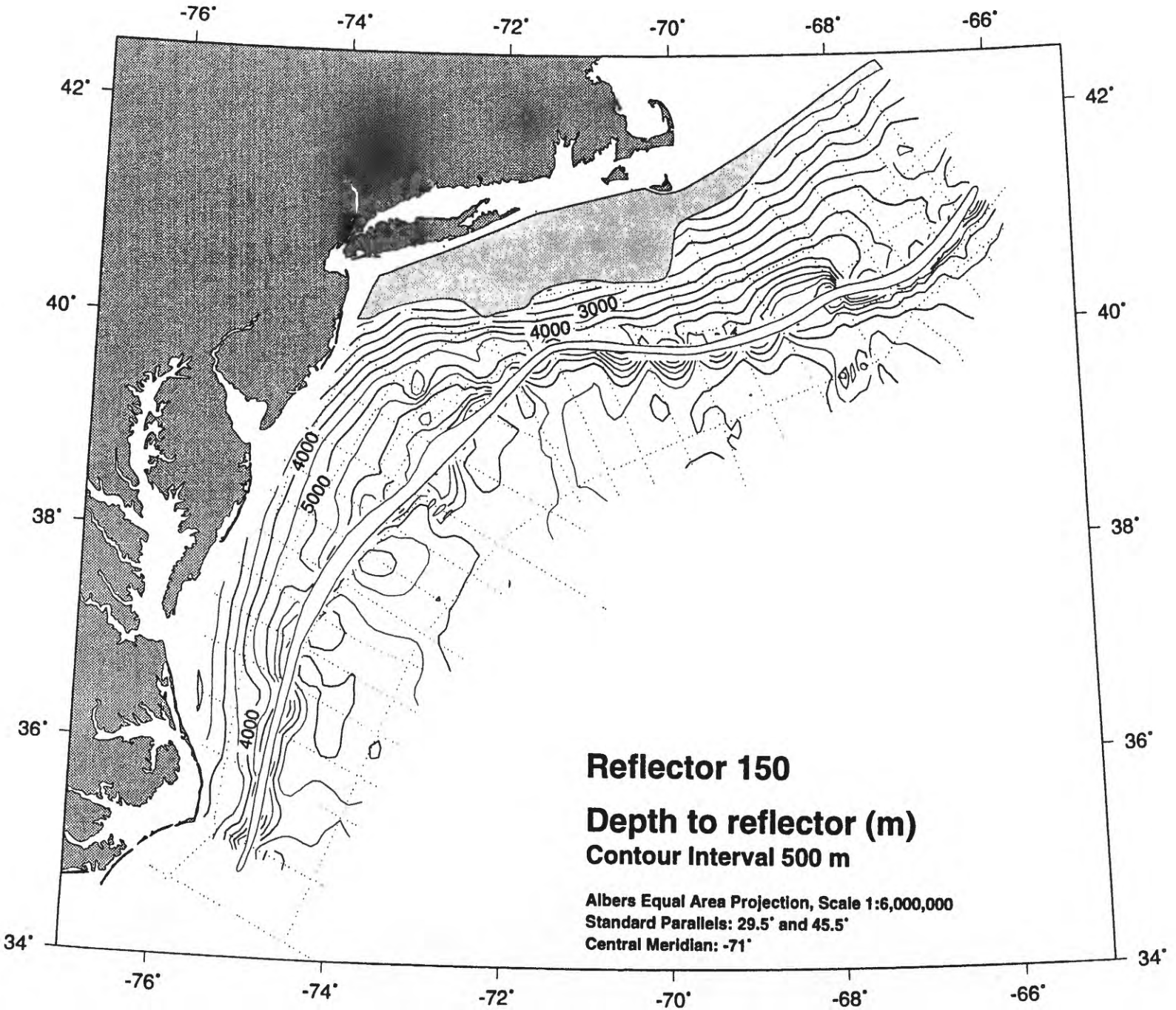
-76°
-74°
-72°
-70°
-68°
-66°
42°
40°
38°
36°
34°
3000
4000
4000
5000
4000
Reflector 150
Depth to reflector (m)
Contour Interval 500 m
Albers Equal Area Projection, Scale 1:6,000,000
Standard Parallels: 29.5° and 45.5°
Central Meridian: -71°

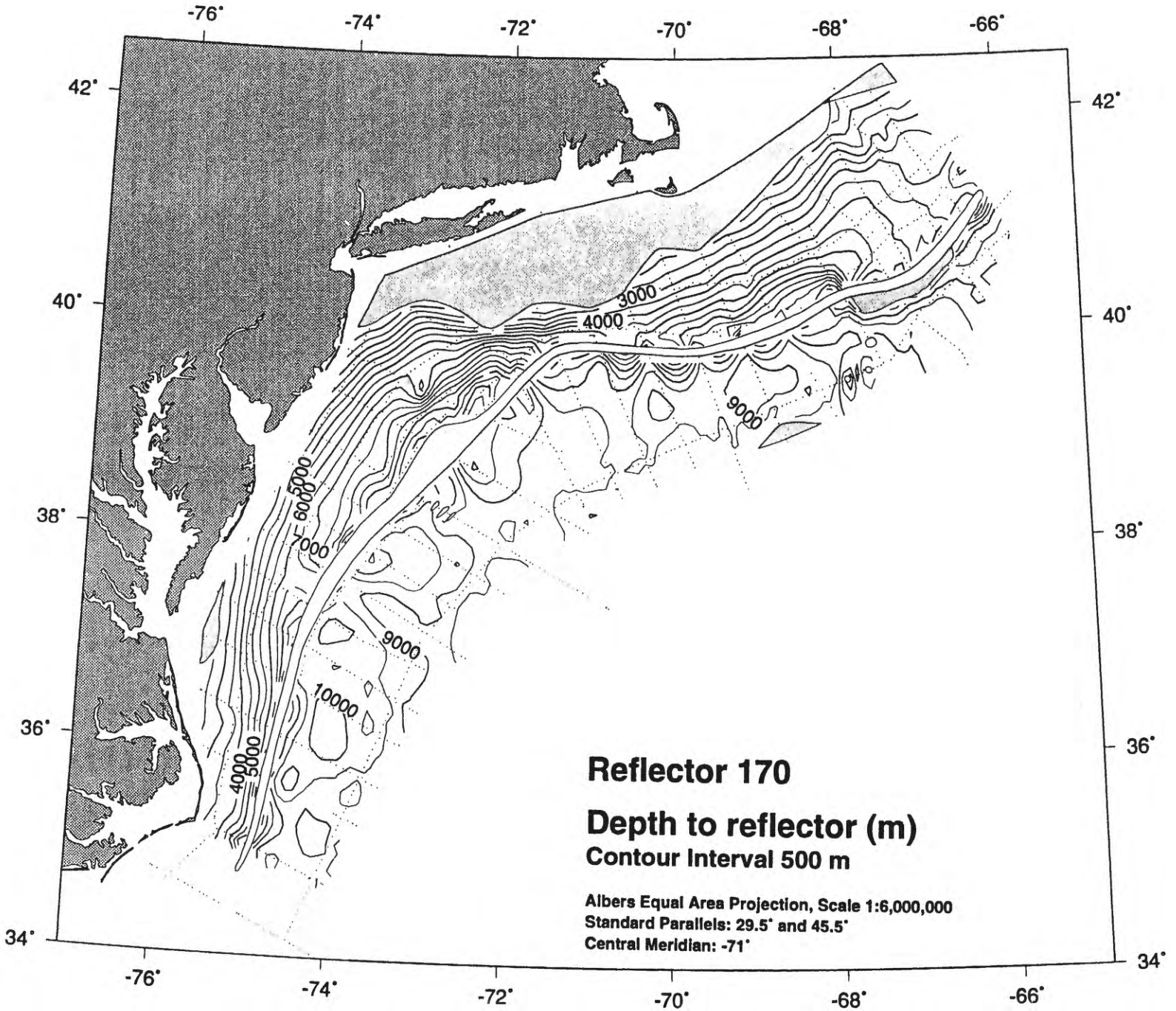
-76°
-74°
-72°
-70°
-68°
-66°
42°
40°
38°
36°
34°
3000
4000
9000
5000
6000
7000
9000
10000
4000
5000
Reflector 170
Depth to reflector (m)
Contour Interval 500 m
Albers Equal Area Projection, Scale 1:6,000,000
Standard Parallels: 29.5° and 45.5°
Central Meridian: -71°

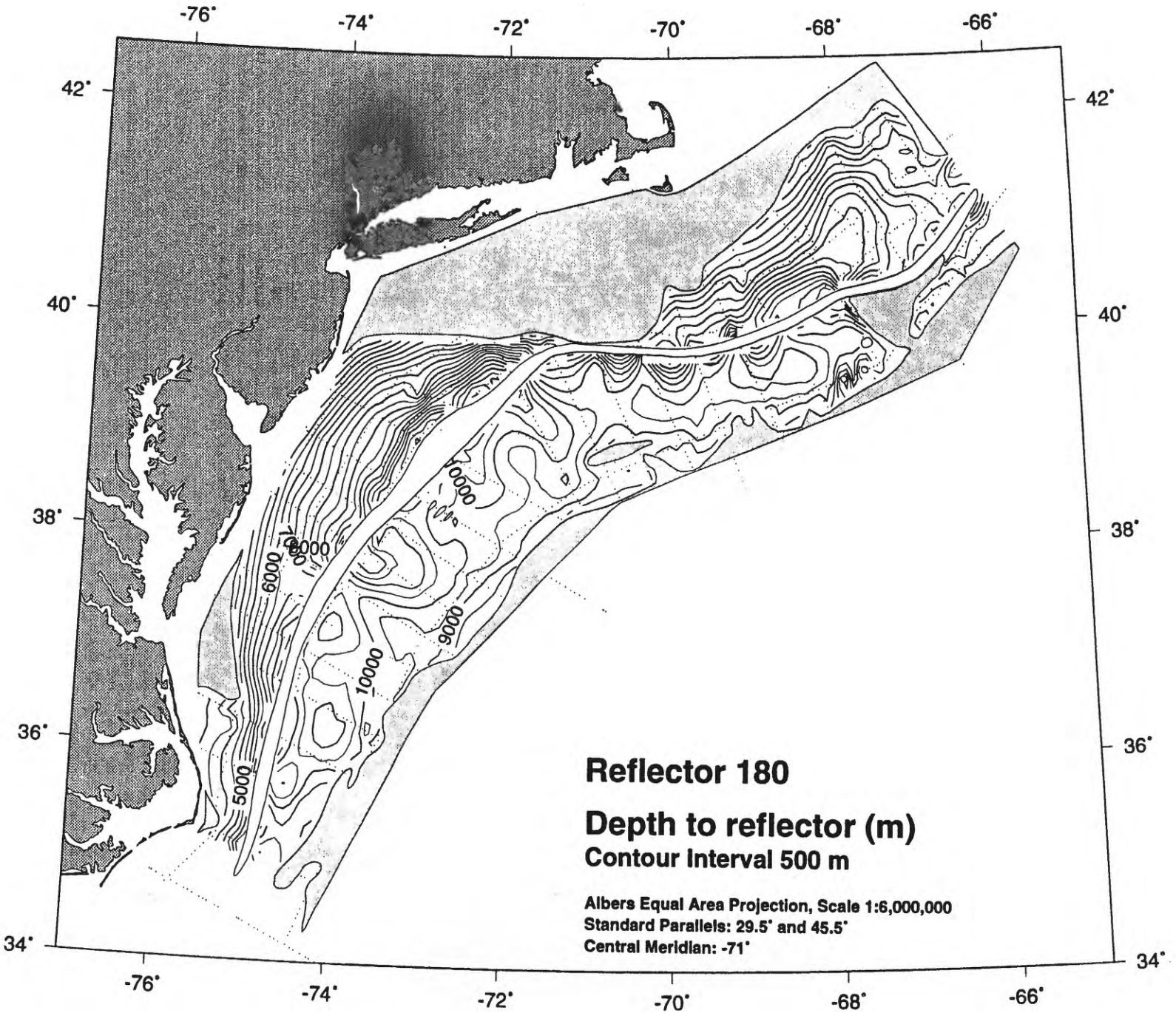
-76°
-74°
-72°
-70°
-68°
-66°
42°
40°
38°
36°
34°
5000
6000
7000
8000
9000
10000
10000
Reflector 180
Depth to reflector (m)
Contour Interval 500 m
Albers Equal Area Projection, Scale 1:6,000,000
Standard Parallels: 29.5° and 45.5°
Central Meridian: -71°

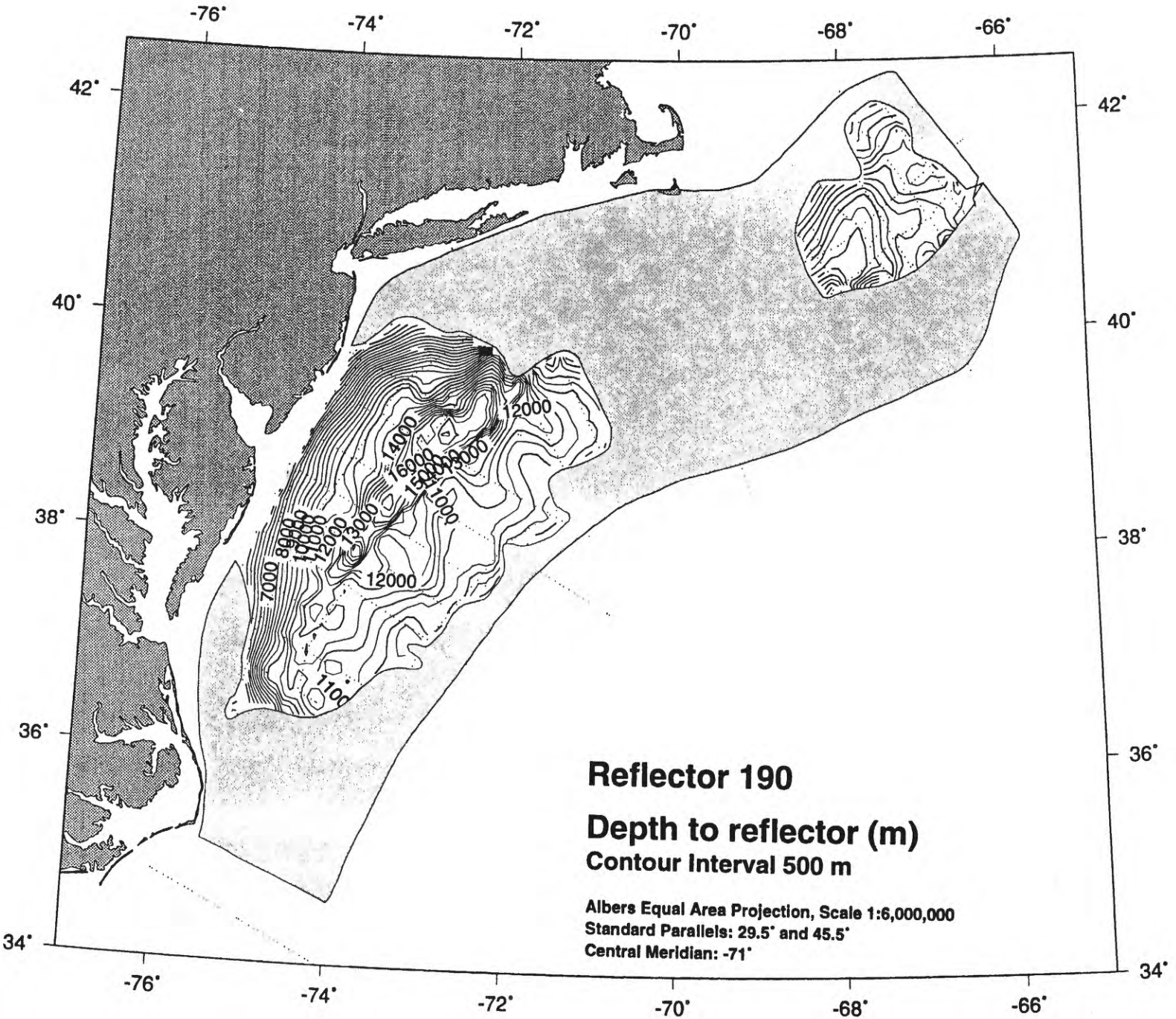
-76°
-74°
-72°
-70°
-68°
-66°
42°
40°
38°
36°
34°
12000
14000
16000
13000
12000
7000
Reflector 190
Depth to reflector (m)
Contour Interval 500 m
Albers Equal Area Projection, Scale 1:6,000,000
Standard Parallels: 29.5° and 45.5°
Central Meridian: -71°

Appendix 6

Thickness-Isopach Contour Maps for Acoustic Units in Digital Database

Isopach contour maps of the thickness, in two-way travel times, of each acoustic unit in this geoacoustic database. The dotted lines represent the seismic line control used to construct each surface. See Figure 8 for the 5-minute grid point map, based on these seismic lines, used to construct the contour map. Shaded masks indicate the regions where a particular surface has been eroded into by an overlying surface. Narrow blank zones in the shelf edge region are where deeper units are obscured by the Jurassic carbonate bank. Contour interval is 0.1 sec.

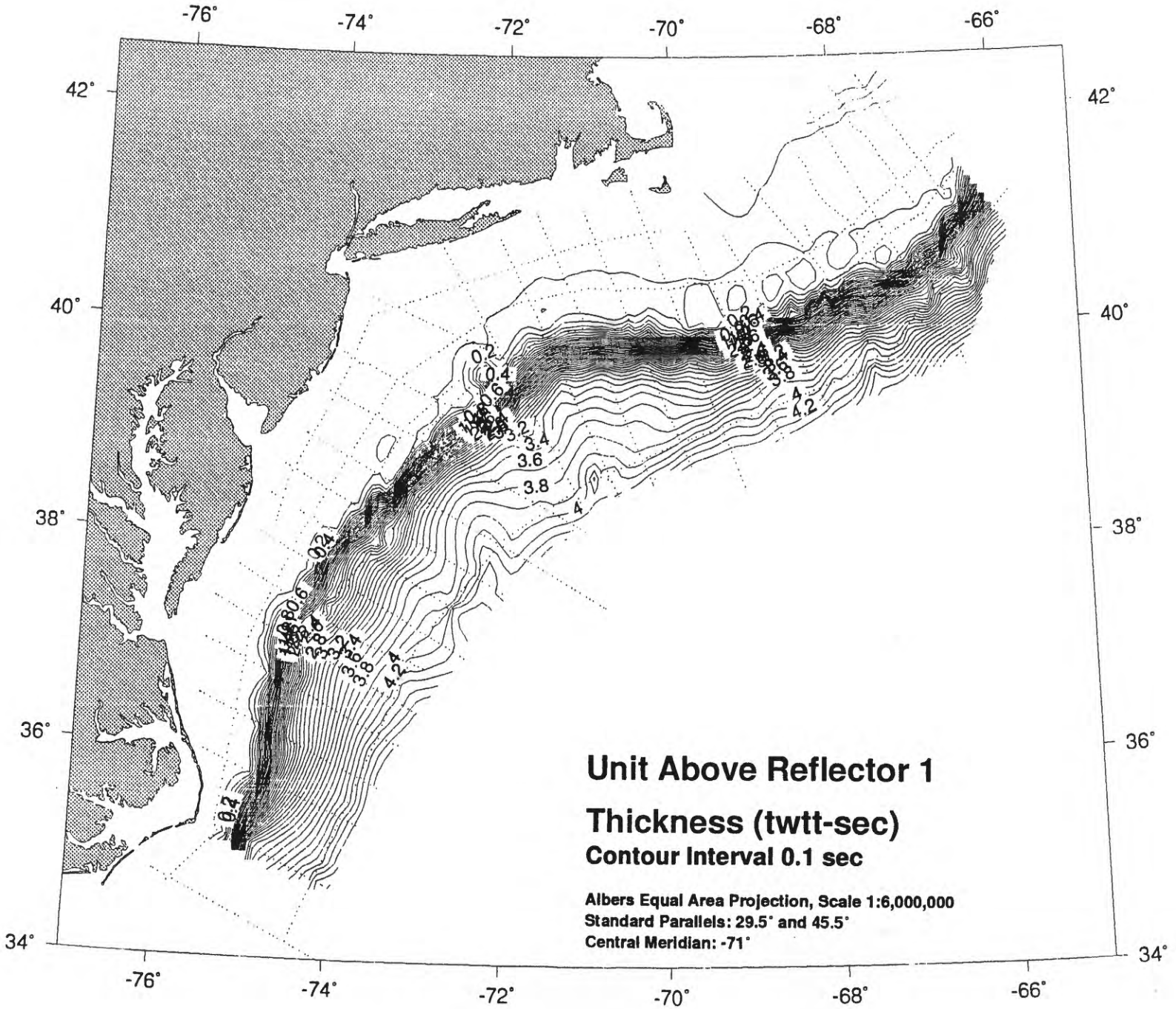
-76°
-74°
-72°
-70°
-68°
-66°
42°
40°
38°
36°
34°
0.2
0.4
0.6
3.2
3.4
3.6
3.8
4
4.2
4.4
Unit Above Reflector 1
Thickness (twtt-sec)
Contour Interval 0.1 sec
Albers Equal Area Projection, Scale 1:6,000,000
Standard Parallels: 29.5° and 45.5°
Central Meridian: -71°

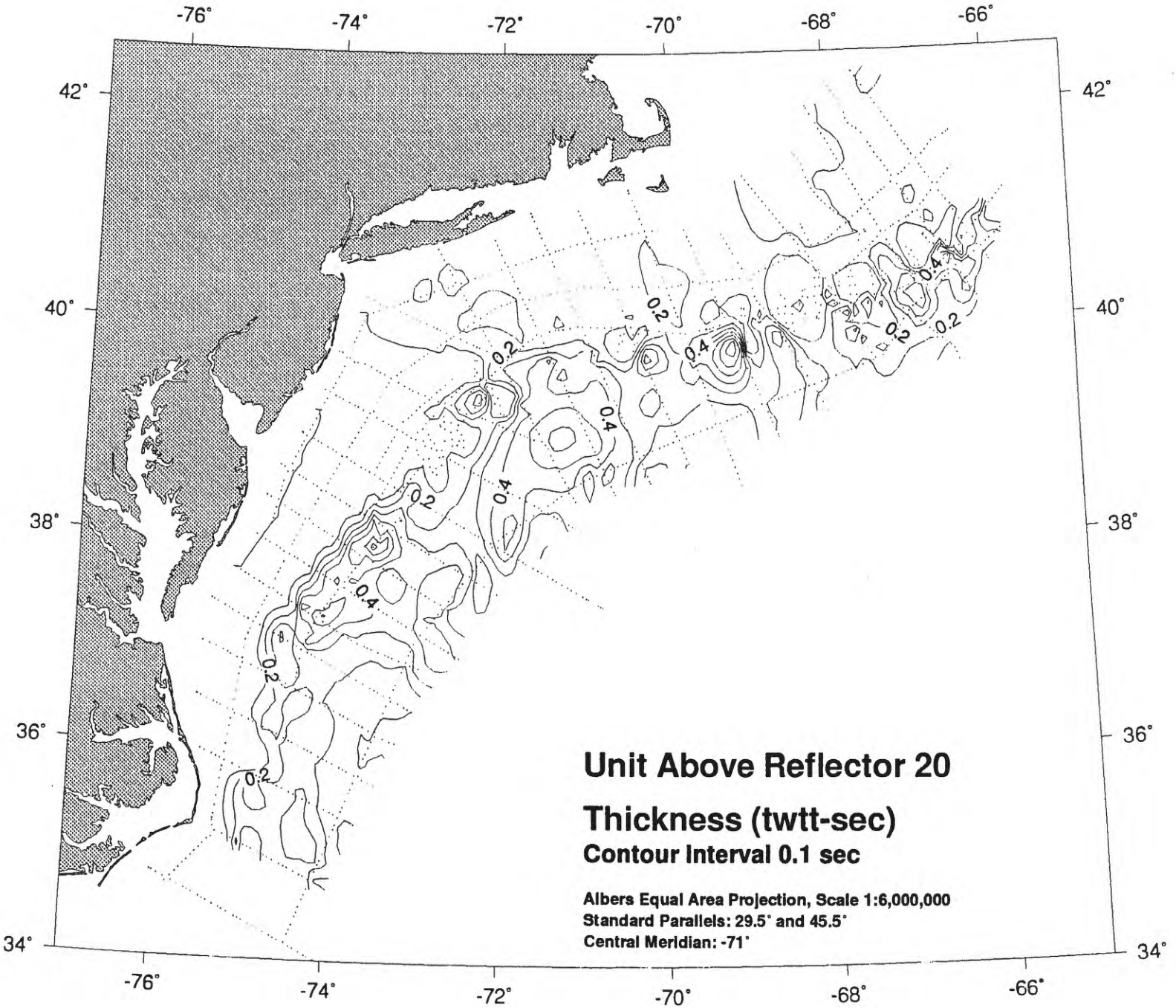
-76°
-74°
-72°
-70°
-68°
-66°
42°
40°
38°
36°
34°
0.2
0.4
Unit Above Reflector 20
Thickness (twtt-sec)
Contour Interval 0.1 sec
Albers Equal Area Projection, Scale 1:6,000,000
Standard Parallels: 29.5° and 45.5°
Central Meridian: -71°

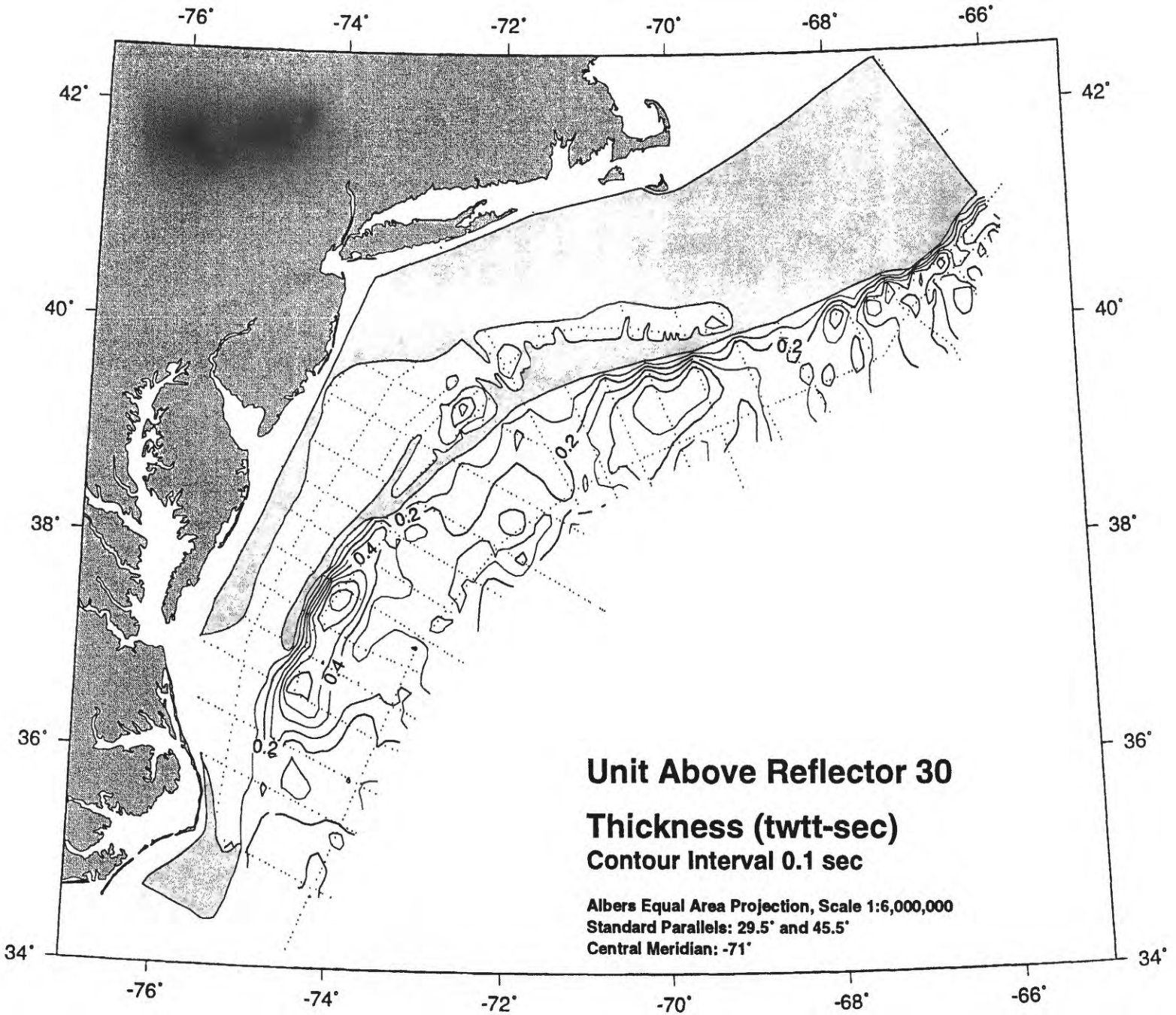
-76°
-74°
-72°
-70°
-68°
-66°
42°
40°
38°
36°
34°
0.2
0.4
Unit Above Reflector 30
Thickness (twtt-sec)
Contour Interval 0.1 sec
Albers Equal Area Projection, Scale 1:6,000,000
Standard Parallels: 29.5° and 45.5°
Central Meridian: -71°

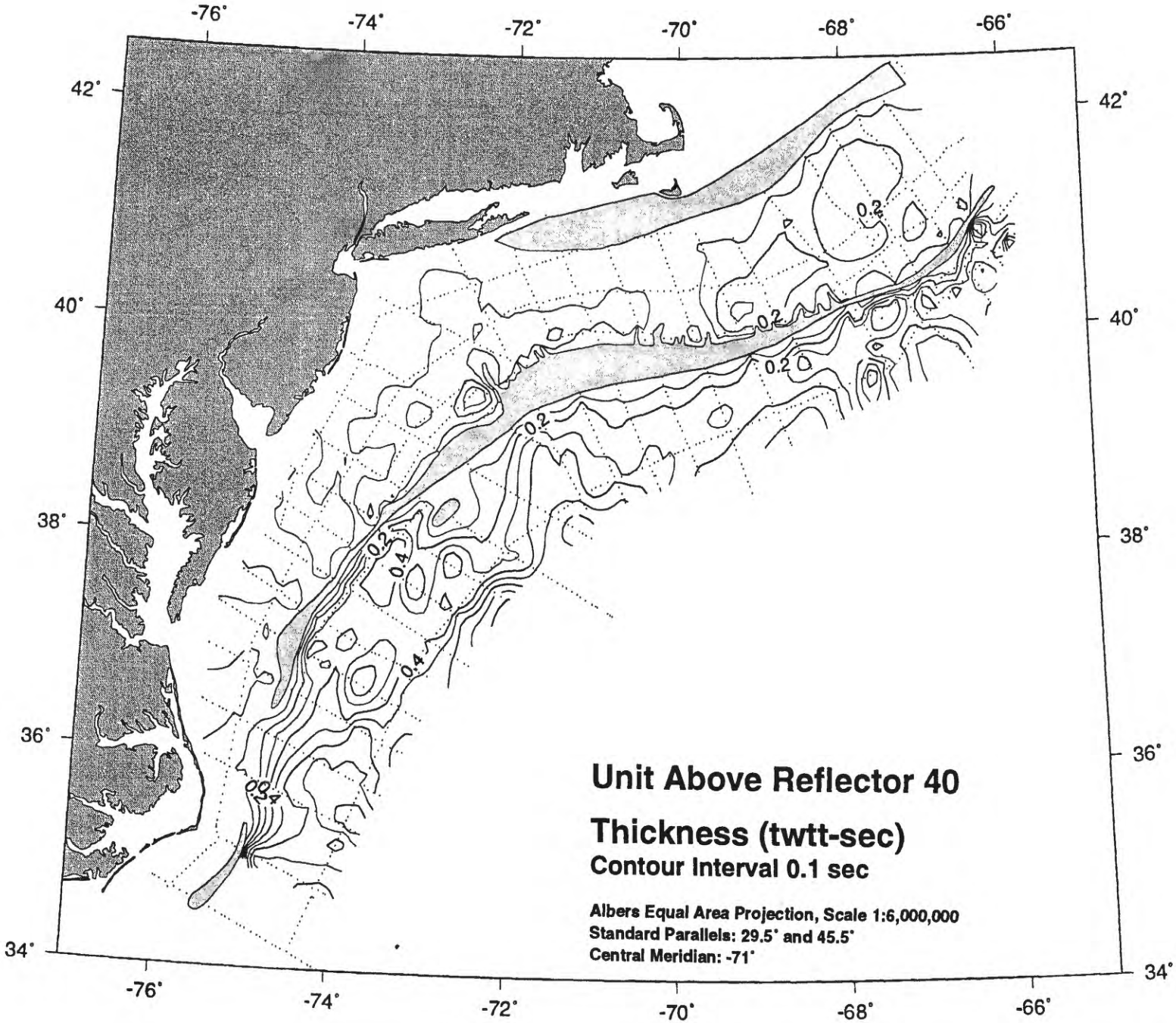
-76°
-74°
-72°
-70°
-68°
-66°
42°
40°
38°
36°
34°
0.2
0.4
Unit Above Reflector 40
Thickness (twtt-sec)
Contour Interval 0.1 sec
Albers Equal Area Projection, Scale 1:6,000,000
Standard Parallels: 29.5° and 45.5°
Central Meridian: -71°

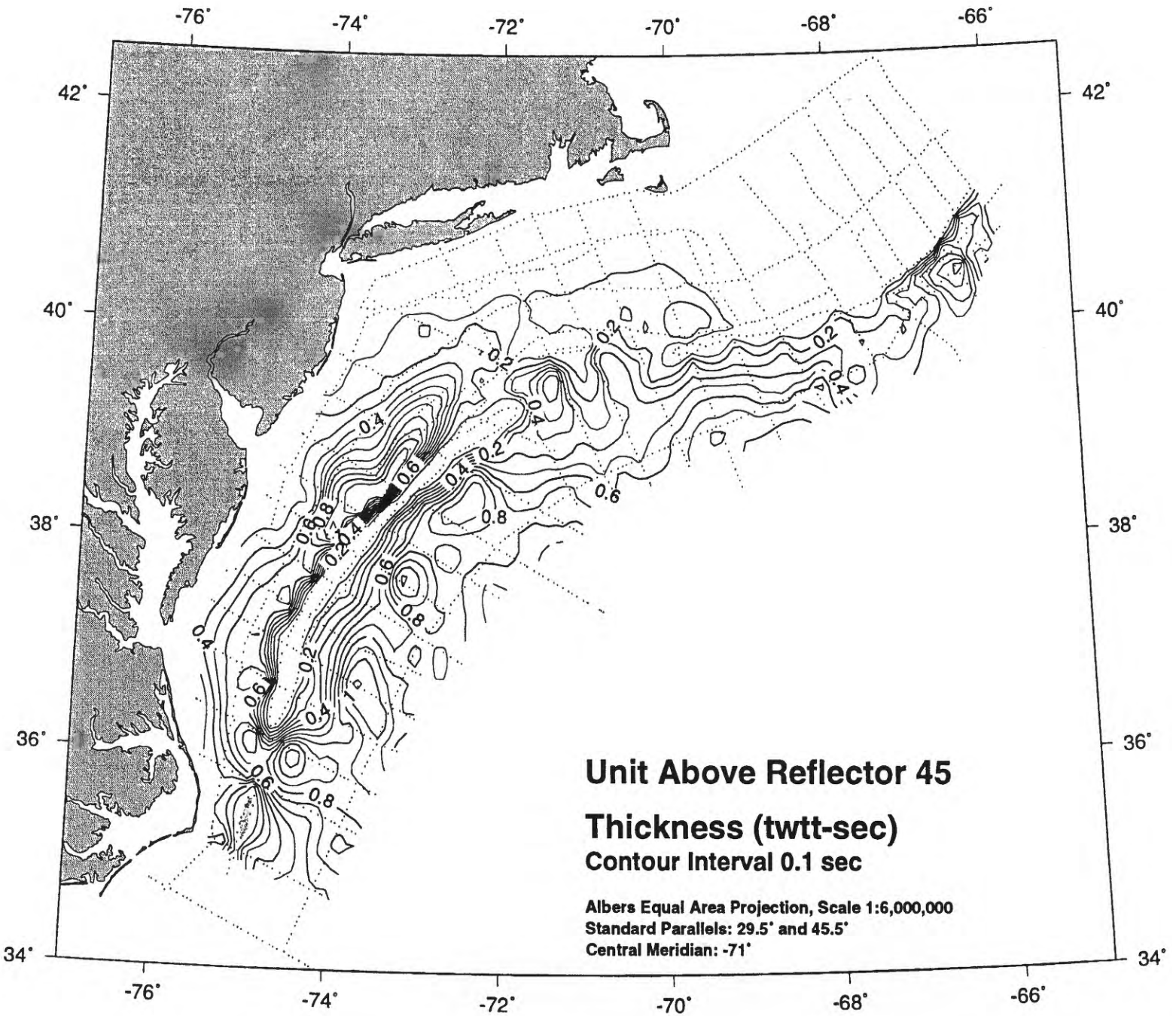
-76°
-74°
-72°
-70°
-68°
-66°
42°
40°
38°
36°
34°
Unit Above Reflector 45
Thickness (twtt-sec)
Contour Interval 0.1 sec
Albers Equal Area Projection, Scale 1:6,000,000
Standard Parallels: 29.5° and 45.5°
Central Meridian: -71°

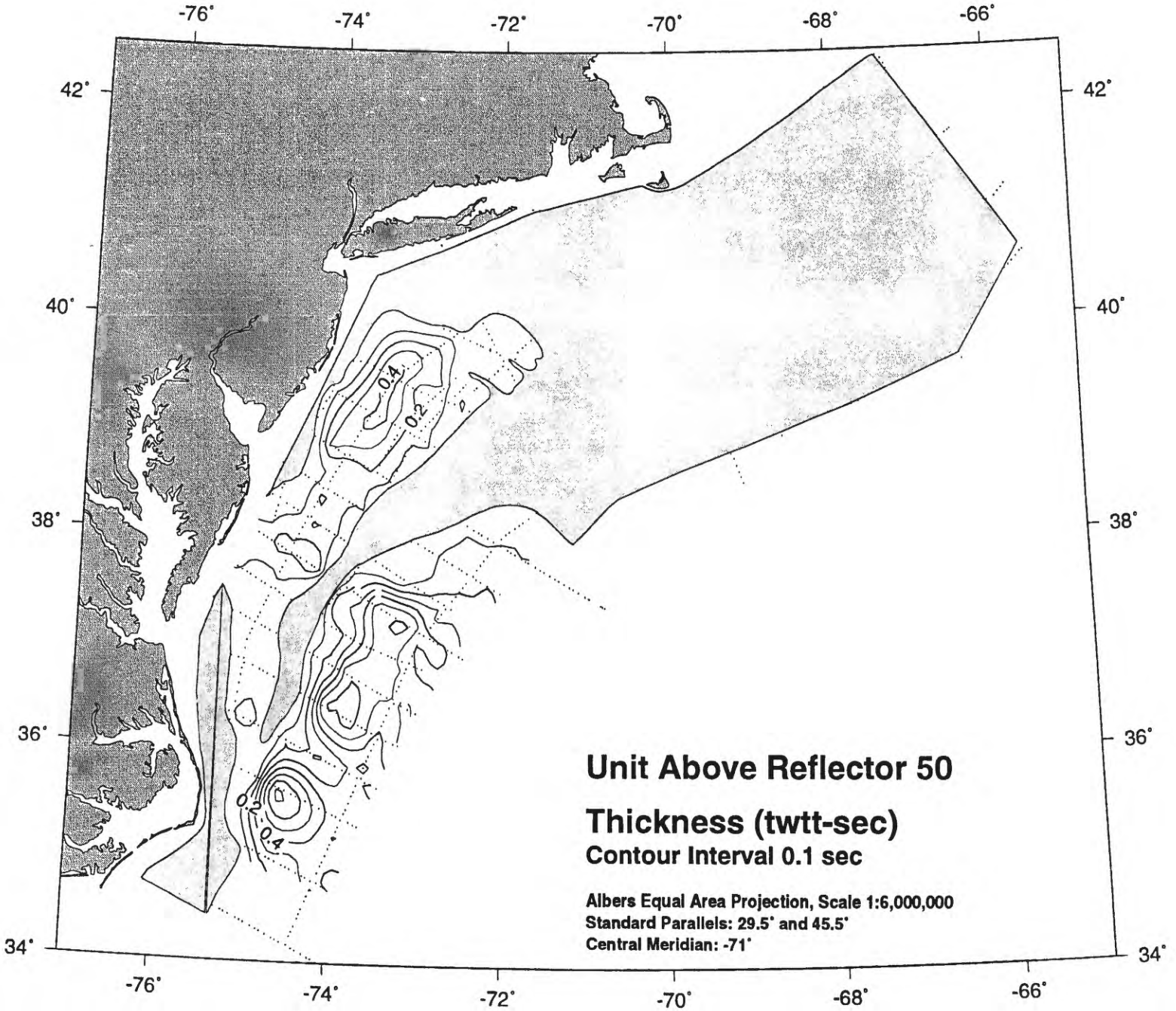
-76°
-74°
-72°
-70°
-68°
-66°
42°
40°
38°
36°
34°
0.4
0.2
0.2
0.4
Unit Above Reflector 50
Thickness (twtt-sec)
Contour Interval 0.1 sec
Albers Equal Area Projection, Scale 1:6,000,000
Standard Parallels: 29.5° and 45.5°
Central Meridian: -71°

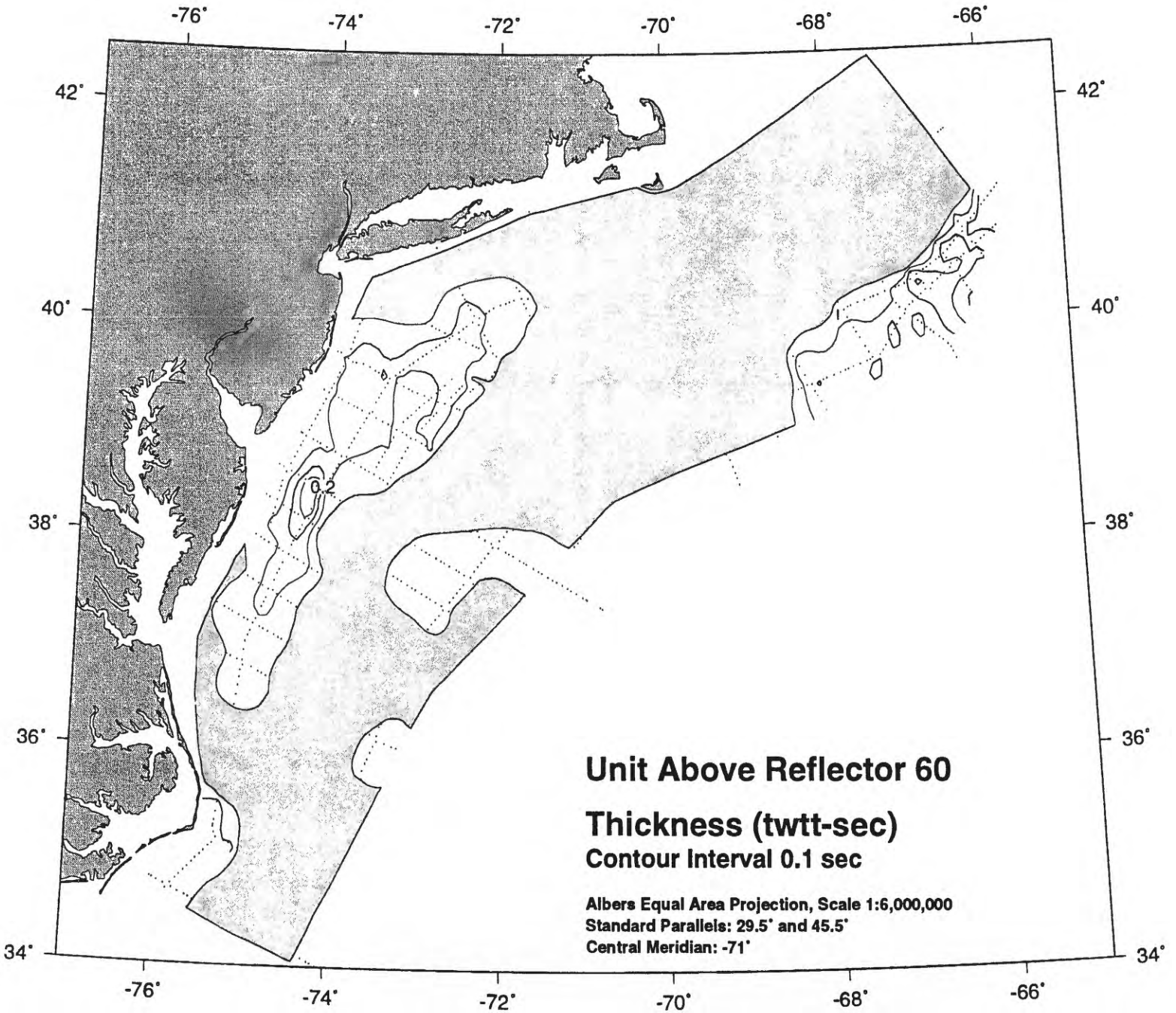
-76°
-74°
-72°
-70°
-68°
-66°
42°
40°
38°
36°
34°
0.2
Unit Above Reflector 60
Thickness (twtt-sec)
Contour Interval 0.1 sec
Albers Equal Area Projection, Scale 1:6,000,000
Standard Parallels: 29.5° and 45.5°
Central Meridian: -71°

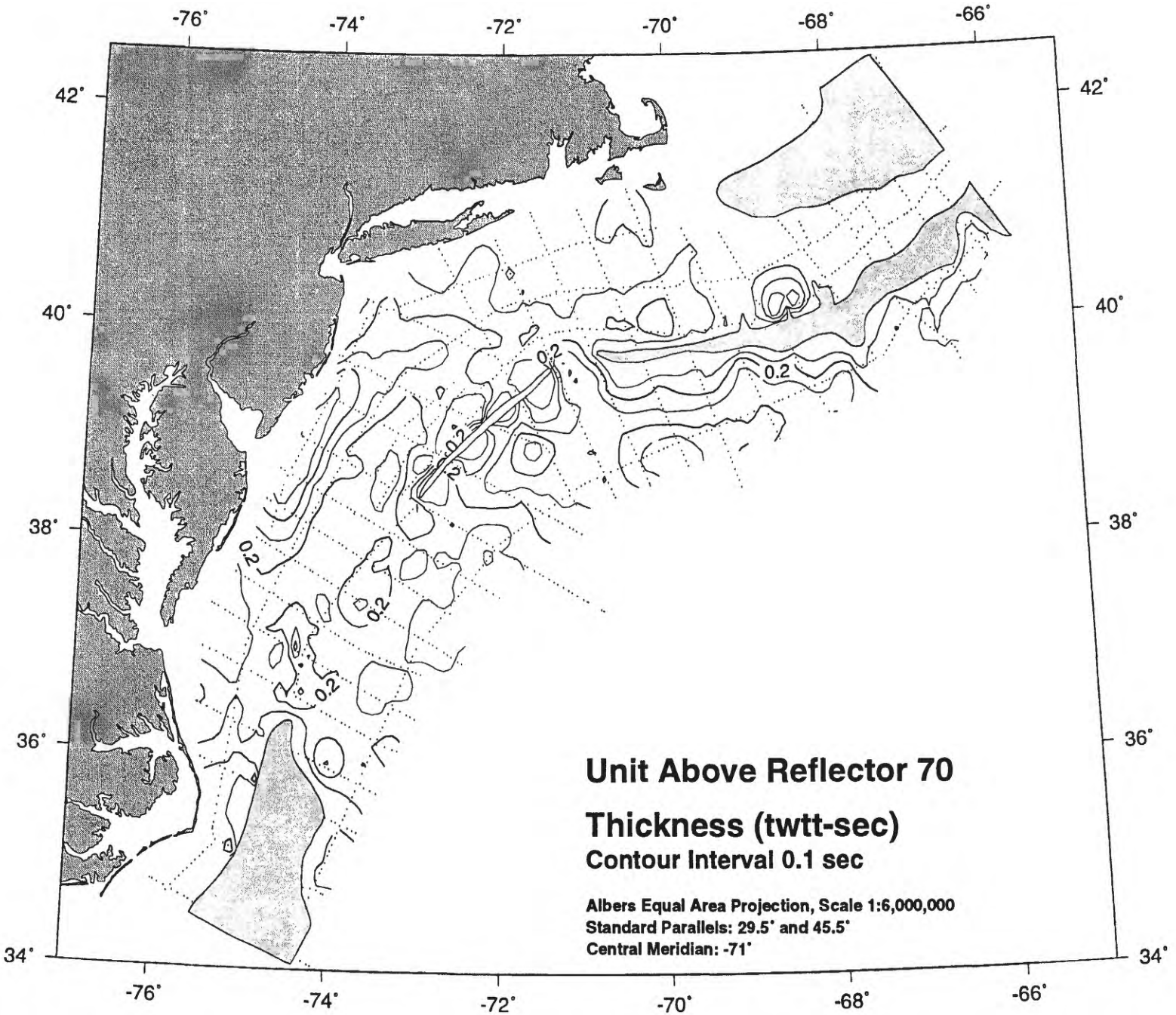
-76°
-74°
-72°
-70°
-68°
-66°
42°
40°
38°
36°
34°
0.2
Unit Above Reflector 70
Thickness (twtt-sec)
Contour Interval 0.1 sec
Albers Equal Area Projection, Scale 1:6,000,000
Standard Parallels: 29.5° and 45.5°
Central Meridian: -71°

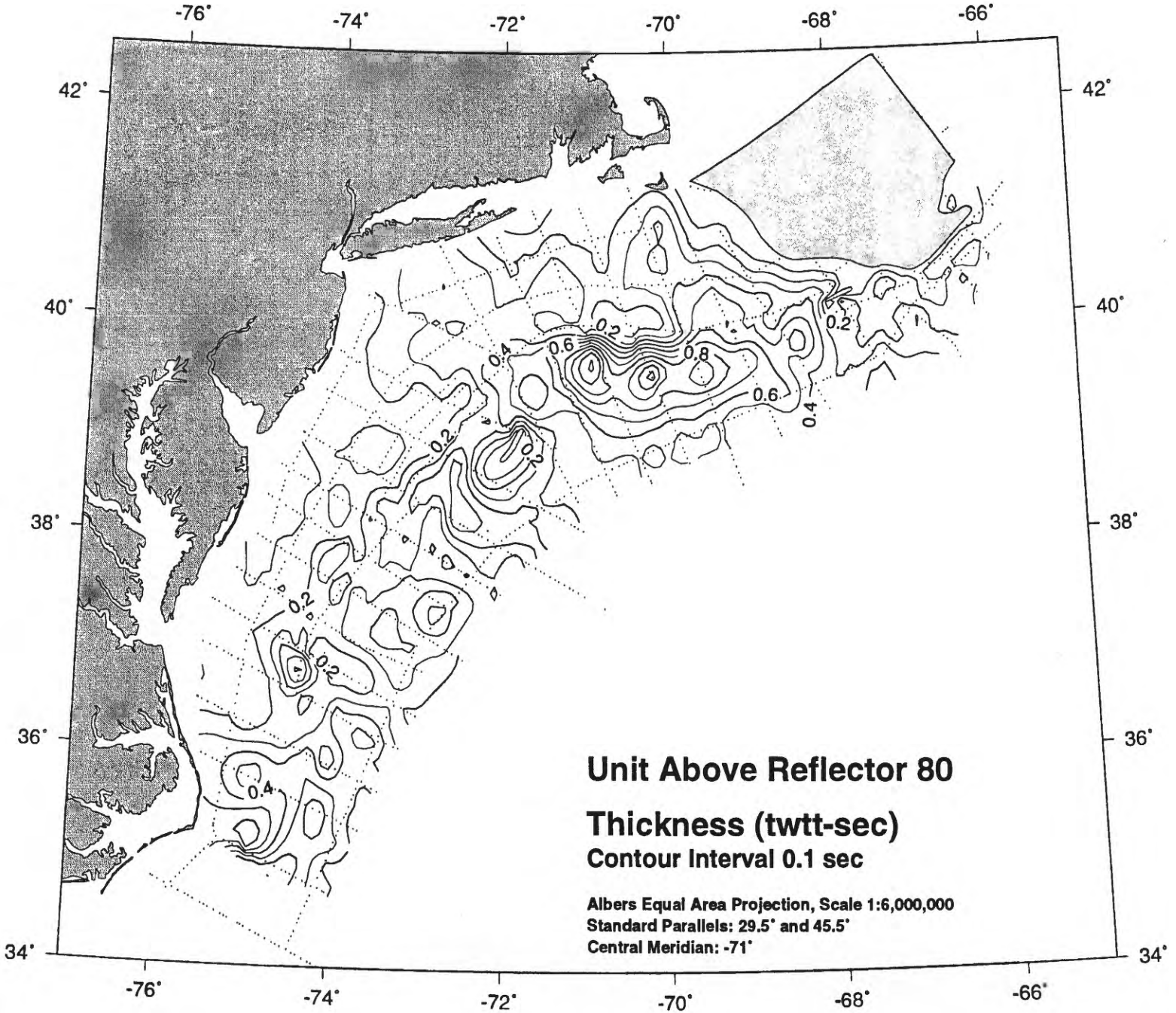
-76°
-74°
-72°
-70°
-68°
-66°
42°
40°
38°
36°
34°
0.2
0.4
0.6
0.8
Unit Above Reflector 80
Thickness (twtt-sec)
Contour Interval 0.1 sec
Albers Equal Area Projection, Scale 1:6,000,000
Standard Parallels: 29.5° and 45.5°
Central Meridian: -71°

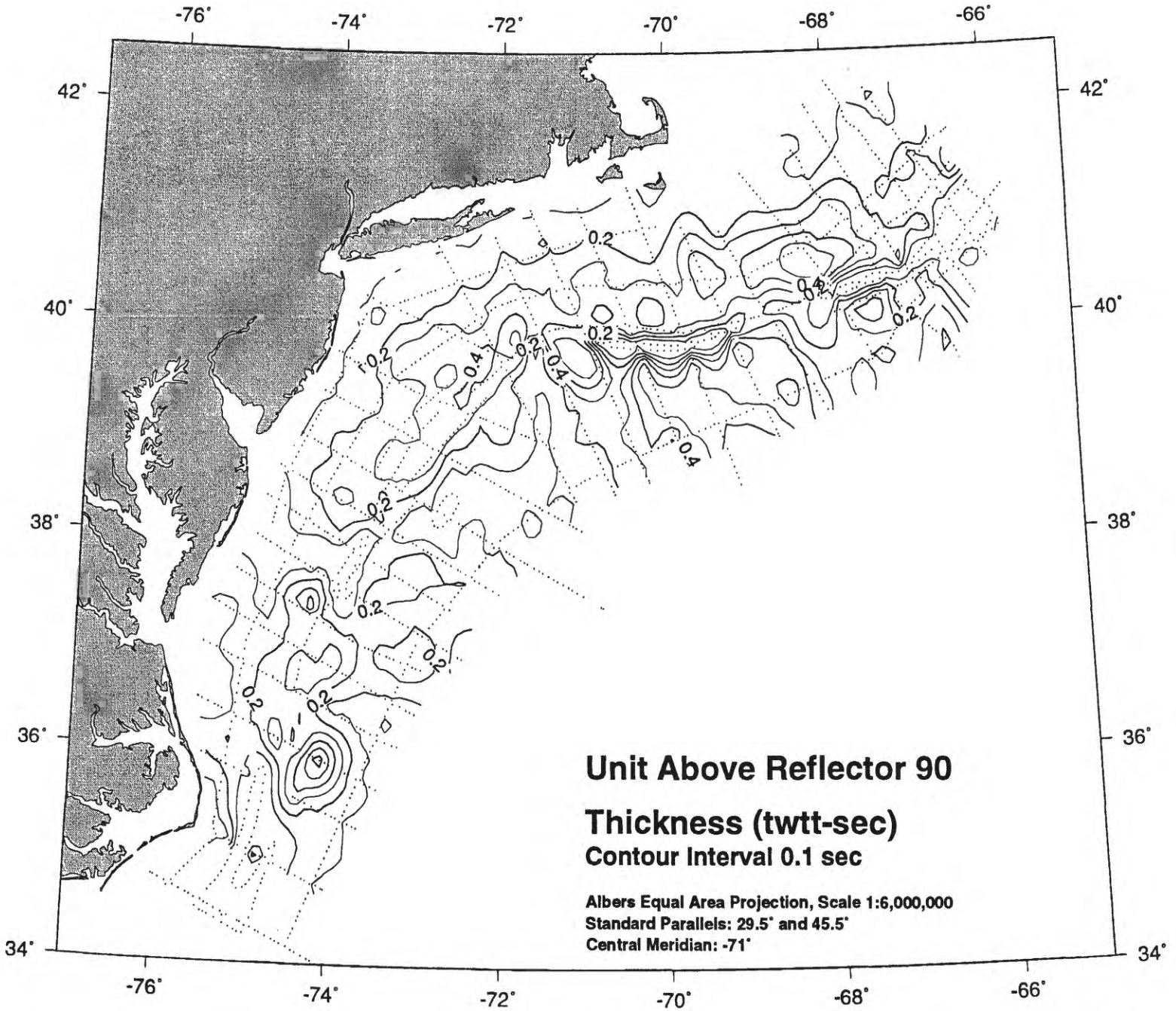
-76°
-74°
-72°
-70°
-68°
-66°
42°
40°
38°
36°
34°
0.2
0.4
Unit Above Reflector 90
Thickness (twtt-sec)
Contour Interval 0.1 sec
Albers Equal Area Projection, Scale 1:6,000,000
Standard Parallels: 29.5° and 45.5°
Central Meridian: -71°

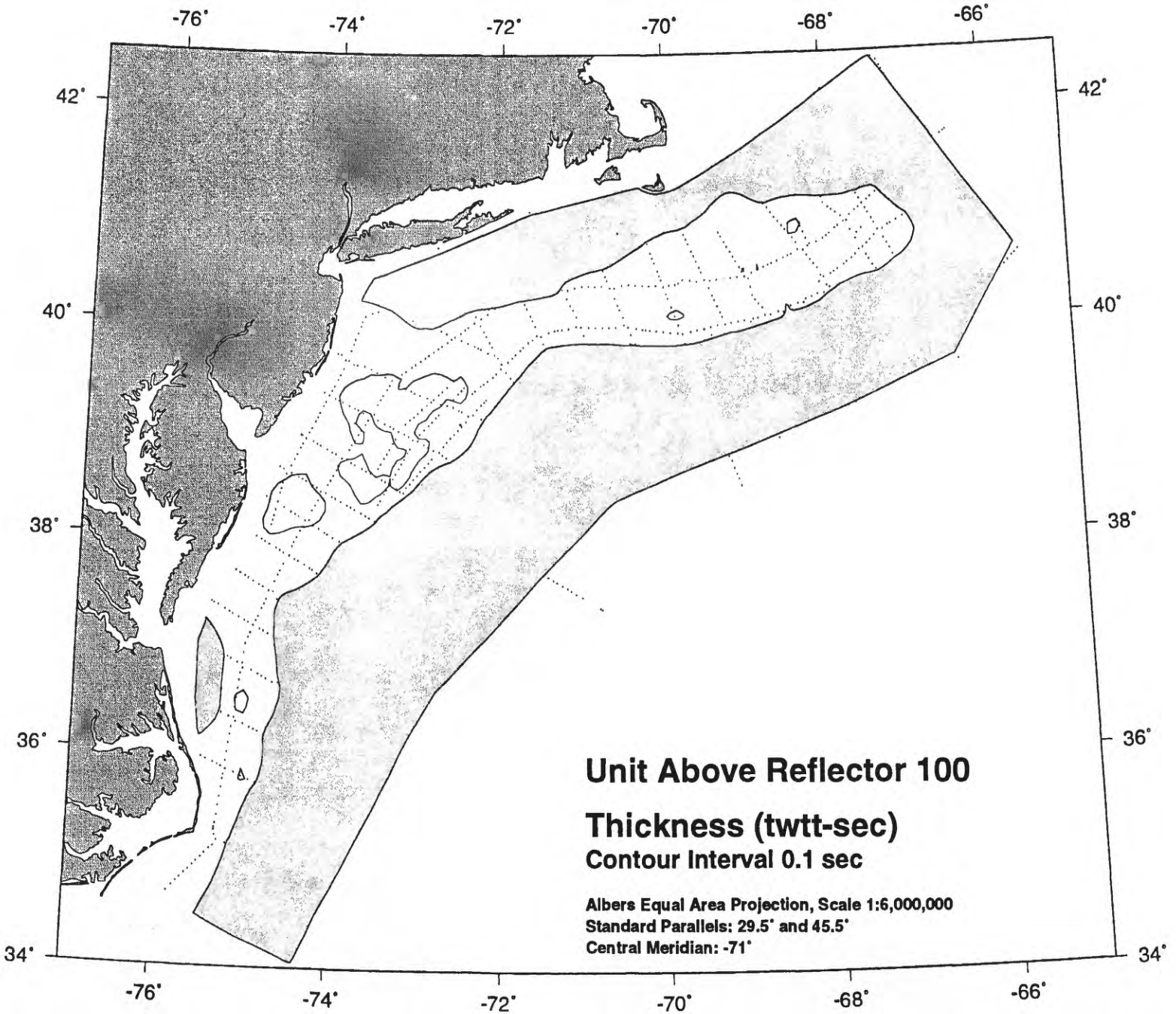
-76°
-74°
-72°
-70°
-68°
-66°
42°
40°
38°
36°
34°
Unit Above Reflector 100
Thickness (twtt-sec)
Contour Interval 0.1 sec
Albers Equal Area Projection, Scale 1:6,000,000
Standard Parallels: 29.5° and 45.5°
Central Meridian: -71°

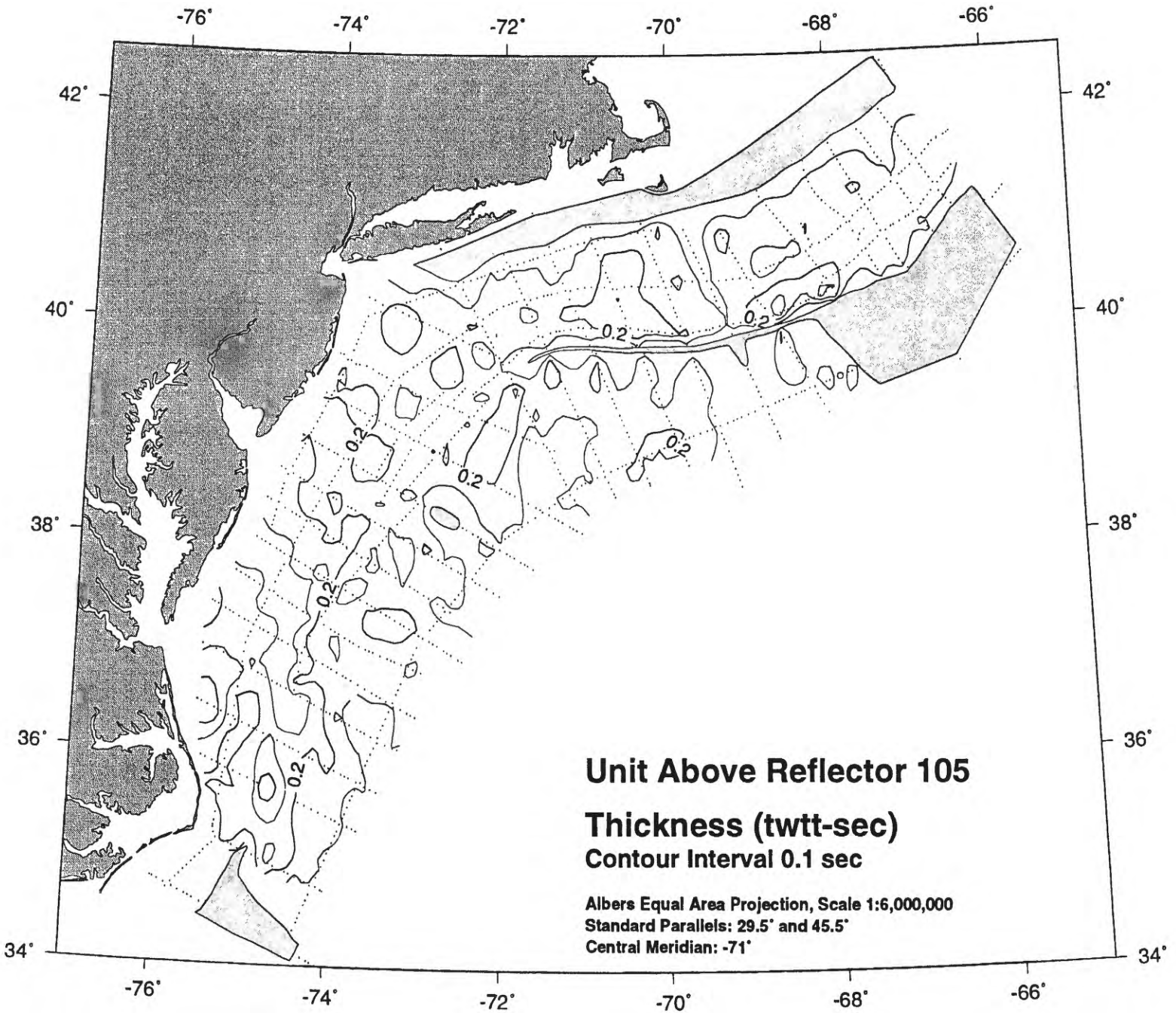
-76°
-74°
-72°
-70°
-68°
-66°
42°
40°
38°
36°
34°
0.2
Unit Above Reflector 105
Thickness (twtt-sec)
Contour Interval 0.1 sec
Albers Equal Area Projection, Scale 1:6,000,000
Standard Parallels: 29.5° and 45.5°
Central Meridian: -71°

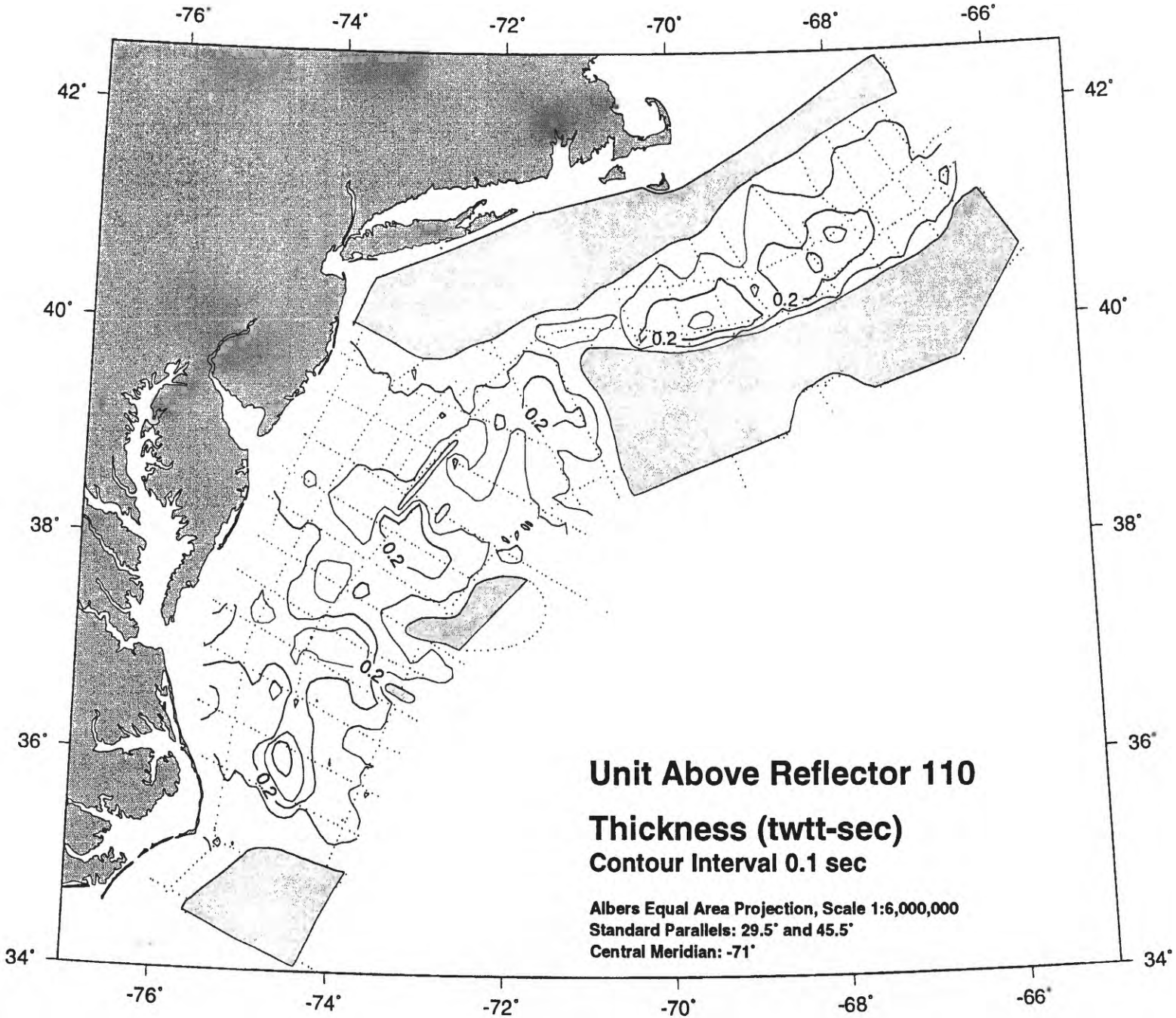
-76°
-74°
-72°
-70°
-68°
-66°
42°
40°
38°
36°
34°
0.2
Unit Above Reflector 110
Thickness (twtt-sec)
Contour Interval 0.1 sec
Albers Equal Area Projection, Scale 1:6,000,000
Standard Parallels: 29.5° and 45.5°
Central Meridian: -71°

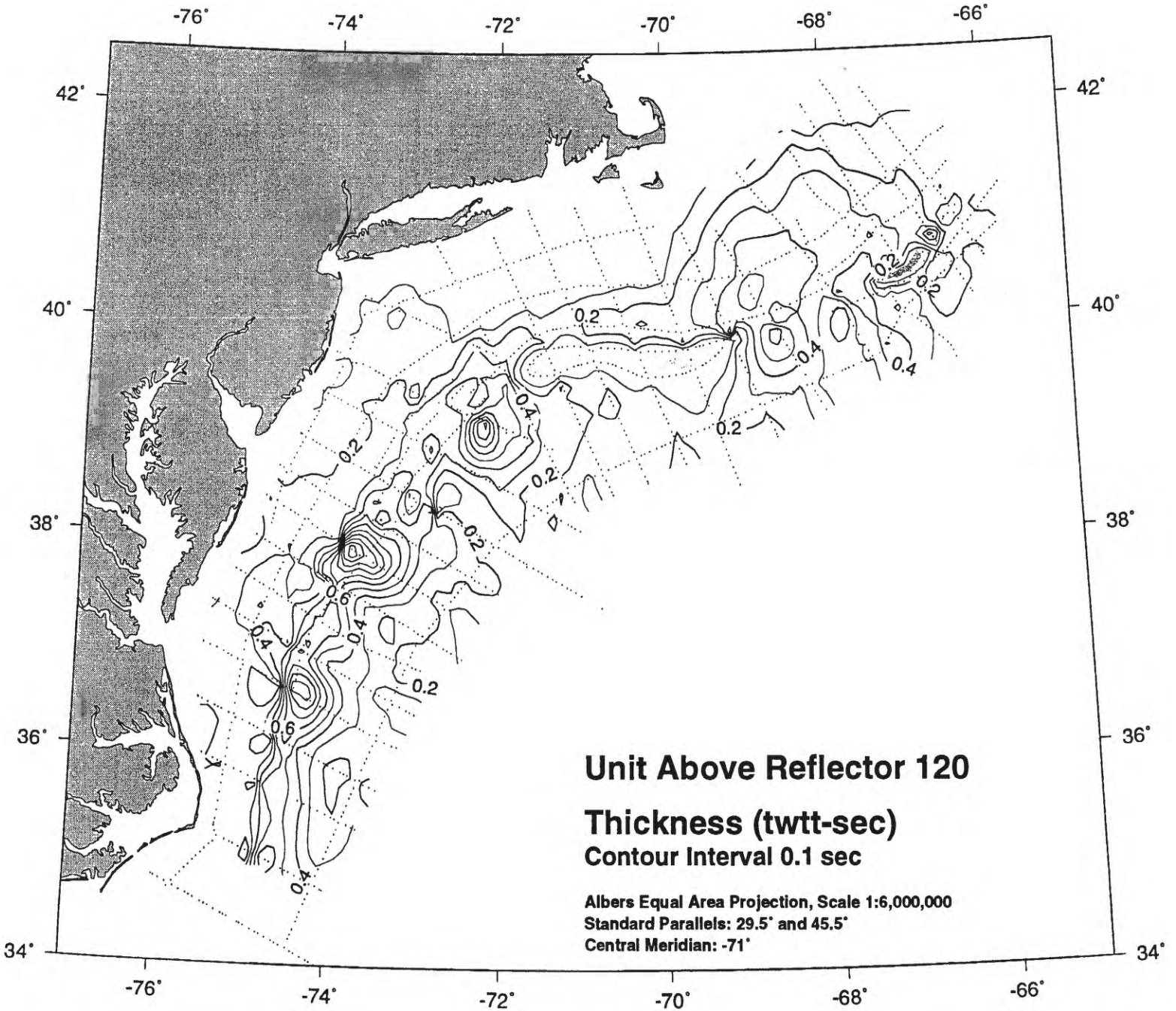
-76°
-74°
-72°
-70°
-68°
-66°
42°
40°
38°
36°
34°
0.2
0.4
0.6
Unit Above Reflector 120
Thickness (twtt-sec)
Contour Interval 0.1 sec
Albers Equal Area Projection, Scale 1:6,000,000
Standard Parallels: 29.5° and 45.5°
Central Meridian: -71°

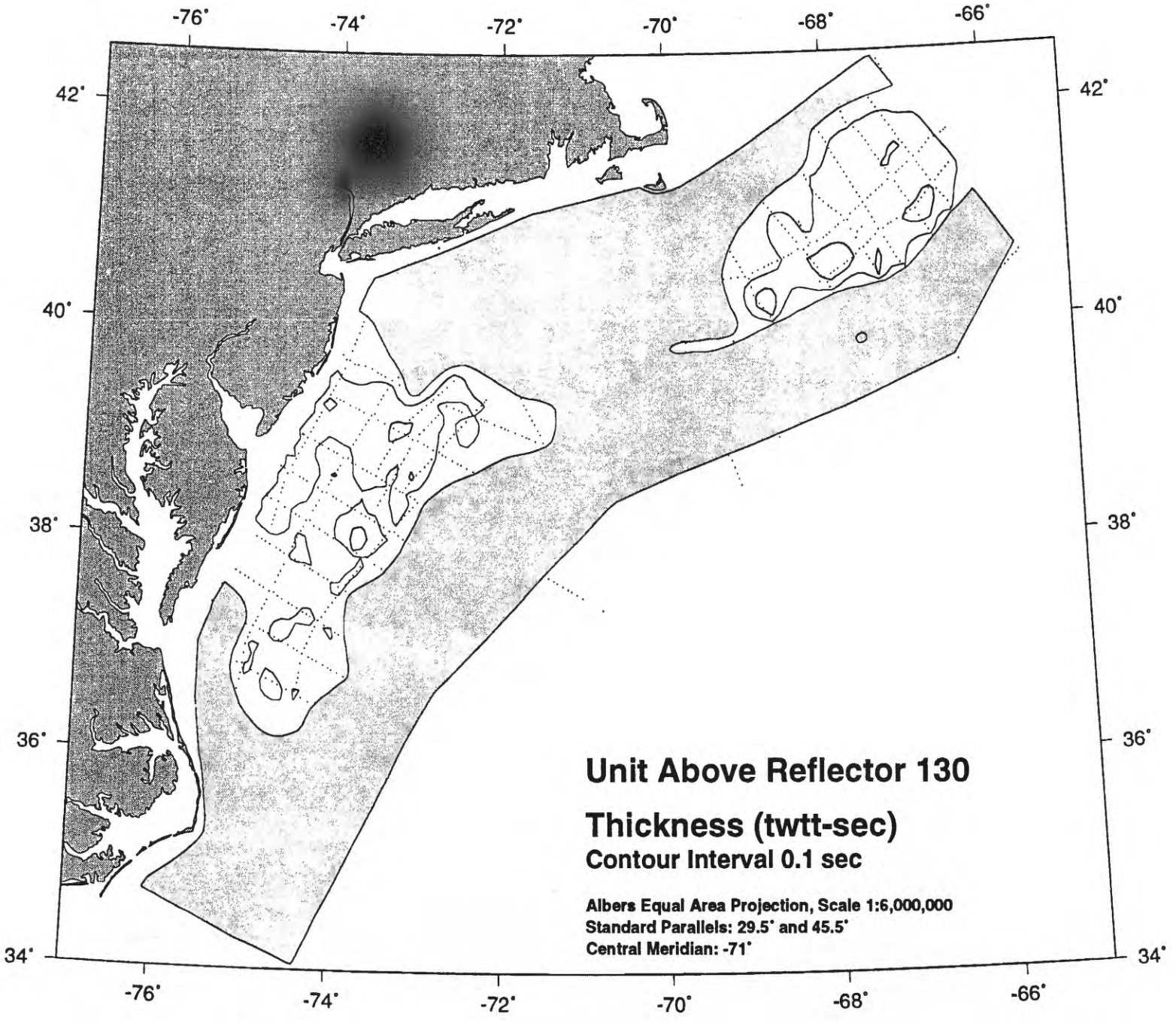
-76°
-74°
-72°
-70°
-68°
-66°
42°
40°
38°
36°
34°
Unit Above Reflector 130
Thickness (twtt-sec)
Contour Interval 0.1 sec
Albers Equal Area Projection, Scale 1:6,000,000
Standard Parallels: 29.5° and 45.5°
Central Meridian: -71°

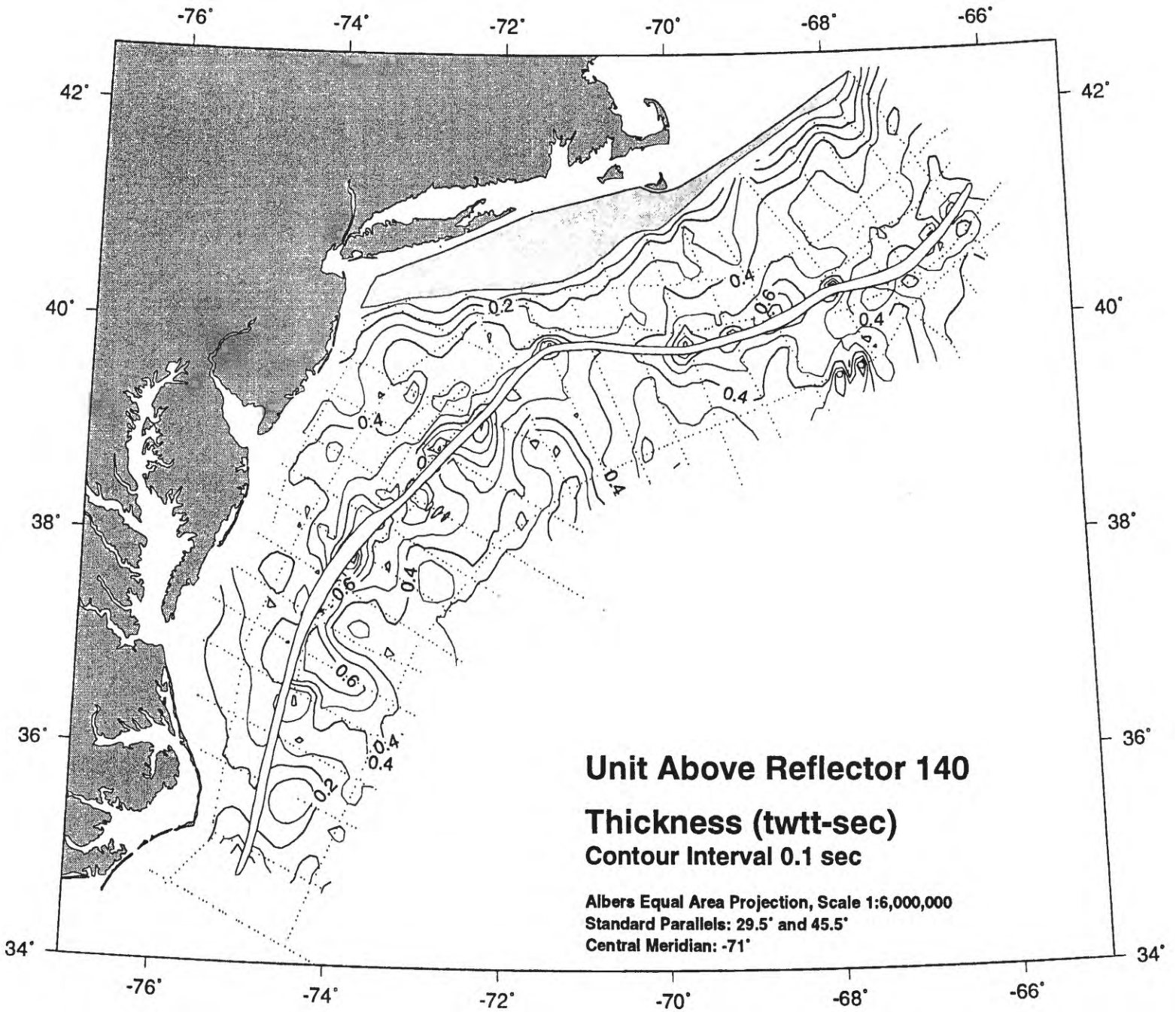
-76°
-74°
-72°
-70°
-68°
-66°
42°
40°
38°
36°
34°
0.2
0.4
0.6
Unit Above Reflector 140
Thickness (twtt-sec)
Contour Interval 0.1 sec
Albers Equal Area Projection, Scale 1:6,000,000
Standard Parallels: 29.5° and 45.5°
Central Meridian: -71°

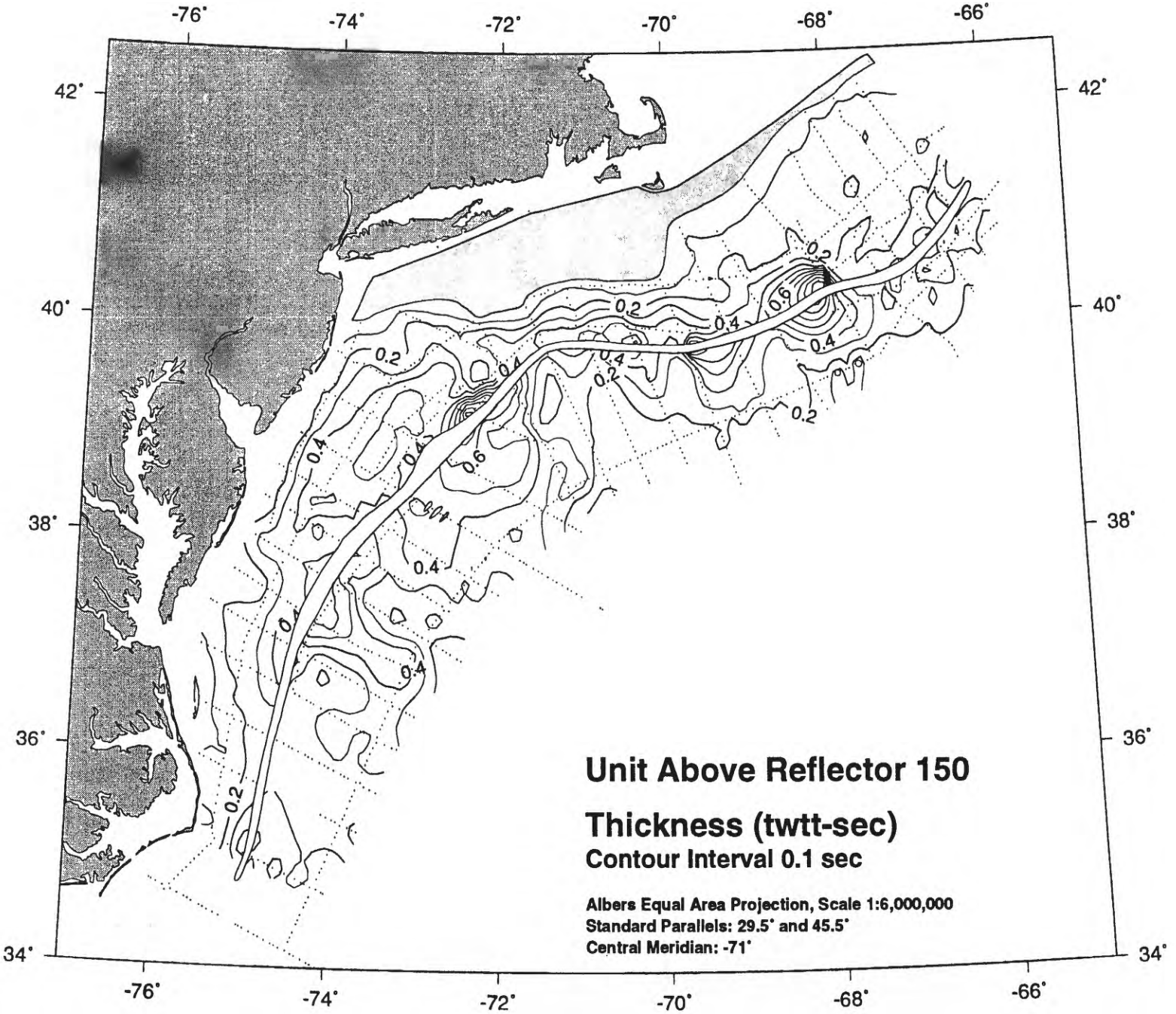
-76°
-74°
-72°
-70°
-68°
-66°
42°
40°
38°
36°
34°
0.2
0.4
0.6
0.9
Unit Above Reflector 150
Thickness (twtt-sec)
Contour Interval 0.1 sec
Albers Equal Area Projection, Scale 1:6,000,000
Standard Parallels: 29.5° and 45.5°
Central Meridian: -71°

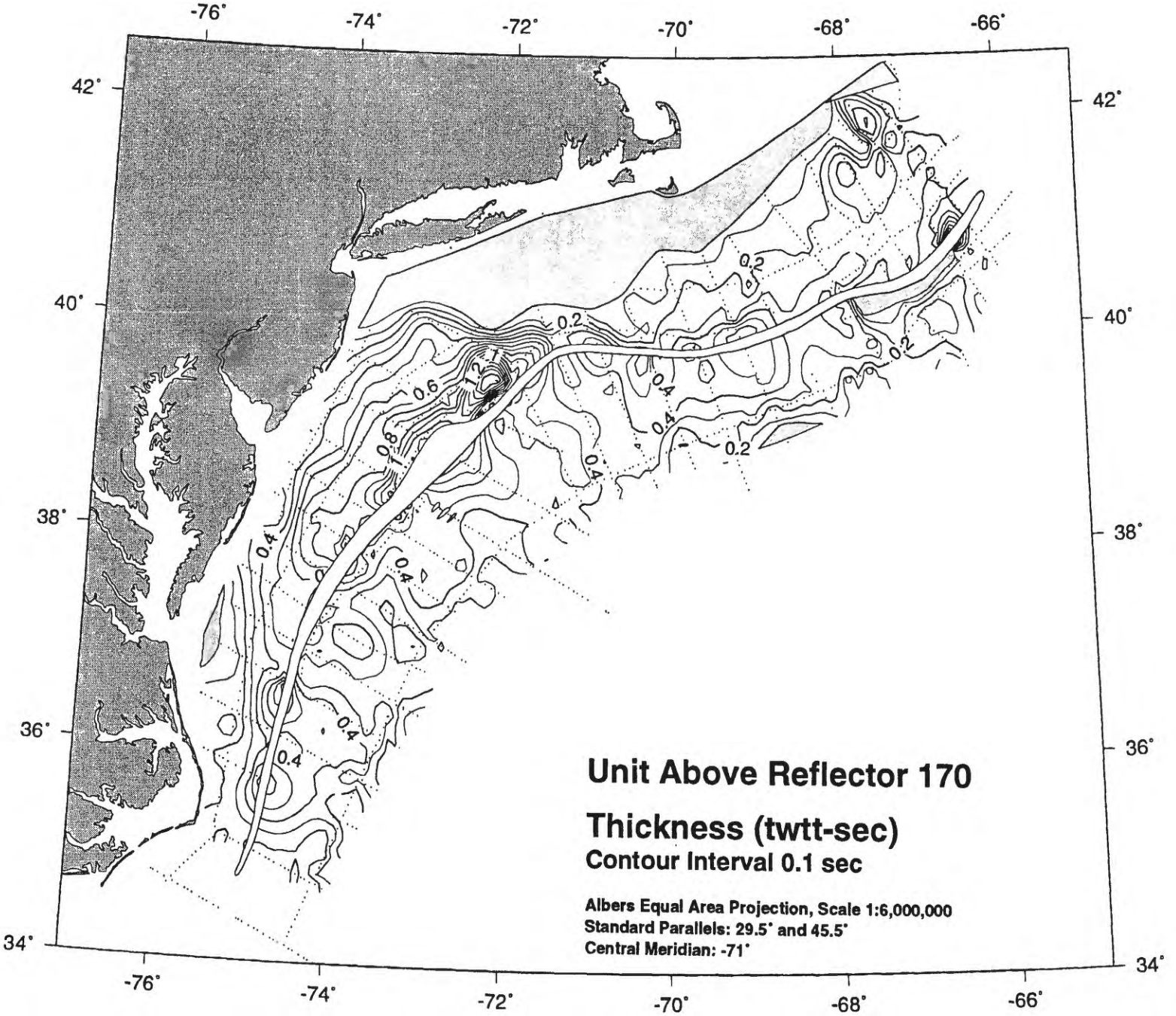
-76°
-74°
-72°
-70°
-68°
-66°
42°
40°
38°
36°
34°
0.2
0.4
0.6
0.8
1
1.2
Unit Above Reflector 170
Thickness (twtt-sec)
Contour Interval 0.1 sec
Albers Equal Area Projection, Scale 1:6,000,000
Standard Parallels: 29.5° and 45.5°
Central Meridian: -71°

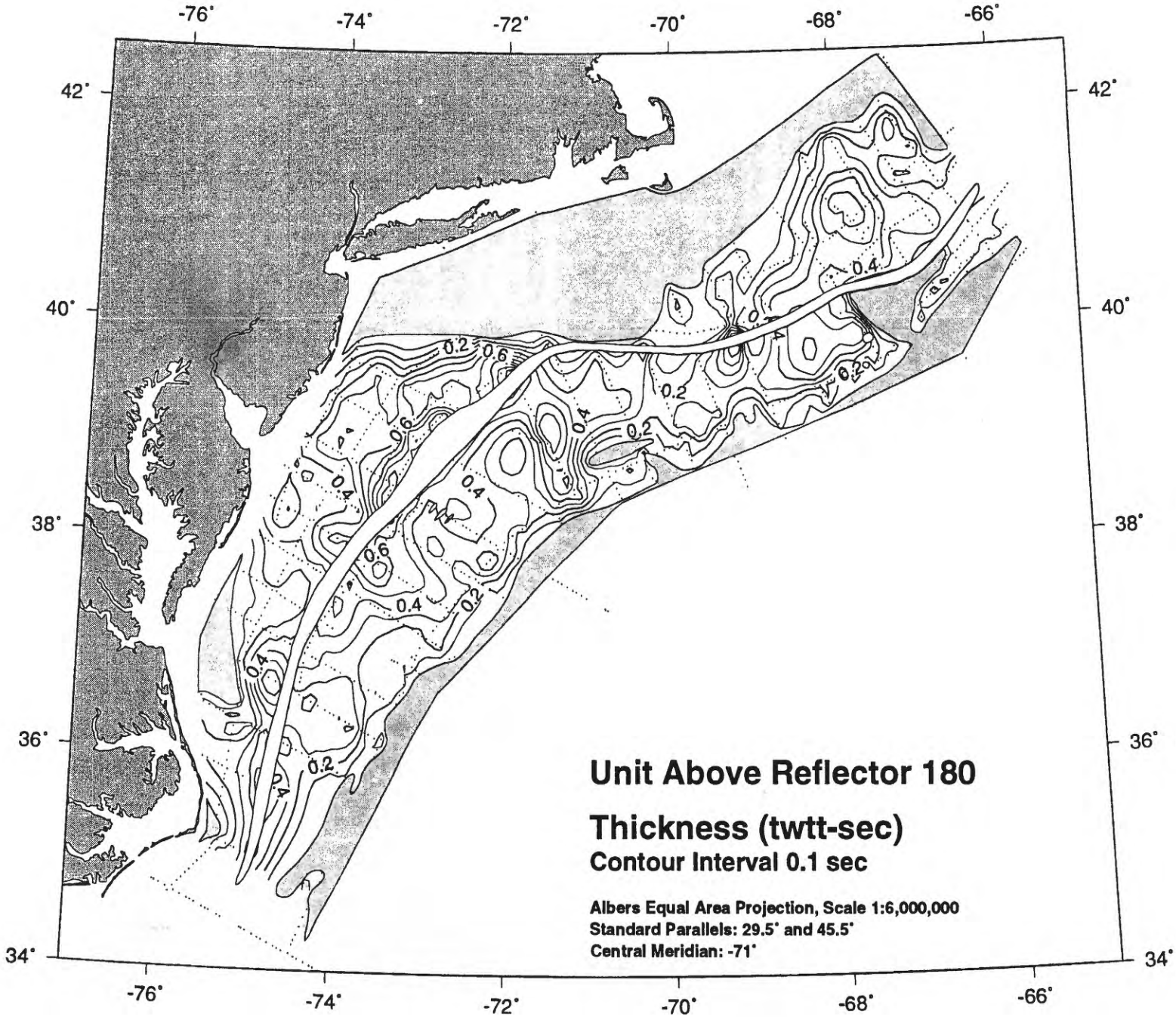
-76°
-74°
-72°
-70°
-68°
-66°
42°
40°
38°
36°
34°
0.2
0.4
0.6
Unit Above Reflector 180
Thickness (twtt-sec)
Contour Interval 0.1 sec
Albers Equal Area Projection, Scale 1:6,000,000
Standard Parallels: 29.5° and 45.5°
Central Meridian: -71°

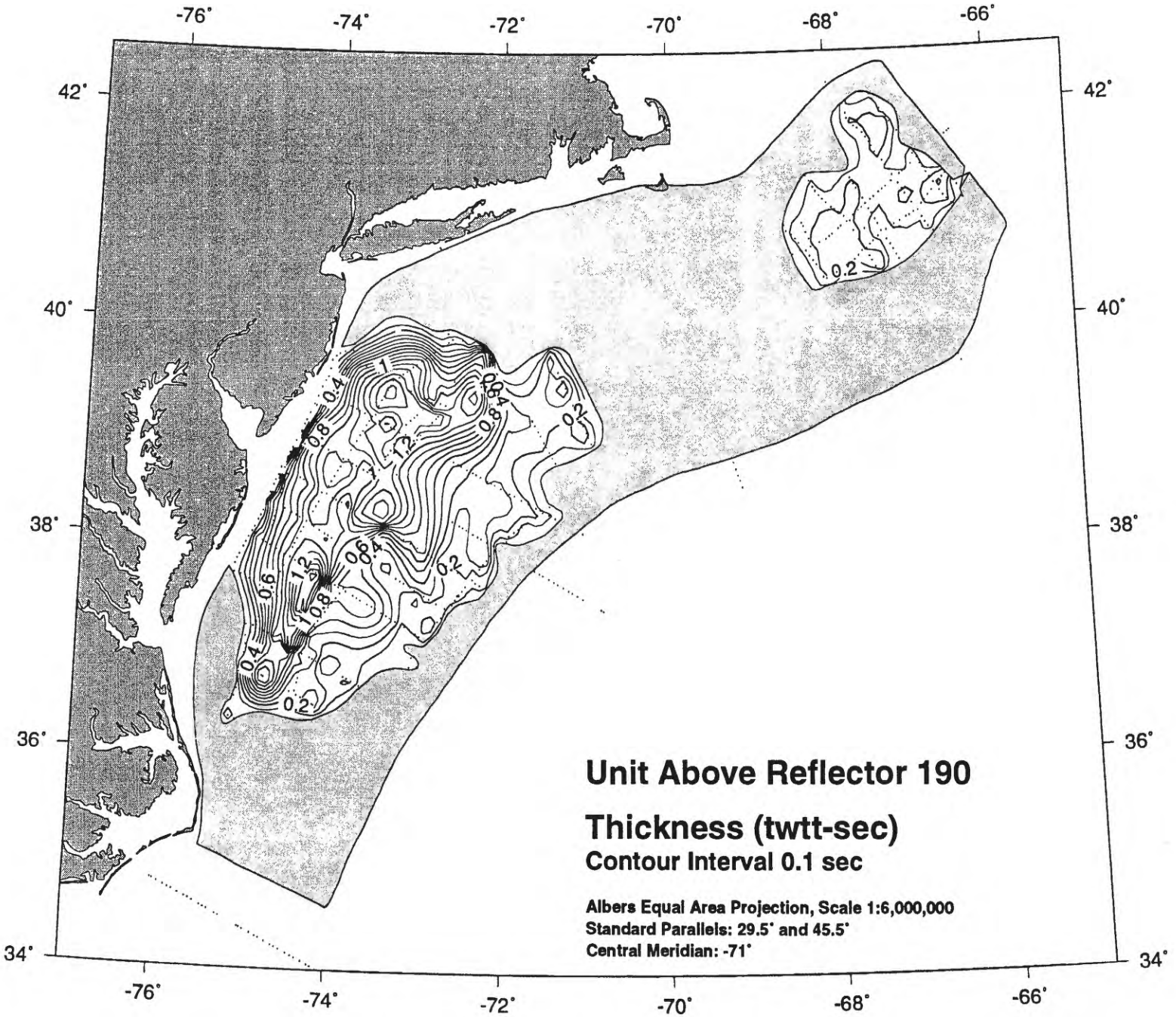
-76°
-74°
-72°
-70°
-68°
-66°
42°
40°
38°
36°
34°
0.2
1
0.4
0.8
1.2
0.6
Unit Above Reflector 190
Thickness (twtt-sec)
Contour Interval 0.1 sec
Albers Equal Area Projection, Scale 1:6,000,000
Standard Parallels: 29.5° and 45.5°
Central Meridian: -71°

Appendix 7

Interval Velocity Contour Maps for Acoustic Units in Digital Database

Contour maps of the interval velocities of each acoustic unit in this geoacoustic database. The dotted lines represent the seismic line control used to construct each surface. See Figure 8 for the 5-minute grid point map, based on these seismic lines, used to construct the contour map. Shaded masks indicate the regions where a particular surface has been eroded into by an overlying surface. Narrow blank zones in the shelf edge region are where deeper units are obscured by the Jurassic carbonate bank. Water velocity (reflector 1) is assumed 1500 m/sec. Contour interval is 100 m/sec.

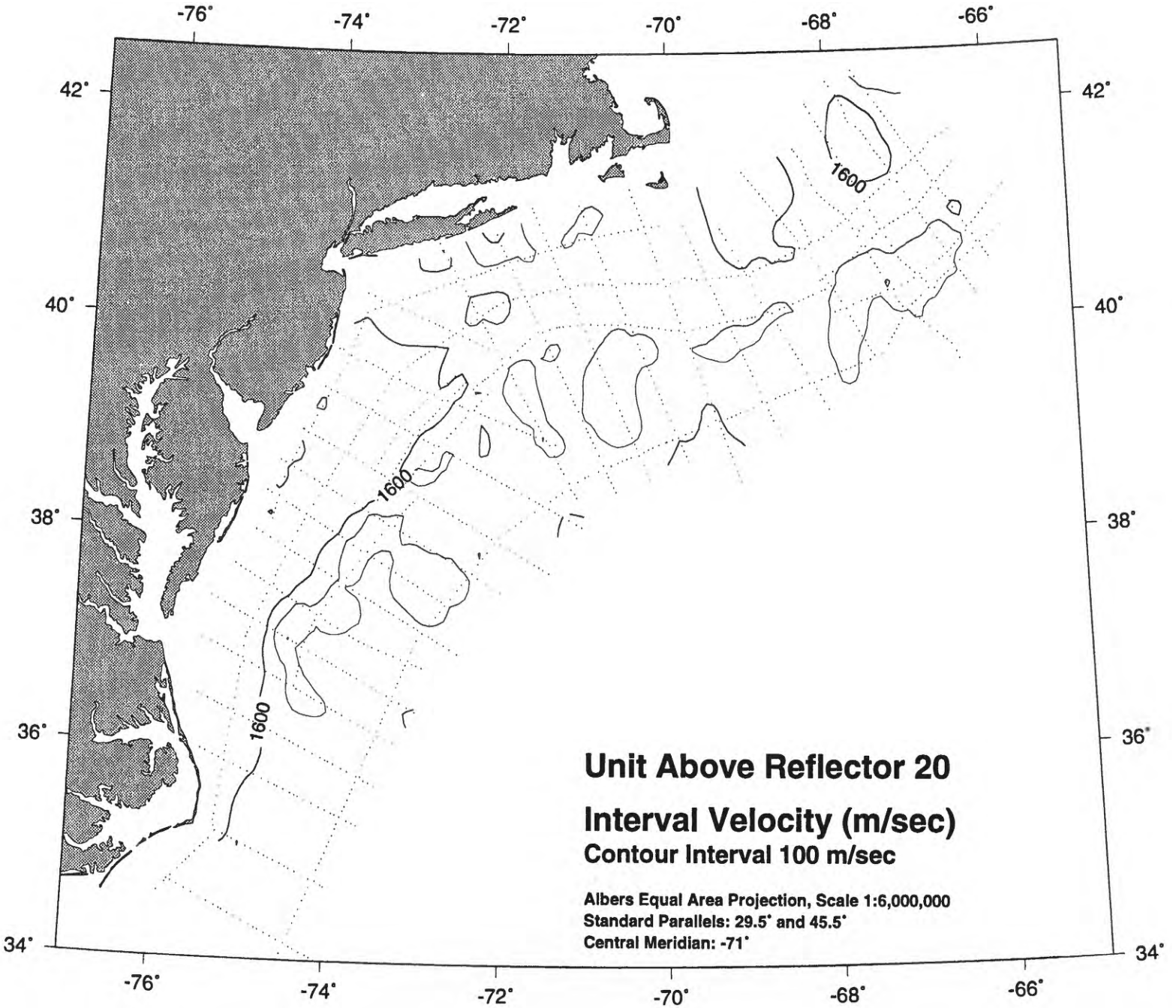
-76°
-74°
-72°
-70°
-68°
-66°
42°
40°
38°
36°
34°
1600
1600
1600
Unit Above Reflector 20
Interval Velocity (m/sec)
Contour Interval 100 m/sec
Albers Equal Area Projection, Scale 1:6,000,000
Standard Parallels: 29.5° and 45.5°
Central Meridian: -71°

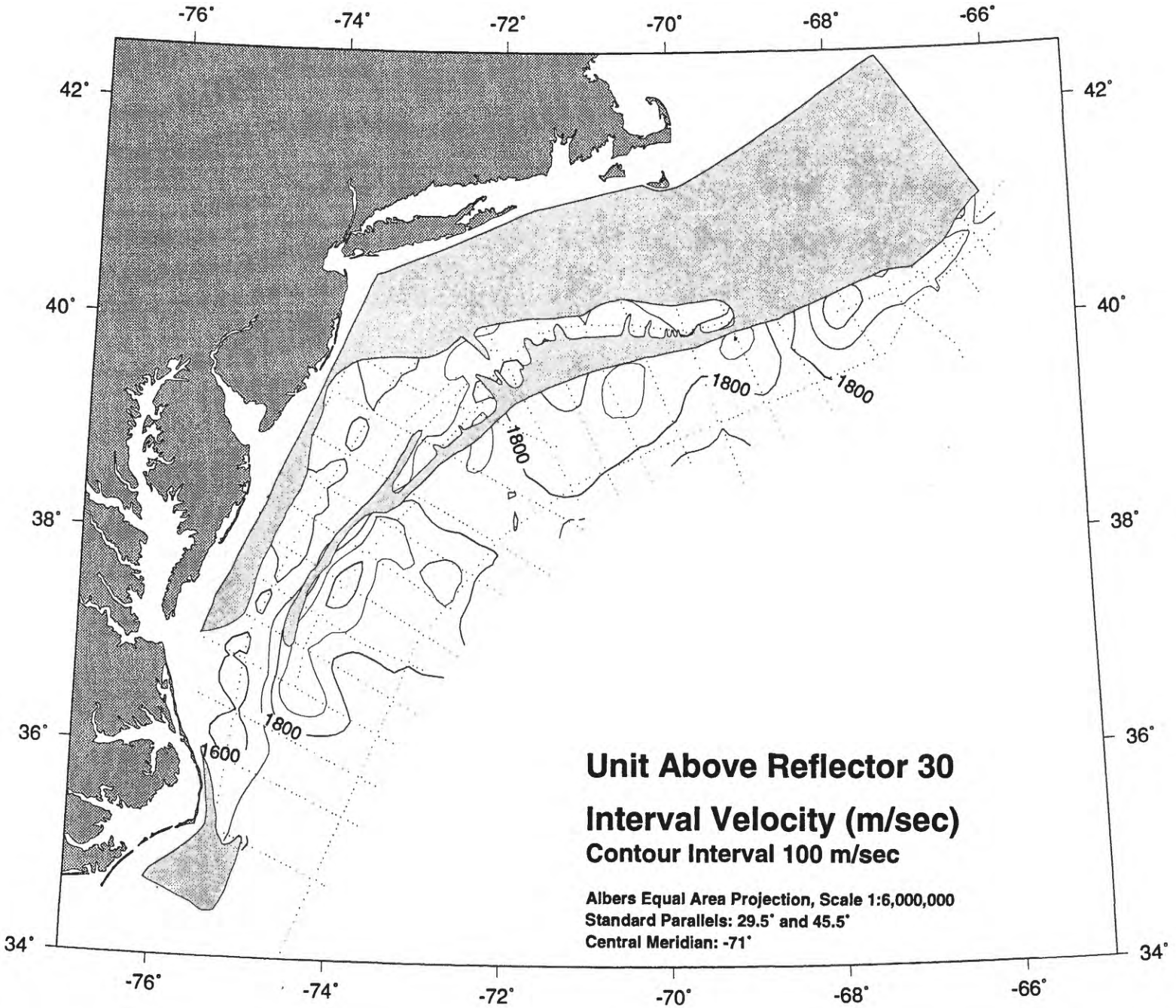
-76°
-74°
-72°
-70°
-68°
-66°
42°
40°
38°
36°
34°
1800
1800
1800
1800
1600
Unit Above Reflector 30
Interval Velocity (m/sec)
Contour Interval 100 m/sec
Albers Equal Area Projection, Scale 1:6,000,000
Standard Parallels: 29.5° and 45.5°
Central Meridian: -71°

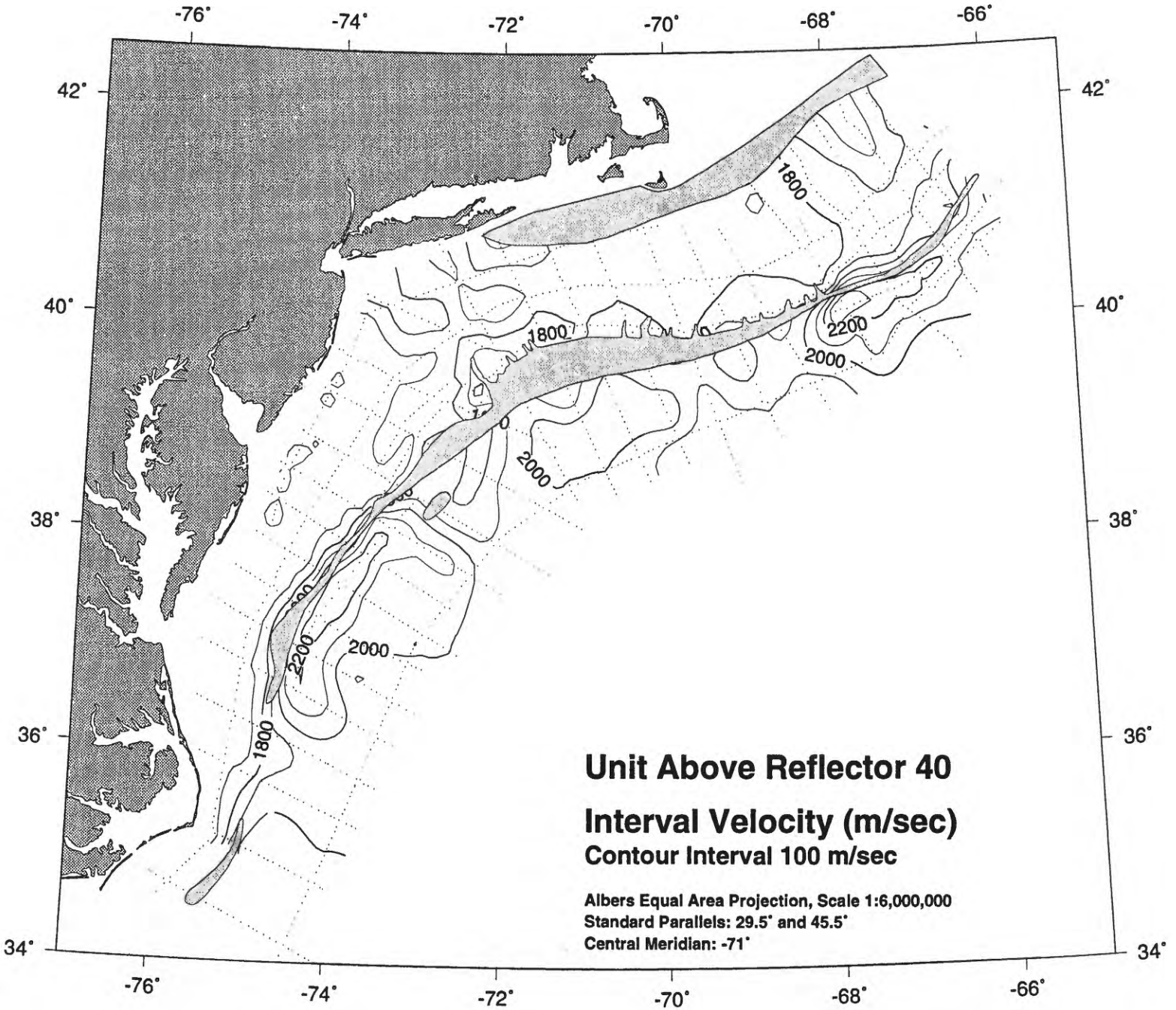
-76°
-74°
-72°
-70°
-68°
-66°
42°
40°
38°
36°
34°
1800
2000
2200
Unit Above Reflector 40
Interval Velocity (m/sec)
Contour Interval 100 m/sec
Albers Equal Area Projection, Scale 1:6,000,000
Standard Parallels: 29.5° and 45.5°
Central Meridian: -71°

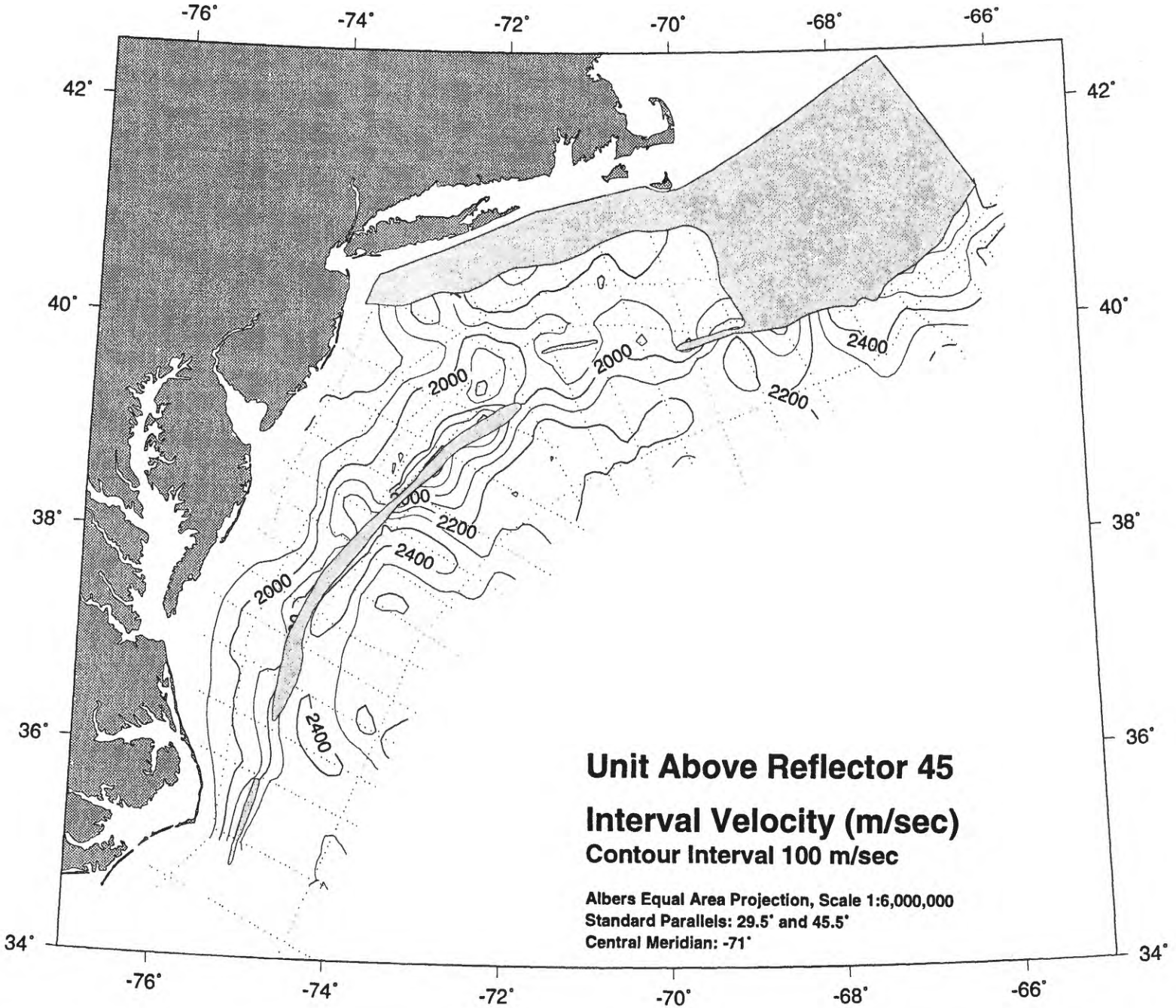
-76°
-74°
-72°
-70°
-68°
-66°
42°
40°
38°
36°
34°
2000
2200
2400
Unit Above Reflector 45
Interval Velocity (m/sec)
Contour Interval 100 m/sec
Albers Equal Area Projection, Scale 1:6,000,000
Standard Parallels: 29.5° and 45.5°
Central Meridian: -71°

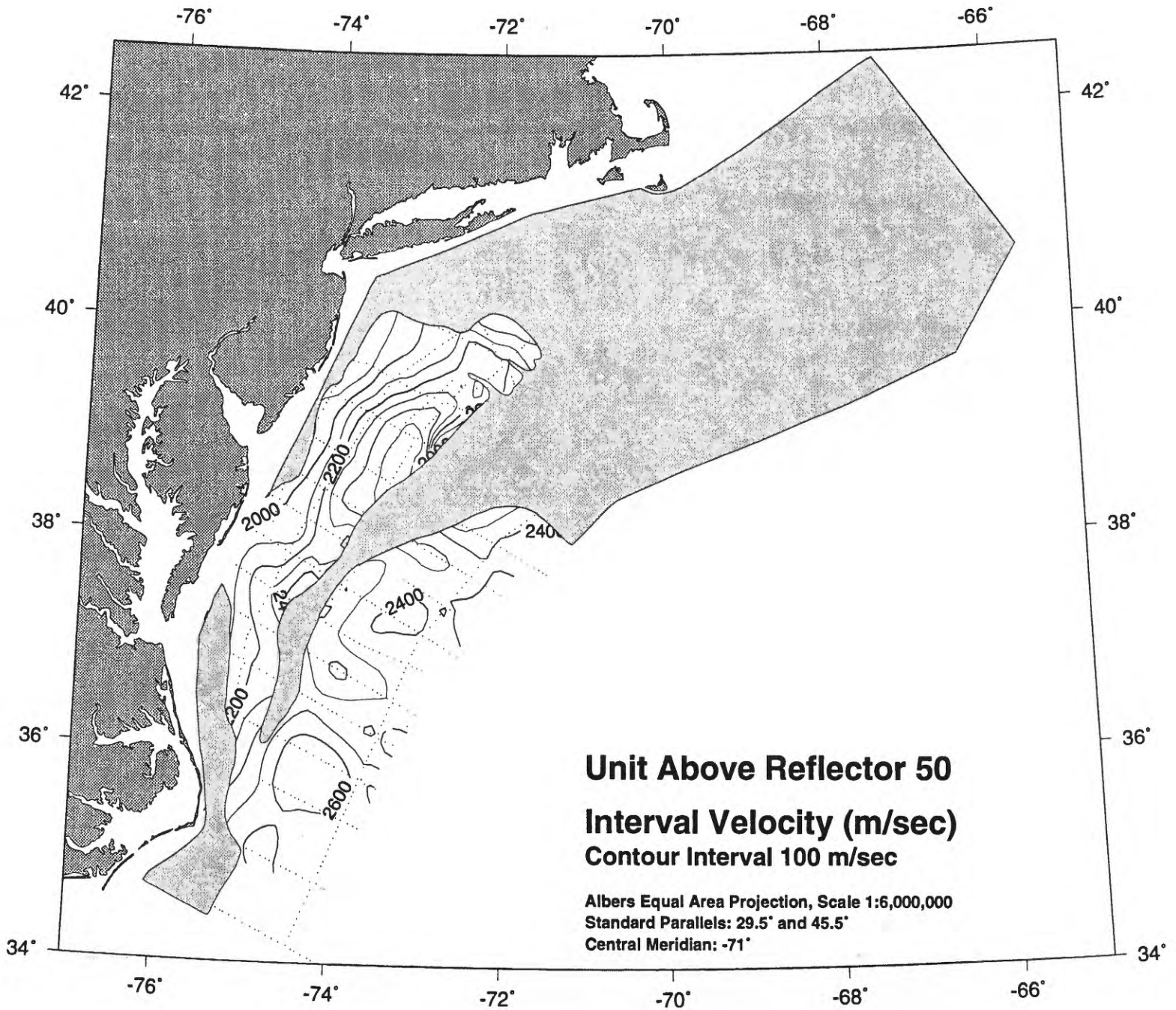
-76°
-74°
-72°
-70°
-68°
-66°
42°
40°
38°
36°
34°
2000
2200
2400
2600
Unit Above Reflector 50
Interval Velocity (m/sec)
Contour Interval 100 m/sec
Albers Equal Area Projection, Scale 1:6,000,000
Standard Parallels: 29.5° and 45.5°
Central Meridian: -71°

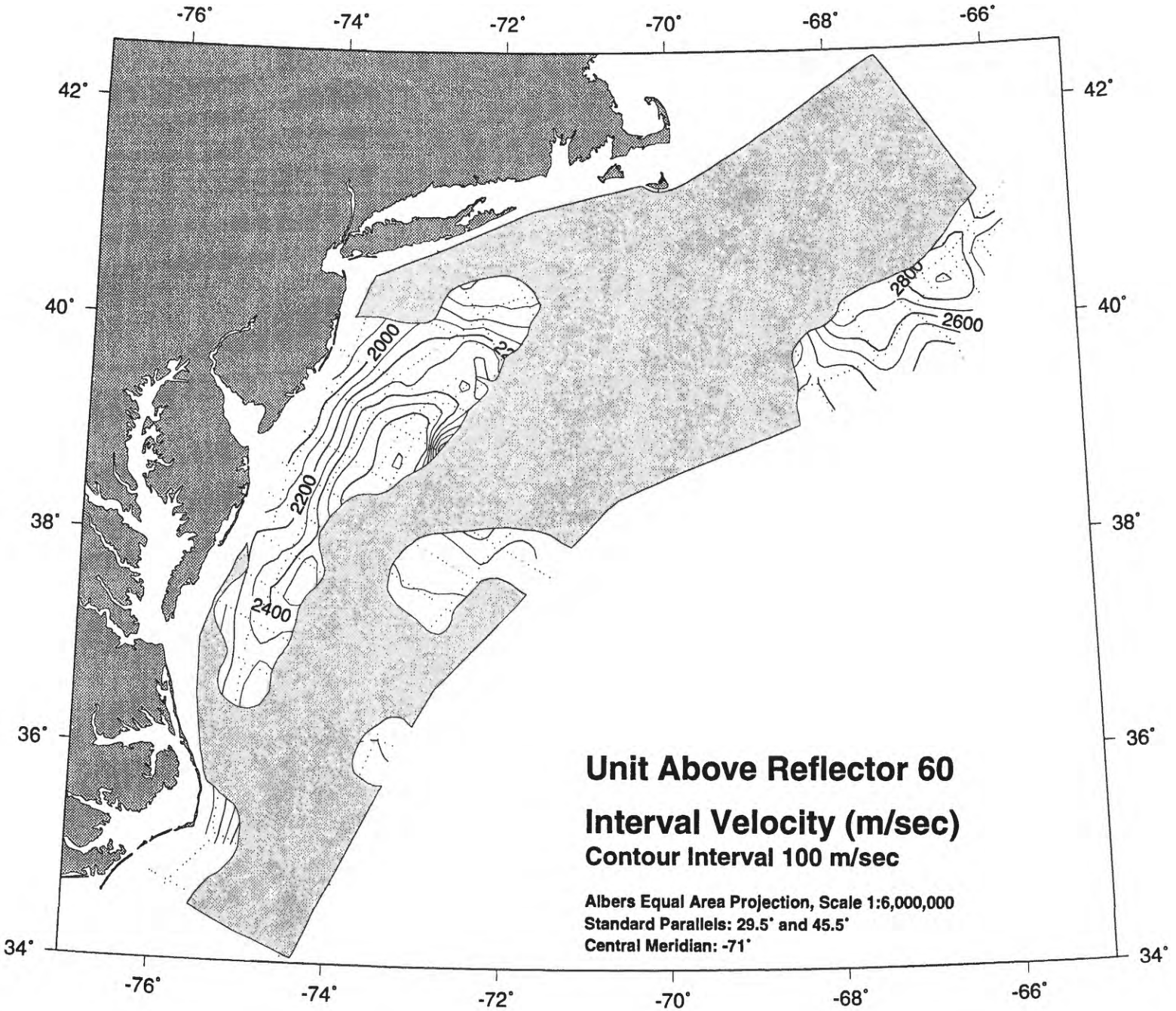
-76°
-74°
-72°
-70°
-68°
-66°
42°
40°
38°
36°
34°
2000
2200
2400
2600
2800
Unit Above Reflector 60
Interval Velocity (m/sec)
Contour Interval 100 m/sec
Albers Equal Area Projection, Scale 1:6,000,000
Standard Parallels: 29.5° and 45.5°
Central Meridian: -71°

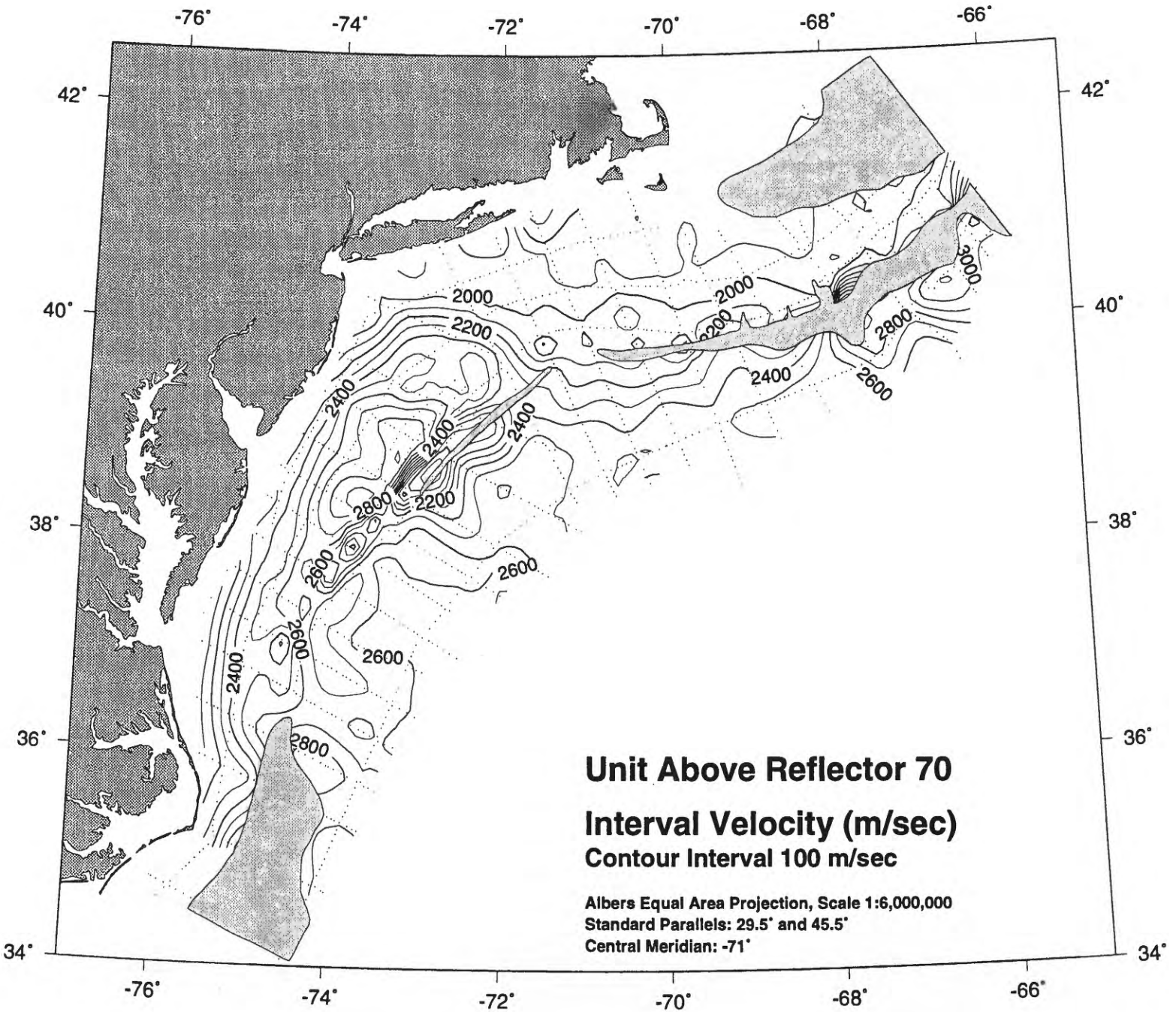
-76°
-74°
-72°
-70°
-68°
-66°
42°
40°
38°
36°
34°
2000
2200
2400
2600
2800
3000
Unit Above Reflector 70
Interval Velocity (m/sec)
Contour Interval 100 m/sec
Albers Equal Area Projection, Scale 1:6,000,000
Standard Parallels: 29.5° and 45.5°
Central Meridian: -71°

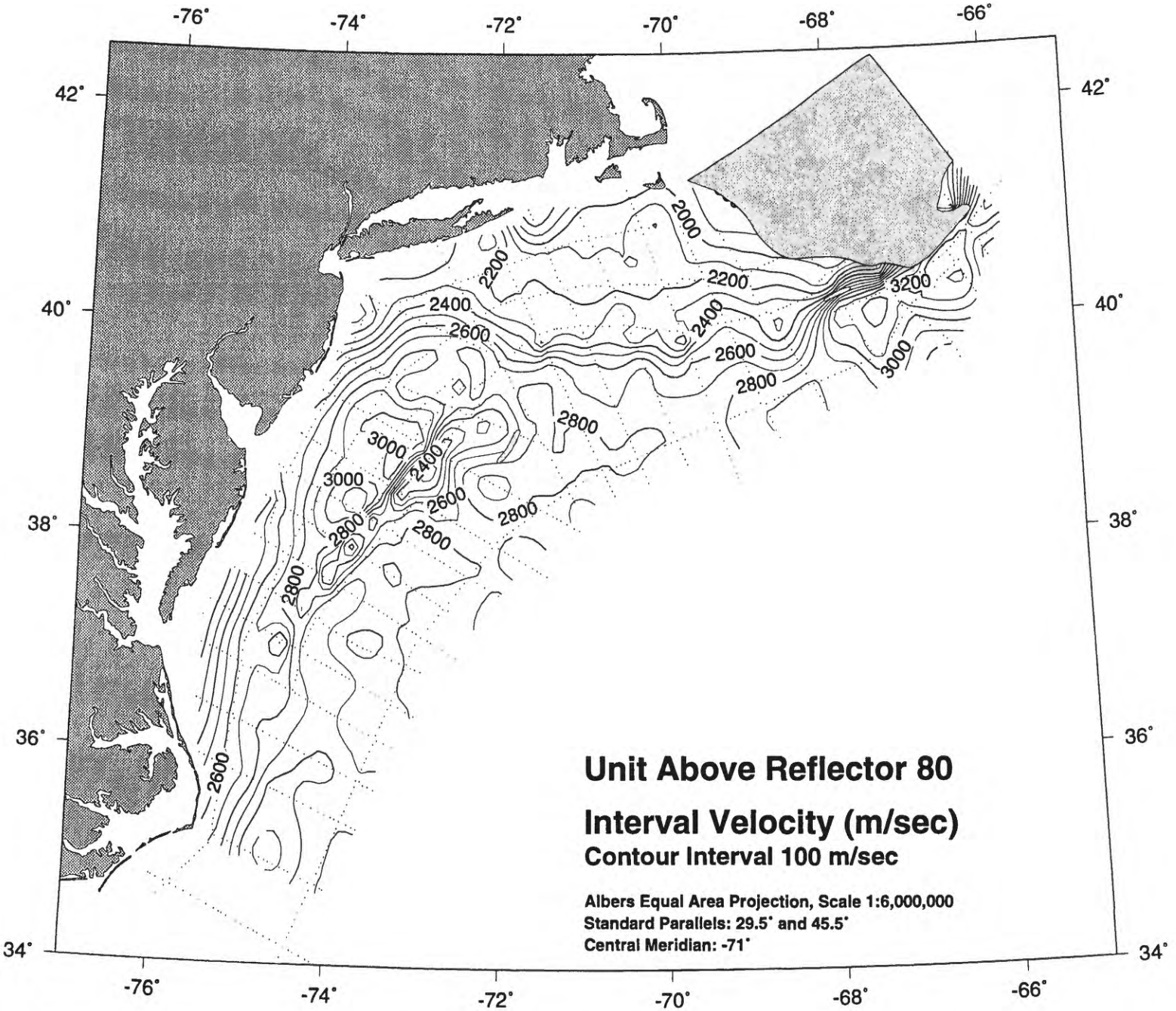
-76°
-74°
-72°
-70°
-68°
-66°
42°
40°
38°
36°
34°
2000
2200
2400
2600
2800
3000
3200
Unit Above Reflector 80
Interval Velocity (m/sec)
Contour Interval 100 m/sec
Albers Equal Area Projection, Scale 1:6,000,000
Standard Parallels: 29.5° and 45.5°
Central Meridian: -71°

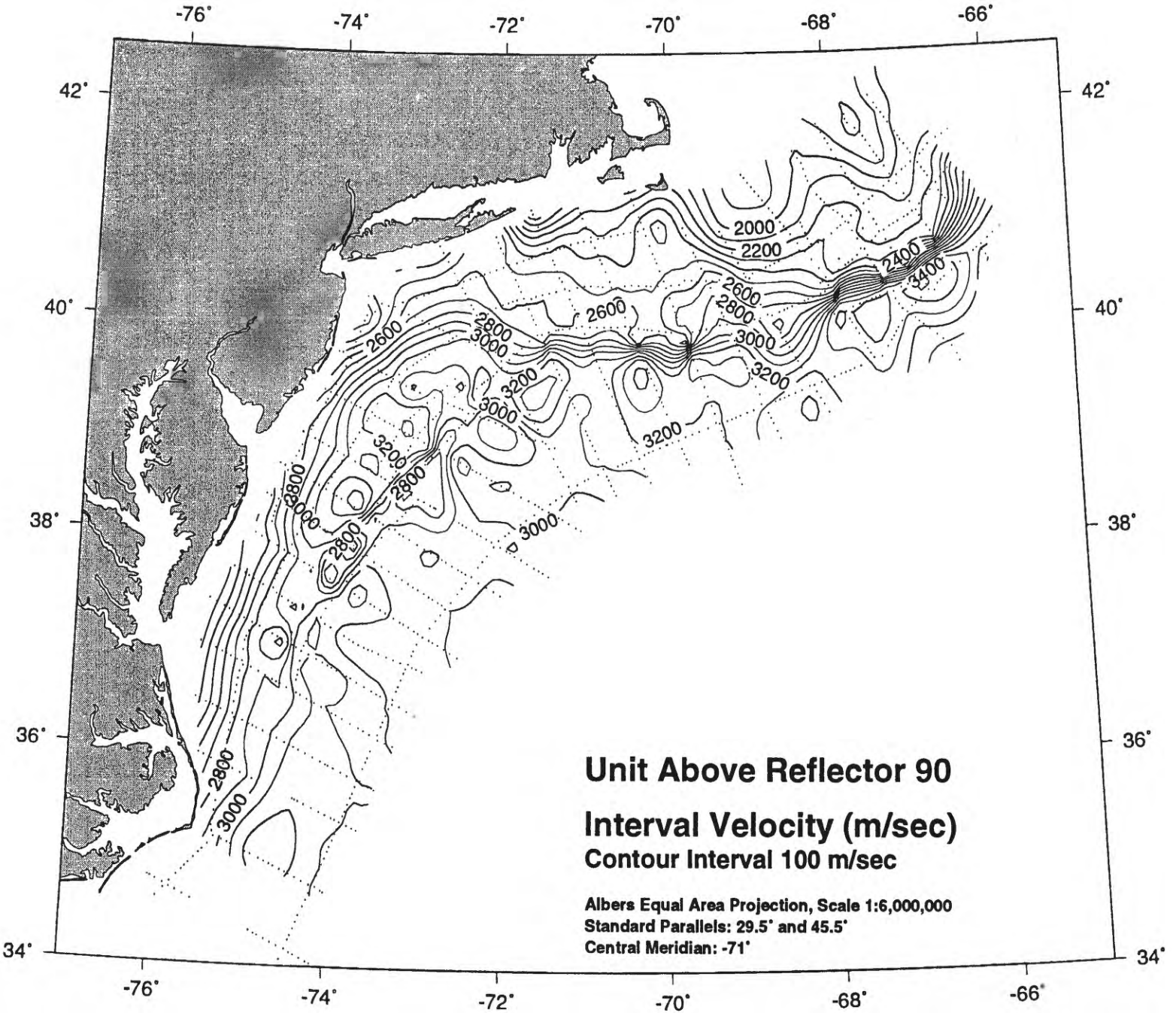
Unit Above Reflector 90
Interval Velocity (m/sec)
Contour Interval 100 m/sec
Albers Equal Area Projection, Scale 1:6,000,000
Standard Parallels: 29.5° and 45.5°
Central Meridian: -71°
-76°
-74°
-72°
-70°
-68°
-66°
42°
40°
38°
36°
34°
2000
2200
2400
2600
2800
3000
3200
3400

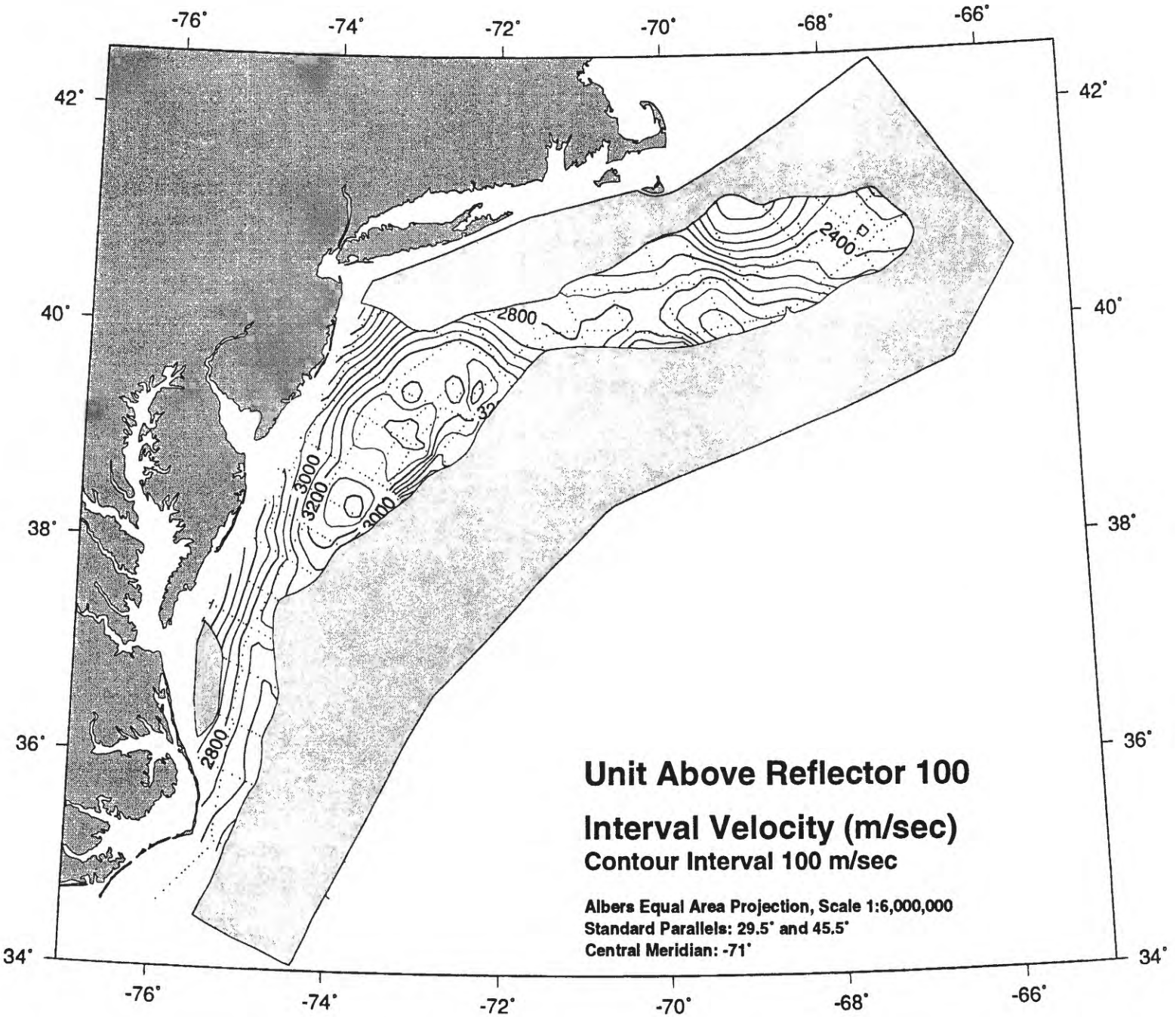
-76°
-74°
-72°
-70°
-68°
-66°
42°
40°
38°
36°
34°
2400
2800
3000
3200
3000
2800
Unit Above Reflector 100
Interval Velocity (m/sec)
Contour Interval 100 m/sec
Albers Equal Area Projection, Scale 1:6,000,000
Standard Parallels: 29.5° and 45.5°
Central Meridian: -71°

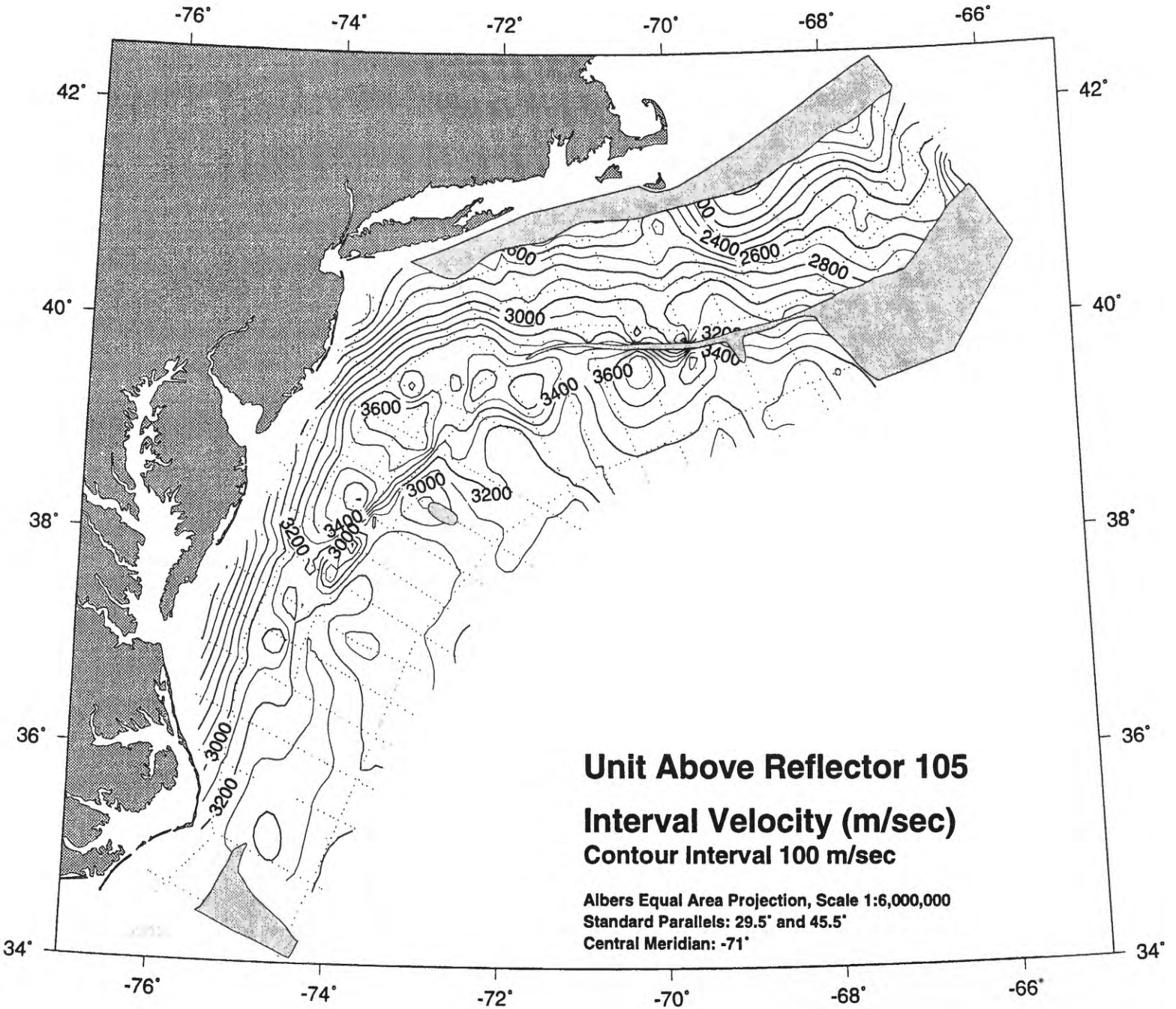
Unit Above Reflector 105
Interval Velocity (m/sec)
Contour Interval 100 m/sec
Albers Equal Area Projection, Scale 1:6,000,000
Standard Parallels: 29.5° and 45.5°
Central Meridian: -71°
-76°
-74°
-72°
-70°
-68°
-66°
42°
40°
38°
36°
34°
2400
2600
2800
3000
3200
3400
3600

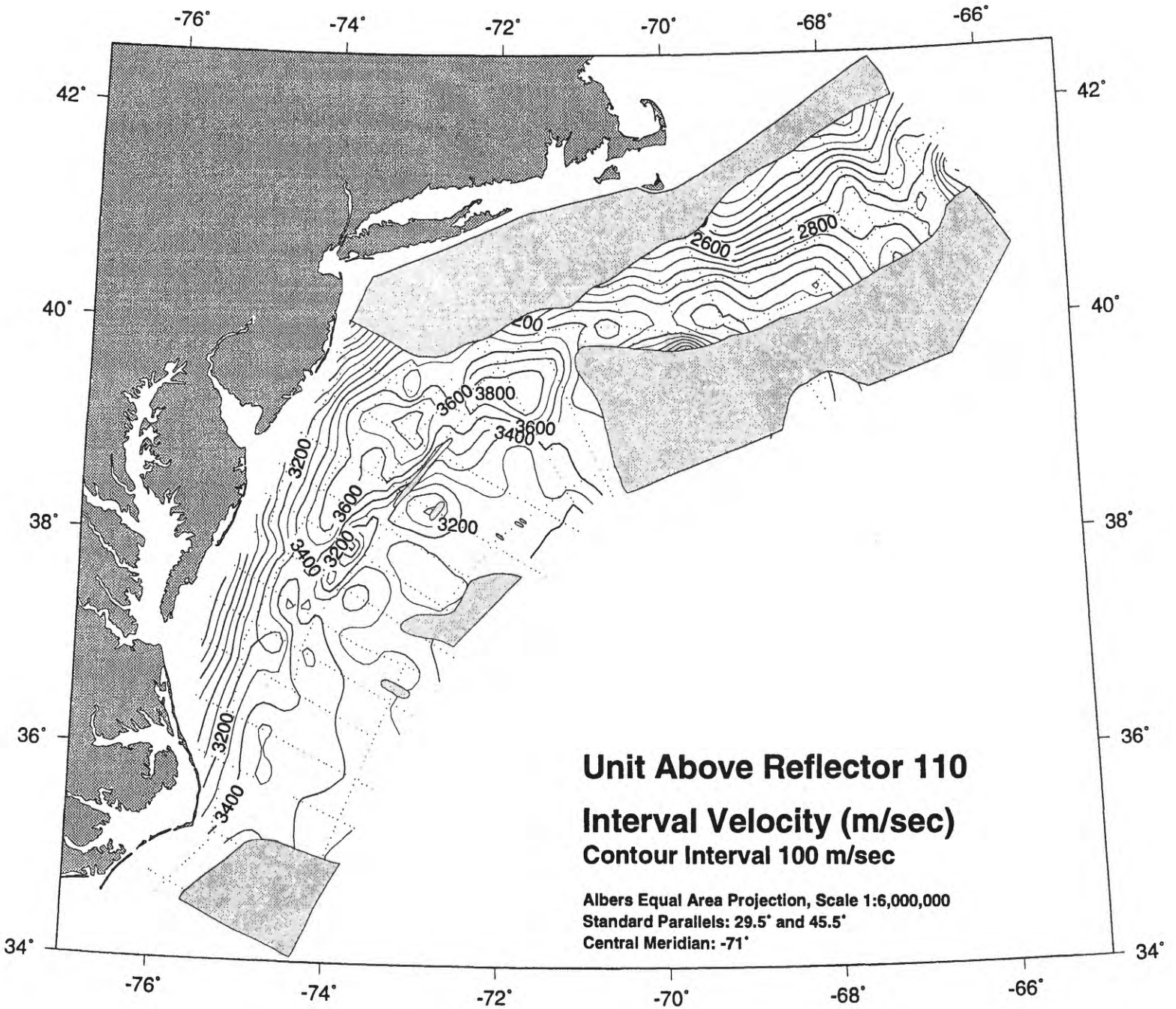
-76°
-74°
-72°
-70°
-68°
-66°
42°
40°
38°
36°
34°
2600
2800
3600
3800
3400
3200
3400
Unit Above Reflector 110
Interval Velocity (m/sec)
Contour Interval 100 m/sec
Albers Equal Area Projection, Scale 1:6,000,000
Standard Parallels: 29.5° and 45.5°
Central Meridian: -71°

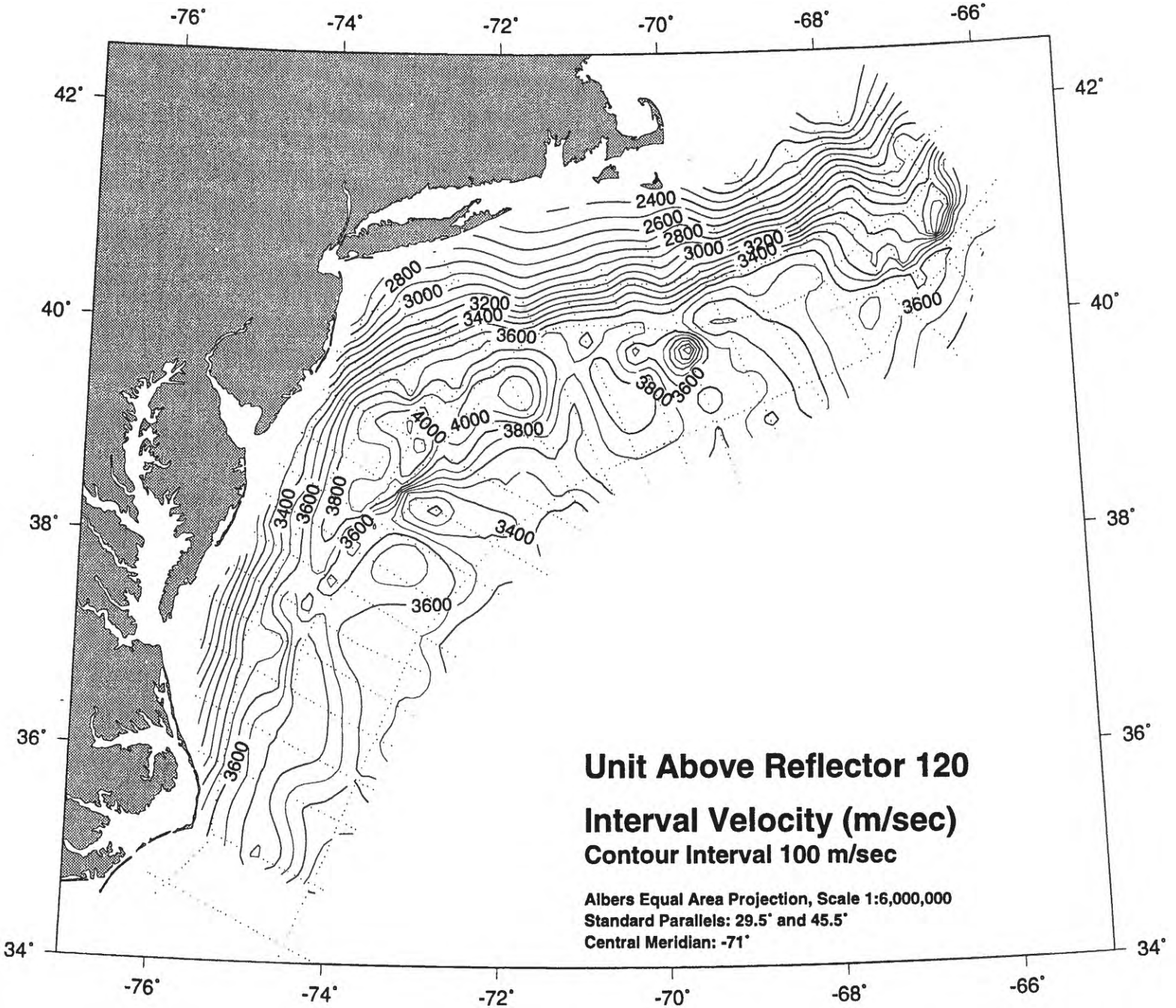
-76°
-74°
-72°
-70°
-68°
-66°
42°
40°
38°
36°
34°
2400
2600
2800
3000
3200
3400
3600
3800
4000
Unit Above Reflector 120
Interval Velocity (m/sec)
Contour Interval 100 m/sec
Albers Equal Area Projection, Scale 1:6,000,000
Standard Parallels: 29.5° and 45.5°
Central Meridian: -71°

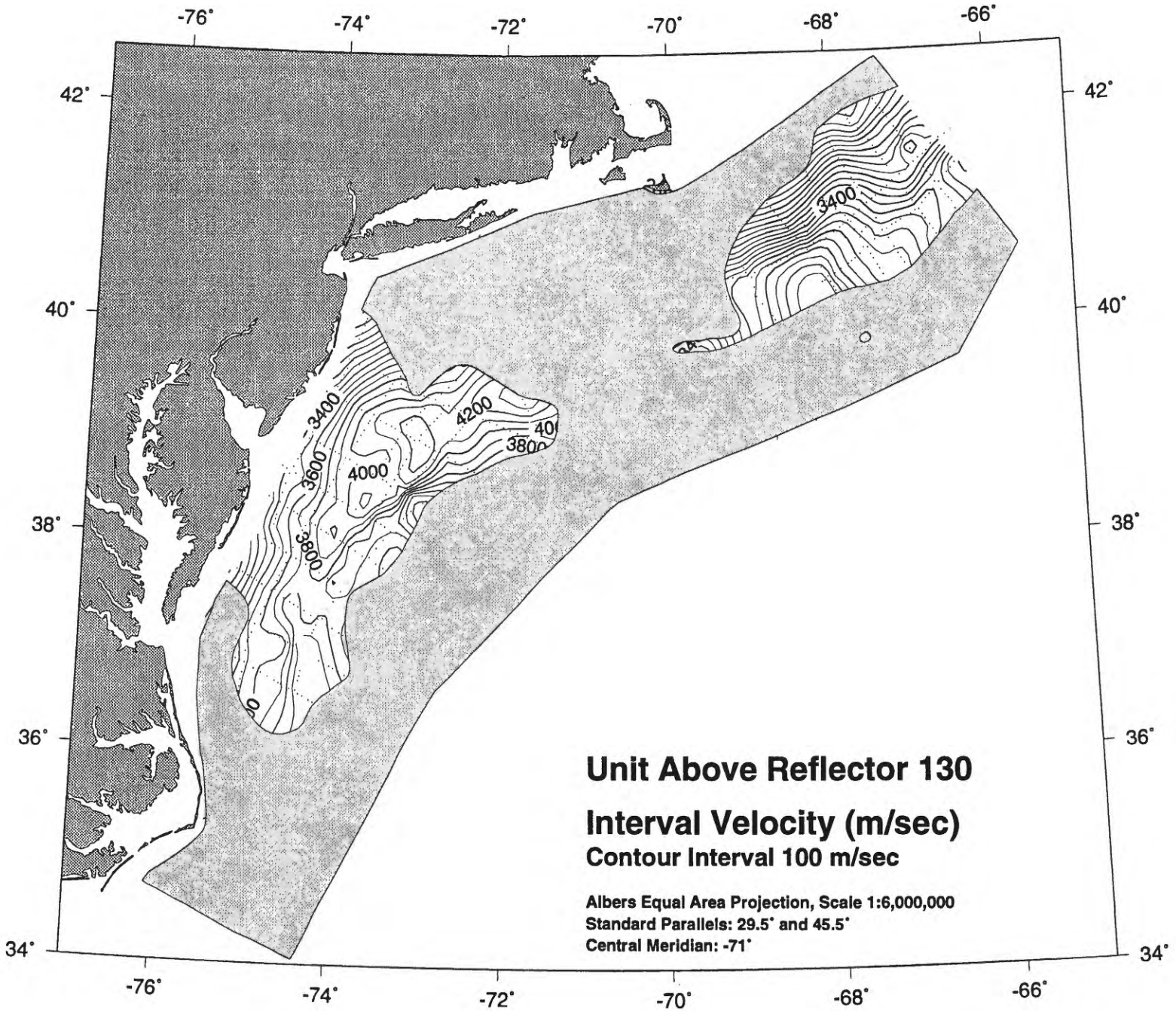
-76°
-74°
-72°
-70°
-68°
-66°
42°
40°
38°
36°
34°
3400
4200
4000
3600
3800
3400
Unit Above Reflector 130
Interval Velocity (m/sec)
Contour Interval 100 m/sec
Albers Equal Area Projection, Scale 1:6,000,000
Standard Parallels: 29.5° and 45.5°
Central Meridian: -71°

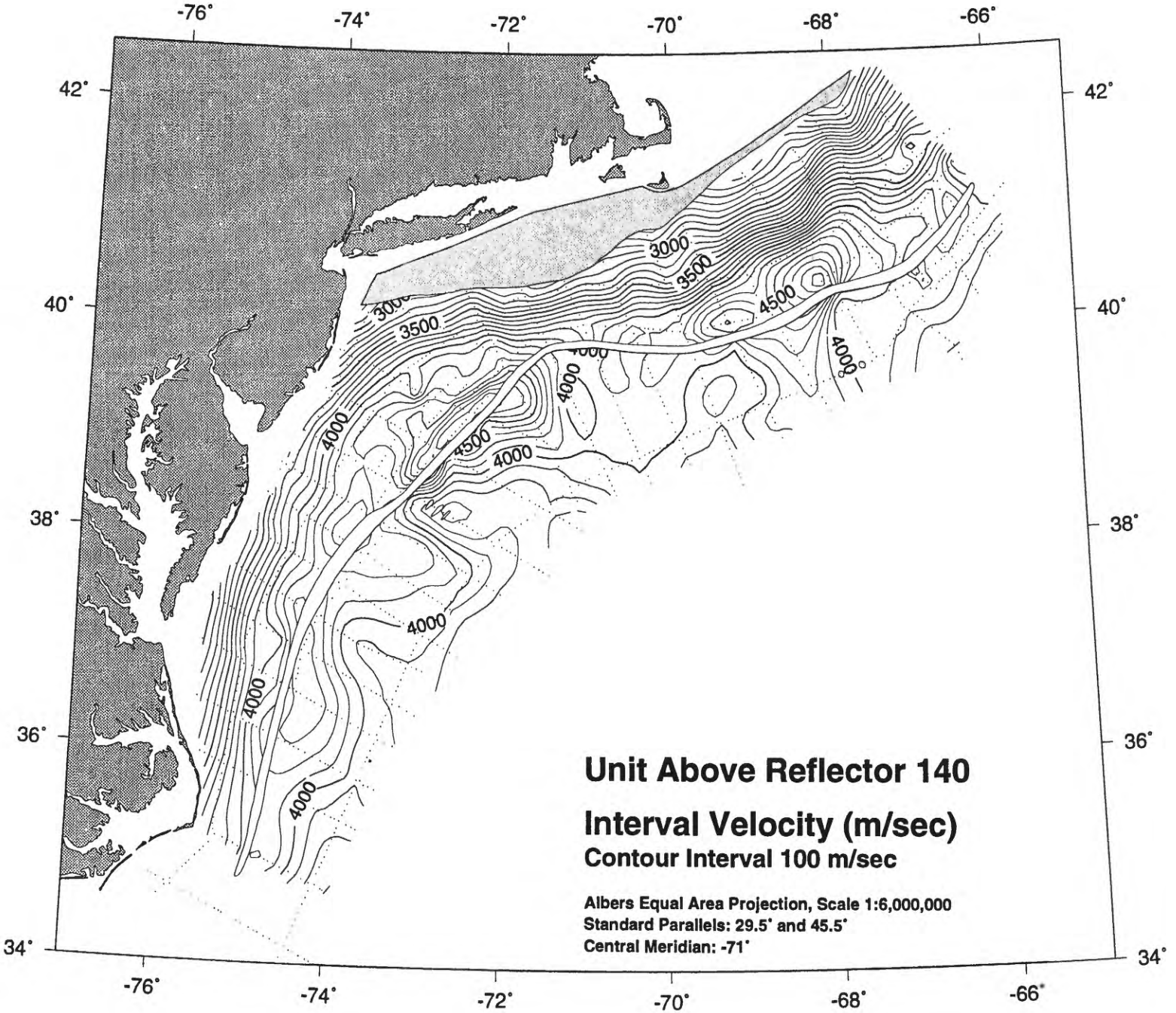
-76°
-74°
-72°
-70°
-68°
-66°
42°
40°
38°
36°
34°
3000
3500
4000
4500
Unit Above Reflector 140
Interval Velocity (m/sec)
Contour Interval 100 m/sec
Albers Equal Area Projection, Scale 1:6,000,000
Standard Parallels: 29.5° and 45.5°
Central Meridian: -71°

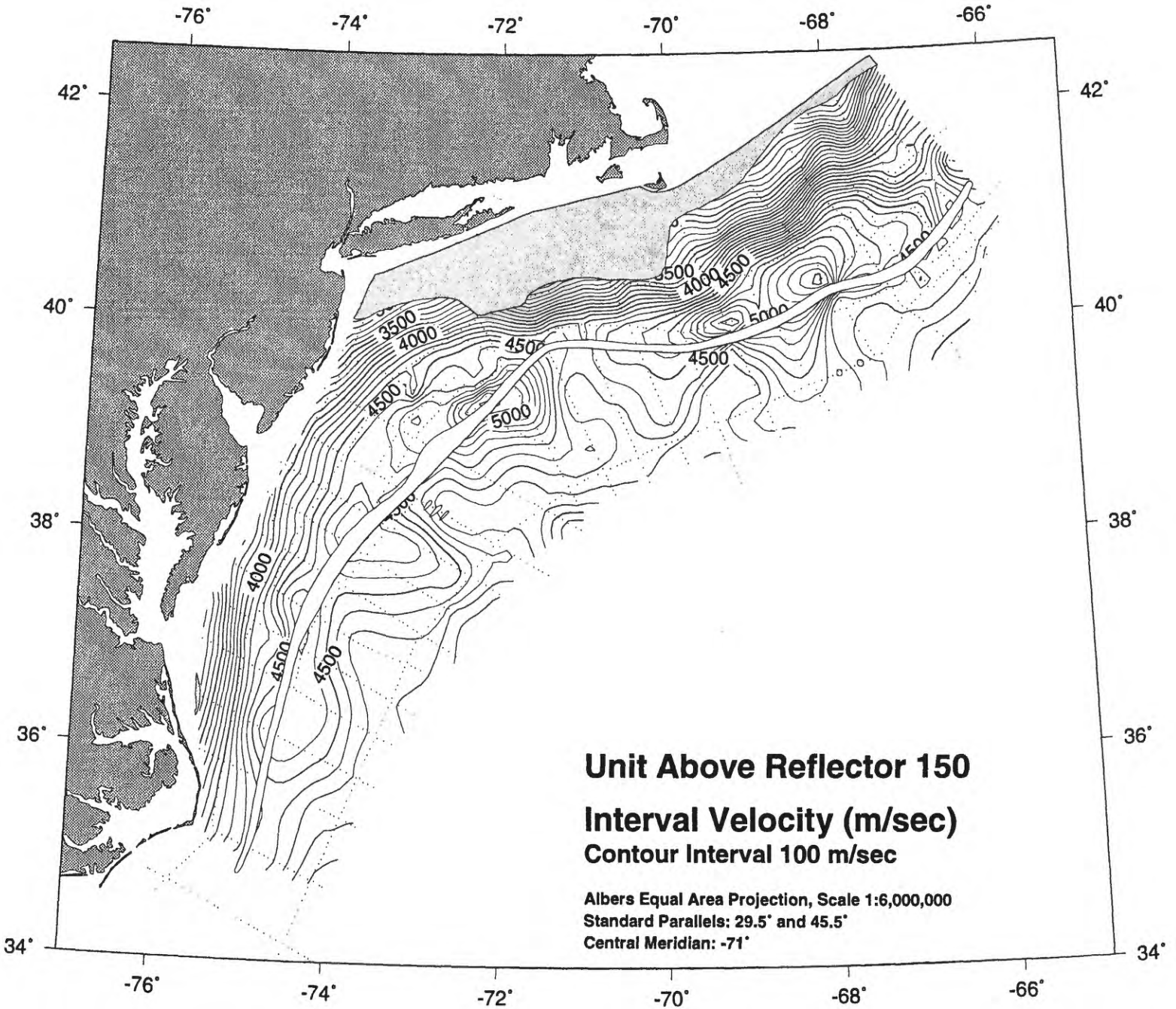
-76°
-74°
-72°
-70°
-68°
-66°
42°
40°
38°
36°
34°
3500
4000
4500
5000
Unit Above Reflector 150
Interval Velocity (m/sec)
Contour Interval 100 m/sec
Albers Equal Area Projection, Scale 1:6,000,000
Standard Parallels: 29.5° and 45.5°
Central Meridian: -71°

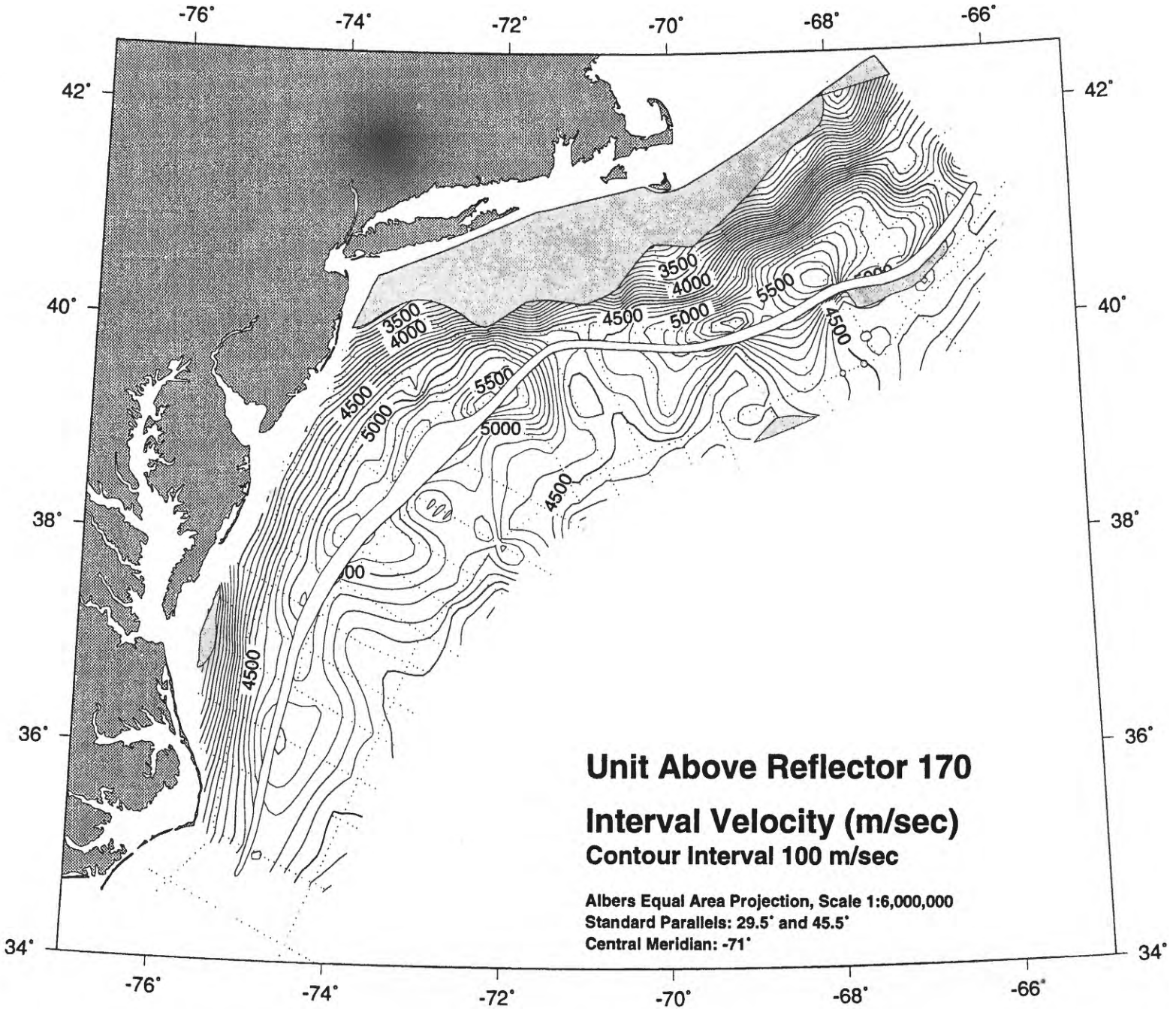
-76°
-74°
-72°
-70°
-68°
-66°
42°
40°
38°
36°
34°
3500
4000
4500
5000
5500
Unit Above Reflector 170
Interval Velocity (m/sec)
Contour Interval 100 m/sec
Albers Equal Area Projection, Scale 1:6,000,000
Standard Parallels: 29.5° and 45.5°
Central Meridian: -71°

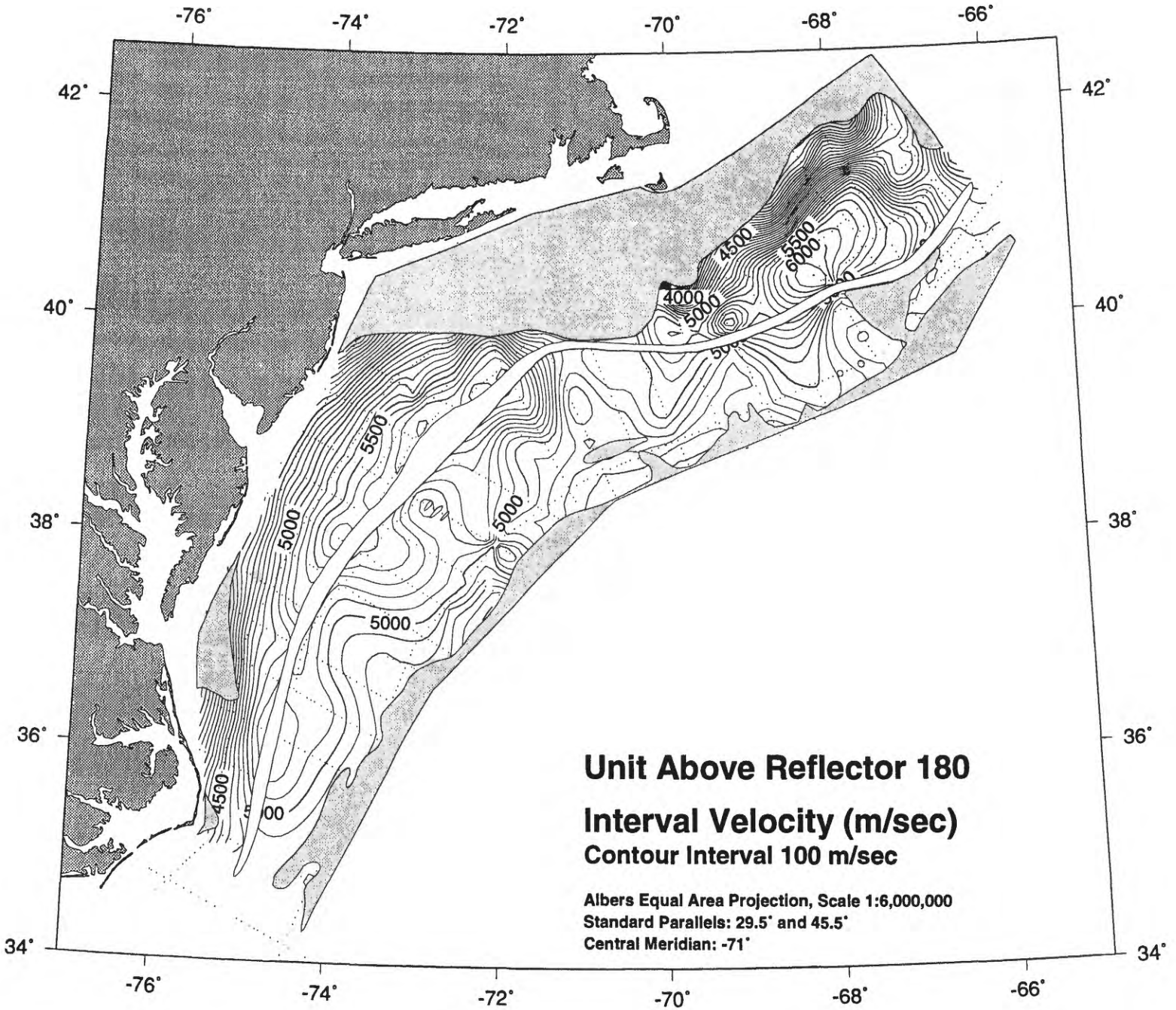
-76°
-74°
-72°
-70°
-68°
-66°
42°
40°
38°
36°
34°
4500
5000
5500
6000
4000
Unit Above Reflector 180
Interval Velocity (m/sec)
Contour Interval 100 m/sec
Albers Equal Area Projection, Scale 1:6,000,000
Standard Parallels: 29.5° and 45.5°
Central Meridian: -71°

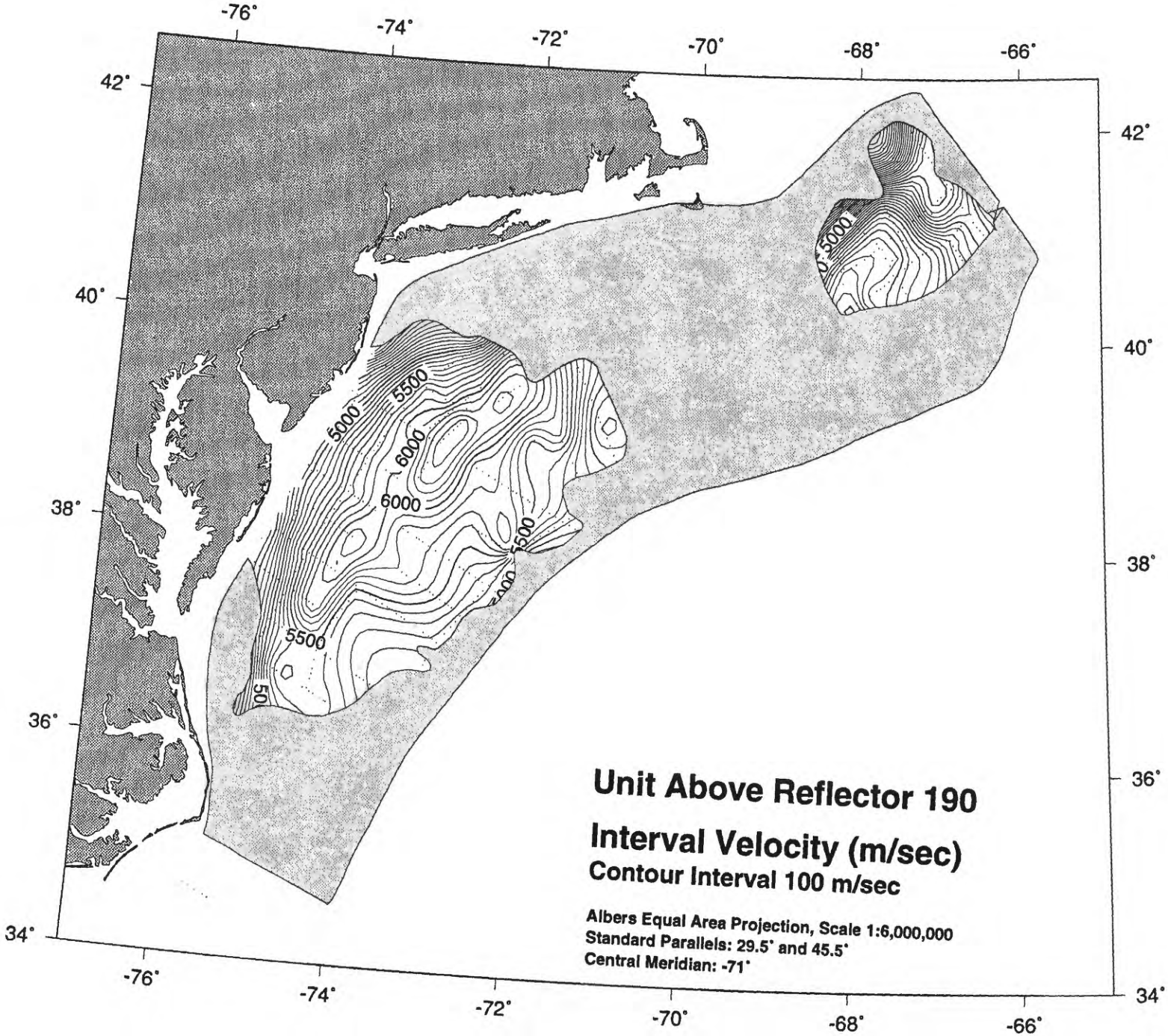
-76°
-74°
-72°
-70°
-68°
-66°
42°
40°
38°
36°
34°
5000
5500
6000
6000
5500
5000
5500
5000
Unit Above Reflector 190
Interval Velocity (m/sec)
Contour Interval 100 m/sec
Albers Equal Area Projection, Scale 1:6,000,000
Standard Parallels: 29.5° and 45.5°
Central Meridian: -71°

Appendix 8

Sediment-Type Distribution Within Acoustic Units in Digital Database

Distribution of sediment types within each acoustic unit in this geoacoustic database. See Figure 7 for the seismic lines used to construct this map. Shaded masks indicate the regions where a particular surface has been eroded into by an overlying surface. Narrow blank zones in the shelf edge region are where deeper units are obscured by the Jurassic carbonate bank.

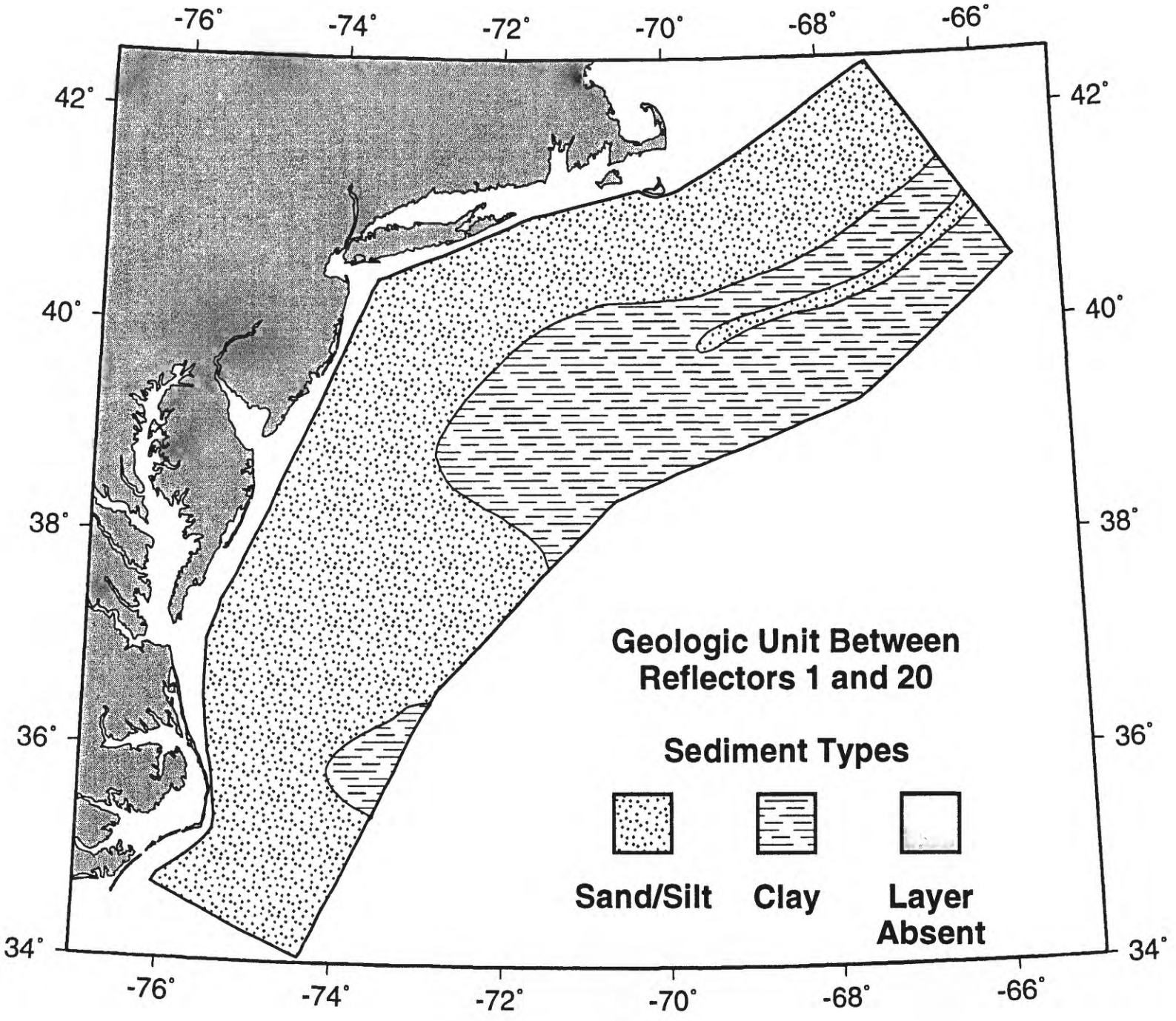
-76°
-74°
-72°
-70°
-68°
-66°
42°
40°
38°
36°
34°
Geologic Unit Between
Reflectors 1 and 20
Sediment Types
Sand/Silt
Clay
Layer
Absent

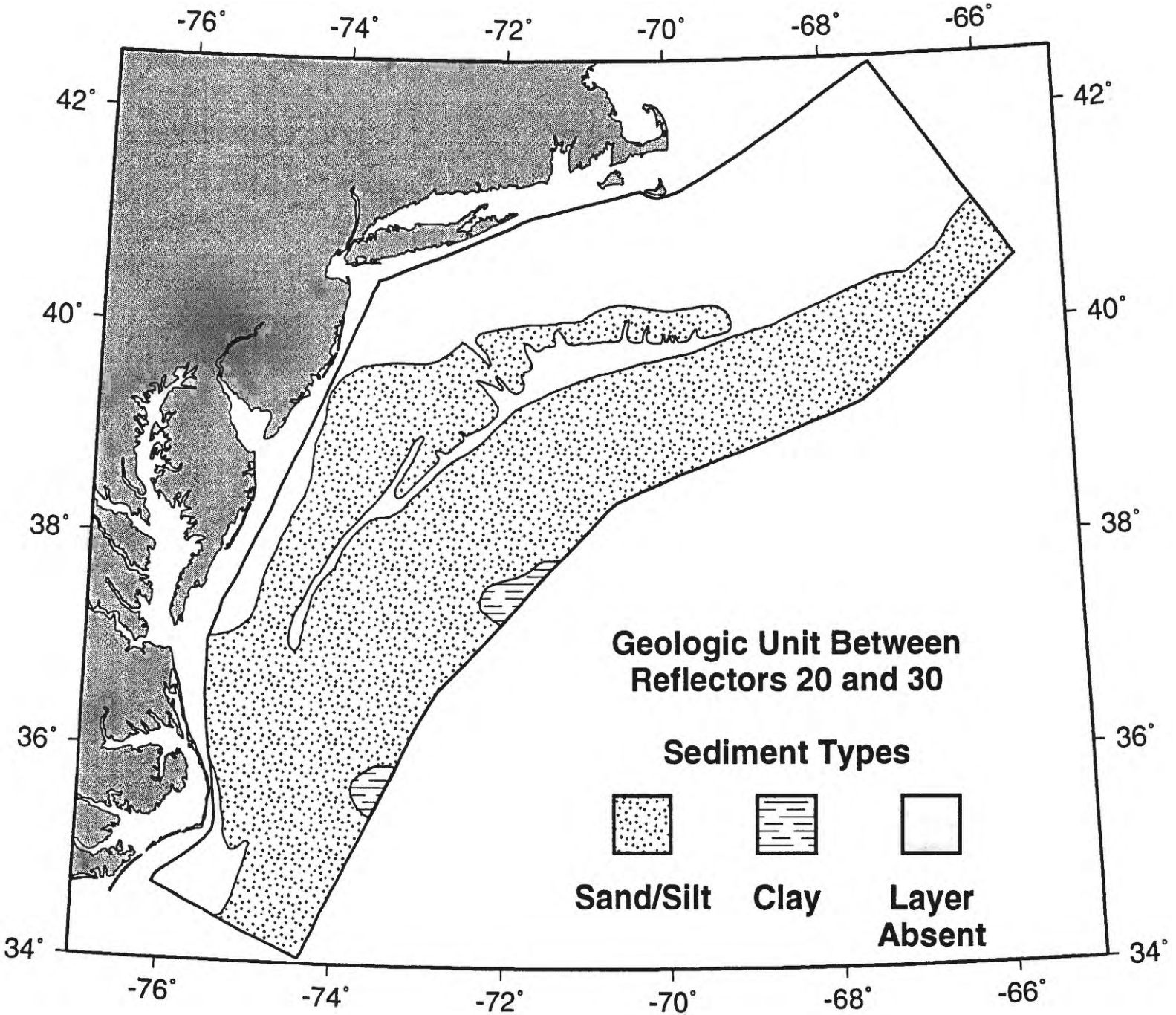
-76°
-74°
-72°
-70°
-68°
-66°
42°
40°
38°
36°
34°
Geologic Unit Between
Reflectors 20 and 30
Sediment Types
Sand/Silt
Clay
Layer
Absent

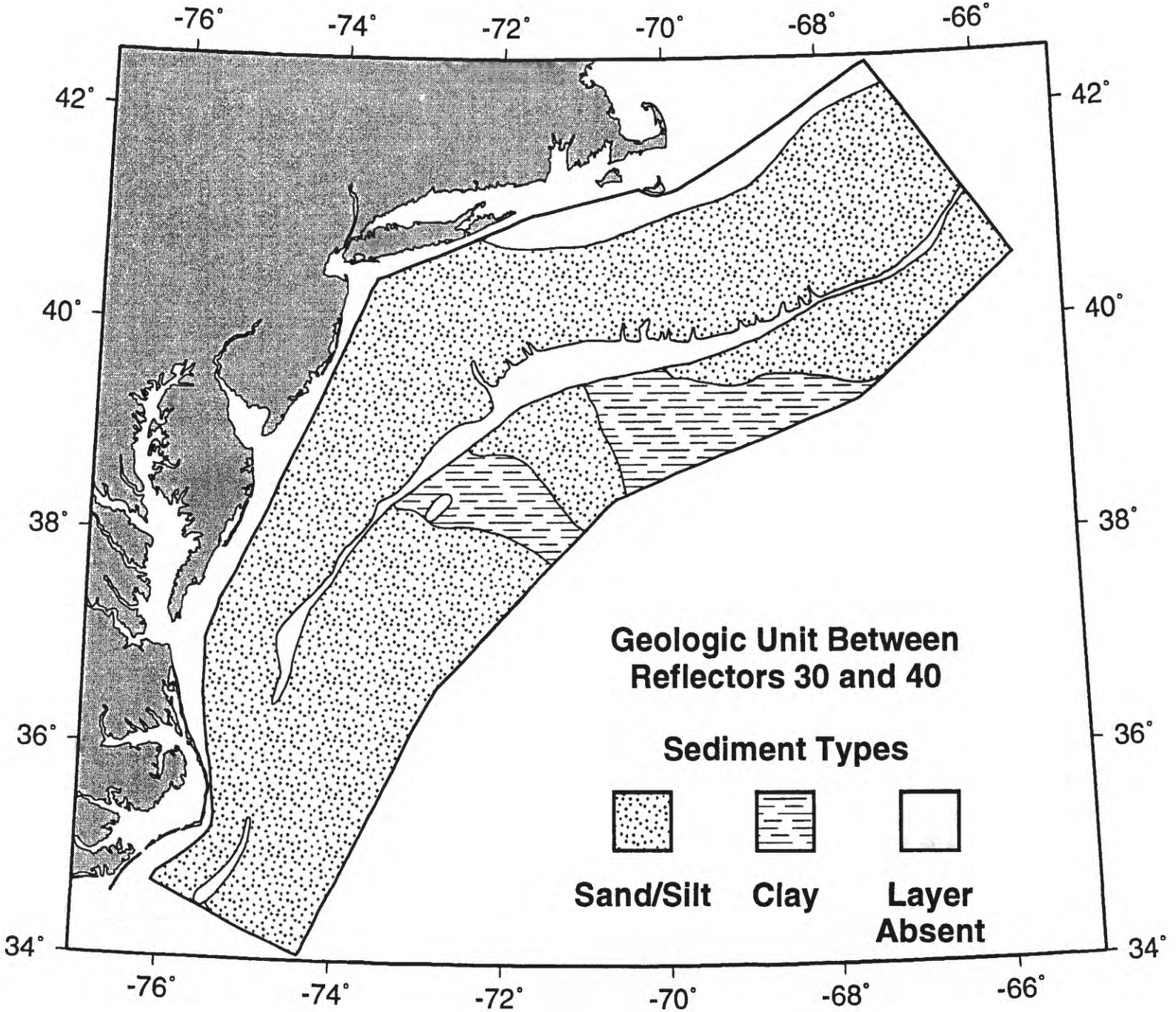
-76°
-74°
-72°
-70°
-68°
-66°
42°
40°
38°
36°
34°
Geologic Unit Between
Reflectors 30 and 40
Sediment Types
Sand/Silt
Clay
Layer
Absent

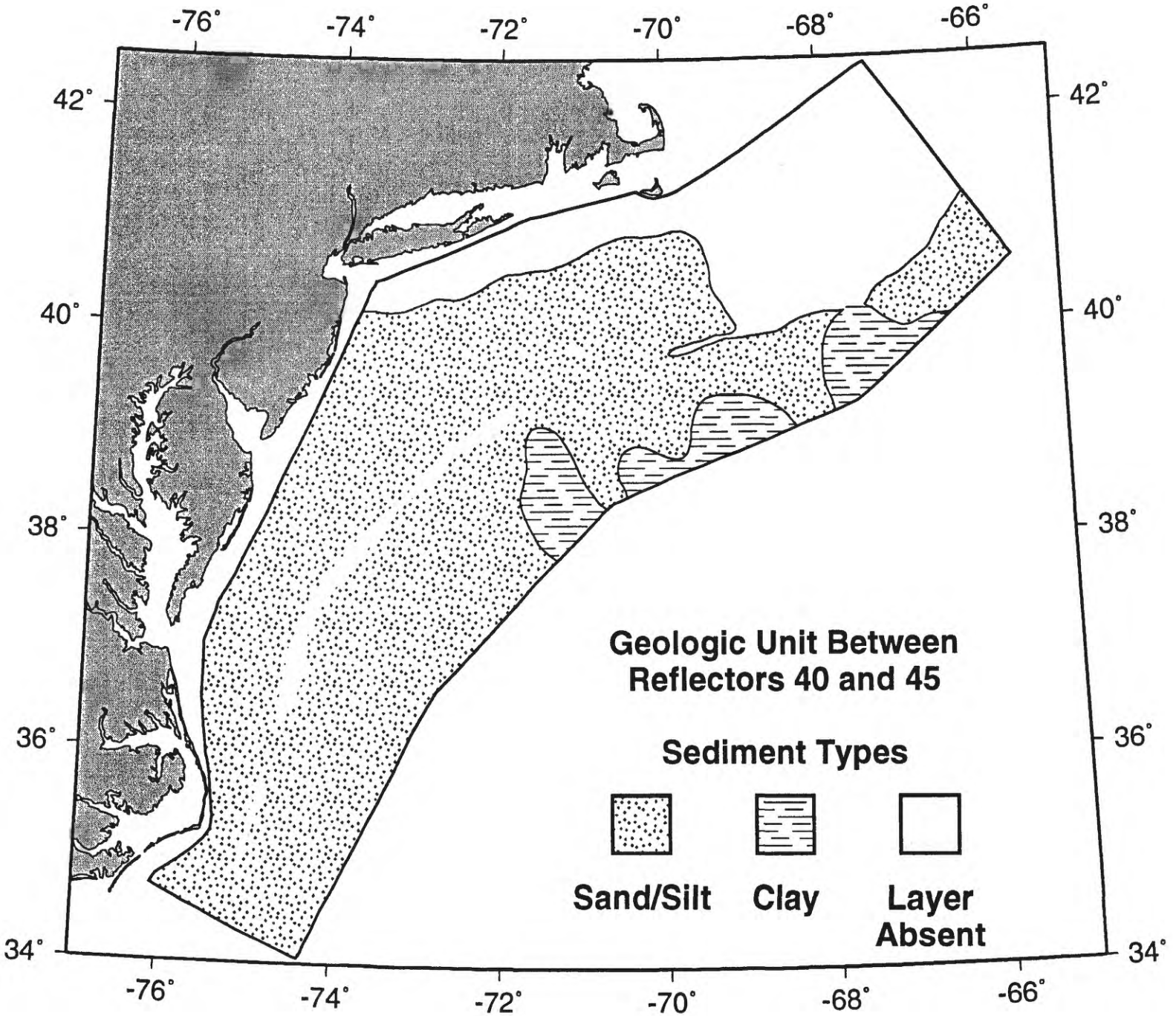
-76°
-74°
-72°
-70°
-68°
-66°
42°
40°
38°
36°
34°
Geologic Unit Between
Reflectors 40 and 45
Sediment Types
Sand/Silt
Clay
Layer
Absent

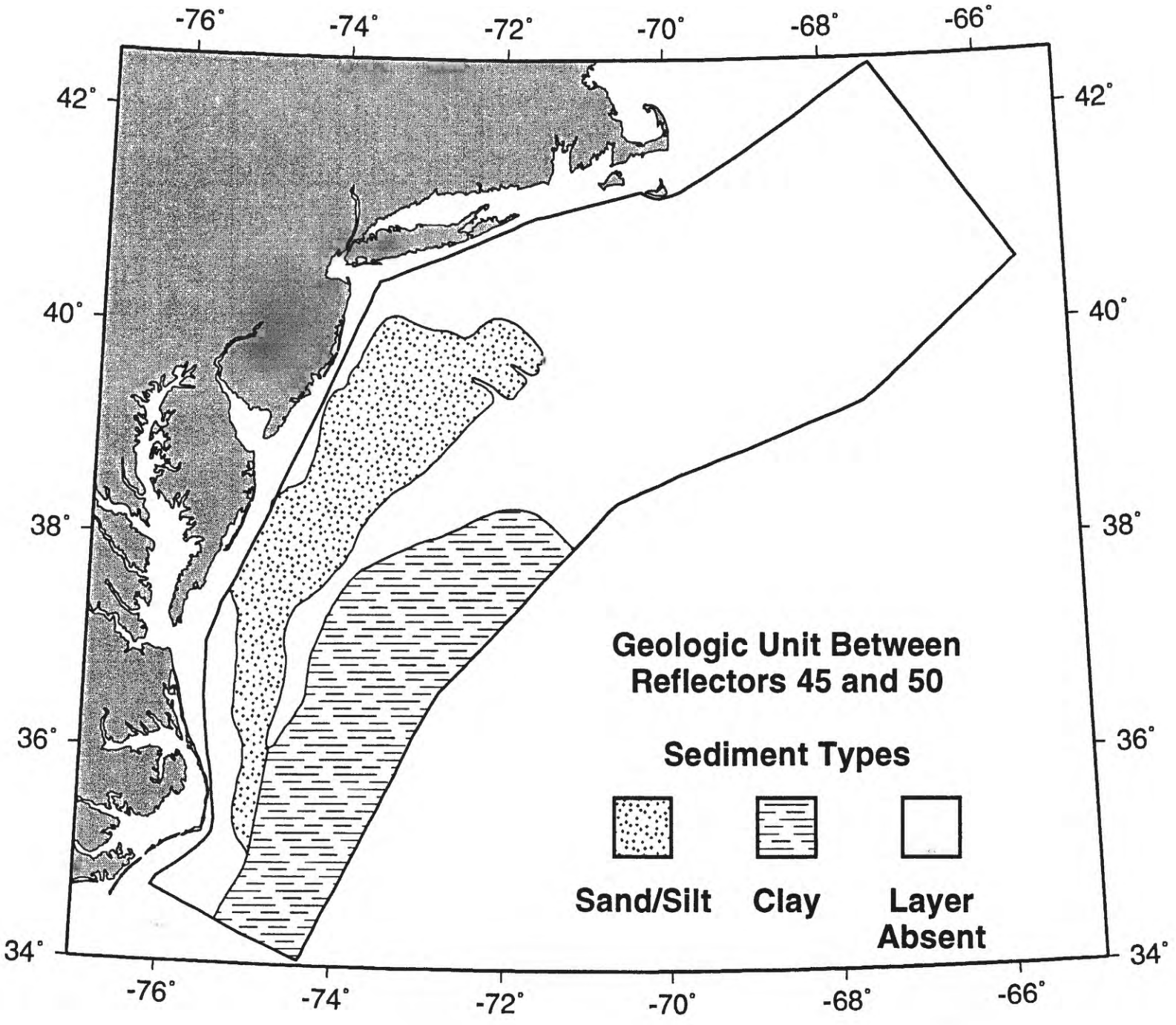
-76°
-74°
-72°
-70°
-68°
-66°
42°
40°
38°
36°
34°
Geologic Unit Between
Reflectors 45 and 50
Sediment Types
Sand/Silt
Clay
Layer
Absent

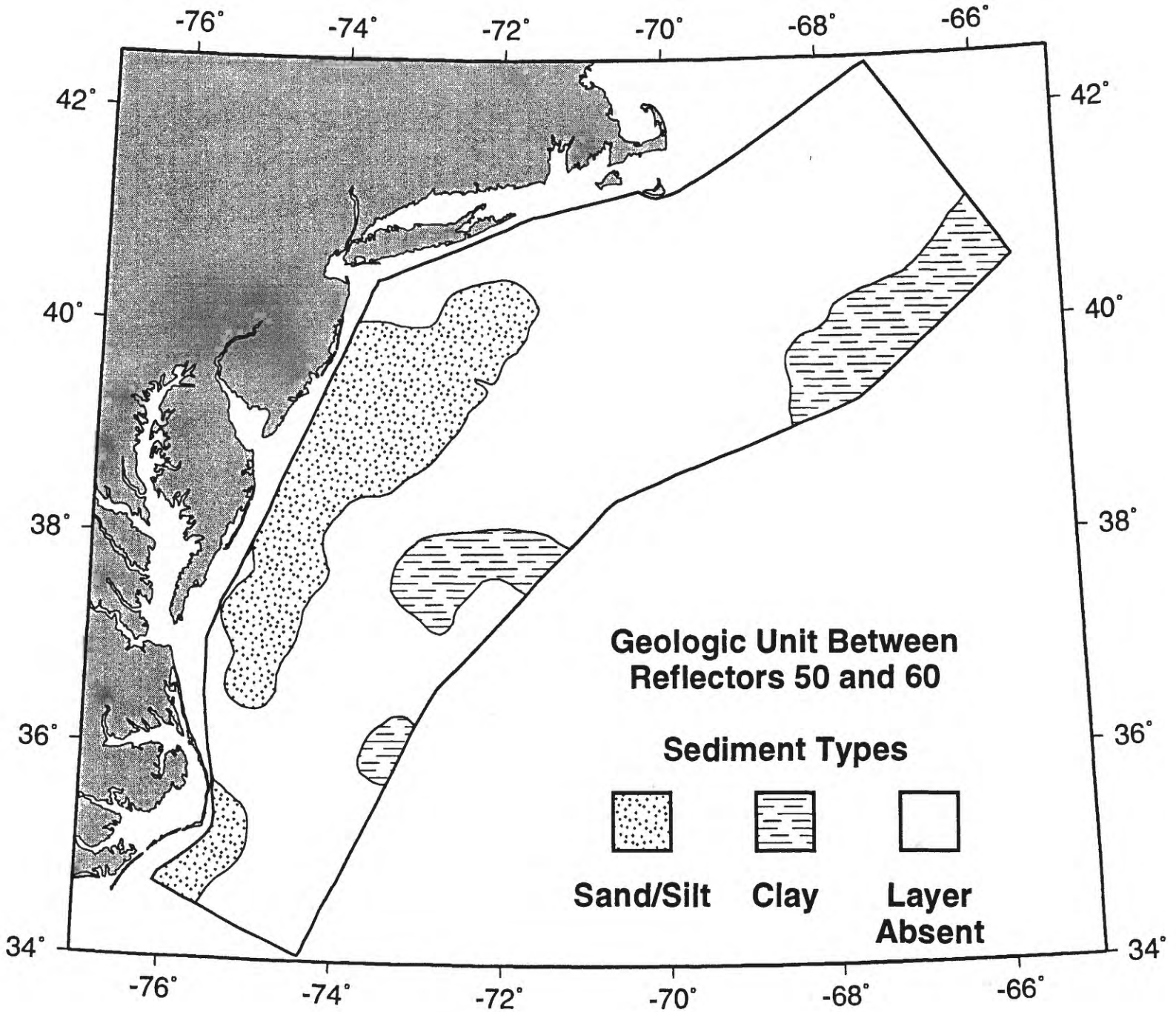
-76°
-74°
-72°
-70°
-68°
-66°
42°
40°
38°
36°
34°
Geologic Unit Between
Reflectors 50 and 60
Sediment Types
Sand/Silt
Clay
Layer
Absent

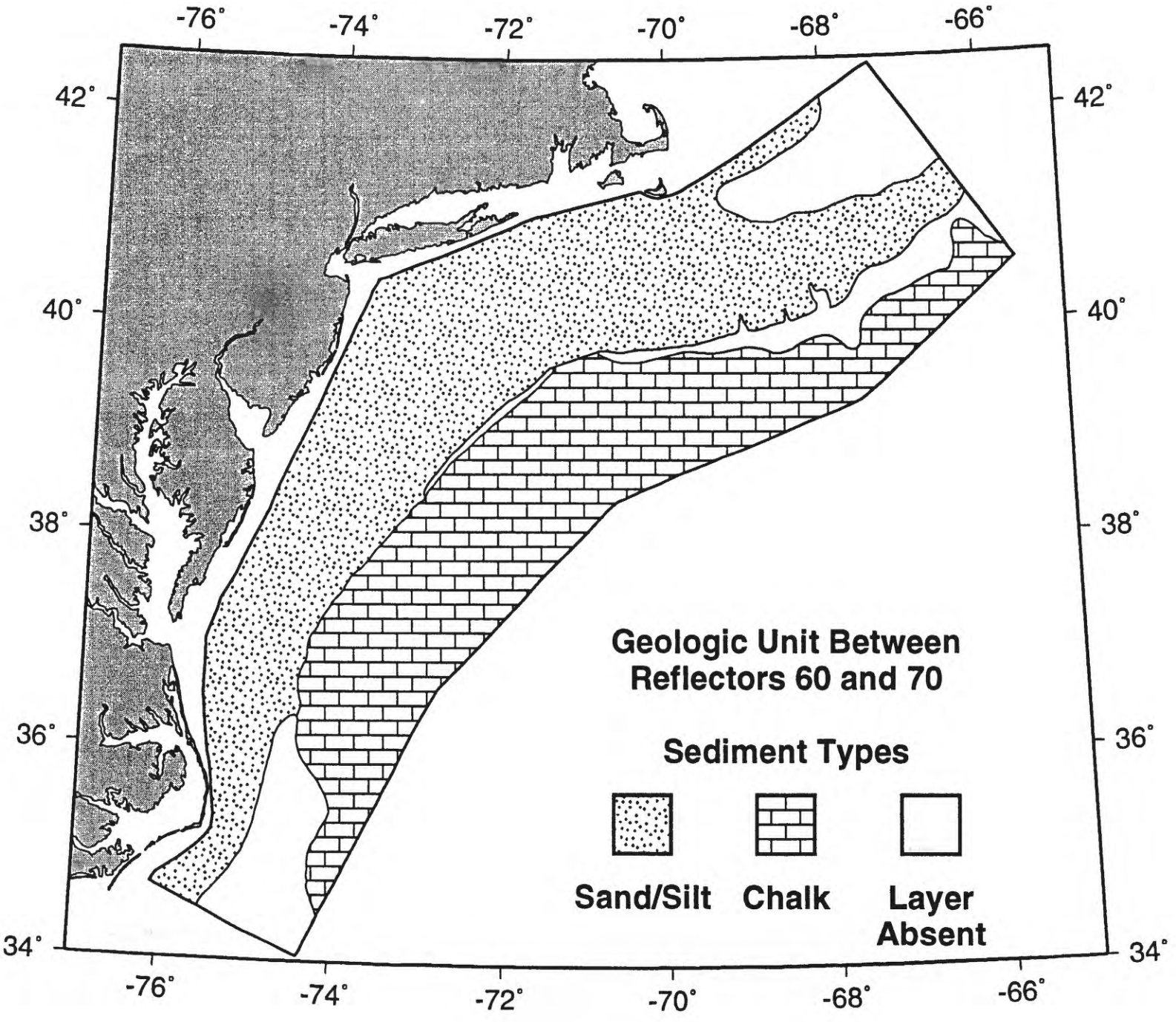
-76°
-74°
-72°
-70°
-68°
-66°
42°
40°
38°
36°
34°
Geologic Unit Between
Reflectors 60 and 70
Sediment Types
Sand/Silt
Chalk
Layer
Absent

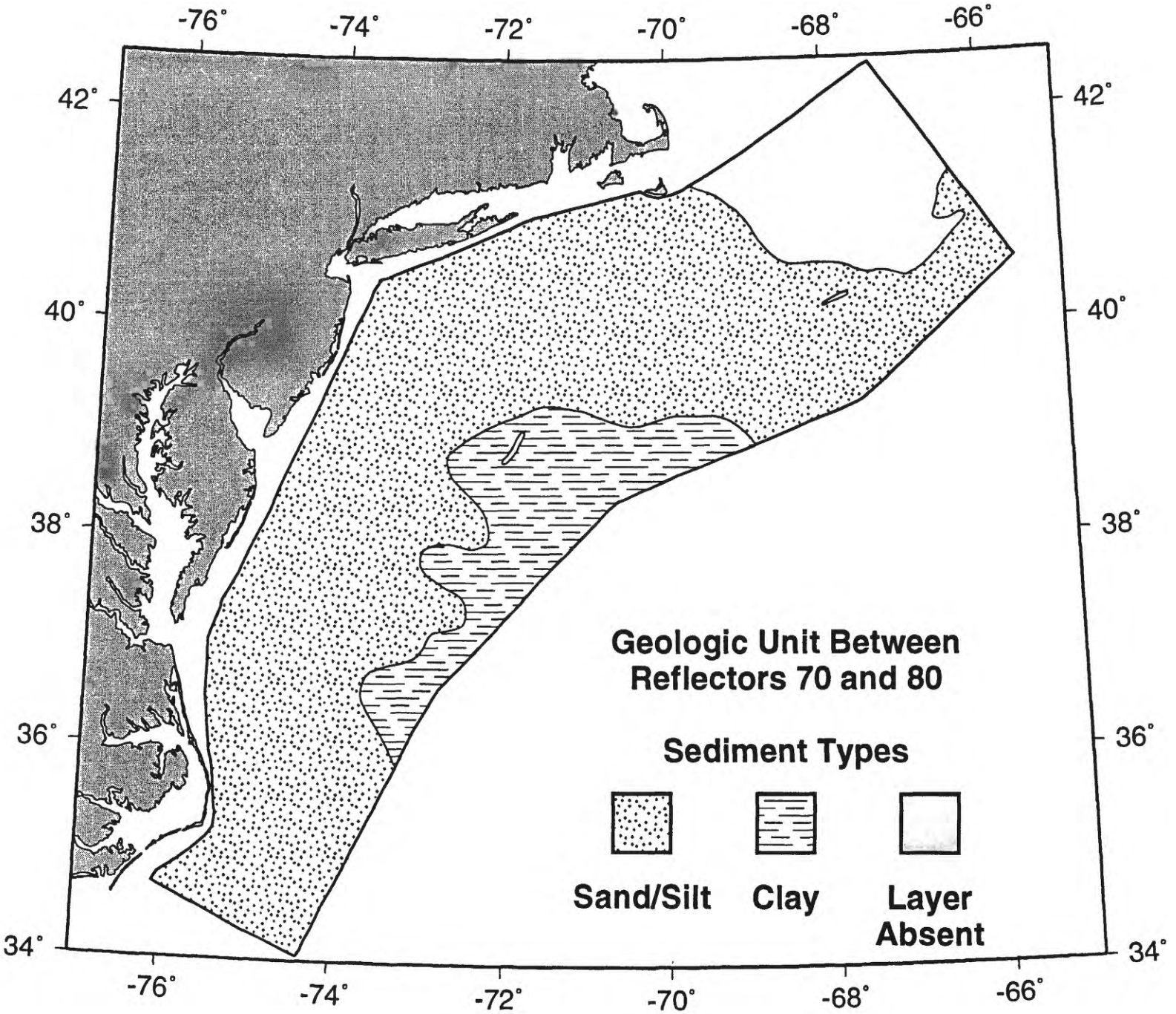
-76°
-74°
-72°
-70°
-68°
-66°
42°
40°
38°
36°
34°
Geologic Unit Between
Reflectors 70 and 80
Sediment Types
Sand/Silt
Clay
Layer
Absent

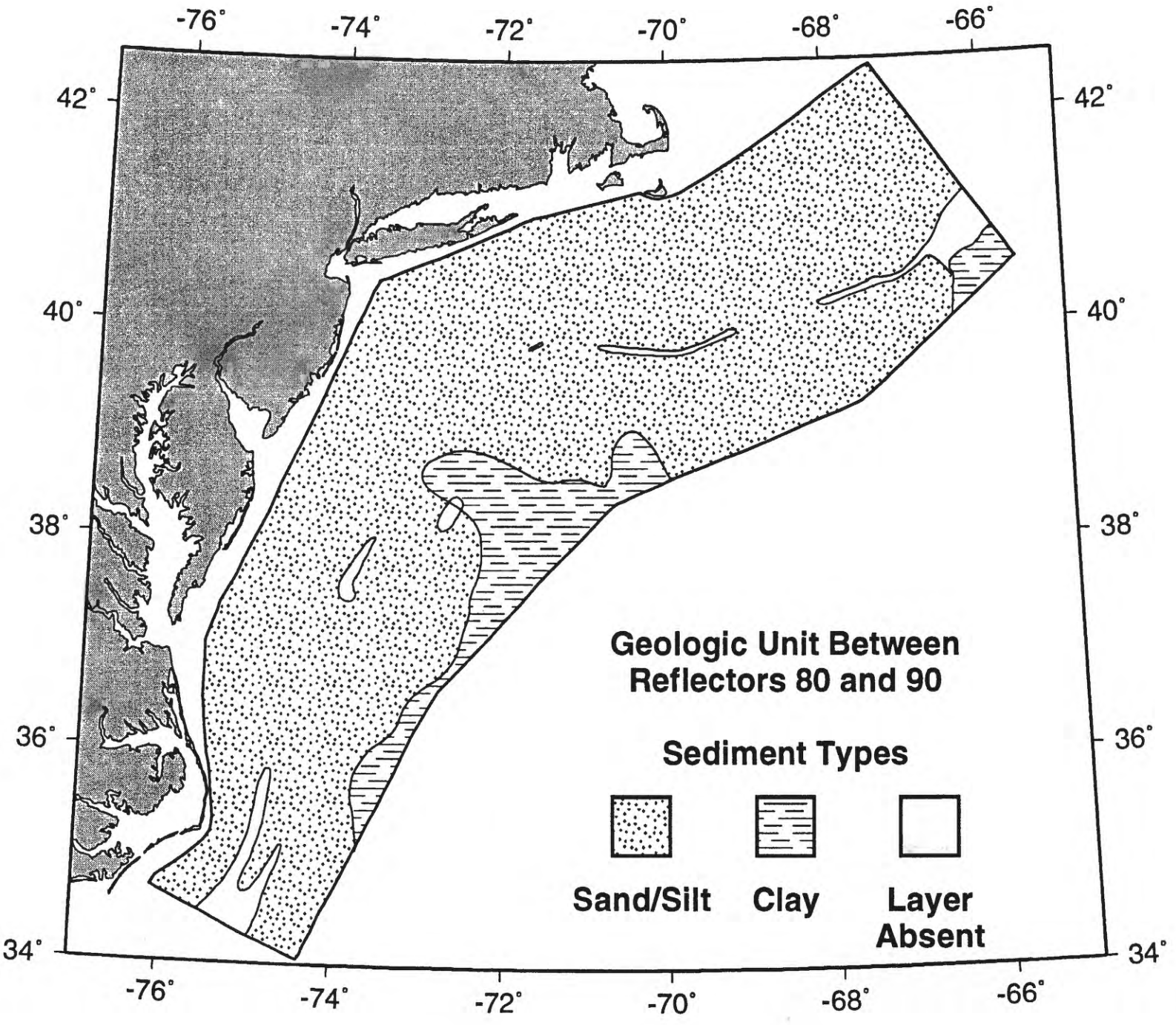
-76°
-74°
-72°
-70°
-68°
-66°
42°
40°
38°
36°
34°
Geologic Unit Between
Reflectors 80 and 90
Sediment Types
Sand/Silt
Clay
Layer
Absent

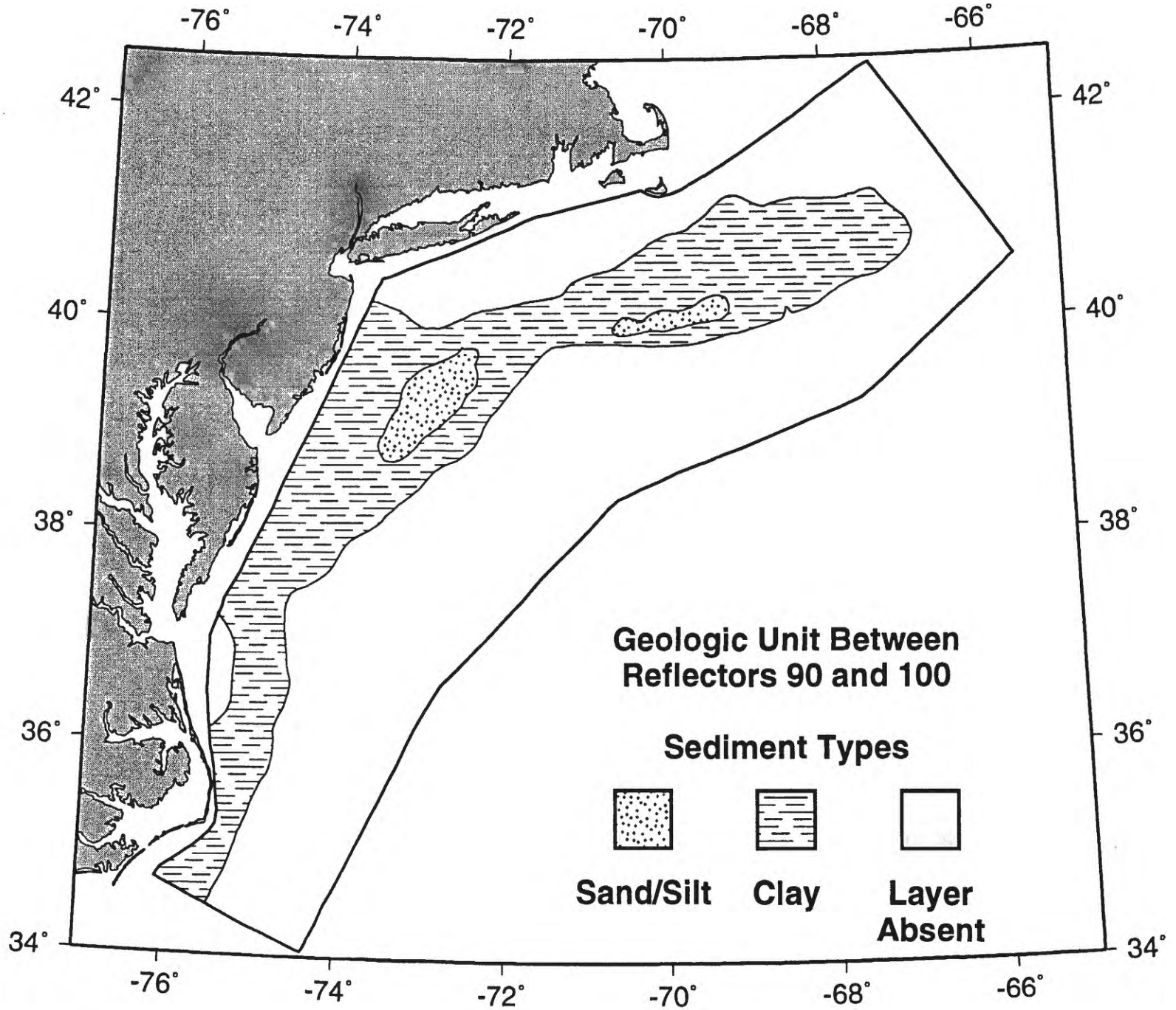
-76°
-74°
-72°
-70°
-68°
-66°
42°
40°
38°
36°
34°
Geologic Unit Between
Reflectors 90 and 100
Sediment Types
Sand/Silt
Clay
Layer
Absent

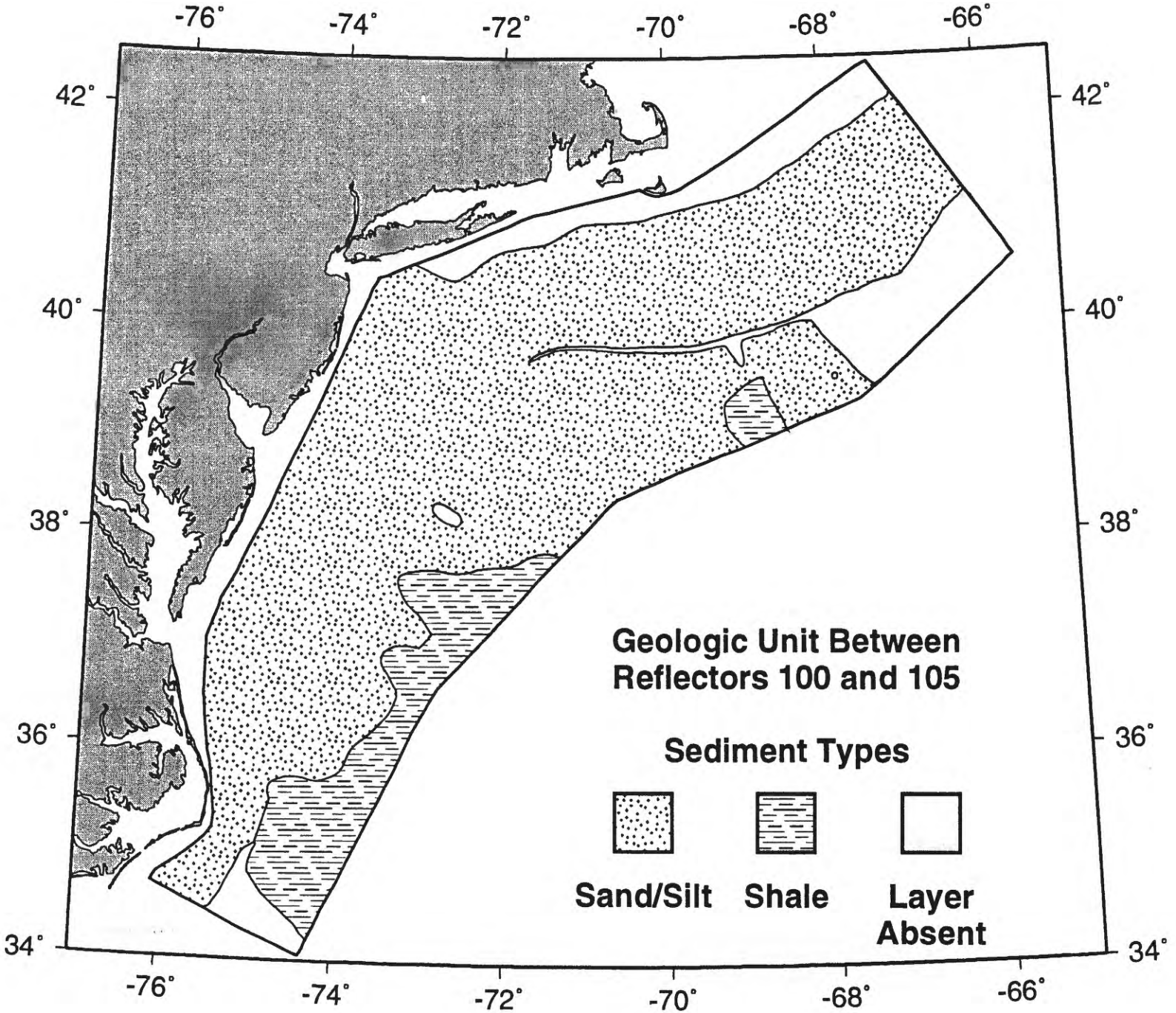
-76°
-74°
-72°
-70°
-68°
-66°
42°
40°
38°
36°
34°
Geologic Unit Between
Reflectors 100 and 105
Sediment Types
Sand/Silt
Shale
Layer
Absent

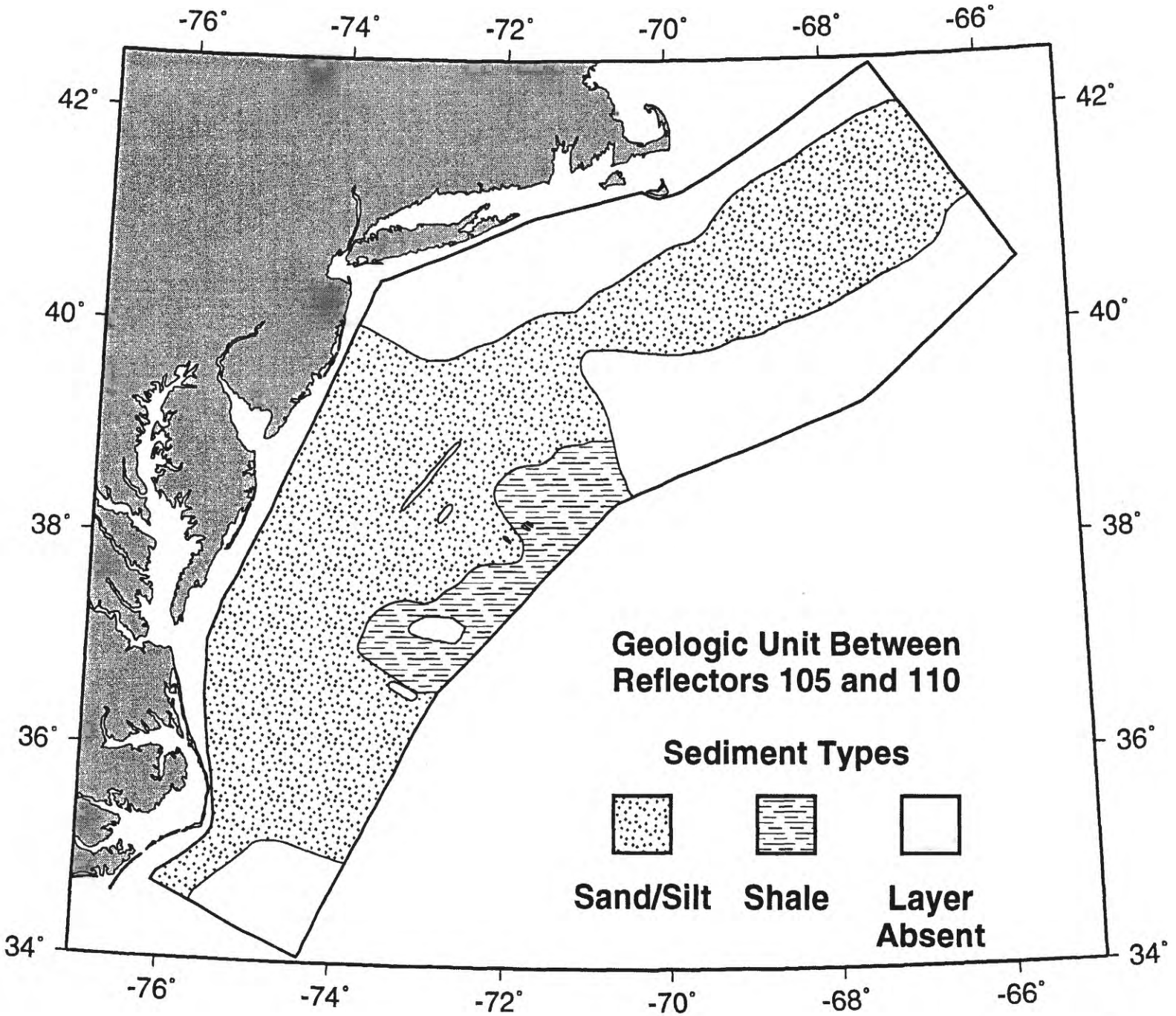
-76°
-74°
-72°
-70°
-68°
-66°
42°
40°
38°
36°
34°
Geologic Unit Between
Reflectors 105 and 110
Sediment Types
Sand/Silt
Shale
Layer
Absent

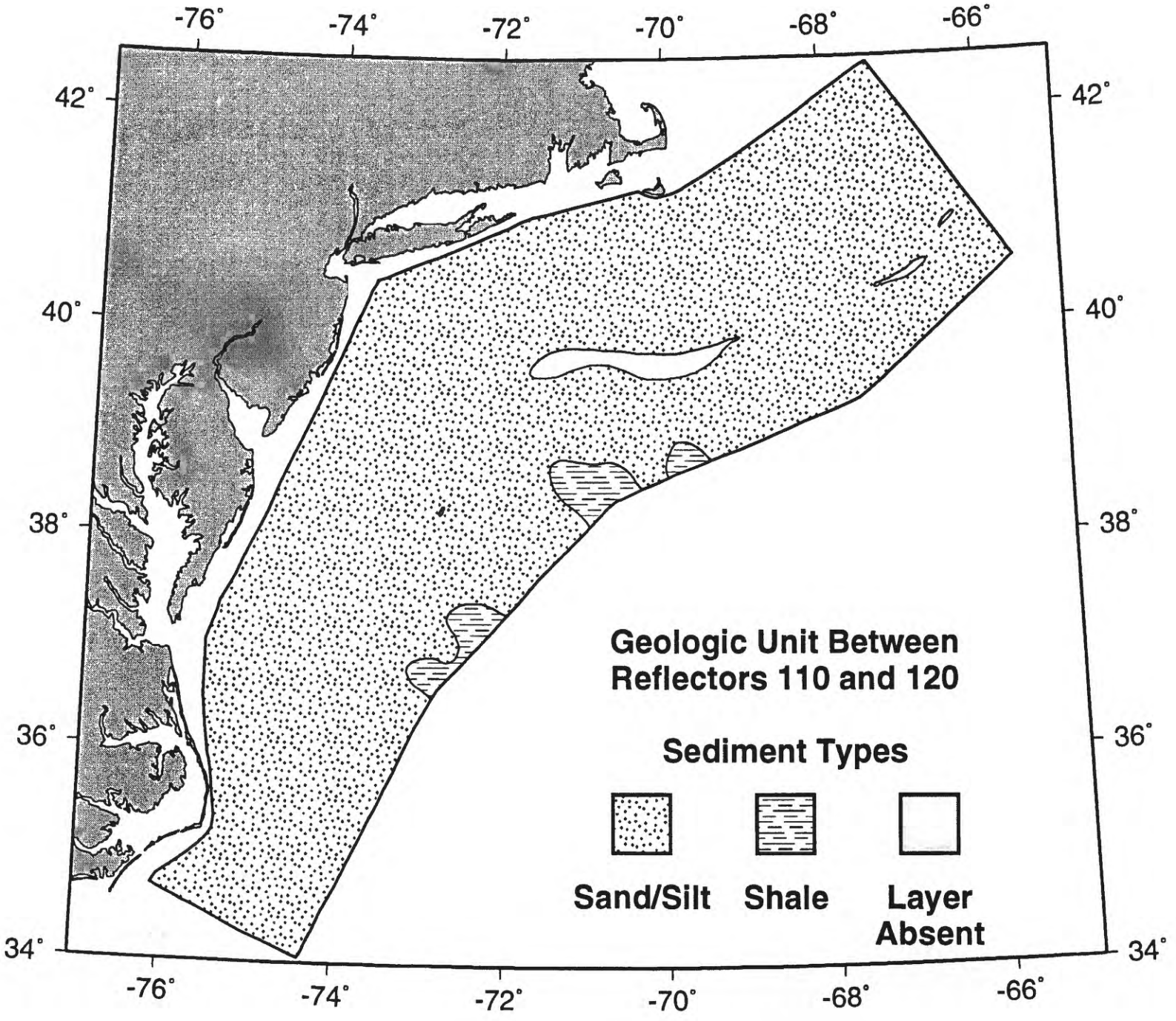
-76°
-74°
-72°
-70°
-68°
-66°
42°
40°
38°
36°
34°
Geologic Unit Between
Reflectors 110 and 120
Sediment Types
Sand/Silt
Shale
Layer
Absent

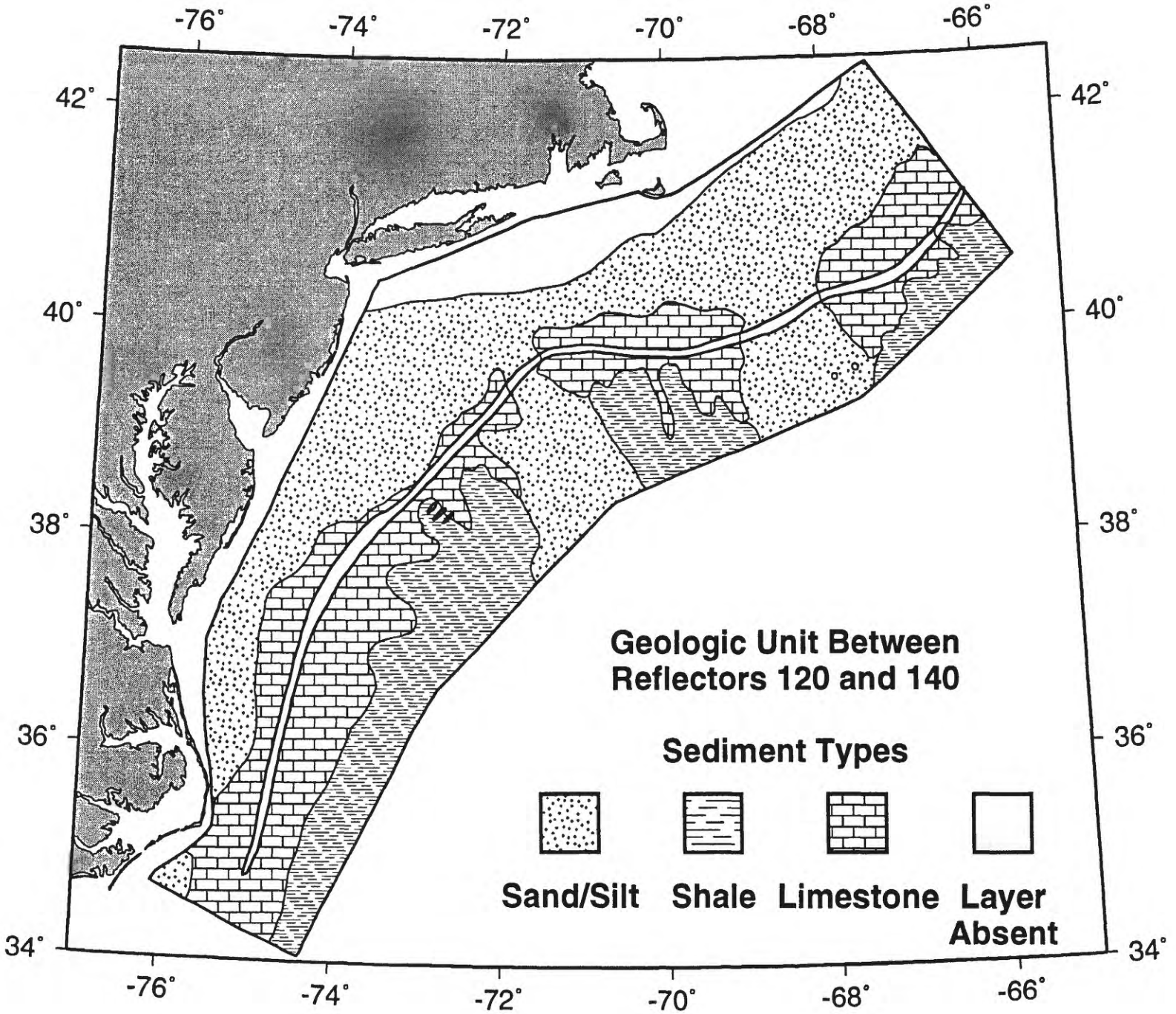
-76°
-74°
-72°
-70°
-68°
-66°
42°
40°
38°
36°
34°
Geologic Unit Between
Reflectors 120 and 140
Sediment Types
Sand/Silt
Shale
Limestone
Layer
Absent

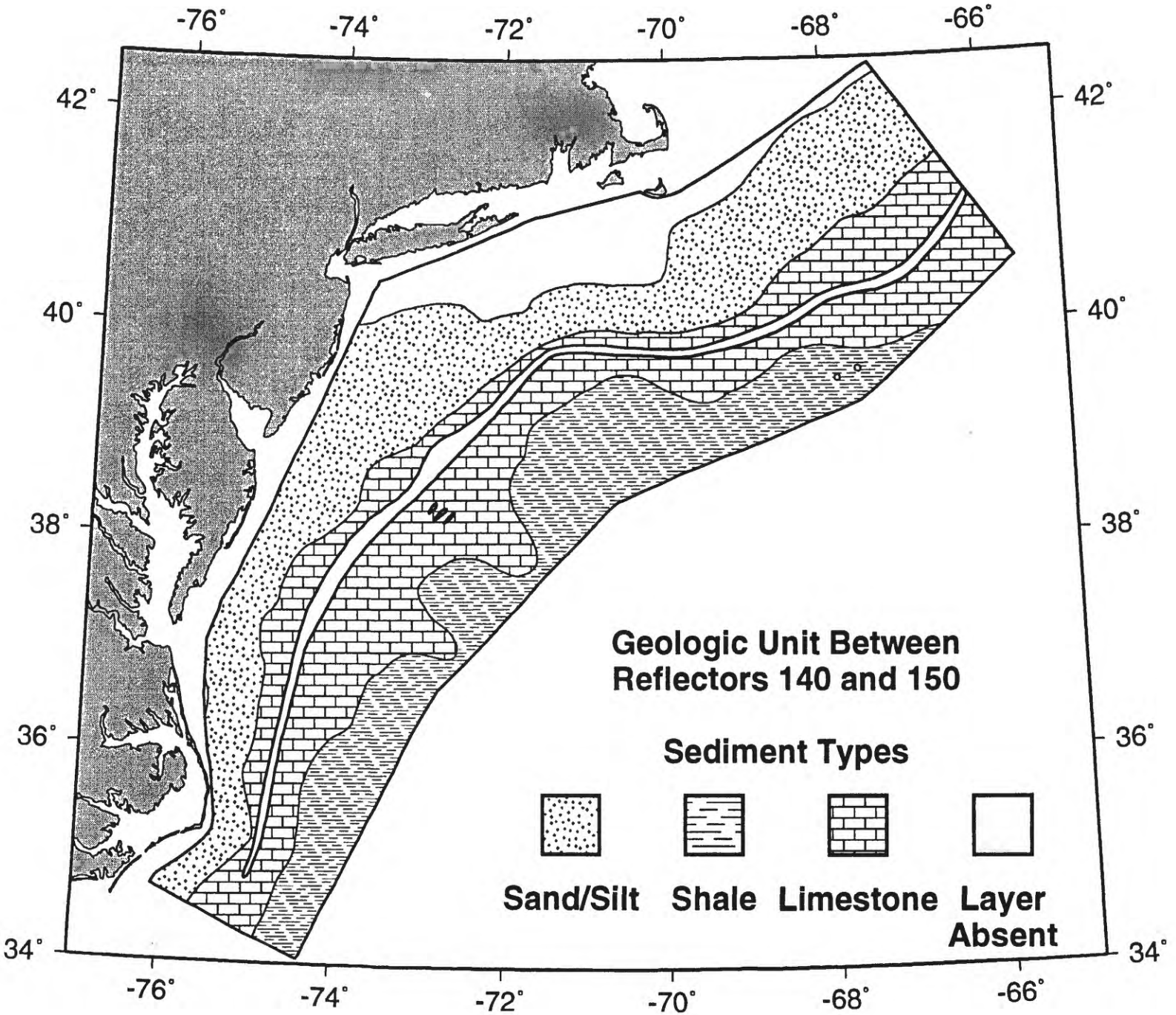
-76°
-74°
-72°
-70°
-68°
-66°
42°
40°
38°
36°
34°
Geologic Unit Between
Reflectors 140 and 150
Sediment Types
Sand/Silt
Shale
Limestone
Layer
Absent

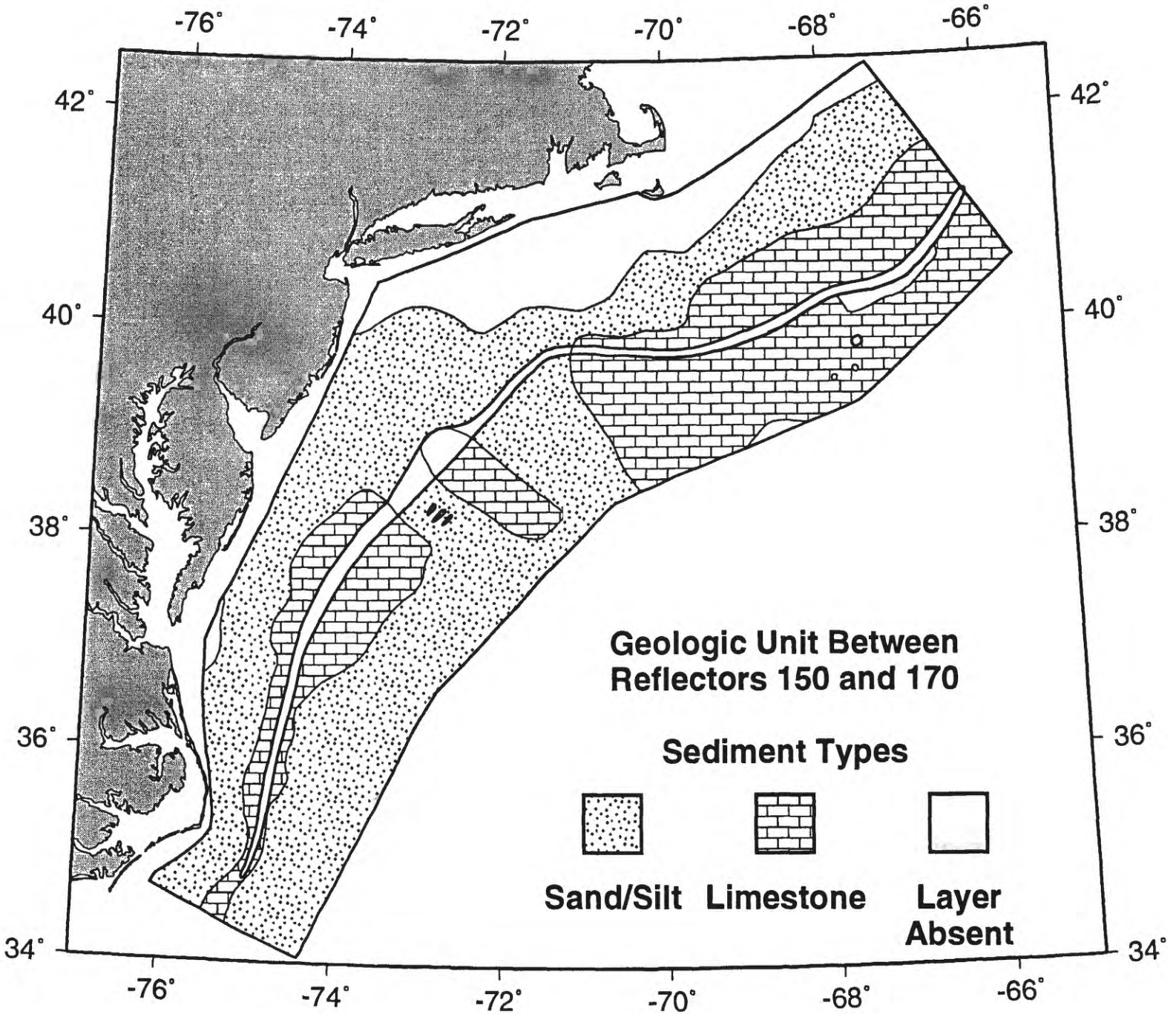
-76°
-74°
-72°
-70°
-68°
-66°
42°
40°
38°
36°
34°
Geologic Unit Between
Reflectors 150 and 170
Sediment Types
Sand/Silt
Limestone
Layer
Absent

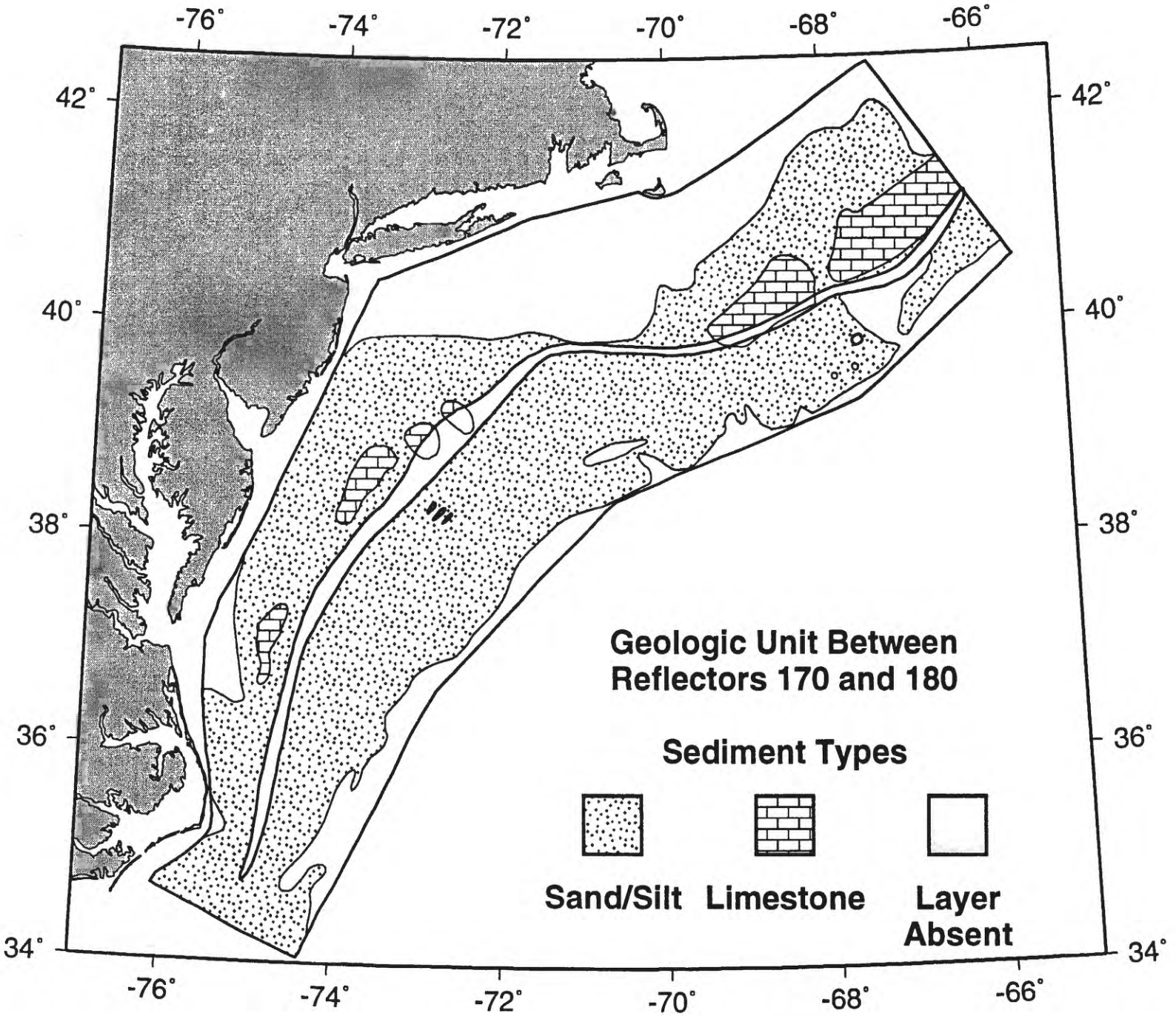
-76°
-74°
-72°
-70°
-68°
-66°
42°
40°
38°
36°
34°
Geologic Unit Between
Reflectors 170 and 180
Sediment Types
Sand/Silt
Limestone
Layer
Absent

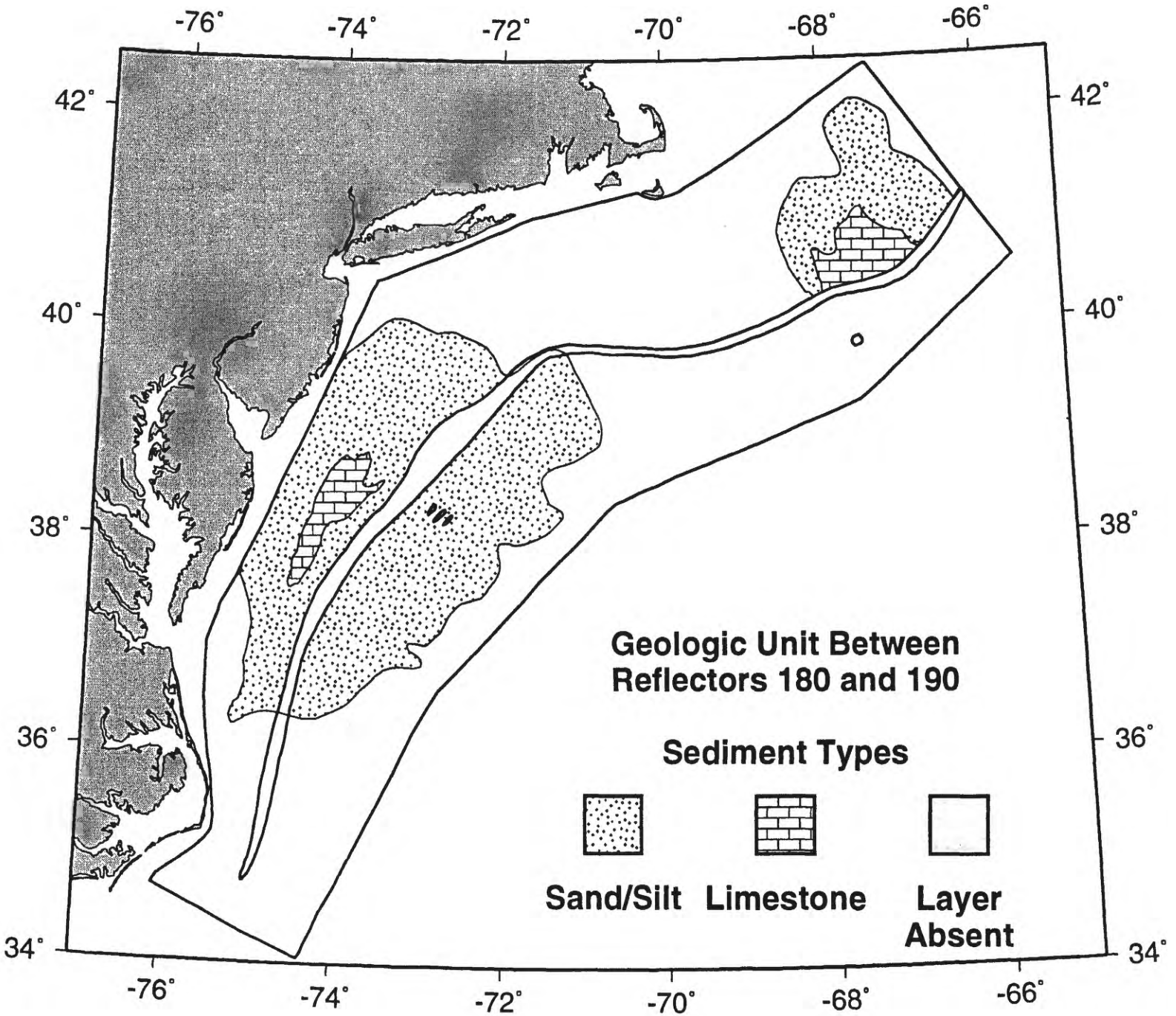
-76°
-74°
-72°
-70°
-68°
-66°
42°
40°
38°
36°
34°
Geologic Unit Between
Reflectors 180 and 190
Sediment Types
Sand/Silt
Limestone
Layer
Absent